Author:
Gurung, Sonam

Title:
Kainate Receptors in various forms of plasticity

Kainate Receptors in various forms of plasticity

Sonam Gurung

August 2018

A dissertation submitted to the University of Bristol in accordance with the requirements for award of the degree of Doctor of Philosophy by advanced study in the School of Biochemistry, Faculty of Life Sciences.

Word Count:46,182

Abstract

Kainate receptors (KARs) are glutamate-gated ion channels that regulate neuronal excitability and network function in the brain. They can signal through both canonical ionotropic and a non-canonical metabotropic pathway. They regulate neuronal excitability by undergoing plasticity themselves while also regulating plasticity of other receptors. Most KARs contain the subunit GluK2 and the precise properties of these GluK2-containing KARs are determined by additional factors including ADAR2-mediated mRNA editing of a single codon that changes a genomically encoded glutamine (Q) to an arginine (R), which affects their assembly, trafficking and channel properties.

I initially set out to study the role of KARs in various forms of plasticity including long term potentiation (LTP) and long term depression (LTD) of AMPA receptors (AMPAR) and homeostatic scaling of KARs themselves. I was unable to reliably replicate previous data showing transient KAR stimulation leads to their increased surface expression which in turn increases AMPAR surface expression. Interestingly however, I discovered that sustained KAR stimulation decreased AMPAR surface expression leading to AMPAR LTD.

In addition, I identified that KARs undergo homeostatic plasticity whereby they upscale and downscale in response to changes in the network activity. My findings show that ADAR2-dependent Q/R editing of GluK2 is dynamically regulated during homeostatic plasticity elicited by the suppression of synaptic activity. This suppression of synaptic activity decreases ADAR2 levels by enhancing their proteasomal degradation, which selectively reduces the numbers of GluK2 subunits that are edited. This loss of editing results in increased KAR oligomerisation and ER exit to increase the surface expression of GluK2-containing KARs. Furthermore, I show that partial ADAR2 knockdown phenocopies and occludes TTX-induced scaling of KARs. These data indicate that activity-dependent regulation of ADAR2 levels and GluK2 Q/R editing provides a mechanism for KAR homeostatic plasticity.

Author’s Declaration

I declare that the work in this dissertation was carried out in accordance with the requirements of the University's *Regulations and Code of Practice for Research Degree Programmes* and that it has not been submitted for any other academic award. Except where indicated by specific reference in the text, the work is the candidate's own work. Work done in collaboration with, or with the assistance of, others, is indicated as such. Any views expressed in the dissertation are those of the author.

SIGNED: ……DATE: ……..

Acknowledgements

First and foremost, thank you Jeremy for the ‘incredible’ supervision! You have been an amazing supervisor and thank you for believing in me more than I did. You have helped me build my confidence. I have learned a lot and enjoyed my PhD throughout.

Thank you, Kev, for teaching me pretty much everything throughout my PhD. All my achievements and everything I learned was all due to your amazing supervision and patience and I am very grateful for it.

Thank you, Ash, for all your help, especially my scaling project; a project I thoroughly enjoyed working with and for my new-found love for ADARs!

Thank you, Suko, for everything, the lab would not have functioned without you and I have learned a lot from you. Thank you to Dan and Ruth for your advice and help throughout my PhD.

To Laura, Alex, Vanilla, Jodie, Caroline and Zsombor, thank you for all the tea breaks and sharing our woes together and all the science advice! Vanilla and Luis, my dissection buddies. Those neurones would not have scaled, if it hadn’t been for the beautiful cells, we dissected every week! Alex again thank you so much for the macros that saved me so much time on analysing hundreds of nuclei!

Thank you, Phil, for helping me settle in the lab when I first started as an undergrad and Chun for your supervision during my rotation months. Everybody in Henley and Hanley lab, past and present, thank you!

Also thank you to my rotation supervisors: Ash Toye and Chrissy Hammond. I got an opportunity to be part of completely different and interesting projects with you both and I enjoyed being part of both of your labs. Thank you my Wellcome course mates: Rob, Lea, Mel and Amy for providing me with all the support, inspiration and fun times I will cherish very much.

Finally, I want to thank my family. My sisters, Sophia and Sarina, for providing me with all the support throughout my life, not just my PhD that I always feel lucky to have and my parents for all the love, belief, support and the food!

To end, I would say everything I have learned and achieved throughout my PhD was due to all the positive support I had around me, so thank you to everyone who helped me throughout my PhD!

Table of Contents

List of Figures

List of Tables

List of Abbreviations

aa	amino acid
aCSF	Artificial Cerebrospinal Fluid
A-I	Adenosine to Inosine
ADAR	Adenosine Deaminases Acting on RNA
AHP	After Hyperpolarisation
AIMP2	Aminoacyl tRNA synthase complex-interacting multifunctional protein 2
ALS	Amyotrophic Lateral Sclerosis
AMPAR	α-amino-3-hydroxy-5-methyl-4-isoxazolepropionic acid receptors
β-Me	β-mercaptoethanol
BCA	Bicinchoninic Acid
BDNF	Brain-derived neurotrophic factor
Bic	Bicuculline
BSA	Bovine Serum Albumin
BTZ	Bortezomib
C1q	complement component 1q
C1ql	complement component 1q like
CaMK	Ca^{2+}/calmodulin–dependent kinase
CHX	Cycloheximide
CIP	Calf Intestinal Alkaline Phosphatase
CNS	Central Nervous System
CP	Ca^{2+} Permeable
Cy	Cyanine
ddH_2O	double-distilled water
DIV	Days In Vitro
DHPG	(S)-3,5-Dihydroxyphenylglycine
DMSO	Dimethyl Sulfoxide
DMEM	Dulbecco’s Modified Eagle Medium
dsRNA	Double stranded RNA
ECL	Enhanced Chemiluminescence
ECS	Editing site Complementary Sequence
EDTA	Ethylenediaminetetraacetic Acid

eEF2	eukaryotic Elongation Factor 2
EGFR	Epidermal Growth Factor Receptor
EGTA	Ethylene Glycol Tetraacetic Acid
EPSC	Excitatory Post Synaptic Currents
EPSP	Excitatory Post Synaptic Potential
FBS	Fetal Bovine Serum
FMRP	Fragile X Mental Retardation Protein
GABA	Gamma-AminoButyric Acid
GFP	Green Fluorescent Protein
GRIP1	Glutamate Receptor-Interacting Protein 1
HBS	HEPES Buffered Solution
HBSS	Hank's Buffered Salt Solution
HCL	Hydrochloric acid
HECT	Homologous to the E6-AP C terminus
HEPES	4-(2-hydroxyethyl)-1-piperazineethanesulfonic acid
HFS	High Frequency Stimulation
HRP	Horse Radish Peroxidase
ICC	Immunocytochemistry
I/V	Isoleucine to Valine
iGluR	Ionotropic Glutamate Receptors
IP6	Inositol hexaphosphate 6
IPSC	Inhibitory Post Synaptic Currents
IPSP	Inhibitory Post Synaptic Potential
IsAHP	Inhibition of Slow After-Hyperpolarizing Potential
KA	Kainate
KAR	Kainate Receptor
KCC2	potassium(K^+)-chloride(Cl^-) co-transporter 2
KD	Knock Down
KO	Knock Out
KPNA	karyopherin subunit alpha
LB	Luria Bertani
LFS	Low Frequency Stimulation

LTD	Long Term Depression
LTP	Long Term Potentiation
mEPSCs	Mini EPSC
mGLuR	Metabotropic Glutamate receptors
MW	Molecular Weight
NES	Nuclear Export Signal
NLS	Nuclear Localisation Signal
NMDAR	N-methyl-D-Aspartate Receptor
NSF	N-ethylmaleimide Sensitive Factor
nt	nucleotide
PBS	Phosphate Buffered Saline
PCR	Polymerase Chain Reaction
PEI	Polyethylenimine
PICK1	Protein Interacting with C Kinase -1
Pin1	Peptidyl-prolyl isomerase NIMA interacting protein 1
PKC	Protein Kinase C
PLC	Phospholipase C
PLL	Poly-L-Lysine
PPR	Paired Pulse Ratio
PSD	Post Synaptic Density
R/G	Arginine to Glycine
rt	Room temperature
RISE	Reduced Intensity Status Epilepticus
SB	Sample Buffer
SDM	Site Directed Mutagenesis
SDS-PAGE	Sodium Dodecyl Sulphate-PolyAcrylamide Gel Electrophoresis
sEPSC	Spontaneous EPSC
shRNA	Short hairpin Ribonucleic Acid
SFFV	Spleen Focus-Forming Virus
SNX27	Sorting Nexin family member 27
SRSF9	Serine and Arginine rich Splicing Factor 9
STP	Short Term Plasticity

SUMO	Small Ubiquitin-like MOdifier
SV	Synaptic vesicle
TARP	Transmembrane AMPA receptor Regulatory Proteins
TD	Thiamine Deficiency
TEMED	Tetramethylethylenediamine
TLE	Temporal Lobe Epilepsy
TM	TransMembrane
TNF	Tumour Necrosis Factor
TTX	Tetrodotoxin
WB	Western Blot
WT	WildType
WWP2	WW domain-containing protein 2
Y/C	Tyrosine to Cytosine

Chapter 1. GENERAL INTRODUCTION

1.1 Synaptic transmission

1.1.1 Synapses

Neurones are specialised cells in the brain comprising of a cell body that projects out long neurites; which can be axons or dendrites. These neurites can extend great lengths into the neighbouring brain regions to form synapses. Synapses are specialised structures that allow neurones to receive and transmit information in the form of chemical or electrical signal. Synapses are junctions where a pre-synaptic membrane of a neurone (axon), that passes the signal, comes into proximity with the post-synaptic membrane of neighbouring neurone (dendrites), which receives the signal [**Figure 1-1**]. A neurone can form around 10,000 such synapses, all of them highly dynamic and responsive (Choquet and Triller 2013, Alberts 2015, Henley and Wilkinson 2016).

1.1.2 Chemical synapses and transmission

Chemical synapses consist of pre- and post-synaptic terminals separated by the synaptic cleft, which is filled with matrix that allows these terminals to adhere. The pre-synaptic terminal (axons) consists of synaptic vesicles (SVs) containing neurotransmitters either as part of the readily releasable pool or as part of the recycling/reserve pool (Denker and Rizzoli 2010). Neurones express voltage-gated sodium and potassium-permeable channels on their plasma membrane that generate action potentials once the depolarisation of the membrane reaches above the threshold level (Catterall 1995, Lodish H 2000).

The action potential is then propagated along the axon and upon reaching the axon terminal leads to Ca^{2+} influx through the opening of voltage-gated Ca^{2+} channels (Llinas, Steinberg et al. 1981). This influx triggers exocytosis whereupon the SVs fuse with the pre-synaptic membrane to release the neurotransmitters into the synaptic cleft (Heuser, Reese et al. 1979, Heidelberger, Heinemann et al. 1994, Hilfiker, Pieribone et al. 1999), which then diffuse across and bind to their specific ionotropic and/or metabotropic receptors on the post synaptic membrane (dendrites) (Wilcox, Buchhalter et al. 1994).

Activation of these ionotropic and metabotropic receptors via neurotransmitter binding results in ion flow or second-messenger signalling cascade in the case of metabotropic receptors (Pin and Duvoisin 1995, Conn and Pin 1997) [**Figure 1-1**]. This triggers changes in the post-synaptic membrane potential and conductance. If the membrane potential changes are above the threshold level, action potential is triggered, and the chemical signal is converted to an electrical signal.

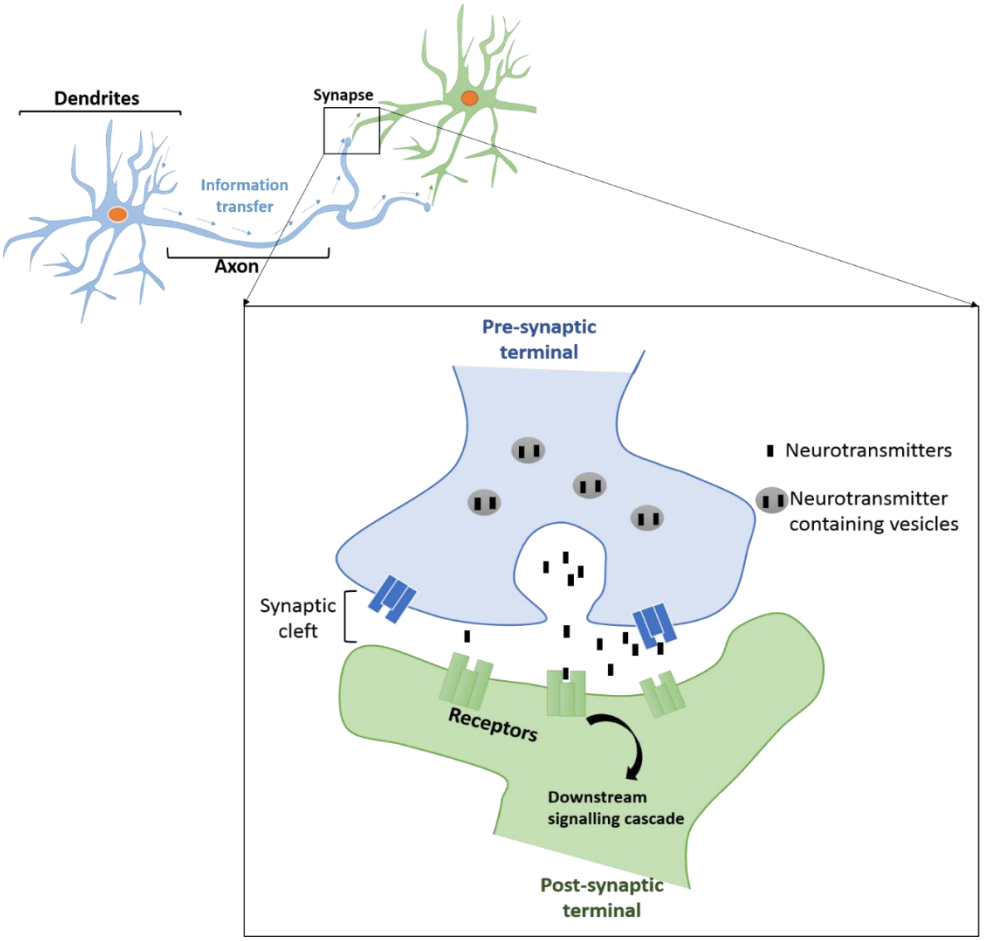

Figure 1-1: Synaptic structure.

Synapse is a specialised structure where a pre-synaptic membrane (axon) is near the post synaptic membrane (dendrites), separated by the synaptic cleft. Upon receiving action potential, the pre-synaptic terminal releases neurotransmitters into the synaptic cleft, which diffuses across and bind to their specific ionotropic and/or metabotropic receptors in the post synaptic membrane. This results in downstream signalling cascades, triggering changes in the post synaptic membrane potential and conductance which generates the action potential, thus allowing information transfer.

1.1.3 Excitatory and inhibitory transmission

Depending on the type of neurotransmitters being released and the subsequent receptor activation, the effect can be excitatory or inhibitory in the

postsynaptic neuron. The excitatory axon terminals typically synapse on to the dendritic spines, which are small protrusions from dendrites; while the inhibitory axon terminals predominantly synapse onto the dendritic shafts (Kandel 2000, Megias, Emri et al. 2001).

Ionotropic glutamate receptors mediate the excitatory neurotransmission, which contribute to the excitatory postsynaptic potential (EPSP) (Wisden and Seeburg 1993). On the other hand, majority of the inhibitory transmission is mediated by inhibitory receptors such as Gamma-AminoButyric Acid (GABA) receptors ($GABA_AR$ and $GABA_BR$), which generate the inhibitory postsynaptic potential (IPSP) (Connors, Malenka et al. 1988, Wilcox, Buchhalter et al. 1994, Sigel and Steinmann 2012).

1.1.4 Measuring synaptic transmission

Excitatory post-synaptic potential (EPSP) is triggered by the momentary depolarisation of cell following the flow of positively charged ions into the postsynaptic cell, which can potentially lead to generation of action potential. Excitatory post synaptic currents (EPSCs) are the flow of ions that cause EPSP. These changes in either the amplitude or frequency of EPSCs can be measured using electrophysiological techniques. Typically, changes in the EPSC frequency are attributed to altered presynaptic neurotransmitter release probability and/or altered numbers of synapses. Changes in the peak amplitude is an indication of altered numbers of postsynaptic receptors and the number of neurotransmitters released in each quantum (2015).

EPSC recordings can be generated with experimental stimulation (evoked) or without experimental stimulation; which can be spontaneous(s) or miniature(m) EPSCs. sEPSC is generated by release of neurotransmitters which can be both action-potential-dependent and independent while mEPSCs are detected in the absence of presynaptic action potentials, solely due to spontaneous SVs release (Holz RW 1999, Kandel 2000, Mozrzymas 2008, Pinheiro and Mulle 2008).

1.2 Ionotropic glutamate receptors

Ionotropic glutamate receptors (iGluRs) mediate almost all of the excitatory neurotransmission in the central nervous system (CNS) (Wisden and Seeburg 1993). They are multi-subunit receptors where each subunit is made up of extracellular N-terminus, 3 membrane spanning domains, one re-entrant loop and an intracellular carboxy-terminal domain (C-terminal) (Henley and Wilkinson 2016) [**Figure 1-2**]. These subunits assemble into a tetramer forming the ion channel which upon glutamate binding is opened to pass ions into the post-synaptic membrane (Safferling, Tichelaar et al. 2001).

There are three main types of glutamate receptors:

- α-amino-3-hydroxy-5-methyl-4-isoxazolepropionic acid receptor (AMPAR)
- Kainate Receptor (KAR)
- N-methyl-D-Aspartate receptor (NMDAR)

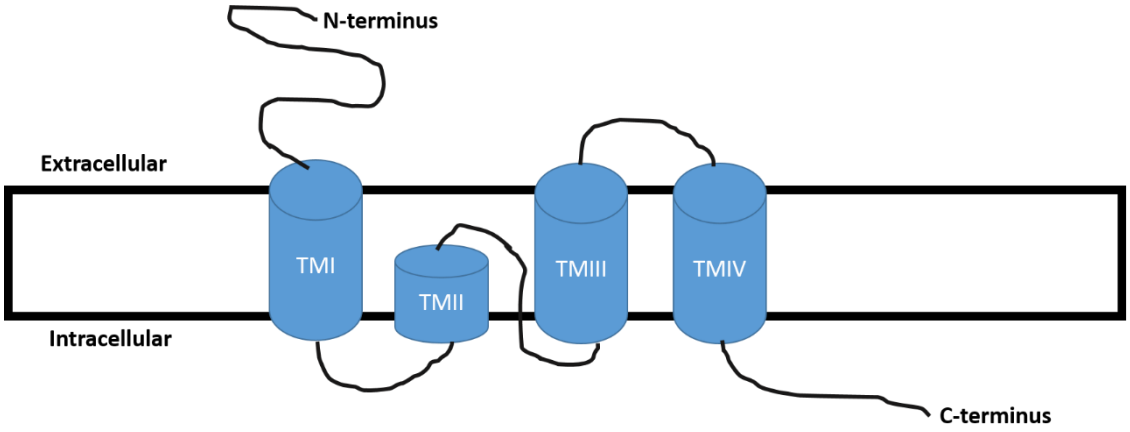

Figure 1-2: General iGluR subunit structure and topology.

iGluRs share similar structure and topology to an extent. Each subunit consists of 3 membrane spanning domains (TMI, III and IV), extracellular N-terminus, one re-entrant loop (TMII) and intracellular carboxy-terminal (C-terminus).

Delta family of ionotropic glutamate receptors (GluD1 and GluD2) also exist however, they do not show typical agonist induced ion channel currents (Yamazaki, Araki et al. 1992, Lomeli, Sprengel et al. 1993). They are unresponsive to glutamate but bind neurotransmitters D-serine and glycine (Naur, Hansen et al. 2007) and have been shown to have an important role in synaptogenesis by interacting with pre-synaptic proteins such as Neurexins

(Yuzaki and Aricescu 2017). For instance, GluD2, which is predominantly expressed in cerebellar Purkinje cells, was shown to bind to Cerebellin 1 (Cbln1) which in turn binds to presynaptic receptor neurexin 1 in parallel fibre terminals. Mice lacking GluD2 had reduced number of these purkinje cells-parallel fibre synapses and restoring GluD2 levels restored normal level of these synapses (Yuzaki 2013). GluD1 was also shown to be able to induce synapse formation by binding to Cbln 1 and Cbln 2 which interacts with neurexin *in vitro* (Matsuda, Miura et al. 2010, Yasumura, Yoshida et al. 2012).

1.2.1 AMPARs

α-amino-3-hydroxy-5-methyl-4-isoxazolepropionic acid receptors (AMPARs) AMPARs are tetrameric assemblies made up of four possible subunits; GluA1, GluA2, GluA3 and GluA4 (previously referred to as GluR1-4), encoded by the genes *GRIA1-4* respectively. They assemble predominantly as heterodimers (Hollmann and Heinemann 1994) but can also assemble as homodimers (Wenthold, Petralia et al. 1996, Lu, Shi et al. 2009).

1.2.1.1 AMPAR subunit diversity

The AMPAR subunits are highly homologous in their domains, with ~70% amino acid residue identity while their C-terminal is the most variable region (Collingridge, Isaac et al. 2004). Additional factors such as alternative splicing and RNA editing add further diversity to the AMPAR subunits. Alternative splicing leads to the so-called flip/flop exon variants being produced that cause alterations in the receptor desensitisation rate and the channel closing kinetics (Lambolez, Ropert et al. 1996, Pei, Huang et al. 2009). This flip/flop alternative splicing occurs in the connecting loop in between transmembrane region TMIII and IV at the C-terminal end (Sommer, Keinanen et al. 1990). There are other forms of post-transcriptional modifications (RNA editing) that occur such as Q/R editing and R/G editing adding further diversity to the subunits and altering their functional ionotropic properties such as Ca^{2+} permeability and desensitisation properties [**Figure 1-3**]. (Sommer, Kohler et al. 1991, Lomeli, Mosbacher et al. 1994) [RNA editing discussed in detail in section 1.5].

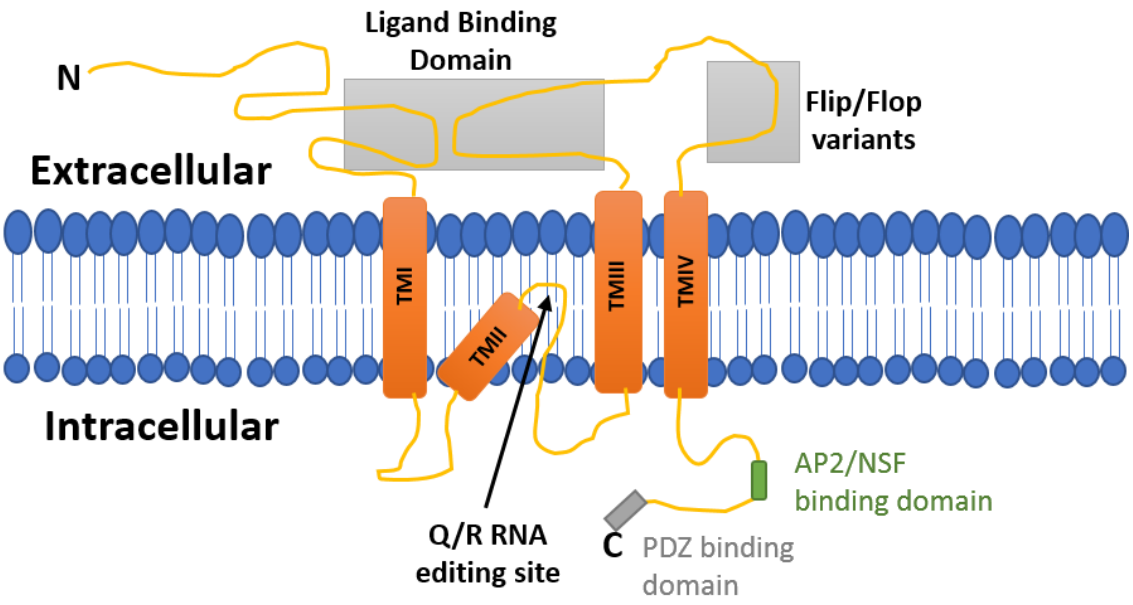

Figure 1-3: Schematic of an AMPAR subunit.

The N-terminal region in combination with the region between TMIII and TMIV form the ligand binding domain. The variable C-terminal region allows for subunit specific protein-protein interactions. Alternative splicing leads to the flip/flop exon variants. GluA2 subunit also undergoes RNA editing process, such as the Q/R editing, which occurs in the TMII region (black arrow).

1.2.1.2 AMPAR expression

AMPARs are enriched at the post synaptic membrane in the excitatory synapses (Henley and Wilkinson 2016). GluA1/A2 form the predominant AMPAR heteromeric complex in adult CA1 hippocampal neurones (Wenthold, Petralia et al. 1996, Shi, Hayashi et al. 2001, Lu, Shi et al. 2009). GluA3 is thought to be expressed at only 10% of the levels compared to GluA1 and GluA2 (Sans, Vissel et al. 2003). However, studies have indicated GluA2/A3 along with GluA1/A2 to be predominant heteromers in rat hippocampus and cortex (Wenthold, Petralia et al. 1996, Lu, Shi et al. 2009). GluA4 is highly expressed during early developmental stages but is expressed sparsely in the adult brain (Zhu, Esteban et al. 2000), though they play a key role in transmission in parvalbumin-containing inhibitory interneurons, where reduced GluA4 expression has been shown to cause a reduction in AMPAR function in these interneurons and hence reduced feedforward inhibition. This resulted in imbalance in excitatory/inhibitory transmission promoting epileptic activity and deficit in spatial learning memory (Bernard, Somogyi et al. 1997, Pelkey, Barksdale et al. 2015).

1.2.1.3 Regulation of AMPAR trafficking and localisation

The variable C-terminal domain of AMPAR subunits allow for subunit specific protein-protein interactions and post-translational modifications that regulates the function and trafficking of the resultant tetramer (Huganir and Nicoll 2013, Henley and Wilkinson 2016). These protein-protein interactions are mostly mediated by the PDZ domain containing proteins such as Protein Interacting with C-Kinase 1 (PICK1) (Hanley 2014), Glutamate receptor-interacting protein 1 (GRIP1) (Dong, O'Brien et al. 1997) and sorting nexin 27 (SNX27) (Hussain, Diering et al. 2014, Loo, Tang et al. 2014), all of which bind to one or more specific AMPAR subunits to maintain their synaptic localisation either basally or during plasticity. Other proteins such as multimeric ATPase N-ethylmaleimide sensitive factor (NSF) (Nishimune, Isaac et al. 1998, Gardner, Takamiya et al. 2005) has been shown to be important in synaptic incorporation of GluA2-AMPARs. AMPAR auxiliary subunits such as the family of transmembrane AMPA receptor regulatory proteins (TARPs) (stargazin and γ3-8) was shown to promote synaptic trapping by binding to post synaptic density protein 95 (PSD-95), a post-synaptic adhesion protein (Tomita, Adesnik et al. 2005, Opazo, Labrecque et al. 2010, Jackson and Nicoll 2011). Moreover, post-translational modifications also regulate the interactions between these proteins and AMPAR subunits. For instance, Protein Kinase C (PKC) can phosphorylate GluA2 in its PDZ region in the C-terminus inhibiting GluA2 binding to GRIP1 but increasing GluA2 binding to PICK1. **Figure 1-4** is a cartoon schematic of majority of known AMPAR interactors.

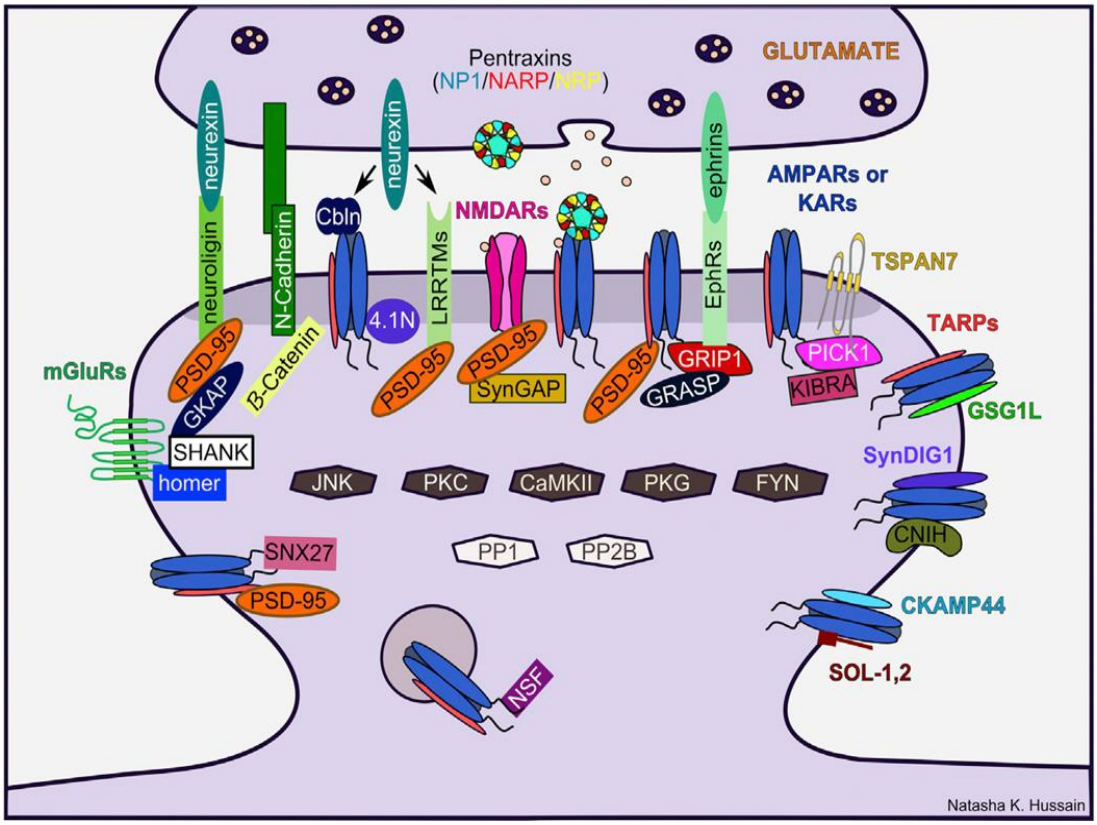

Figure 1-4: Cartoon diagram of scaffolding and trafficking proteins implicated in AMPAR trafficking and localisation.

Proteins such as PICK1, GRIP1, NSF and SNX27 regulate AMPAR endocytosis and exocytosis. AMPAR auxiliary subunits such as TARPs enhance AMPAR synaptic trapping. Signalling proteins such as protein kinases and phosphatases regulate receptor trafficking. PSD structural complex including PSD-95 interact with other proteins to regulate structure and function of the synapse. Figure taken from (Huganir and Nicoll 2013).

1.2.1.4 AMPARs function

AMPARs mediate majority of the fast-excitatory neurotransmission in the central nervous system as such regulating AMPAR surface expression and localisation underlies the ultimate mechanism that regulates plasticity of majority of excitatory neurotransmission (Chater and Goda 2014). The number, composition and/or properties of AMPARs on the post-synaptic surface can be altered and regulated to respond to the incoming stimulus. The mechanisms regulating AMPAR properties, trafficking and localisation are reinforced to allow AMPARs to fulfil their role in plasticity. These also include properties that regulate AMPAR diversity for instance Ca^{2+} permeability of AMPARs via GluA2 Q/R editing [see section 1.5.4]. In fact, AMPAR regulation provides basis of plasticity mechanisms such as Long Term Potentiation

(LTP), Long Term Depression (LTD) and homeostatic scaling [more detail on plasticity in Section 1.3] (Huganir and Nicoll 2013, Henley and Wilkinson 2016).

1.2.1.5 AMPARs in diseases

Due to the vastly important role of AMPARs in synaptic function, any defect in their trafficking, subunit composition or activity can result in neurological disorders and neurodegenerative diseases (Henley and Wilkinson 2016). For instance, reduced synaptic AMPARs and aberrations in LTP and LTD are the early hallmarks of dementia in Alzheimer's disease (Walsh and Selkoe 2007, Shankar, Li et al. 2008). Reports have shown that soluble amyloid-β (Aβ) oligomers disrupts AMPAR trafficking (Zhao, Santini et al. 2010) while intracellular Aβ also causes enhancement of synaptic Ca^{2+} permeable AMPARs resulting in excitotoxicity (Whitcomb, Hogg et al. 2015). Moreover, other pathological conditions such as in epilepsy, alterations in AMPAR subunit compositions are also observed where loss of GluA1 containing AMPARS occur (Grigorenko, Glazier et al. 1997) while cocaine exposure causes increase in levels of Ca^{2+} permeable AMPARs (Heshmati 2009).

1.2.2 Kainate Receptors

Kainate Receptors (KARs) are ionotropic glutamate receptors that play key roles in regulating synaptic function and neuronal network activity (Evans, Gurung et al. 2017). They are involved in processes ranging from neuronal development and differentiation to neuronal cell death and neurodegeneration (Lerma and Marques 2013). Functional KARs are tetrameric assemblies composed of five possible subunits: low-affinity (for kainate ligand) GluK1, GluK2, GluK3 and high-affinity GluK4 and GluK5 (previously named as GluR5, GluR6, GluR7, KA1 and KA2 respectively), encoded by gene *GRIK1-5* respectively (Collingridge, Olsen et al. 2009).

Studies using recombinant proteins have shown that GluK1, GluK2 and GluK3 can form functional ion channels as homomeric assemblies while GluK4 and GluK5 can only form functional ion channels as heteromeric assemblies with GluK1-3 (Ayalon and Stern-Bach 2001). GluK4 and GluK5 have ER retention sequences and so cannot be released from ER and express on the surface

without forming heteromers with GluK1-3 (Gallyas, Ball et al. 2003, Ruiz, Sachidhanandam et al. 2005, Vivithanaporn, Yan et al. 2006, Ball, Atlason et al. 2010). Moreover, at least one of the GluK4/5 subunit is needed for KAR's ionotropic function (Fernandes, Catches et al. 2009). Interestingly, along with their canonical ionotropic function, KARs can also signal through a non-canonical metabotropic pathway where KARs signal through coupled heterotrimeric G-proteins and second messengers (Contractor, Mulle et al. 2011). This metabotropic signalling pathway regulates various neurological functions of KARs which will be explored below.

1.2.2.1 KAR subunit diversity

KAR subunits undergo alternative splicing in their N- and C-terminal domains adding to their subunit diversity. GluK1 can produce two N-terminal variants ($GluK1_{1\text{-}2}$), where $GluK1_1$ has an insertion of 15-amino-acid (aa) cassette in its N-terminus, and 4 C-terminal alternative splice variants ($GluK1_{a\text{-}d}$) (Bettler, Boulter et al. 1990, Sommer, Burnashev et al. 1992, Pinheiro and Mulle 2006). GluK2 and GluK3 can also undergo editing in their C-terminal region to produce splice variants ($GluK2_{a\text{-}c}$ and $GluK3_{a\text{-}b}$ respectively) (Schiffer, Swanson et al. 1997, Jaskolski, Coussen et al. 2004) [**Figure 1-5**]. For GluK2, $GluK2_{a\text{-}b,}$ which differs in their C-terminus domain, can equally co-assemble in native receptors and are found to be expressed within the same brain regions, while $GluK2_c$ consists of exon insertion in the C-terminus and have only been described in humans as of yet. For $GluK3_a$, the whole of C-terminus is replaced by an unrelated 55aa sequence (Pinheiro and Mulle 2006). Similar to the AMPARs, the C-terminal variations in KARs affect KAR trafficking, regulation, interaction and expression (Pahl, Tapken et al. 2014).

In addition, GluK1 and GluK2 subunits of KAR can undergo RNA editing adding to their diversity. These editing processes include I/V, Y/C and Q/R editing [**Figure 1-5**] [Discussed in section 1.5 and 1.6] (Evans, Gurung et al. 2017).

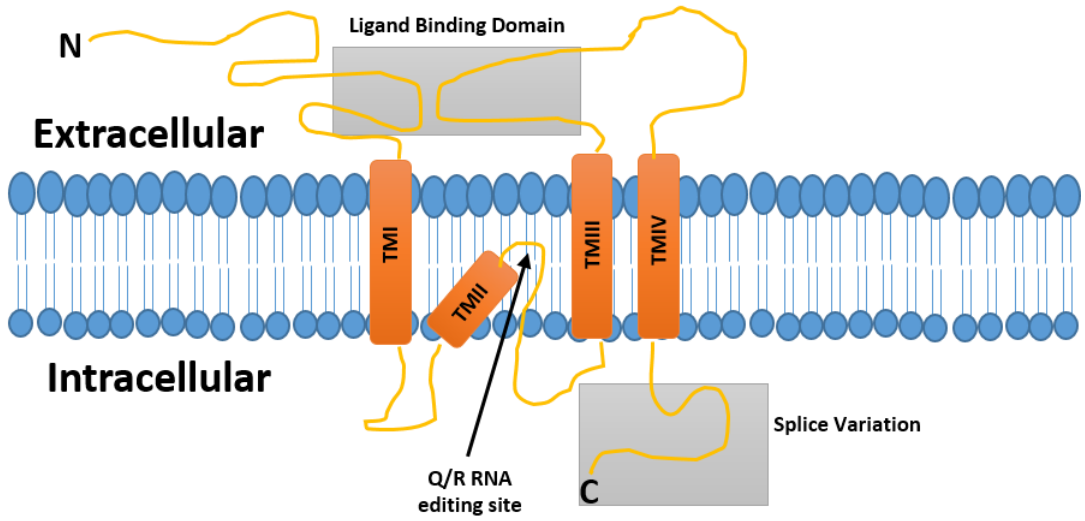

Figure 1-5: Structure and Topology of GluK2 KAR subunit.

The N-terminal region in combination with the region between TMIII and TMIV form the ligand binding domain. The C-terminal region is prone to splicing producing alternatively spliced variants. GluK2 along with GluK1 subunit also undergoes RNA editing process such as the Q/R editing site which occurs in the TMII region. Figure adapted from (González-González 2012).

1.2.2.2 KAR subunit expression

mRNA studies have shown high expression of KAR subunits throughout the brain and spinal cord (Wisden and Seeburg 1993, Bahn, Volk et al. 1994, Bettler and Mulle 1995). Within the CA3 region and in dentate gyrus cells, there are high levels of GluK2, GluK4 and GluK5. GluK1 is thought to express predominantly in the CA3 interneurons and GluK3 in the dentate granule cells (Bahn, Volk et al. 1994, Bureau, Bischoff et al. 1999, Paternain, Herrera et al. 2000). Lack of reliable specific antibodies have limited the expression studies of KARs to mRNA levels. However, GluK2-GluK5 heteromeric complex is thought to be the most abundant KAR complex in the adult hippocampus (Petralia, Wang et al. 1994, Kumar, Schuck et al. 2011).

1.2.2.3 Post-translational regulation of KARs

Activity-dependent regulation of KARs has been shown in many previous studies (Martin and Henley 2004, Martin, Bouschet et al. 2008, Gonzalez-Gonzalez and Henley 2013) [see Chapter 3.1]. Post translational modifications such as palmitoylation, phosphorylation, SUMOylation and ubiquitination

regulate both KAR trafficking and their post-synaptic localisation [**Figure 1-6**], discussed below.

Small Ubiquitin like Modifier (SUMO) proteins are small 97 residue proteins (11kDa), which covalently conjugate to the lysine residue of the target proteins altering the protein stability, inducing conformation changes and/or altering protein interactions either by masking or introducing new interaction sites (Wilkinson and Henley 2010). In the case of GluK2, it's SUMOylation in the intracellular C-terminus, K886, allows agonist-induced internalisation of GluK2-containing KARs (Martin, Nishimune et al. 2007).

Phosphorylation is the major post translational modification mechanism through which protein function is regulated in response to various stimuli. GluK2 phosphorylation by PKC at S846 and S868 site has been shown to regulate GluK2 trafficking through the secretory pathway by reducing ER exit and hence their surface expression (Evans, Gurung et al. 2017). Basally, phosphorylation at S846 promotes internalisation of GluK2-containing KARs while both the serine sites are also phosphorylated in response to the agonist stimulation, with the phosphorylation at S868 in particular being required for agonist-induced endocytosis. Interestingly, phosphorylation at S868 also enhances GluK2 SUMOylation to allow basal and activity-induced internalisation of GluK2-containing KARs. However, in the absence of SUMOylation GluK2 phosphorylation at S868 leads to the recycling of endocytosed GluK2 back to the plasma membrane (Nasu-Nishimura, Jaffe et al. 2010, Konopacki, Jaafari et al. 2011, Chamberlain, Gonzalez-Gonzalez et al. 2012, Wilkinson, Konopacki et al. 2012). This suggests the role of phosphorylation in both insertion and removal of KARs from the plasma membrane.

Palmitoylation is another form of post-translational modification where palmitic acid is added to specific cysteine residues regulating protein trafficking and function, acting as a form of reversible lipid modification (Fukata and Fukata 2010). Palmitoylation of GluK2 (C858 and C871) was shown to promote its interaction with scaffolding protein 4.1N resulting in stable KAR surface expression while phosphorylation of GluK2 inhibited this interaction and

enhanced KAR endocytosis instead (Pickering, Taverna et al. 1995, Copits and Swanson 2013). This also shows existence of dynamic crosstalk between these various forms of post translational modifications that regulate KAR surface expression.

Ubiquitin on the other hand is a highly conserved 76-amino acid protein, which tags target proteins for degradation in the proteasomes (Hallengren, Chen et al. 2013). GluK2 containing KARs are also targeted for ubiquitination and degradation by various E3 ubiquitin ligases. Cullin 3 (Cul3) interacts with the C-terminus of GluK2 via an adaptor protein actinofilin (Salinas, Blair et al. 2006). Recently, it was shown that another E3 ubiquitin ligase, Parkin, can ubiquitinate GluK2 in its C-terminus. Loss of Parkin increases GluK2 surface expression which results in increased susceptibility of the hippocampal neurones to kainate-induced excitotoxicity (Maraschi, Ciammola et al. 2014).

While above mentioned modifications have focused on GluK2 containing KARs, other subunits of KAR can also be regulated by post translational modifications. For instance, CaMKII has been shown to phosphorylate the C-terminal domain of GluK5 which is required for KAR-LTD at MF-CA3 synapses by antagonising GluK5 interaction with the post synaptic adhesion protein PSD95 (Carta, Opazo et al. 2013). Hence, posttranslational modification of KARs play a major role in KAR localisation and function both basally and during activity.

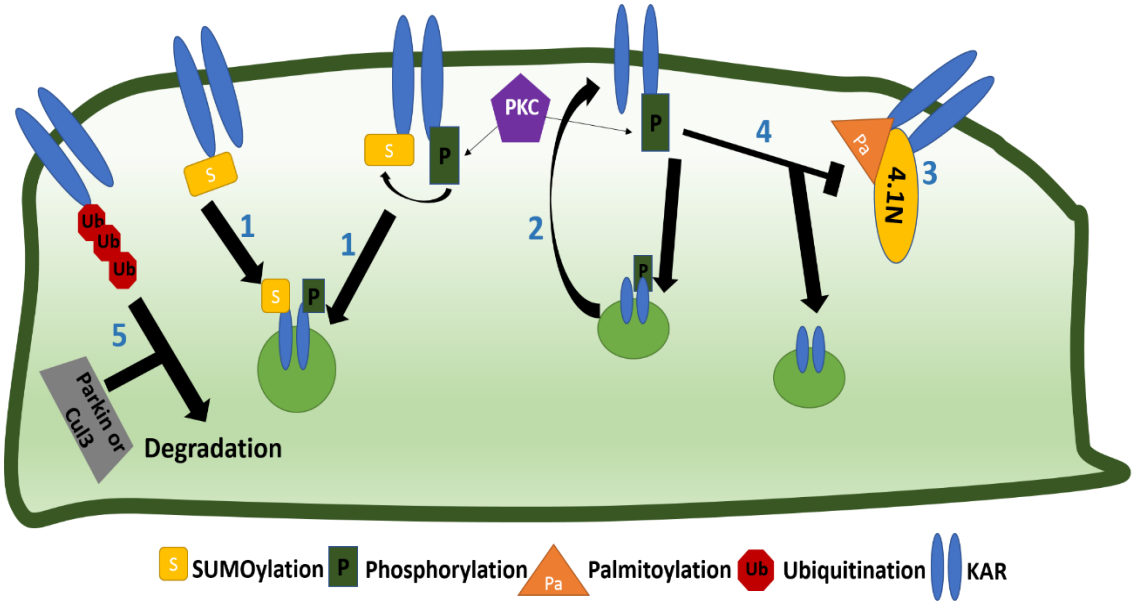

Figure 1-6: Post translational modifications regulating GluK2-KAR surface expression.

Agonist induced phosphorylation of GluK2-KAR by PKC at S868 enhances GluK2-KAR SUMOylation at K886 leading to KAR endocytosis (1). Phosphorylation at S868 in the absence of SUMOylation leads to receptor recycling back to the plasma membrane, increasing the surface expression of KAR (2). PKC phosphorylation of GluK2 at S846 and S868 reduces ER exit of GluK2 basally (not shown). Palmitoylation of KAR enhances its surface expression by interaction with 4.1N scaffolding protein (3). PKC mediated phosphorylation of KAR inhibits this interaction and promotes endocytosis (4). Finally, ubiquitination of GluK2-KAR by Parkin or Cul3 has been shown to mediate KAR internalisation and degradation (5).

1.2.2.4 Regulation of KAR localisation

Various mechanisms have been shown to regulate KAR synaptic positioning. This includes subunit dependent regulation, protein-protein interactions and post-translational modifications as mentioned above.

1.2.2.4.1 Protein-protein interactions

Many KAR protein interactors have been identified which play a major role in their post-synaptic localisation. Single pass transmembrane proteins Neto1 and Neto2 have been shown to bind to GluK1-3 subunits (Zhang, St-Gelais et al. 2009, Straub, Hunt et al. 2011). Neto1 is highly expressed in the hippocampus while Neto2 is more expressed in the cerebellum (Evans, Gurung et al. 2017). However, there is contradiction in terms of whether Netos do play a role in trafficking and targeting of GluK2-containing KARs as some studies have reported enhanced GluK2 surface expression with overexpression of Neto1 and Neto2 (Palacios-Filardo, Aller et al. 2016) and

reduction in synaptic GluK2 in Neto2 knockout (Wyeth, Pelkey et al. 2014). Other studies have reported no difference in GluK2-KAR responses in CA1 pyramidal neurones when co-expressed with Neto1 or Neto2 (Sheng, Shi et al. 2015). Interestingly for GluK1, expressing Neto1 or Neto2 along with GluK1 in CA1 pyramidal cells enhanced synaptic targeting of GluK1 containing KARs (Copits, Robbins et al. 2011). However, importance of Neto proteins *in vivo* have not been examined as of yet. While Netos role in KAR localisation remain debatable, the association of Netos to KAR has been shown to mediate the slow deactivation kinetics of KARs, which is not detected on recombinant KARs (Tomita and Castillo 2012).

Recently, C1q-like protein (c1ql), a synaptically secreted soluble factor (Matsuda 2017), was reported to be a key contributor in KAR localisation in mossy fibre synapses in the CA3 neurones (Matsuda, Budisantoso et al. 2016, Straub, Noam et al. 2016) [**Figure 1-7**]. C1ql2 and 3 were shown to bind to N-terminal domain of GluK2, GluK4 (Matsuda, Budisantoso et al. 2016) and GluK5 (Straub, Noam et al. 2016) while the pre-synaptic adhesion molecule neurexin 3 binds to c1ql2/3. Interestingly, using co-cultures of HEK293T cells expressing neurexin 3 and c1ql2/3 with neurones, the neurexin3-c1ql-KAR complex could be isolated (Matsuda, Budisantoso et al. 2016). Other adhesion molecules such as N-cadherin and PSD95 also binds KAR subunits and maintain their postsynaptic localisation, interaction of which are mediated by the PDZ ligand (Garcia, Mehta et al. 1998, Coussen, Normand et al. 2002, Hirbec, Francis et al. 2003).

PSD95, synaptic scaffolding protein has been shown to interact with the C-terminal PDZ ligands of GluK1, GluK2 and GluK5 subunits of KARs (Garcia, Mehta et al. 1998). While it is not known whether this binding is direct or not, PSD95 knockout mice showed decreased synaptic KAR component in MF-CA3 synapses, showing their importance in KAR synaptic localisation (Suzuki and Kamiya 2016). Similarly, expression of dominant negative N-cadherin, which is a neuronal cell adhesion protein, and knockdown of N-cadherin both reduce KAR synaptic components in the MF-CA3 synapses. The C-terminal region of GluK2 again has been shown to mediate KAR interaction with N-

cadherin, identifying it to be important for GluK2 incorporation in MF-CA3 synapses [**Figure 1-7**] (Fievre, Carta et al. 2016).

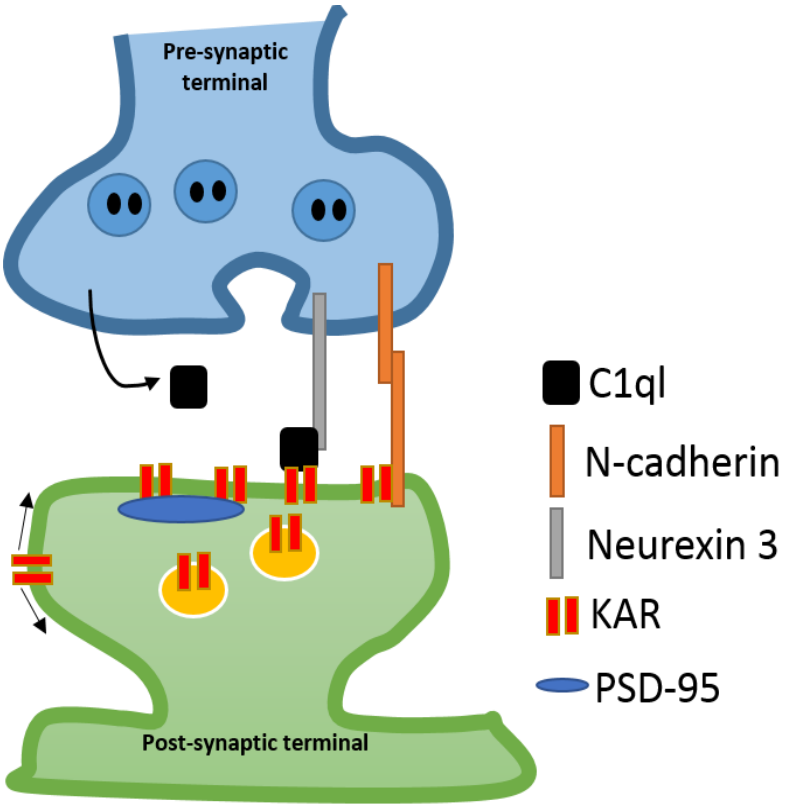

Figure 1-7: Protein-protein interactors that regulate KAR post synaptic localisation.

Soluble c1ql proteins secreted from the pre-synaptic terminal cluster the post synaptic KARs and pre-synaptic neurexin 3. N-cadherin and PSD95 also interact with the C-terminus of KAR subunits promoting KAR synaptic incorporation and maintenance. Figure adapted from (Evans, Gurung et al. 2017).

1.2.2.4.2 Subunit mediated regulation

The GluK2 C-terminus itself also plays an important role in synaptic stability of KARs but not necessarily in KARs surface expression in general (Yan, Yamasaki et al. 2013, Straub, Noam et al. 2016). Ablating Neto2 or GluK5 had no effect on the postsynaptic density abundance of GluK2/Neto2 or GluK2/GluK5. However, mice lacking C-terminus of GluK2 lacked synaptic responses in mossy fibre-CA3 synapses but had no effect on surface or total levels of GluK2 in the cerebellum thus suggesting, their importance in synaptic stabilisation of KARs, which is most likely through interaction with synaptic adhesion proteins.

Interestingly however, the study did show the importance of subunits GluK4 and GluK5 in providing synapse specificity in hippocampus. GluK4/5 knockout

mice showed lack of postsynaptic KARs at MF-CA3 synapses (Fernandes, Catches et al. 2009). Furthermore, the GluK2 subunit was observed to be redistributed in more distal dendrites within the CA3 pyramidal neurones (Straub, Noam et al. 2016). This was suggested to be via GluK5 ability to bind c1q-like proteins, which is present in abundance in mossy fibre synapses, through the N-terminal region of GluK5. Therefore, GluK2 C-terminus was shown to be important for synaptic localisation but the high affinity GluK4/5 are needed for KAR synapse specificity (Straub, Noam et al. 2016).

1.2.2.5 Forward trafficking of KARs

We have recently shown that GluK2 containing KARs can use local secretory pathways to be delivered to the cell surface and its trafficking itself can be regulated in various activity contexts (Evans, Gurung et al. 2017). Briefly, we showed that KARs can use local secretory pathways to be delivered to the cell surface and this can be activity dependently regulated as activating surface KARs using kainate stimulation results in a negative feedback mechanism where less *de novo* KARs are trafficked to the surface. Moreover, the PDZ ligand mediated interaction of GluK2 was shown to be important for this regulation however, the interactors are not known as of yet (Evans, Gurung et al. 2017). Finally, GluK5 also regulates KAR trafficking as its heteromerization with GluK2 and binding to 14-3-3ζ promotes KAR forward trafficking (Vivithanaporn, Yan et al. 2006).

1.2.2.6 KAR in excitatory neurotransmission

KARs are expressed at both pre- and post-synaptic membranes where they fulfil distinct functional roles (Contractor, Mulle et al. 2011).

1.2.2.6.1 Pre-synaptic KARs

Pre-synaptic KARs can bidirectionally modulate glutamate release to regulate excitatory neurotransmission. At MF-CA3 synapses they can decrease glutamate release upon stimulation with relatively high (>100nM) concentration of kainate (Vignes, Clarke et al. 1998, Contractor, Swanson et al. 2000, Kamiya and Ozawa 2000, Schmitz, Frerking et al. 2000). Both metabotropic and ionotropic functions of KAR have been implicated in its function to regulate this release. It has been proposed that KAR activation at

these concentrations of kainate may inactivate the sodium and Ca^{2+} channels and promote electrical shunting, which in turn depresses the evoked glutamate release by reducing the terminal excitability (Kamiya and Ozawa 2000, Schmitz, Mellor et al. 2001). However, KAR mediated depression of glutamate release was also sensitive to the treatment of pertussis toxin (PTx) which inhibits the $G_{i/o}$ pathway, thus suggesting it to be a metabotropic function instead (Rodriguez-Moreno and Sihra 2004). This second messenger signalling cascade involved adenylate cyclase(AC)/cAMP/PKA activation [**Figure 1-8** A].

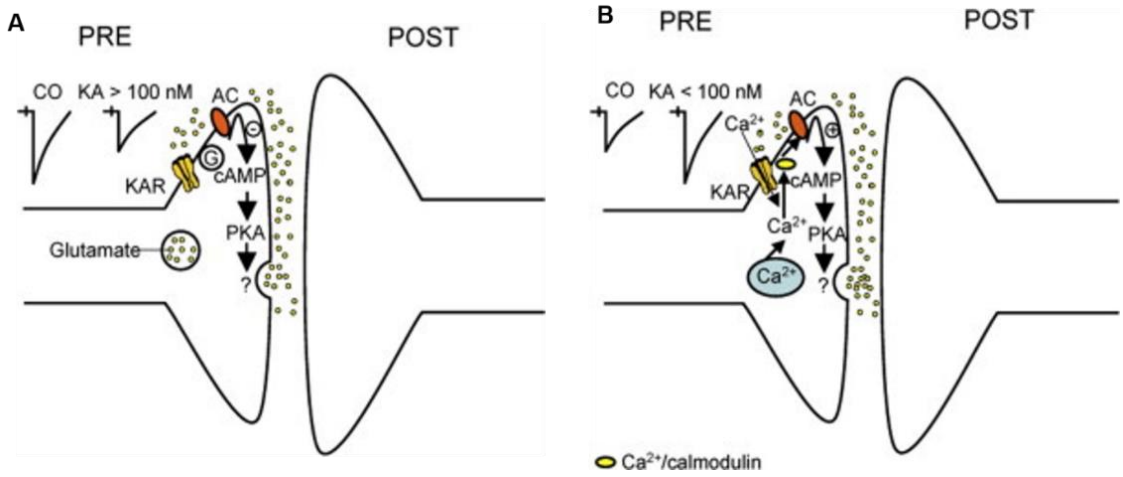

Figure 1-8: Pre-synaptic KARs regulate bi-directionally modulate glutamate release.

Pre-synaptic KARs can both depress (A) and enhance glutamate release (B). KARs depress glutamate release via its metabotropic function activating G-protein and downstream signalling cascade of AC/cAMP and PKA. Pre-synaptic KARs can also enhance glutamate release by inducing Ca^{2+} release from internal stores, which results in Ca^{2+}-calmodulin complex formation thereby activating PKA. Figure taken from (Sihra and Rodriguez-Moreno 2013).

Interestingly when activated at lower kainate concentrations, pre-synaptic KARs can facilitate glutamate release in the MF-CA3 synapses (Schmitz, Mellor et al. 2001). Subsequent studies also showed the role of presynaptic KARs in the facilitation of glutamate release (Lauri, Bortolotto et al. 2001, Lauri, Bortolotto et al. 2003, Pinheiro, Perrais et al. 2007, Andrade-Talavera, Duque-Feria et al. 2013). This release action was shown to be dependent on the increase in cytosolic Ca^{2+} concentration, potentially through the Ca^{2+} permeable KARs (Lauri, Bortolotto et al. 2003, Pinheiro, Perrais et al. 2007, Andrade-Talavera, Duque-Feria et al. 2013). Interestingly, downstream signalling mechanism for this pathway also involves the adenylate

cyclase/cAMP/PKA signalling cascade, similar to the pathway of inhibiting glutamate release, but the facilitation is not dependent on the G-protein activation as it is not sensitive to the inhibitors of G-protein function (Negrete-Diaz, Sihra et al. 2006, Negrete-Diaz, Sihra et al. 2007) . It is instead thought that the intracellular Ca^{2+} increase by KAR activation directly leads to the activation of the adenylate cyclase (Andrade-Talavera, Duque-Feria et al. 2013) [**Figure 1-8** B].

1.2.2.6.2 Post synaptic KARs

Post synaptic KARs upon activation through synaptically released glutamate yields EPSCs which have small amplitudes and characteristic slow kinetics i.e. slow activation and deactivation (Castillo, Malenka et al. 1997), potentially providing unfulfilled integrative capacities for information transfer (Frerking and Ohliger-Frerking 2002, Pinheiro, Lanore et al. 2013). KAR EPSCs have been found in few central synapses for instance the MF-CA3 pyramidal neurones. This is unlike that of the AMPARs and NMDARs, which are localised in majority of postsynaptic glutamatergic synapses in the brain (Castillo, Malenka et al. 1997, Vignes and Collingridge 1997). Along with this long-lasting depolarisation, KARs also regulate the slow afterhyperpolarization current (I_{SAHP}) (Melyan, Wheal et al. 2002, Melyan, Lancaster et al. 2004). AHP is the state post action potential generation which can last up to several seconds and has several phases; fast, medium and slow, each being generated due to activation of different potassium channels. The slow AHP has relatively slower kinetics in that it has slow rising phase and lasts up to several seconds and is easily detected after a train of action potentials (Storm 1990, Sah 1996). The noncanonical metabotropic signalling of KARs were shown to be responsible for regulating the $I_{SAHP.}$ This metabotropic downstream signalling pathway activates $G_{i/o}$ protein leading to PKC activation (Melyan, Wheal et al. 2002) and potentially PKA and MAP kinases activation (Grabauskas, Lancaster et al. 2007). Together, these characteristics of post synaptic KARs regulate the neuronal excitability.

Moreover, postsynaptic KARs can undergo plasticity themselves undergoing LTD that can be induced by various stimulation protocols whilst also undergoing activity-dependent up- or down-regulation on the surface upon

agonist activation (Martin, Bouschet et al. 2008, Carta, Opazo et al. 2013, Chamberlain, Sadowski et al. 2013). Recently, studies in our lab have shown that activation of postsynaptic KARs at CA3-CA1 synapses induces a novel form of AMPAR-LTP via its noncanonical metabotropic signalling pathway (Petrovic, Viana da Silva et al. 2017).

KAR role in excitatory synaptic transmission is further explored in Chapter 3.1.

1.2.2.7 KARs in inhibitory neurotransmission

While KARs are known to mediate excitatory neurotransmission [Chapter 3.1, (Evans, Gurung et al. 2017)], they can also regulate inhibitory transmission. Pre-synaptic KARs regulate pre-synaptic GABA release from interneurones (Rodriguez-Moreno and Lerma 1998). This pertussis toxin (PTx) sensitive pathway was mediated by downstream signalling through G-protein coupled receptors activating kinases Phospholipase C (PLC) and PKC, which reduces the inhibitory postsynaptic currents (IPSCs) (Rodriguez-Moreno and Lerma 1998).

Moreover, KARs mediate activation of potentiated extrasynaptic $GABA_A$ receptors via intracellular PKC pathway while depressing the synaptic $GABA_A$ receptors. It is thought that the potentiation of extrasynaptic $GABA_A$ receptors may depress feedforward and feedback inhibition thereby facilitating LTP induction. On the other hand, depression of synaptic $GABA_A$ receptors have a protective effect by preventing neuronal over-excitation (Jiang, Kang et al. 2015).

Furthermore, KARs also control the surface expression of chloride transporter KCC2 (potassium(K^+)-chloride(Cl^-) co-transporter) (Pressey, Mahadevan et al. 2017). KCC2 is required to maintain low intracellular Cl^- concentration. This is important to attain the required electrochemical gradient that allows $GABA_A$Rs signalling to maintain postsynaptic inhibition (Woodin, Ganguly et al. 2003). KCC2 and KAR were shown to exist in a macromolecular complex, and KAR itself was shown to be required for KCC2 oligomerisation and surface expression (Mahadevan, Pressey et al. 2014). In particular, the phosphorylation in the GluK2 C terminal residues S846 and S868 was shown

to regulate GluK2 mediated increase in KCC2 surface expression through enhanced recycling of KCC2 to the surface (Pressey, Mahadevan et al. 2017).

Hence, it is becoming increasingly evident that KARs can regulate both excitatory and inhibitory neurotransmission and is a likely key regulator of excitation-inhibition balance.

1.2.2.8 KAR signalling through non-canonical metabotropic pathway

As well as signalling through the canonical ionotropic receptors, KARs can also signal via an additional non-canonical metabotropic signalling pathway, which I have alluded to in previous sections. This non-canonical signalling is G-protein receptor mediated [**Figure 1-9**] and is pertussis toxin-sensitive. This metabotropic signalling pathway is known to be involved in KAR modulation of GABA release within the inhibitory synapses in the CA1 hippocampal region, which is prevented by the inhibition of PKC or PLC activation (Rodriguez-Moreno and Lerma 1998). This signalling also regulates KAR mediated inhibition of the slow after-hyperpolarizing potential (I_{SAHP}) resulting in continuing enhancement of neuronal excitability (Melyan, Wheal et al. 2002).

While the metabotropic signalling is essential for various KAR functions, the mechanism behind this is not fully known and is a subject of some controversy. KAR subunits such as GluK2, GluK1 and GluK5 have all been implicated in this function (Fisahn, Heinemann et al. 2005, Ruiz, Sachidhanandam et al. 2005, Gonzalez-Gonzalez and Henley 2013, Rutkowska-Wlodarczyk, Aller et al. 2015). The kainate evoked upregulation of KAR surface expression was shown to require metabotropic signalling via a GluK2-dependent mechanism (Gonzalez-Gonzalez and Henley 2013). Similarly, the metabotropic regulation of I_{SAHP} was absent in GluK2-/- mice but retained in GluK1-/- mice (Fisahn, Heinemann et al. 2005, Ruiz, Sachidhanandam et al. 2005). However, other studies suggested interactions between GluK5 and $G_{\alpha q}$ to be involved in KAR metabotropic regulation of its I_{SAHP} (Ruiz, Sachidhanandam et al. 2005) while another proteomic study suggested interactions between GluK1 subunit and G_o proteins to mediate the metabotropic signalling (Rutkowska-Wlodarczyk, Aller et al. 2015). Recently, KAR signalling that regulates AMPAR surface expression was attributed to its metabotropic signalling mediated by the GluK2

subunit (Petrovic, Viana da Silva et al. 2017). It is also not known if a KAR subunit can signal via both metabotropic and ionotropic pathways. Despite these unknowns, it is well accepted that KAR metabotropic signalling regulates various neurological functions of KARs.

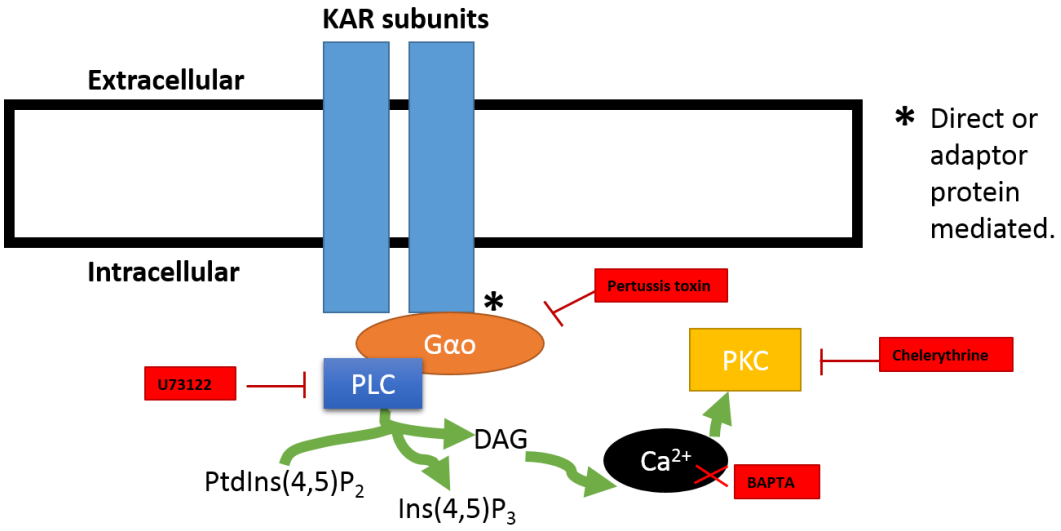

Figure 1-9: Metabotropic Signalling by KARs.

GluK1, GluK2 and GluK5 have all been shown as potential metabotropic signalling subunit of KAR. While it is not known if the interaction with the G-protein is direct or adaptor protein mediated, the downstream signalling pathway involves PLC mediated Ca^{2+} signalling which activates the PKC pathway. This metabotropic signalling is pertussis toxin sensitive, and inhibiting PLC and PKC activation inhibits the G-protein downstream signalling.

1.2.2.9 KARs during development

KARs have been shown to play key roles in development by controlling filopodial motility, growth cone dynamics and synapse formation/stabilisation (Bahn, Volk et al. 1994, Cherubini, Caiati et al. 2011). KARs can enhance axonal motility in immature rat hippocampal slices but inhibit motility in mature slices (Tashiro, Dunaevsky et al. 2003). KARs are also expressed early during development in thalamocortical synapses, which are slowly replaced by AMPARs via NMDAR mediated Ca^{2+} entry (Kidd and Isaac 1999). Having KARs early on in development is thought to help integrate synaptic inputs over longer period in young synapses as KARs have longer lifetime per individual current flow (Frerking and Ohliger-Frerking 2002).

KARs are also known to drive the network activity during development. For instance, during development in early neonatal hippocampus KARs regulate

both GABAergic and glutamatergic synaptic transmission and thus control the neuronal network by regulating the balance between these two forms of transmission (Lauri, Segerstrale et al. 2005). Moreover, in neonatal CA3 synapses, presynaptic KARs can be activated by endogenous glutamate which regulates the frequency of mEPSCs and spontaneous network activity (Lauri, Segerstrale et al. 2005). KARs in CA1 synapses were also shown to be activated by ambient glutamate which also developmentally regulates glutamatergic transmission by regulating the probability of release (Lauri, Vesikansa et al. 2006). Moreover, mice lacking the GluK2 subunit were shown to have transient reduction in their synaptic strength during development as they had delayed functional and structural maturation at MF-CA3 synapses compared to the WT mice (Lanore, Labrousse et al. 2012). Therefore, there are increasing evidences supporting KAR role during development in regulating synaptic function and network activity.

1.2.2.10 KARs in diseases

KARs have been linked to many neurodegenerative disorders including epilepsy, schizophrenia and autism, where KAR mutations have been associated with increased susceptibility to these conditions (reviewed in (Lerma and Marques 2013)). Application of kainate induces acute seizures like those found in the temporal lobe epilepsy (TLE) patients (Ben-Ari and Cossart 2000). Intriguingly, study in *in vitro* and *in vivo* models of TLE showed that mice lacking GluK2 or by treating with GluK2/GluK5 receptor antagonist, mice exhibit reduced seizure-like activity (Peret, Christie et al. 2014). Moreover, using hypoxia model in neonatal mice, it was shown that the KARs lacking GluK2 subunit or blockade of KAR ionotropic function decreased their seizure susceptibility, implying the role of GluK2-KARs in mediating hypoxic seizures particularly during the reoxygenation period (Grosenbaugh, Ross et al. 2018).

Additionally, both gain or loss of GluK2 function have led to Autism spectrum like disorder (ASD) phenotypes (Lanore, Labrousse et al. 2012, Micheau, Vimeney et al. 2014, Guzman, Ramsey et al. 2017). Studies on GluK2 KO mice showed abnormalities in CA3 functional maturation, where both structural and functional maturation of MF-CA3 synapses were delayed in the GluK2 KO mice (Lanore, Labrousse et al. 2012). This was followed by

behavioural analysis on the GluK2 KO mice where the mice displayed phenotypes similar to the ASD phenotypes in the social and cognition tasks. For instance, social interaction behavioural task performed on the GluK2 KO mice showed these mice to be less sociable and have reduced locomotor activity (Micheau, Vimeney et al. 2014). However, a patient study associated the gain of function mutation in the *GRIK2* (A657T) gene to be associated with neurodevelopmental abnormalities in the patient displaying characteristics of intellectual disability and speech and motor delay. KARs with this single point mutation were also shown to be constitutively active in their channel function (Guzman, Ramsey et al. 2017).

Recently, it was shown that complete knockout of all kainate receptor subunits in mice results in compulsive and obsessive behaviours such as over-grooming while also displaying motor problems (Xu, Marshall et al. 2017). These observations support the importance of KARs in higher brain function as their disruption can lead to various neurological disorders.

1.3 Synaptic plasticity

Synaptic plasticity is the biological process in which functional and structural changes in synapses cause changes in synaptic transmission. Hebbian Plasticity and Homeostatic plasticity represent the two most studied forms of synaptic plasticity.

1.3.1 Hebbian plasticity

Hebbian form of plasticity refers to activity dependent long-lasting changes in the synaptic efficacy resulting in either enhancement of synaptic transmission (Long-term Potentiation (LTP)) or depression of synaptic transmission (Long-term depression (LTD)) (Morris 1999). These synaptic changes are associative, rapidly induced and input specific. Together, LTP and LTD form the cellular models of cognition, learning and memory, as these processes allow the information to be built and retained in the neurones by strengthening connections in between cells (Citri and Malenka 2008) and are implicated in many physiological and pathological processes (Malenka and Bear 2004).

1.3.1.1 Long Term Potentiation (LTP)

LTP, which is the enhancement of synaptic transmission, was first described using high frequency stimulation (HFS) in the dentate area of hippocampus which was stable over months (Bliss and Lomo 1973). A classical LTP induction involves the activation of NMDARs. Typically, HFS leads to sodium influx through AMPARs, depolarising the postsynaptic compartment and activating NMDARs. NMDAR activation involves magnesium dissociation, allowing Ca^{2+} influx through the Ca^{2+} permeable NMDAR ion channel leading to a rise in the intracellular Ca^{2+} levels (Collingridge, Kehl et al. 1983, Mayer, Westbrook et al. 1984, Kauer, Malenka et al. 1988, Bliss and Collingridge 1993, Malenka and Nicoll 1993). NMDAR activation can also be induced chemically by bath application of NMDAR co-agonist glycine (chem-LTP) (Lu, Man et al. 2001). One of the main characteristic change that occurs during LTP is the increase in the number of AMPARs inserted in the post-synaptic membrane which strengthens the synapse [**Figure 1-10**]. AMPARs can be inserted either via lateral diffusion (Makino and Malinow 2009, Penn, Zhang et al. 2017) and/or by increased AMPAR exocytosis (Lu, Man et al. 2001, Pickard, Noel et al. 2001). The Ca^{2+} influx also leads to kinase mediated activation of proteins involved in AMPAR trafficking and insertion. For instance, Ca^{2+} calmodulin–dependent kinase II (CaMKII) is transiently activated following LTP induction, which leads to phosphorylation of C termini of AMPAR subunits which in turn alters the single channel conductance and trafficking of AMPARs (Hayashi, Shi et al. 2000, Soderling and Derkach 2000, Lee, Escobedo-Lozoya et al. 2009). CaMKII can also phosphorylate scaffolding proteins in the post synaptic density to accommodate for additional AMPARs i.e. creating slots (Tomita, Stein et al. 2005, Lisman, Yasuda et al. 2012). Moreover, CaMKII also regulates the actin cytoskeleton to physically enlarge spines supporting increased synaptic efficiency (Patterson and Yasuda 2011, Bosch, Castro et al. 2014). These alterations combined with additional protein synthesis allows the LTP to be maintained over a longer period of time (Reymann and Frey 2007).

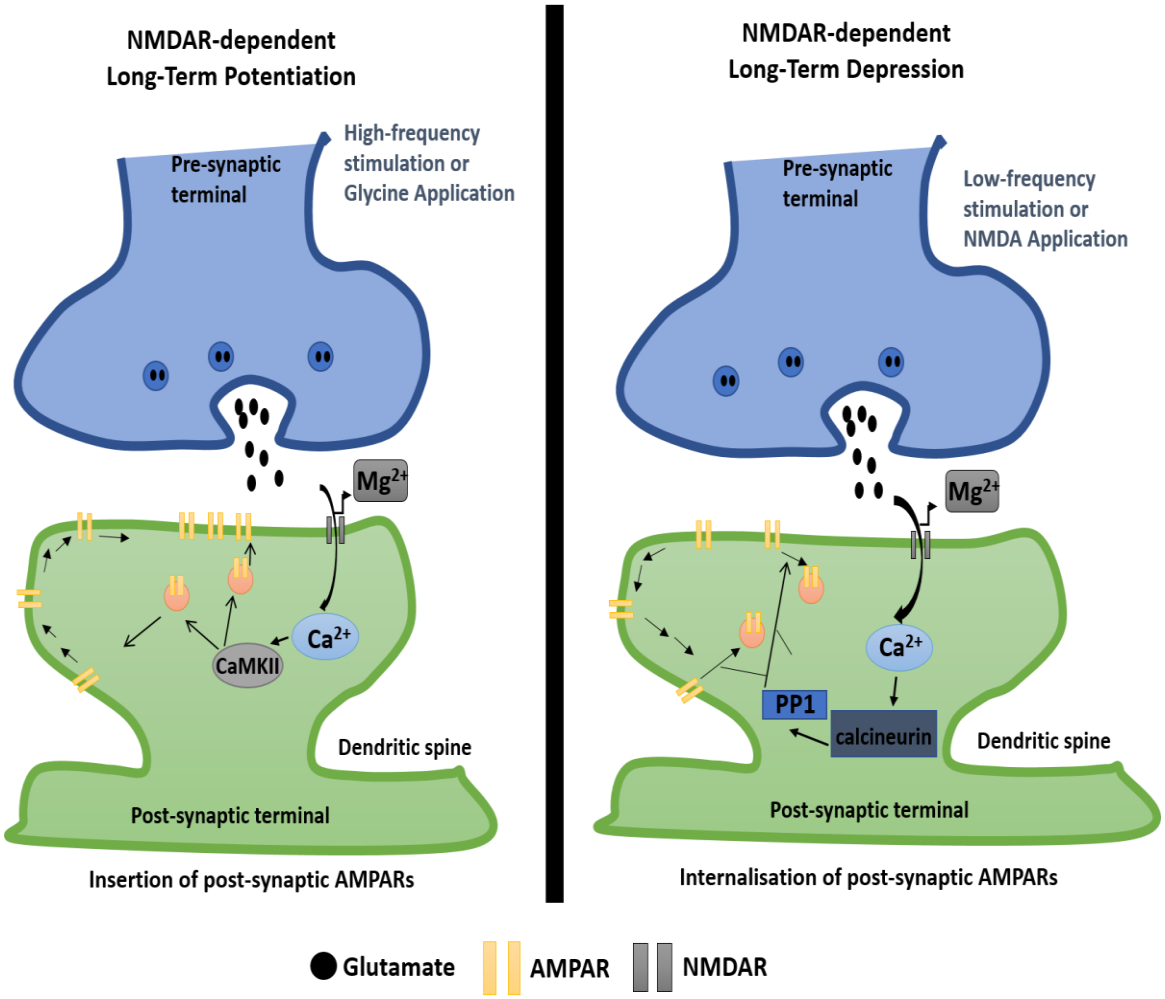

Figure 1-10: NMDAR mediated Long-Term Potentiation (LTP) and Long-Term Depression (LTD).

Both LTP and LTD inducing protocols release the magnesium block from the NMDARs, resulting in Ca^2 ion flow. In LTP, the Ca^2 ion flow activates CaMKII kinase resulting in insertion of more AMPARs on the post-synaptic surface. In contrast the LTD protocol results in lower Ca^{2+} influx, activating protein phosphatase cascade instead, causing internalisation of AMPARs from the post-synaptic surface.

NMDAR independent forms of LTP have also been reported. For instance, mGluR dependent LTP was first described in the hippocampal region where a group I/II mGluR antagonist blocked both NMDAR dependent and independent forms of LTP (Bashir, Bortolotto et al. 1993). mGluRs belong to the G-protein coupled receptor superfamily, which are activated by neurotransmitters such as glutamate resulting in intracellular signalling cascade through interactions with G-proteins (Niswender and Conn 2010). It has however been a matter of controversy since, as to whether these receptors can directly induce LTP (Fitzjohn, Bortolotto et al. 1998, Doherty, Palmer et al. 2000, Mellor and Nicoll 2001, Bortolotto, Collett et al. 2005), and

so is not as well accepted. It has nevertheless been suggested that mGluRs can act as a molecular switch whereupon their activation is important to induce LTP in a pathway that has not previously experienced LTP induction (Bortolotto, Collett et al. 2005).

KARs have also been shown to induce LTP whereupon they can undergo plasticity themselves and have recently been shown to regulate AMPAR expression independently of NMDARs [discussed in Chapter 3.1.2].

1.3.1.2 Long Term Depression (LTD)

LTD on the other hand, is weakening of synapses and like LTP, is classically generated by NMDAR activation (Dudek and Bear 1992). This can be induced either by low frequency stimulation (LFS) or bath application of NMDA (chem-LTD) (Lee, Kameyama et al. 1998). LFS triggers prolonged NMDAR activation, but below the threshold levels that induces LTP. While both LTP and LTD are generated by postsynaptic Ca^{2+} influx, the strength and the length of the Ca^{2+} accumulation impacts on the plasticity direction (Lee, Kameyama et al. 1998). The spatio-temporal nature of the Ca^{2+} rise during LTD induction activates protein phosphatase cascade (Mulkey, Herron et al. 1993, Mulkey, Endo et al. 1994). It is thought that the signalling pathways with higher Ca^{2+} affinity are activated (Mulkey, Endo et al. 1994). Upon NMDAR activation, downstream Ca^{2+} sensing molecules such as calcineurin and their phosphoprotein substrate; inhibitor-1 and PP1 are activated. This triggers AMPARs removal by targeted dephosphorylation events causing reduction in the synaptic strength. GluA1 is one of the downstream substrates that are dephosphorylated at serine 845 (S845) site causing their endocytosis and decrease in channel conductance of AMPARs (Lee, Takamiya et al. 2010). Moreover, it was shown that AKAP interaction with calcineurin is also important for NMDAR mediated LTD (Jurado, Biou et al. 2010). Other interactions such as clathrin adaptor AP2 with GluA2 (Lee, Liu et al. 2002) and phosphorylation mediated interaction of GluA2 with PICK1 (Kim, Chung et al. 2001, Steinberg, Takamiya et al. 2006, Rocca, Martin et al. 2008) also induces internalisation of these GluA2-AMPARs during NMDAR mediated LTD **[Figure 1-10]**.

Like LTP, NMDAR-independent forms of LTD can also occur and mGluR-LTD is a well-studied form of LTD (Palmer, Irving et al. 1997, Fitzjohn, Kingston et al. 1999). Activation of these receptors using DHPG (potent agonist of group I mGluRs) induces removal of AMPARs like that of NMDAR-dependent LTD (Snyder, Philpot et al. 2001). While both forms of LTD can coexist, they follow mechanistically distinct routes to induce LTD (Oliet, Malenka et al. 1997, Bhattacharyya, Biou et al. 2009). mGluR pathway also involves post synaptic Ca^{2+} release, though in this case through mGluR-dependent G protein signalling through Gq (Luscher and Huber 2010) leading to activation of downstream signalling cascades such as NCS-1 and PICK1 (Jo, Heon et al. 2008). While both pathways involve internalisation of AMPARs, AMPAR internalisation in the presence of both NMDA and DHPG is additive (Casimiro, Sossa et al. 2011), in that they target distinct populations of AMPARs.

KARs can also undergo LTD themselves independent of NMDARs and AMPARs, which will be also explored in chapter 3.1.3.

1.3.1.3 LTP and LTD associated with learning and memory

Both LTP and LTD are key cellular processes that underlie learning and memory. It was initially shown that inhibiting NMDAR using antagonist APV into hippocampus impaired learning (Morris, Anderson et al. 1986). Moreover, preventing CaMKII activation (T286A CaMKII knock-in mice which prevents autophosphorylation), showed normal NMDAR function but LTP was absent which in turn impaired learning and memory in these mice (Giese, Fedorov et al. 1998). Alternative approaches where LTP was studied during learning using processes such as fear-conditioning in amygdala (a type of associative learning) (Rogan, Staubli et al. 1997) and one-trial inhibitory avoidance learning in CA1 hippocampus (Whitlock, Heynen et al. 2006) also showed LTP induction.

LTD, while initially proposed to underlie forgetting (Tsumoto 1993), have also been implicated in promoting memory formation. Blocking *in vivo* exocytosis in the perihinal cortex was shown to prevent visual memory formation (Griffiths, Scott et al. 2008, Cazakoff and Howland 2011). Another interesting study using fear conditioning in amygdala showed that associative learning

can be inactivated and reactivated by LTD and LTP respectively (Nabavi, Fox et al. 2014). Hence, these studies show interplay between these different forms of plasticity and highlights their importance in synaptic learning and memory processes.

1.3.2 Homeostatic plasticity

Because they are both potentially positive-feedback systems the synaptic changes induced by LTP and LTD can lead to destabilization of the neuronal circuits. Therefore, compensatory mechanisms exist to account for these changes in the network activity and maintain global stability. This phenomenon is referred to as homeostatic plasticity or scaling which acts as a negative feedback mechanism to allow neurones to globally scale up or down their synaptic strength relative to the input. This stabilises neuronal firing within a usable range necessary for information processing and storage (Turrigiano, Leslie et al. 1998, Turrigiano 2008, Pozo and Goda 2010). This also prevents runaway excitation thereby maintaining synaptic stability, critical to network formation, development and stability and defects in this process has been implicated in neurological diseases such as epilepsy and schizophrenia (Wondolowski and Dickman 2013).

1.3.2.1 Glutamate receptors in synaptic scaling

Homeostatic synaptic response was first demonstrated in visual cortical cultures which were treated with various channel blockers chronically over period of 48 hours. Treatment with tetrodotoxin (TTX), which blocks voltage gated sodium channels, thus dampening the network activity (Narahashi 2008), increased the mEPSC amplitude, resulting from an increase in synaptic AMPARs. On the other hand, treatment with bicuculline, $GABA_A$ blocker (Straughan, Neal et al. 1971) which enhances the network activity, decreased this AMPAR mEPSC amplitude (Turrigiano, Leslie et al. 1998). Hence, the synaptic AMPARs were altered to counteract the external changes in activity [**Figure 1-11**]. This activity-dependent bidirectional changes to adjust the strength of neuronal excitatory synapses to stabilise firing is also termed as ‘synaptic scaling’ (Turrigiano 2008). Importantly, these scaling processes

retain the changes in the original strength of the connections to maintain the input-specific LTP and LTD information (Chater and Goda 2014).

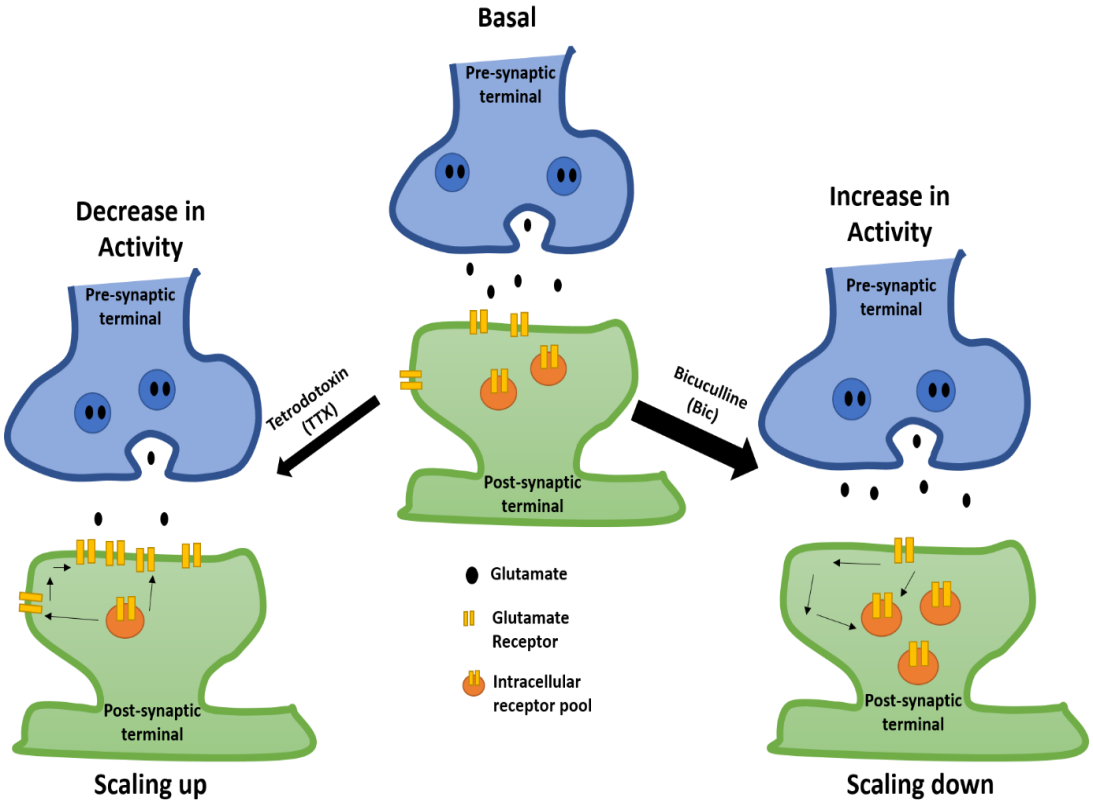

Figure 1-11: Role of glutamate receptors in homeostatic scaling.

Chronic decrease or increase in network activity can be induced following treatments with TTX or bicuculline respectively. Based on decrease or increase in network activity, the surface expression of glutamate receptors (mainly AMPARs) increase or decrease respectively to compensate for the changes in the synaptic activity, bringing the activity level back to basal.

Regarding glutamate receptors role in homeostatic scaling, predominant studies have focused mainly on the changes in AMPAR expression and composition. Majority of the post synaptic changes that occur during homeostatic plasticity are due to changes in the composition and abundance of AMPARs (Pozo and Goda 2010, Chater and Goda 2014, Henley and Wilkinson 2016). Both GluA1 and GluA2 subunit-containing AMPARs are known to scale up or down (Watt, van Rossum et al. 2000). However, there are some controversies on which AMPAR subunit plays the more important role. Both GluA1 and GluA2 have been shown to be upregulated in response to chronic activity changes (O'Brien, Kamboj et al. 1998, Wierenga, Ibata et al. 2005) while some studies have suggested GluA2 to have a more prominent

role during homeostatic up-scaling (Cingolani, Thalhammer et al. 2008). For instance, overexpressing GluA2 C-terminal domain peptide blocked homeostatic scaling in cultures, most likely by acting as a dominant negative and GluA2 KD was also shown to occlude synaptic scaling (Gainey, Hurvitz-Wolff et al. 2009). Particularly, GluA2 C-terminal interaction with GRIP1 was shown to be important for this as WT GluA2 could rescue the loss of synaptic scaling but not a mutant form of GluA2 (Y876E) that cannot bind GRIP1 (Gainey, Tatavarty et al. 2015) . Another study also showed the importance of GluA2 C-terminal on synaptic scaling, however emphasised more on the importance of GluA2 proximal C-terminal domain (residues A841 and A843). Nevertheless, the study showed that GluA2 subunit is both necessary and enough for synaptic scaling (Ancona Esselmann, Diaz-Alonso et al. 2017). However, other reports show postsynaptic enhancement of GluA1 recruitment, but not necessarily of GluA2, during synaptic scaling (Ju, Morishita et al. 2004, Thiagarajan, Lindskog et al. 2005, Sutton, Ito et al. 2006). Nonetheless, despite these discrepancies that remain to be resolved, it is well accepted that changes in AMPAR accumulation administers synaptic scaling.

NMDARs at the post synapses also upscale or downscale in response to opposing changes in the network activity (Rao and Craig 1997, Watt, van Rossum et al. 2000, Mu, Otsuka et al. 2003). In cortical neurones, it was shown that they can both upscale and downscale in proportional manner to that of AMPARs thereby maintaining the ratio of NMDA to AMPA receptors at individual synapses (Watt, van Rossum et al. 2000). Furthermore, increased forward trafficking through the early secretory pathway of newly synthesised NMDARs was shown to increase their surface expression during chronic inactivity (Mu, Otsuka et al. 2003)

Scaling responses can also be induced by locally perturbing synapses as opposed to globally altering network activity. Local enhancement of homeostatic plasticity can be achieved by simultaneously blocking postsynaptic firing with TTX and blocking NMDARs. This was shown to selectively increase GluA1, by relieving the brake on local (dendritic) protein synthesis to promote insertion of GluA1 (Sutton, Wall et al. 2004, Sutton, Ito et al. 2006). This local dendritic protein synthesis was mediated by regulating

phosphorylation state of eukaryotic elongation factor-2 (eEF2). The dephosphorylated eEF2, which is the active form, was activated upon chronic silencing promoting dendritic protein synthesis (Sutton, Taylor et al. 2007). This also suggests distinct mechanisms for LTP and homeostatic up-scaling as LTP is caused by NMDAR activation while scaling can be induced by NMDAR blockade (Ju, Morishita et al. 2004, Thiagarajan, Lindskog et al. 2005, Sutton, Ito et al. 2006).

In contrast to AMPARs and NMDARs, prior to our work there are very few reports in the literature for the homeostatic scaling of KARs, which is summarised in Chapter 3.1.4.

1.3.2.2 Homeostatic plasticity mechanisms

The cellular and molecular properties of homeostatic plasticity have been studied intensively (Turrigiano, Leslie et al. 1998, Shepherd and Huganir 2007). The compensatory changes in the surface expression of postsynaptic glutamate receptors in particular AMPARs are governed by multiple cellular processes such as endo/exocytosis, lateral diffusion of receptors in between synaptic and extrasynaptic sites and changes in protein-protein interactions that deliver and/or stabilise synaptic AMPARs (Bredt and Nicoll 2003, Collingridge, Isaac et al. 2004, Harms, Tovar et al. 2005, Ehlers, Heine et al. 2007, Shepherd and Huganir 2007).

1.3.2.2.1 Protein interactions

On an individual level, many cellular processes and their signalling molecules have been identified that play a role in homeostatic plasticity [**Figure 1-12**]. For instance, the transcriptional regulator Arc/Arg3.1 can basally upregulate or downregulate synaptic strength when removed or overexpressed from the system respectively (Shepherd, Rumbaugh et al. 2006, Craig, Jaafari et al. 2012). Furthermore, secretory molecules such as BDNF and TNF-α (Leslie, Nelson et al. 2001, Leonoudakis, Zhao et al. 2008); cell adhesion molecules such as N-cadherin/β-catenin complex and integrins and AMPAR interactors such as PICK1, GRIP1, PSD93 and PSD95 regulate synaptic AMPARs during scaling, also summarised in **Table 1-1** (Okuda, Yu et al. 2007, Cingolani, Thalhammer et al. 2008, Frank, Pielage et al. 2009, Anggono, Clem et al.

2011, Sun and Turrigiano 2011, Tan, Queenan et al. 2015). Interestingly, like LTP and LTD, Ca^{2+} dependent signalling pathways such as CaMKIV also play a role in scaling up and down of synaptic AMPARs (Thiagarajan, Lindskog et al. 2005, Ibata, Sun et al. 2008). Moreover, post-translational modifications such as phosphorylation and SUMOylation of effector proteins can each regulate synaptic AMPARs during homeostatic scaling (Noritake, Fukata et al. 2009, Craig, Jaafari et al. 2012). For instance, PKA levels are increased during chronic inactivity resulting in increased GluA1 S845 phosphorylation resulting in increased AMPAR up-scaling (Diering, Gustina et al. 2014). Suppression of network activity increases SUMOylation of Arc resulting in their increased stability which in turn increases AMPAR surface expression (Craig, Jaafari et al. 2012).

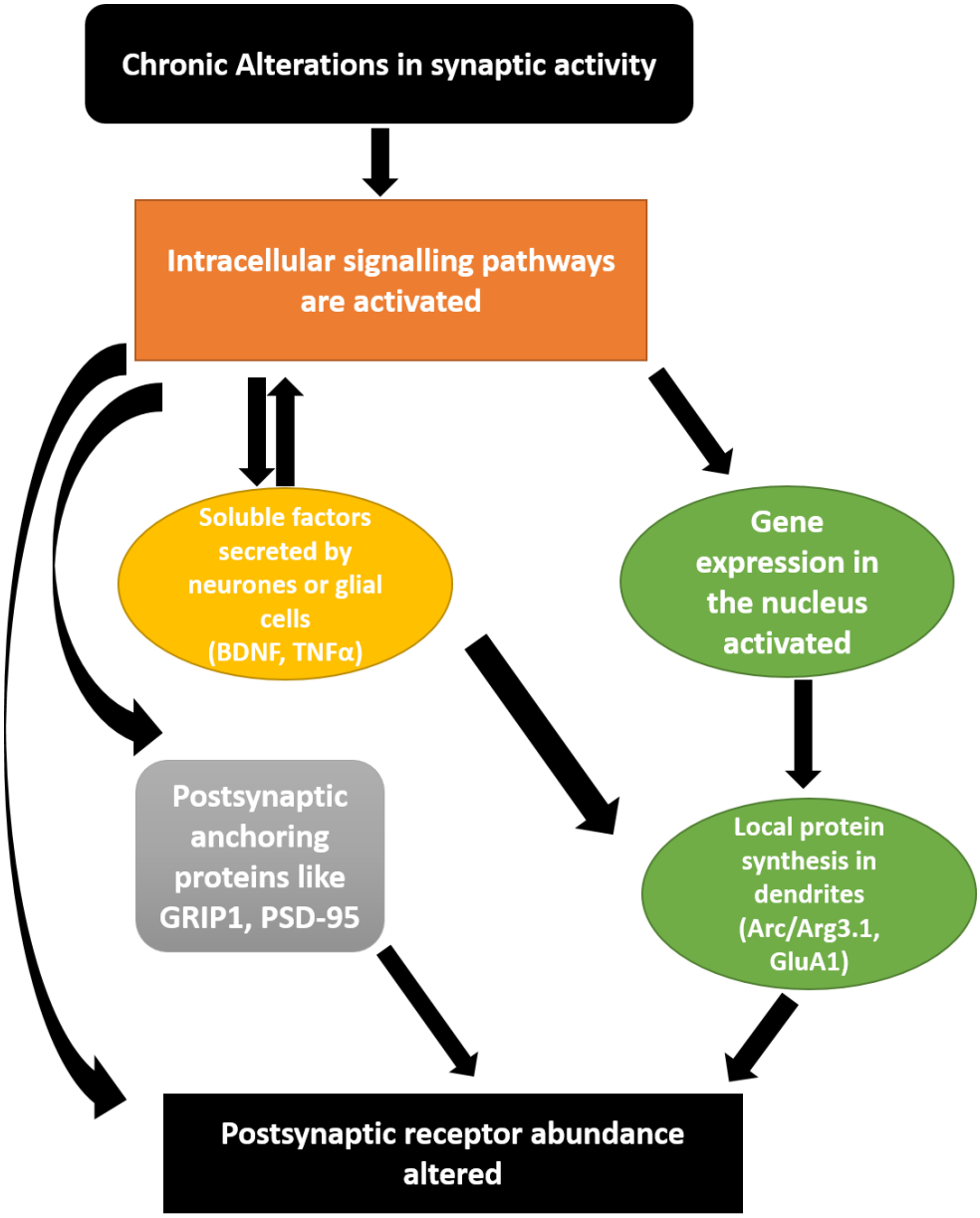

Figure 1-12: Various molecular players implicated in homeostatic scaling.

Upon chronic alterations in the synaptic activity, certain intracellular signalling pathways are activated which can either activate gene expression enhancing local protein synthesis or secrete soluble factors that enhances or reduces receptor abundance on the surface. Equally, these intracellular signalling pathways can also act by altering post-synaptic anchoring proteins to either enhance or reduce glutamate receptor abundance on the surface. Figure adapted from (Pozo and Goda 2010).

Table 1-1: Regulators of AMPAR mediated Homeostatic Plasticity. Table adapted from (Fernandes and Carvalho 2016).

Protein	Function	Role in Homeostatic Plasticity	Biological Models used	References
Transcriptional Regulator				
Arc/Arg3.1	Immediate early gene; regulates AMPAR endocytosis.	During chronic inactivity Arc levels↑; activity enhancement Arc levels↓; Blocks scaling up; Arc KO blocks scaling up and down.	Mouse/rat hippocampal+ cortical neurones. Mouse visual cortex slices.	(Shepherd, Rumbaugh et al. 2006)
Secreted Molecules				
BDNF	Regulates AMPAR trafficking.	During chronic inactivity BDNF levels↓; reduced BDNF scales up synapses and prevents down-scaling.	Rat visual cortical neurons.	(Leslie, Nelson et al. 2001, Reimers, Loweth et al. 2014)

TNF-α	Pro-inflammatory cytokine.	During chronic inactivity TNFα↑; secreted by glial cells; TNFα KO abolishes scaling up and increase in TNFα results in upscaling.	Mouse/rat hippocampal cortical neurones+ hippocampal acute slices.	(Stellwagen and Malenka 2006, Steinmetz and Turrigiano 2010)
Cell Adhesion				
N-cadherin/β-catenin	Regulates AMPAR surface expression and synapse formation.	Scaling impaired in conditional KO, binding mutant and Dominant negative N-cadherin mutant.	Rat hippocampal neurones.	(Okuda, Yu et al. 2007)
Integrin	Regulates AMPAR surface expression and synapse formation.	During chronic inactivity β3 integrin surface levels ↑; activity enhancement their levels ↓.	Mouse/rat hippocampal neurones and organoptypic slices.	(Cingolani, Thalhammer et al. 2008)

		KO blocks synaptic upscaling.		
AMPAR interactors				
PICK1	Regulates AMPAR endocytosis by interacting with GluA2.	During chronic inactivity PICK1 levels ↓; PICK1 KD or KO occludes scaling up.	Mouse cortical neurones.	(Anggono, Clem et al. 2011)
GRIP1	AMPAR synaptic anchoring by interacting with GluA2.	During chronic inactivity GRIP1 levels↓; activity enhancement levels↑. Loss of function blocks upscaling.	Mouse cortical and rat visual cortical neurones.	(Sun and Turrigiano 2011)
PSD95/93	Post synaptic scaffolding proteins.	During chronic inactivity synaptic expression of PSD95↑; activity enhancement PSD95↓;	Postnatal rat visual cortical neurones.	(Sun and Turrigiano 2011)

		No changes in PSD93. Double KD of PSD95 and 93 prevents upscaling. PSD95 is required for downscaling.		
Ca^{2+} signalling				
CaMKIV	Regulate transcription.	Chronic inactivity CaMKIV activation↓. Upscaling induced by reduced CaMKIV activation.	Rat cortical neurones.	(Ibata, Sun et al. 2008)
CaMKII	Regulated by Ca^{2+}.	In chronic inactivity CaMKIIα levels↓ and CaMKII β levels↑. KD of CaMKIIβ prevents upscaling.	Hippocampal neurones.	(Thiagarajan, Lindskog et al. 2005)

1.3.2.2.2 Proteome changes

Studies have also looked at global level compensatory changes during scaling. Translation of over 300 proteins were differentially regulated during up-scaling and down-scaling including proteins involved in regulation of

cellular processes such as axon guidance and neurite outgrowth, excitatory synapses and glutamate receptor complexes. Interestingly, rather than individual proteins, opposing pathways were targeted to adjust the proteome (Schanzenbächer, Sambandan et al. 2016). Furthermore, comparing early (2 hour) to late set responses (24 hour) during scaling, there was no overlap in newly synthesised proteins, rather there were overlaps in functional groups that were regulated in early and later phases (Schanzenbacher, Langer et al. 2018). This suggests instead of altering specific proteins, set of proteins with functional overlap are regulated variably during 'early' and 'late' phase of synaptic scaling. These functional groups included voltage gated Ca^{2+} channels, synaptosomes, cell adhesion, actin cytoskeleton, polarity and protein kinases and phosphatases (Schanzenbacher, Langer et al. 2018).

1.3.2.2.3 Protein turnover

In addition, a quantitative study in the post synaptic density (PSD) fraction showed that ubiquitination targeted degradation plays a key role in regulating PSD molecular reorganisation during chronic activity changes. For instance, in response to increased activity, certain postsynaptic proteins and scaffolding proteins get ubiquitinated and degraded rapidly, which would in turn alter the global molecular character and signalling properties of the post synaptic membrane (Ehlers 2003).

Understanding how the interplay between all these cellular processes are regulated globally during scaling, will help give clearer understanding of mechanisms that regulate synaptic scaling.

1.3.2.2.4 Post-transcriptional modifications

Post transcriptional processes also play a role in scaling. Interestingly for NMDARs, their forward trafficking at the endoplasmic reticulum regulates their synaptic accumulation during chronic activity blockade. ER export of NR1 subunit of NMDARs were shown to be accelerated by their alternatively spliced C2' domain and slowed by the C2 splice cassette. C2' variant was shown to be predominant during activity blockade which enhances their recruitment to ER exit sites by binding of a divaline motif within C2' to COPII coats, thus

allowing their increased surface expression. On the other hand, increased chronic activity, increased C2 variant abundance (Mu, Otsuka et al. 2003).

1.3.2.3 Physiological relevance and diseases associated with homeostatic plasticity

While majority of the work has been performed in dissociated cultures, several reports have investigated the physiological relevance of this form of synaptic plasticity. Homeostatic scaling has been studied in visual cortex in *in vivo* model where network activity was blocked by intraocular injection of TTX or exposing and depriving animals of light (altering sensory inputs) to induce experience dependent scaling of glutamate receptors. Depriving animals of light increased the glutamatergic quantal size which correlated with increased AMPAR abundance, and re-introducing light reversed these changes (Desai, Cudmore et al. 2002, Goel, Jiang et al. 2006). A recent study showed that homeostatic down-scaling functions during sleep to remodel synapses in rodents for memory consolidation. During sleep, synapses were shown to undergo weakening by removal of AMPARs (Diering, Nirujogi et al. 2017). This further demonstrates the importance of homeostatic scaling in intact brain.

Unsurprisingly, inability of the system to balance the network activity can have many pathological consequences. For instance, it has been proposed that the neural excitability disorder epilepsy is thought to be a pathological consequence of synaptic imbalance (Treiman 2001). The balance of excitation and inhibition needs to be maintained to avoid epileptogenic states (Swann and Rho 2014). Interestingly, global scale changes in translation during homeostatic scaling uncovered changes in over 166 proteins that are implicated in various neural diseases such as epilepsy (960 genes), Alzheimer's disease (66 genes), Parkinson's disease (39 genes) and schizophrenia (71 genes) (Schanzenbächer, Sambandan et al. 2016). In addition, molecular links to diseases such as Autism spectrum disorders, Fragile X syndrome, schizophrenia and Alzheimer's disease are also becoming increasingly evident (Soden and Chen 2010, Blackman, Djukic et al. 2012, Wondolowski and Dickman 2013, Jang and Chung 2016). Hence, homeostatic scaling does play a key role in both physiological and pathophysiological function in the brain and defining the molecular

mechanisms behind homeostatic scaling will help better understand the underlying physiology and pathology.

1.4 Adenosine to Inosine RNA editing by ADARs

Glutamate receptors undergo the process of Adenosine to Inosine (A to I) RNA editing which adds further diversity to their subunits. Both AMPAR and KAR subunits have been shown to undergo various RNA editing processes, all of which are named based on the resultant amino acid alterations; Q/R editing (Glutamine to Arginine), R/G (Arginine to Glycine), I/V (Isoleucine to Valine) and Y/C (Tyrosine to Cysteine). This editing is mediated by the family of enzymes called Adenosine Deaminases acting on RNA (ADARs) (Nishikura 2016).

1.4.1 Adenosine Deaminases Acting on RNA (ADAR)

Adenosine Deaminases acting on RNA (ADARs) are enzymes that convert adenosine bases to inosine in double stranded RNA by hydrolytic deamination at the C6 position (Bass and Weintraub 1988, Wagner, Smith et al. 1989) [**Figure 1-13**]. The resultant inosine is read as guanosine by the cellular translational machinery, base-pairing it with cytosine and allowing incorporation of amino acids that are not genomically encoded.

These ADAR family members are conserved in the animal kingdom and are essential for normal development in mammals (Jin, Zhang et al. 2009, Nishikura 2016). There is one ADAR found in *D. melanogaster* (dADAR) and two found in *C. elegans* (CeADAR1-2). In vertebrates, there are three families of ADARs known: ADAR1, ADAR2 and ADAR3 (Kim, Wang et al. 1994, Melcher, Maas et al. 1996, Chen, Cho et al. 2000, Bass 2002, Barraud and Allain 2012).

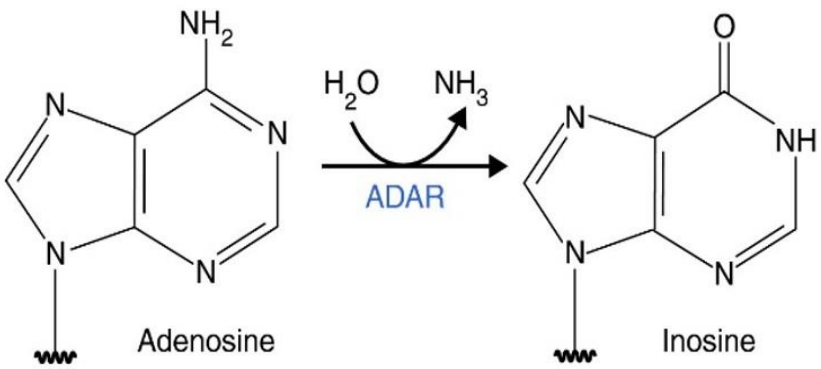

Figure 1-13: Catalytic conversion of Adenosine to Inosine.

Adenosine is hydrolytically deaminated to an inosine, which is read as guanosine by the cellular translational machinery. Figure taken from (Slotkin and Nishikura 2013).

Studies using KO mice have demonstrated the importance of ADAR1 and ADAR2 for survival. Lack of ADAR1 is embryonically lethal, showing overproduction of interferons and hematopoietic failures (Hartner, Schmittwolf et al. 2004, Hartner, Walkley et al. 2009). ADAR2 KO mice are viable however are increasingly seizure prone and die post birth (Higuchi, Maas et al. 2000).

Along with editing protein coding sequences, ADARs also have other substrates such as precursors of certain primary microRNAs (pre-mRNA), regulating the expression and function of non-coding miRNAs (Nishikura 2016).

1.4.2 ADAR structure

All three ADARs share common functional domains [**Figure 1-14**]. The double stranded RNA binding domain (dsRBD) is roughly 65 aa long and consists of α-β-β-α configuration which allows ADARs to interact with its double stranded RNA substrate (Stefl, Xu et al. 2006). ADAR1 consists of three dsRBDs while ADAR2 and ADAR3 consists of two dsRBDs each. The deaminase domain, which lies in the carboxy-terminal region, allows the enzymatic catalysis to occur.

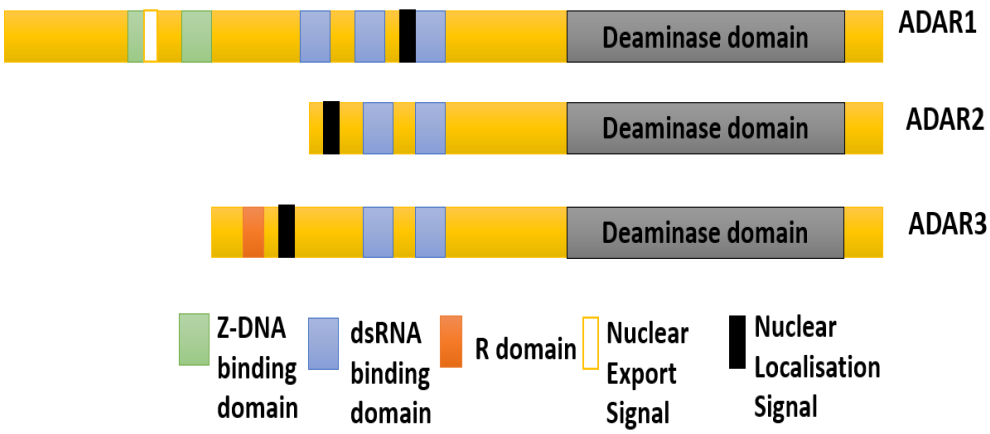

Figure 1-14: Structure of ADARs.

All ADARs consist of a deaminase domain, various numbers of dsRNA binding domains and nuclear localisation signal. ADAR1 consists of additional nuclear export signal and Z-DNA-binding domains while ADAR3 consists of arginine-rich single-stranded RNA binding domain (R-domain). Figure adapted from (Slotkin and Nishikura 2013).

In addition, all ADARs have putative nuclear localisation sequence (NLSs). ADAR1 also consists of two additional Z-DNA-binding domains (Zα and Zβ) (Herbert, Alfken et al. 1997), while ADAR3 has an Arginine(R)-rich domain in its amino-terminal region (R-domain) (Chen, Cho et al. 2000). While the functional significance of these two regions are not fully understood, it is thought that the R-domain in ADAR3 allows ADAR3 to bind single-stranded RNA (ssRNA) (Chen, Cho et al. 2000) and also aid nuclear localisation of ADAR3 (Maas and Gommans 2009). On the other hand, amongst the Z-DNA binding domains in ADAR1, the Zα domain has been shown to successfully bind Z-DNA structures. As Z-DNA structures are usually formed upstream of an active RNA polymerase, additional binding of ADAR1 to Z-DNA is thought to assist efficient mRNA binding by ADAR1 before splicing (Barraud and Allain 2012). Zβ domain however cannot bind Z-DNA but has been suggested to have a role in ADAR1 dimerisation instead (Athanasiadis, Placido et al. 2005). Interestingly for Zα domain it is also thought to allow ADAR1 to bind Z-RNA structures (Placido, Brown et al. 2007).

Studies in flies and mammalian ADARs shows ADARs to act as a dimer (Cho, Yang et al. 2003, Gallo, Keegan et al. 2003). Mammalian ADAR1 and ADAR2 form homodimers, needed for its editing activity *in vitro* (Cho, Yang et al.

2003). Homodimerisation is mediated by the dsRBDs in both ADAR1 (it's third dsRBD) (Ota, Sakurai et al. 2013) and ADAR2 (it's first dsRBD) (Poulsen, Jorgensen et al. 2006, Ota, Sakurai et al. 2013). However, binding to the dsRNA substrate itself is not required for their dimerisation (Valente and Nishikura 2007). Interestingly, FRET analysis showed that ADAR1 and ADAR2 could also form heterodimers, suggesting heterodimerisation of ADAR1 and ADAR2 could play a regulatory role in their editing activity (Chilibeck, Wu et al. 2006). ADAR3, unlike 1 and 2, cannot homodimerise (Cho, Yang et al. 2003, Cenci, Barzotti et al. 2008).

1.4.3 ADAR isoforms

ADAR2 can undergo multiple splicing events that generate several isoforms (ADAR2a-f) (Lai, Chen et al. 1997, Rueter, Dawson et al. 1999, Filippini, Bonini et al. 2018). This creates various lengths of ADAR2 affecting their ability to interact with and edit its substrates. The first splicing event is self-editing producing 2e and 2f isoforms that have no catalytic domain or RNA binding domains (Rueter, Dawson et al. 1999). Isoform 2c and 2d have shorter C terminus disrupting the deaminase domain and as such display no editing activity (this is only known to occur in human). The final splicing event leads to an inclusion of 30 nucleotides in rat and mouse (120nt in human) producing isoforms ADAR2a and 2b (Gerber, O'Connell et al. 1997). ADAR2a and 2b are the only known functional and active isoforms of ADAR2 and they differ with each other by 10aa. ADAR2b includes the additional 10aa cassette. Study in rat cortical cultures showed ADAR2a to be the more active isoform, showing higher editing activity compared to the b isoform. The extra 10aa loop is thought to interfere with the RNA binding. However, both display the same level of substrate specificity and dimerisation properties (Filippini, Bonini et al. 2018). Moreover, they were shown to be equally expressed in rat cortical cultures, but their relative expression levels have not been studied *in vivo* (Filippini, Bonini et al. 2018). Additional splicing variants for ADAR2 have also been detected, one of which has extended open reading frames, referred to as ADAR2R. This extension also consists of sequence motif similar to the R-domain of ADAR3 and shows the highest expression in the cerebellum, but

their functional significance has not been explored yet (Maas and Gommans 2009).

ADAR1 has two main isoforms generated due to alternative splicing at exon 1 producing an interferon induced 150kDa protein and a constitutively expressed 110kDa protein, where the N-terminal portion of the protein including the first Z-DNA binding domain is absent (Patterson and Samuel 1995).

1.4.4 ADAR tissue expression and cellular localisation

ADAR1 and ADAR2 is ubiquitously expressed but ADAR2 is highly expressed in the brain and has many targeted substrates there (Kim, Wang et al. 1994, Melcher, Maas et al. 1996). ADAR3 on the other hand is expressed exclusively in the brain (Melcher, Maas et al. 1996).

ADARs are usually nuclear localised where they interact with their pre-mRNA substrates. For ADAR3, importin alpha KPNA2 (importin subunit alpha 2) interacts with its R-domain, acting as a classical NLS, allowing controlled nuclear import. On the other hand, ADAR2 which is entirely nuclear retained, consists of NLS that interacts with KPNA1 (importin subunit alpha-5) and KPNA3, but not KPNA2 (Maas and Gommans 2009). A later study also showed specific interaction of ADAR2 with importin subunit-alpha 4 (KPNA3) to regulate ADAR2 import during cortical development (Behm, Wahlstedt et al. 2017). However, ADAR2R isoform which consists of ADAR3-like NLS due to the presence of R-domain, allows ADAR2 to interact with importin alpha KPNA2 (Maas and Gommans 2009). This further shows the role of ADAR3 R-domain in allowing specific interactions with importins.

On the other hand, ADAR1 lacked any binding to all the importins. However, nonconventional import pathways for ADAR1 into the nucleus has been suggested where nonclassical NLS within the third dsRBD of ADAR1 is recognised by nuclear import factor transportin-1 (Fritz, Strehblow et al. 2009). Interestingly, ADAR1 also consists of nuclear export signal (NES) within its Zα binding domain that allows it to shuttle between the nucleus and cytoplasm (Poulsen, Nilsson et al. 2001). Moreover, the first dsRBD of ADAR1 has also been implicated in its cytoplasmic localisation (Strehblow, Hallegger et al.

2002). As the NES signal is missing within the p110 isoform of ADAR1 (constitutively expressed form and lacking the Zα binding domain), it is mostly localised in the nucleus but can still export out to the cytosol to an extent through interaction with transportin-1 and exportin-5 through its first dsRBD (Fritz, Strehblow et al. 2009).

Finally, both ADAR1 and ADAR2 can shuttle in and out of the nucleoplasm and nucleoli, along with ADAR1 (Desterro, Keegan et al. 2003, Sansam, Wells et al. 2003).

1.4.5 ADAR substrate preference and specificity

ADARs bind to dsRNA and efficiently deaminate specific adenosines in the duplex RNA without modifying other adenosines within the sequence (Li, Levanon et al. 2009). It is generally thought that the ADARs can bind to any dsRNA regardless of the sequence, but it is the deaminase domain that confers the specificity of target adenosine after binding (Wong, Sato et al. 2001). The variable number of copies of dsRNA binding domains in different ADARs is also thought to contribute to the substrate binding affinity and selectivity from other non-ADAR RNA Binding domains (Liu, Lei et al. 2000, Stephens, Haudenschild et al. 2004).

Following these speculations many studies have investigated the preferences and specificities of ADAR1 and ADAR2 activity as certain sites are edited exclusively by either ADAR1 or ADAR2. However, there are many other sites that can be edited equally by both ADAR1 and ADAR2 [see **Table 1-2**] (Nishikura 2016). Moreover, ADAR1 and ADAR2 can act on the same protein but at different sites [**Table 1-2**]. While ADAR1 edits majority of the substrates in the mammals, it has been shown to predominantly edit repetitive sites while ADAR2 accounts for more non-repetitive coding sites editing (Tan, Li et al. 2017). There is a preference to edit adenosine in neighbouring 5’ uridine for both ADAR1 and ADAR2 but preferential 3’ guanosine editing for ADAR2 (Lehmann and Bass 2000).

Further specificity to editing target substrates by ADARs are mostly mediated through secondary structures formed by the substrate mRNA. These secondary structures could include terminal and internal loops, bulges and/or

mismatches (Barraud and Allain 2012). For instance, Q/ R editing of glutamate receptors are more specific to ADAR2 editing [see section 1.5.1] while the Zα binding domain in ADAR1 is thought to target ADAR1 to sites that are likely to form Z-RNA structures (Placido, Brown et al. 2007). Due to the importance of RNA structures, the dsRBDs are thought to play a more important role in the target specificity.

Recently, structural studies also revealed RNA-binding loops within the catalytic domain of ADAR1 and ADAR2. This loop was conserved in the family of ADAR2 but varied among other family of ADARs (Matthews, Thomas et al. 2016). This difference in RNA binding loop was later shown to contribute to the ADARs specificity as chimeric human ADAR1, where it's RNA binding loop was replaced with the loop from human ADAR2, showed ADAR2-like selectivity in editing of target substrates (Wang, Park et al. 2018). Thus, both the catalytic domains and the RBDs are important in ADAR's editing specificity.

1.4.6 Potential co-factor involvement in the deamination

Structural study of human ADAR2 bound to dsRNA revealed important catalytic domains (His394, Glu396, Cys451 and C516) that coordinate the zinc ion in the active site and form the catalytic centre (Macbeth, Schubert et al. 2005). The adenosine to be deaminated is thought to be targeted to the catalytic pocket by a base-flipping mechanism (Matthews, Thomas et al. 2016). Base-flipping is a well-studied mechanism where a single nucleotide within the double helix is rotated outside to allow access to the enzymes to the site of reaction (Roberts and Cheng 1998). This study also showed that inositol hexakisphosphate (IP6) acts as a potential co factor in the enzyme core to aid the protein fold, important for its enzyme activity (Macbeth, Schubert et al. 2005). As of now, no such studies have been performed using ADAR1.

1.4.7 ADAR3 lacks catalytic activity

While both ADAR1 and ADAR2 act on many substrates (Kim, Wang et al. 1994, Melcher, Maas et al. 1996, Barbon and Barlati 2011), ADAR3 has not been shown to have any functional role as it's deaminase domain is inactive as such it cannot edit the substrates (Melcher, Maas et al. 1996, Chen, Cho et

al. 2000, Schneider, Wettengel et al. 2014). ADAR3 is thought to play a more regulatory role by altering availability of various ADAR substrates as it can still bind the substrates through its RNA binding domain (Oakes, Anderson et al. 2017). While both ADAR1 and ADAR2 have conserved arginine residue within their RNA-binding loop, this is absent within ADAR3, which may add to its catalytic inactivity (Matthews, Thomas et al. 2016, Wang, Park et al. 2018). Moreover, ADAR3 lack of ability to form dimers may also be contributing to their lack of activity (Cho, Yang et al. 2003, Cenci, Barzotti et al. 2008).

Recently, behavioural study has shown that mice expressing ADAR3 which lacks the dsRBDs have increased anxiety levels and are deficient in short-term and long-term memory formation (Mladenova, Barry et al. 2018). This is likely due to its inability to sequester substrates from ADAR1 and ADAR2 and thus provides a novel role of ADAR3 in cognitive processes.

1.5 Q/R editing of glutamate receptor by ADARs

Q/R editing is the process in which a genomic codon encoding for a glutamine (Q) (CAG) is altered post-transcriptionally to code for an arginine (R) (CGG). The arginine codon is introduced by converting the adenosine base to inosine (A to I) which is read as guanosine by the cellular machinery. The AMPAR subunit GluA2 (at 607amino acid) and KAR subunits GluK1 (at 636 amino acid) and GluK2 (at 621 amino acid) undergo this process of Q/R editing. **Table1-2** shows the list of Q/R editing sites present in both AMPAR and KAR subunits along with other known editing sites in these subunits.

Table 1-2: List of known glutamate receptor RNA editing sites and the ADARs implicated.

Gene	Protein	Editing	Implicated ADARs
GRIK1	GluK1 (KAR)	Q to R	ADAR2 ADAR1
GRIK2	GluK2 (KAR)	Q to R	ADAR2
GRIK2	GluK2 (KAR)	I to V	ADAR1 ADAR2
GRIK2	GluK2 (KAR)	Y to C	ADAR2
GRIA2	GluA2 (AMPAR)	Q to R	ADAR2
GRIA2	GluA2 (AMPAR)	R to G	ADAR1 ADAR2
GRIA3	GluA3 (AMPAR)	R to G	ADAR1 ADAR2
GRIA4	GluA4 (AMPAR)	R to G	ADAR1 ADAR2

1.5.1 ADAR2 in Q/R editing of KARs and AMPARs

Among the two functional ADARs, ADAR2 is the key mediator of Q/R editing for both GluK2 and GluA2 (Melcher, Maas et al. 1996, Belcher and Howe 1997, Lai, Chen et al. 1997). *In vivo* studies in ADAR2 KO mice (which had intact ADAR1 levels) exhibited huge deficiencies in GluA2 editing (reduced from 98% to 10%) and in GluK2 editing (reduced from ~86% to 29%). There was comparatively lower decrease in the GluK1 editing (reduced from 64% to 40%) (Higuchi, Maas et al. 2000). ADAR1 can also mediate the Q/R editing of these substrates (but to a much lower extent compared to ADAR2) as there are also *in vitro* studies showing a role for ADAR1 in Q/R editing of both GluK2 and GluA2 (Dabiri, Lai et al. 1996, Herb, Higuchi et al. 1996). This perhaps explains the remaining low levels of editing of GluA2 and GluK2 observed in ADAR2 KO mice. Nevertheless, all the available evidence points to ADAR2 being the predominant mediator of Q/R editing.

Q/R editing by ADAR2 for both AMPAR and KAR subunits require intramolecular dsRNA structure mediated by the interaction between exonic

sequences surrounding the editing site and the editing site complementary sequence (ECS) downstream in the adjacent intron [**Figure 1-15**]. These exonic and the intronic regions where the base pairing occurs do not necessarily need to occur nearby. In the case of GluK1 and GluK2 Q/R editing site, the ECS is as far as 1900 nucleotides (nt) down the Q/R site (Herb, Higuchi et al. 1996). In contrast for GluA2, nearby ECS sites in the intronic region, ~310 nucleotides distal of the 5' splice sites, is recruited for base pairing (Higuchi, Single et al. 1993). These findings are consistent with the RNA editing being a nuclear event that occurs in the pre-mRNA prior to the splicing. This also provides examples of the secondary structure of ds(pre-)mRNA allowing for substrate editing specificity, which was eluded to earlier in the section 1.4.4.

As the ECS site is required for ADAR2 activity in Q/R editing, this intronic region has been manipulated to produce GluK2 editing deficient mice. However, these mice showed residual 5% edited GluK2 despite the deletion of the ECS site, perhaps suggesting a minor mechanism of ECS-independent editing of GluK2 as ADAR1 also requires this ECS site to deaminate (Vissel, Royle et al. 2001). The intronic ECS region required for the GluA2 editing has also targeted to produce GluA2 editing deficient mice, whereby this region was replaced by loxP. As expected, these mice completely lacked in Q/R editing, further showing the ECS element to be crucial for the GluA2 Q/R editing (Brusa, Zimmermann et al. 1995, Feldmeyer, Kask et al. 1999).

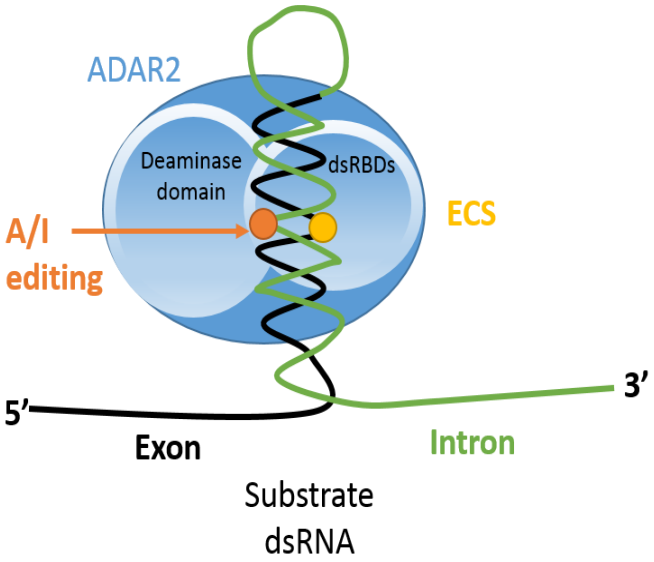

Figure 1-15: Interaction between dsRNA and ADAR2.

The adjacent intronic region of AMPAR and KAR consist of editing complementary site (ECS) which forms dsRNA with the exon consisting of the Q/R editing site. This can be as close as 350nt and as far as 1900nt. Upon binding of the ADAR2 enzyme, it's deaminase domain recognises and edits the adenosine to inosine within the glutamine coding sequence in the Q/R site.

1.5.2 Effects of Q/R editing on glutamate receptor properties

Q/R editing occurs in the transmembrane II (TMII) region of both AMPAR and KAR subunits. As arginine is positively charged, its presence in the inner channel pore forming region results in reduction in the Ca^{2+}permeability along with low single channel conductance and a linear current voltage relationship of the resultant tetramer in AMPARs (Sommer, Kohler et al. 1991, Burnashev and Rozov 2000, Cull-Candy, Kelly et al. 2006) [**Figure 1-16**].

Similar to AMPARs, KARs with edited GluK1 and GluK2 have reduced Ca^{2+} permeability (Egebjerg and Heinemann 1993, Köhler, Burnashev et al. 1993), channel conductance (Swanson, Feldmeyer et al. 1996, Vissel, Royle et al. 2001) and linear current voltage relationship while the unedited KARs display inwardly rectifying response (Bowie and Mayer 1995, Kamboj, Swanson et al. 1995) [**Figure 1-16**].

Q/R editing also affects receptor oligomerisation, assembly and trafficking properties. This was shown to be the case for GluA2 and GluK2 subunits of AMPARs and KARs respectively (Greger, Khatri et al. 2002, Greger, Khatri et al. 2003, Ball, Atlason et al. 2010). The Q/R editing for both GluA2 and GluK2 reduces its assembly/oligomerisation, with the edited subunits accumulating mostly as a monomer/dimer and as a result are more likely to be ER retained (Greger, Khatri et al. 2002, Greger, Khatri et al. 2003, Ball, Atlason et al. 2010).

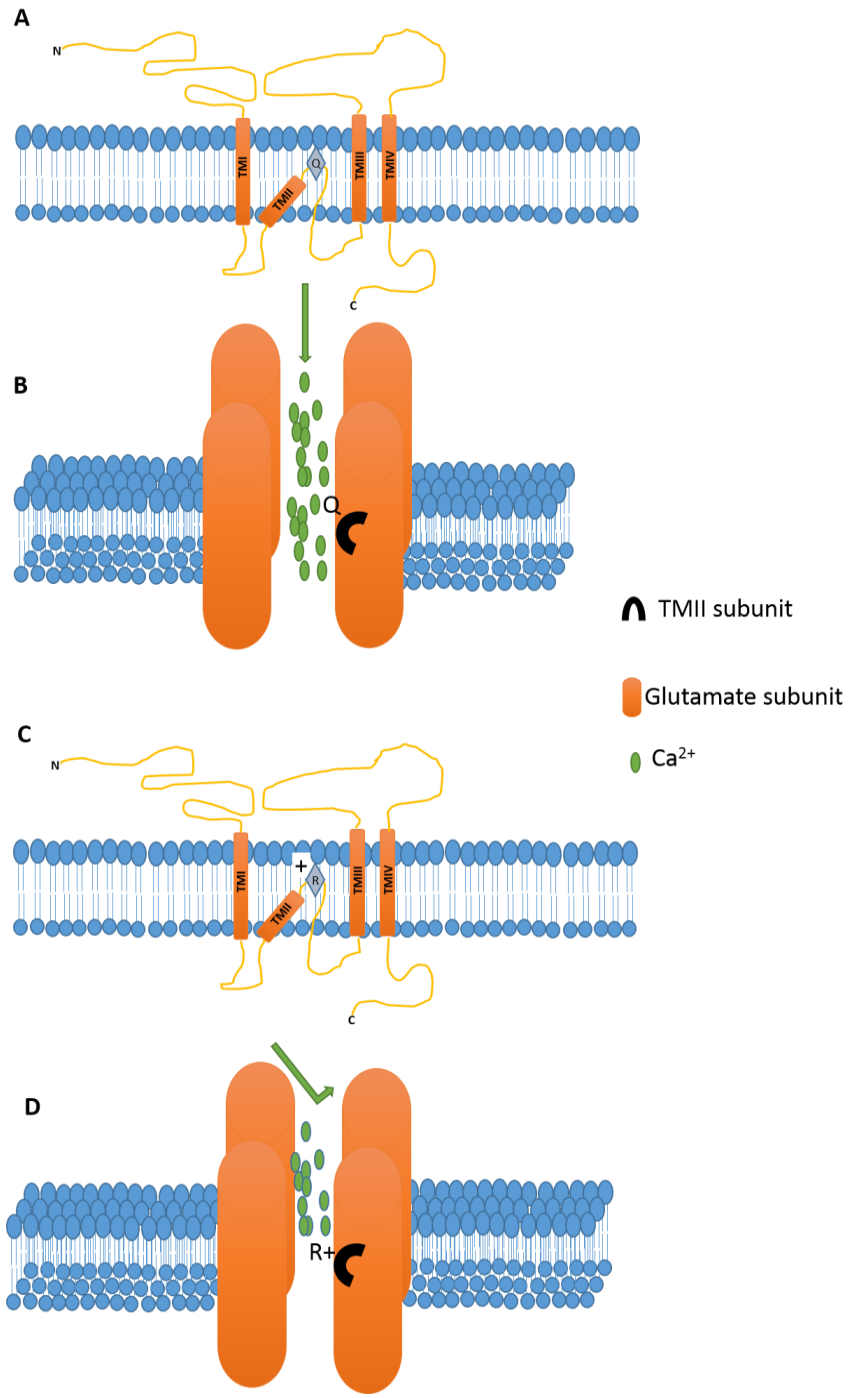

Figure 1-16: Glutamate receptor Q/R editing regulates their ionotropic function.

The Q/R editing occurs in the channel pore forming region (A). As arginine is positively charged (C), this alters their ionotropic properties by altering Ca^{2+} permeability (B and D), channel conductance and current voltage relationship. As arginine is positively charged, its incorporation next to the channel pore region (D) prevents Ca^{2+} flow altering ion permeability of the resultant tetramer.

1.5.3 Q/R editing of GluA2 is important for survival

ADAR2 KO mice show increased seizure activity and premature death. Adding back edited GluA2 in this system by replacing the alleles for GluA2 with alleles

encoding the edited version exonically rescued the lethal phenotype (Higuchi, Maas et al. 2000). Similar results were obtained in GluA2 editing deficient mice, which expressed AMPARs with increased Ca^{2+} permeability resulting in mice developing seizures followed by death within 3 weeks (Brusa, Zimmermann et al. 1995). Moreover, studies in mouse models which express unedited AMPARs at different levels, were shown to be capable of inducing inappropriate/excessive NMDAR-independent LTP in hippocampal pyramidal connections and suffered from neurological dysfunctions such as epilepsy and deficient dendritic architecture (Feldmeyer, Kask et al. 1999). All these studies show that ADAR2 mediated Q/R editing in mice is important for brain function and survival.

1.5.4 Developmental and plasticity role of Q/R editing in AMPARs

In contrast to KAR Q/R editing, GluA2 is fully edited (>99%) before birth, however the developmental stage at which this editing occurs is not fully known (Burnashev, Monyer et al. 1992, Higuchi, Single et al. 1993, Wahlstedt, Daniel et al. 2009). There have been some reports of the potential importance of unedited GluA2 during development, as ~60% unedited GluA2 Q/R transcripts are present in human neuronal progenitor cells (Whitney, Peng et al. 2008). However, contradicting this, a study in neuroepithelial precursor cells found fully edited GluA2 present throughout, implying the lack of significance of unedited GluA2 during development. Perhaps this discrepancy in cell lines could be due to their variable expression of ADAR2 (Pachernegg, Munster et al. 2015). Furthermore, a study from mice engineered to constitutively express arginine (R) (edited site) at GluA2 Q/R site, did not produce any obvious defects and displayed a normal phenotype (Kask, Zamanillo et al. 1998), hence suggesting the lack of importance of unedited GluA2. Moreover, a zebrafish model lacking Q/R editing at GluA2 site showed abnormal neural development (Li, Chen et al. 2014). Thus, the functional relevance of these unedited GluA2 is not well understood and it is a mystery as to why the critical arginine residue in the GluA2 Q/R site is generated via site-selective RNA editing and not by exon coding.

Because over 99% of GluA2 are edited in adults, GluA2 containing receptors in adults are mostly Ca^{2+} impermeable and incorporation of single edited GluA2 subunit in the receptor tetramer assembly causes the entire AMPAR complex channel to be Ca^{2+} impermeable (Hollmann, Hartley et al. 1991, Burnashev, Monyer et al. 1992). As such, many studies on synaptic plasticity have explored the importance of incorporation of GluA2-lacking Ca^{2+} permeable (CP) and GluA2-containing Ca^{2+} impermeable receptors. It is generally thought that the CP-AMPARs are required for the initial stage of activity induction but not necessarily for the maintenance of plasticity (Man 2011, Henley and Wilkinson 2016). The CP-AMPARs are replaced by Ca^{2+} impermeable GluA2 containing AMPARs post activity induction. For instance, LTP studies have shown that CP-AMPARs initially recruited during LTP stimulation are soon replaced by GluA2-containing AMPARs (Plant, Pelkey et al. 2006, Jaafari, Henley et al. 2012). This was also suggested in homeostatic plasticity where activity blockade showed a rapid increase in the surface expression of CP-AMPARs in the early stages followed by the increase in GluA2-containing AMPARs (Leonoudakis, Zhao et al. 2008). However, the role of Ca^{2+} permeable and impermeable AMPARs in homeostatic scaling is controversial, as other studies have also specified the importance of incorporation of GluA2 containing AMPARs for scaling induction itself (Gainey, Hurvitz-Wolff et al. 2009). Nevertheless, Q/R editing of GluA2 plays an important role in plasticity while its role in development is not known.

1.5.5 Developmental and plasticity role of Q/R editing in KARs

GluK1 and GluK2 are edited at low-levels during development in the Q/R site and increases up to 40% and 80% respectively, within the first few days after birth (Belcher and Howe 1997, Paschen, Schmitt et al. 1997, Bernard, Ferhat et al. 1999). There are also regional differences in the extent of GluK1 and GluK2 editing. Studies on rat hippocampus showed GluK2 to reach its maximal editing of ~80% by P10, which remains stable through to adulthood, while at E18 the editing is at only 20%. On the other hand, GluK1 in hippocampus at E18 and P0 stage is edited ~15% which increases up to 40% by P4 and is stabilised through to adulthood (Bernard, Ferhat et al. 1999).

Since, unedited GluK1 and GluK2 are present at significantly higher levels in early life, it is thought that they play an important role during development. A study focusing specifically on GluK2 editing deficient mice showed that these mice continue to display a juvenile form of NMDAR-independent LTP in adulthood (Vissel, Royle et al. 2001). One possibility suggested was that this is an important unedited KAR-dependant mechanism for LTP induction in early development that is lost in the wildtype mice. Moreover, KAR containing synapses during development in thalamocortical synapses are modified in an activity dependent manner, whereby the KAR contribution to transmission decreases during experience dependent plasticity (Kidd and Isaac 1999). The increased editing of GluK2 could be playing a role in this decreased transmission. Therefore, GluK2 editing seems to have more significant role during development, while its role in plasticity in adult brain is not as well characterised.

GluK1 Q/R editing deficient mice, on the other hand, did not show any developmental abnormalities, behavioural defects or any obvious effects to kainate induced seizures (Sailer, Swanson et al. 1999). Hence their role is not fully understood. However, a study into pre-synaptic KARs showed that the Ca^{2+} permeable unedited GluK1-KARs have a potential role in increasing functional presynaptic release sites as suggested by increased synaptophysin (pre-synaptic protein) puncta (Sakha, Vesikansa et al. 2016).

1.5.6 GluK2 Q/R editing and seizures

While GluK2 editing deficient mice are fully viable, their increased vulnerability to induced seizures suggests that increased GluK2 editing during development can act as a critical regulator in reducing seizure vulnerability in adults. This is in line with previously suggested ideas that editing dysregulation can be the pathological mediator of seizure generation (Bernard, Ferhat et al. 1999) and unedited GluK2 may be playing a major role in seizure generation in developing brain (Johnston 1996), further demonstrating the role of KARs in epilepsy (Mulle, Sailer et al. 1998, Bernard, Ferhat et al. 1999, Vincent and Mulle 2009). This shows that GluK2 Q/R editing play important role in plasticity and in pathological processes.

1.6 Other forms of Glutamate receptor RNA editing

The AMPAR subunits GluA2, GluA3 and GluA4 also undergo RNA editing at the R/G (Arginine to Glycine) site, in the extracellular domain close to the glutamate binding site, preceding the flip/flop splice site (GluA2 at 764aa, GluA3 at 769 aa and GluA4 at 765aa) [**Figure 1-17**, **Table 1-2**]. Editing at this site has been shown to be functionally important for AMPAR kinetic properties. The G-edited subunits were shown to have enhanced rate of recovery from desensitisation. As this editing site occurs close to the neurotransmitter binding site, the channel of unedited GluA2 receptor complex at this site exhibit rapid responses to the new glutamate stimulus (Lomeli, Mosbacher et al. 1994). This editing site is also shown to work in coordination with the flip/flop splice site (Laurencikiene, Kallman et al. 2006). During neuronal cell maturation, R/G editing increases (Orlandi, La Via et al. 2011). Moreover, editing at this site was also shown to be regulated during neuronal activity [(Sanjana, Levanon et al. 2012, Balik, Penn et al. 2013), Chapter 4].

The KAR GluK2 subunit also undergoes editing at two additional sites; I/V (at 567aa) (Isoleucine to Valine) and Y/C (Tyrosine to Cysteine) at (571aa) [**Figure 1-17**]. These editing occur at the transmembrane domain I (TMI) of GluK2. They regulate the ion permeability of the GluK2 containing KARs along with the Q/R site and are associated with finer modification of ionic properties (Köhler, Burnashev et al. 1993, Burnashev, Zhou et al. 1995). Editing at Y/C site increases during development reaching up to 90% in rat brain while the I/V site was found to be edited up to 60% in adult rat brain (Belcher and Howe 1997). However, the function and relevance of these editing sites is not well studied.

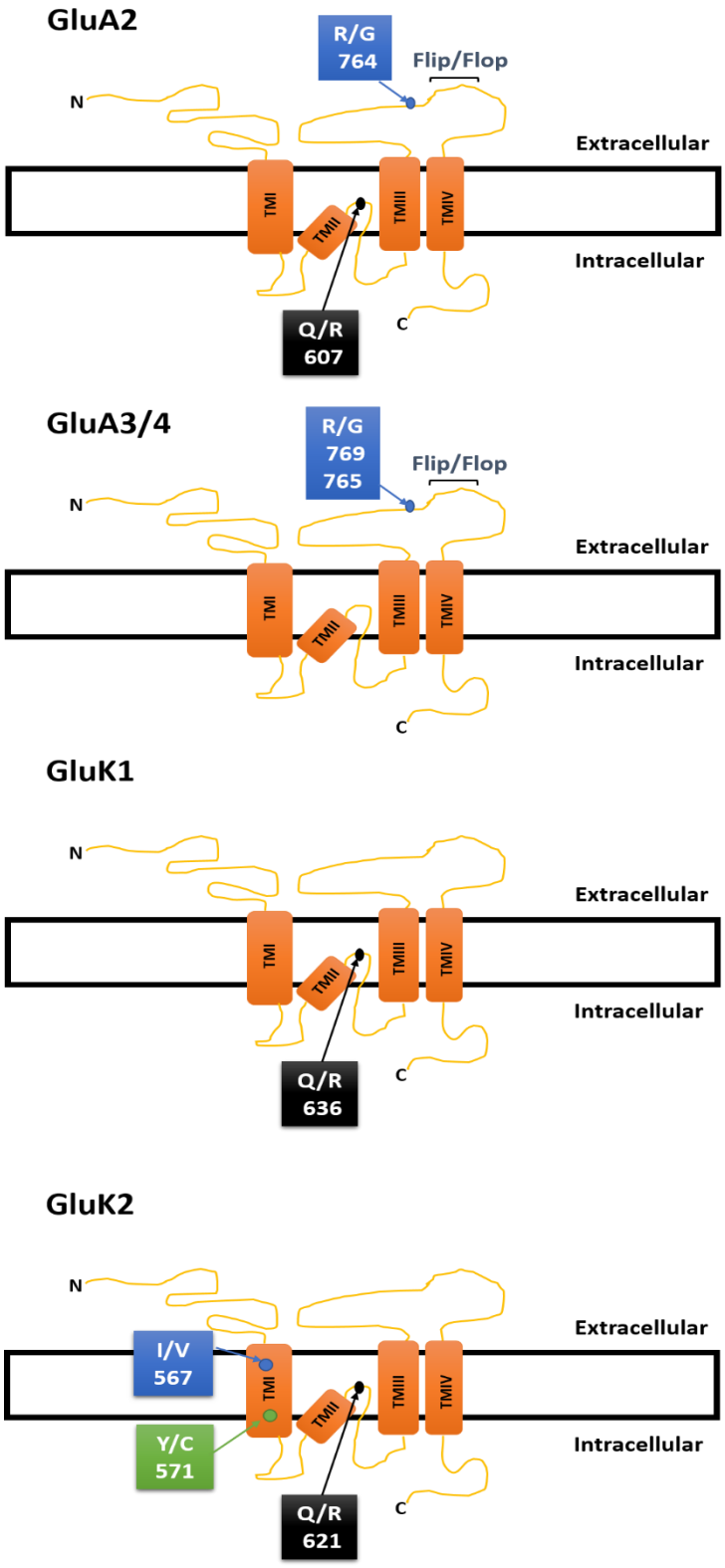

Figure 1-17: RNA editing sites in glutamate receptors.

Q/R editing for GluK1, GluK2 and GluA2 occurs at the TMII region as shown while GluA2/A3 and A4 undergo R/G editing in the loop connecting TMIII and TMIV. GluK2 can also undergo additional I/V and Y/C site editing in the TMI region.

1.7 Glutamate receptor RNA editing in diseases

Dysfunction of ADAR1 and ADAR2 have been implicated in range of cancers and viral infections (Gallo and Locatelli 2012, Fritzell, Xu et al. 2017). Moreover, as ADAR2 is highly enriched in the brain, the majority of the pathological consequences of alterations in ADAR2 editing is mediated by changes in the CNS substrates GluA2 and GluK2 (Filippini, Bonini et al. 2017). Some of these neurological diseases are also mediated by alterations in ADAR1 editing (Slotkin and Nishikura 2013). Many neural pathological conditions have been identified in which glutamate receptor RNA editing has been shown to be altered.

ADAR2 mediated editing of GluK2 and GluA2 has been implicated in a range neurological disease (Barbon and Barlati 2011, Slotkin and Nishikura 2013). As RNA editing is very important for learning, memory and behaviour, its dysregulation is altered in diseases such as epilepsy (Brusa, Zimmermann et al. 1995, Higuchi, Maas et al. 2000). GluA2 Q/R editing, mediated by ADAR2, for instance was shown to be altered in forebrain ischemia (Peng, Zhong et al. 2006), amyotrophic lateral sclerosis (ALS) (Kawahara, Ito et al. 2004), schizophrenia (Akbarian, Smith et al. 1995), Alzheimer's disease (Gaisler-Salomon, Kravitz et al. 2014) and in tumors such as glioblastoma (Ishiuchi, Yoshida et al. 2007) and astrocytoma (Cenci, Barzotti et al. 2008).

While majority of ADAR2 dysfunction is thought to be mediated via alterations in GluA2 Q/R editing, ADAR2 mediated GluK2 Q/R editing have also been implicated particularly in epilepsy (Kortenbruck, Berger et al. 2001), spinal cord injury (Caracciolo, Fumagalli et al. 2013) and schizophrenia (Barbon, Fumagalli et al. 2007). Alterations in GluK2 editing has also been observed in hippocampal and neocortical tissue of epileptic patients (Grigorenko, Bell et al. 1998). Interestingly, increased GluK2 editing was observed in murine model of schizophrenia (phenylcyclidine-treated rats) (Barbon, Fumagalli et al. 2007). Another study also reported a slight decrease in GluK2 Q/R editing following kainate-induced seizures (Bernard, Ferhat et al. 1999). This is interesting as GluK2 editing deficient mice have increased susceptibility to kainate induced seizures (Vissel, Royle et al. 2001). A similar observation of reduced GluK2 editing has also been reported following cerebral ischemia (Paschen, Schmitt

et al. 1996). While not fully known, it can be speculated that increased calcium conductance through increased unedited receptors during ischemia, contributes to the ischemic cell damage and death (Zhu, Kong et al. 2014).

Other forms of A-to-I RNA editing such as GluA2 R/G editing has been implicated in spinal cord injury (Barbon, Fumagalli et al. 2010), excitotoxicity (Bonini, Filippini et al. 2015), and Alzheimer's diseases (Khermesh, D'Erchia et al. 2016). Similarly, I/V and Y/C site editing of GluK2 have also been linked to spinal cord injury (Caracciolo, Fumagalli et al. 2013) and bipolar disorder (Silberberg, Lundin et al. 2012).

All these links are from varieties of studies performed in murine models and/or cell culture model of diseases and samples from human patients. While most of the studies have linked these editing deficiencies to the changes in ADAR2 (in some cases ADAR1) levels, not all studies show the editing deficiency to be consequential. Nevertheless, all these studies highlight the key role of ADAR2 (and ADAR1) mediated RNA editing plays in brain function and dysfunction of this leads to neurological disorders.

1.8 Objectives

Kainate receptors play a major in synaptic plasticity. They undergo plasticity themselves and can be activity dependently regulated while also mediating plasticity. This has been studied to an extent in Hebbian forms of plasticity: LTP and LTD. However, their role in homeostatic plasticity is not as well explored.

Building on recently published work showing that KARs regulate AMPAR plasticity, I wanted to determine how KAR signalling can regulate AMPAR expression. I also wanted to determine what role if any do KARs play in homeostatic scaling.

Finally, ADAR2-mediated (Q/R) RNA editing has been shown to be an important regulator of KAR diversity, trafficking and physiological and pathological function. I also wanted to explore its potential function in KAR plasticity. So, my project objectives were to address the following questions:

- Can KARs mediate AMPAR plasticity (LTP and LTD)? If so, what are the mechanisms?
- Do KARs play a role in homeostatic plasticity? If so, what are the mechanisms?
- Do Q/R editing of GluK2 play a role in KAR plasticity? If so, is this regulation mediated by the ADAR enzymes?

Chapter 2. MATERIALS AND METHODS

2.1 Materials

2.1.1 Chemicals

All reagents were purchased from Sigma-Aldrich Company limited unless stated otherwise.

All acids were purchased from Fisher Scientific unless stated otherwise.

2.1.2 Bacterial reagents

2.1.2.1 Escherichia Coli (E.Coli)

Table 2.1 consists of all the E. coli strains used:

Table 2-1: E.Coli strains used.

Strain	Purpose	Supplier	Genotype
DH5α	Cloning and amplification	Thermo Fisher	*Φ80 lacZΔ M15 supE44 Δlac U169 hsdR17 recA1 endA1 gyrA96 thi-1 relA1*
XL1-Blue	Cloning into viral vector and amplification (low recombination activity)	Agilent, Thermo Fisher	*recA1 endA1 gyrA96 thi-1 hsdR17 supE44 relA1 lac [F´ proAB lacI^q ZΔM15 Tn10)*

*Competent DH5α were bought from the indicated suppliers originally and were made in house (protocol described in (Inoue, Nojima et al. 1990)).

*Commercial XL1-blue competent cells (Agilent) were used for cloning into viral vector purposes.

2.1.2.2 Bacterial growth media and agar plates

E.coli bacteria were grown in in house Luria Bertani (LB) media (University of Bristol central stores) for cloning and amplification of DNA stocks. Agar plates to culture E.coli were made using LB and 1.5% agar under sterile conditions. Bacterial growth media and agar plates were supplemented with appropriate antibiotics: Ampicillin (100µg/ml diluted from 100mg/ml stock in 50% ethanol; Sigma-Aldrich) and kanamycin (25µg/ml diluted from 10mg/ml stock; Sigma).

2.1.3 Molecular biology reagents

2.1.3.1 Plasmids

Following plasmids were used for cloning purposes:

- pcDNA3.1 (Invitrogen)
- pEGFP-N1 (Clontech)
- pSUPER-neo-GFP (OligoEngine)

2.1.3.2 Restriction endonucleases

All restriction enzymes and their compatible buffers used were supplied by New England Biolabs (NEB) and stored at -20^{o}C.

2.1.3.3 Other enzymes

T4 DNA ligase to ligate vector and inserts was purchased from Takara (BioWhittaker). Calf Intestinal Alkaline Phosphatase (CIP) was purchased from NEB.

2.1.3.4 Polymerase Chain Reaction (PCR) kit

KOD Hot Start DNA Polymerase kit was purchased from Merck Millipore which included KOD Hot start polymerase, 10x buffer, dNTPs and $MgSO_4$. DMSO was also added to PCR mixture obtained from Sigma.

2.1.3.5 Agarose gel DNA

Agarose gels (0.8%, 1.5% or 4%) for gel electrophoresis were made in house using ultra-pure agarose (Bioline). 1kb and 50bp DNA ladder were purchased from Thermo Scientific. Ethidium Bromide added to the agarose gel to visualise the DNA were purchased from Sigma.

2.1.3.6 DNA purification

DNA purification was performed using GeneJET^{TM} Gel extraction, Miniprep and Midiprep kits obtained from Thermo Scientific.

2.1.3.7 RNA extraction and cDNA synthesis

RNA extraction kit was obtained from Qiagen and cDNA synthesis kit from ThermoFisher Scientific.

2.1.3.8 Primers and sequencing

All primers were ordered from Sigma-Aldrich synthesised as oligonucleotides and resuspended in 1xTE (10 mM Tris-HCl pH8.0, 1mM EDTA) buffer made in house. Plasmids were sequenced using Eurofins MWG Services.

2.1.4 Protein biochemistry reagents

cOmplete™ Protease inhibitor tablets were obtained from Roche, resuspended in 2ml of distilled water to make 20x stock and stored at 4°C. Phosphatase inhibitor cocktail solution 2 was obtained from Sigma. 30% v/v acrylamide was obtained from Geneflow limited to make SDS-PAGE gels. For protein transfer, Polyvinylidene difluoride (PVDF) 0.45µM immobilin membrane was obtained from Millipore and Whatman™ Grade 3MM Chr Cellulose Chromatography Papers from GE Healthcare Life Sciences. PageRuler protein ladder was obtained from ThermoScientific. For membrane blocking, non-fat milk powder from The Co-operative own brand and Bovine Serum Albumin (BSA) from Sigma-Aldrich were obtained. Following HRP Substrates were used to develop western blot images:

- SuperSignal® West Pico Enhanced Chemiluminescence (ECL)- Thermo Scientific
- Luminata™ Crescendo- Merck Millipore
- Luminata™ Forte- Merck Millipore
- West Femto ECL- Thermo Scientific

CL-Xposure™ Xray Film was obtained from ThermoScientific and Hypercasette™ from Amersham Biosciences. The fixer and developer solutions were from Fixaplus.

EZ-Link® Sulfo-NHS-SS-Biotin were obtained from ThermoScientific and Streptavidin-Agarose from *Streptomyces Avidinii* beads were from Sigma. GFP Trap beads were obtained from Chromotek and BCA Assay kit from Pierce ThermoFisher Scientific.

2.1.5 Mammalian clonal cell line reagents

Human Embryonic Kidney (HEK) 293T cells lines were obtained from The European Collection of Cell Cultures (ECACC). Stocks were maintained in 1% DMSO and stored in liquid nitrogen.

Dulbecco's Modified Eagle's Medium (DMEM) were obtained from Lonza or Sigma-Aldrich and were supplemented with 10% heat-inactivated fetal bovine serum (FBS) (Sigma-Aldrich), 1% Glutamine (Gibco, Invitrogen) and 1000 units Penicillin and 0.1mg Streptomycin (Gibco). Poly-L-Lysine (PLL) was from Sigma-Aldrich and Lipofectamine® 2000 transfection reagent from ThermoFisher.

2.1.6 Electronic equipment

Sterile cell culture hoods were set up by Holten LaminAir and cell culture incubators and shaking bacterial incubators were from LTE Scientific and New Brunswick Scientific respectively. Mini bacterial incubator was from IKA® KS 3000i control. Bench top microcentrifuges were from Biofuge and Eppendorf. High speed Centrifuges and rotors were from Beckman-Coulter or Jouan. Low speed centrifuges were from Jouan and Hettick. Electrophoresis power pack for western blot were from Bio-Rad Laboratories, agarose gel electrophoresis tank from Takara and thermal cycler PCR was from MJ Research PTC-2000. The X-Ray film developer was from Konica (SRX-101A automatic medical X-ray film developer) and Odyssey Fc detection system was from LI-COR. Microscopes for dissection were from Leica and for fixed cell imaging Leica SP5-II confocal laser scanning microscope attached to Leica DMI 6000 inverted epifluorescence was used. Plate reader was from Versamax Microplate reader, Molecular devices. Heat block was from Eppendorf, waterbath from Grant and Benchtop UV Transilluminator from BioDoc-It™ Imaging System.

2.1.7 Plasticware and glassware

Non-sterile plastic pipette tips (10µl to 1000µl) were from StarLabs and Gel loading tips from Fisher. Stripettes (5ml to 25ml) from CellStar. 25mm glass coverslips and glass slides were from VWR International.Cell culture plasticware were from Cellstar. PCR tubes (0.5ml and 0.2ml) were from

Starlab. 0.5ml and 1.5ml tubes from Eppendorf and 15ml and 50ml tubes from Falcon. Syringes and Needles from Sarotorius and BD Microlance^{TM3} respectively. RNAse free 1.5ml microfuge tubes were from Ambion.

2.1.8 Fixed cell imaging reagents

16% Formaldehyde stock was obtained from Electron Microscopy Sciences and Fluoromount-G mounting^{TM} media with DAPI from Thermo Fisher.

2.1.9 Antibodies used

2.1.9.1 Primary antibodies

Following primary antibodies were used for western blotting (WB) and immunocytochemistry (ICC). All the primary antibodies for WB were diluted in 2.5% milk in PBS-T and for ICC were diluted in 3% BSA in PBS.

Table 2-2: List of primary antibodies used for WB and ICC.

Antibody Use	Species	Supplier	Catalogue Number	Dilution	Type
ADAR2 WB	Rabbit	Sigma	SAB4500090	1:1000	Polyclonal
ADAR2 ICC	Rabbit	Abcam	Ab64830	1:400	Polyclonal
ADAR1 WB	Mouse	SantaCruz	sc73408	1:1000	Monoclonal
Actin	Mouse	Sigma	A5441	1:10000	Monoclonal
EGFR WB	Rabbit	Abcam	Ab52894	1:1000	Monoclonal
Fibrillarin ICC	Mouse	Abcam	Ab4566	1:400	Monoclonal
GAPDH	Mouse	Abcam	Ab8245	1:10000	Monoclonal
GluA1 WB	Rabbit	Millipore	Ab1504	1:1000	Polyclonal
GluA1 ICC	Mouse	Millipore	Mab2263	1:100	Monoclonal
GluA2 WB	Rabbit	Synaptic Systems	182103	1:1000	Polyclonal
GluA2 ICC	Mouse	Millipore	MAB397	1:70	Monoclonal
GluK2 WB	Rabbit	Millipore	04-921	1:1000	Monoclonal
GluK5 WB	Rabbit	Millipore	06-315	1:1000	Polyclonal
GFP WB	Rat	Chromotek	3h9-100	1:10000	Monoclonal
GFP ICC	Chicken	Abcam	Ab13970	1:1000	Polyclonal
HA WB	Mouse	Sigma	43663	1:2000	Monoclonal
HA ICC	Mouse	Sigma	43663	1:600	Monoclonal
LaminB	Goat	SantaCruz	Sc-6217	1:1000	Polyclonal
Pin1 WB	Mouse	Santacruz	G-8	1:1000	Monoclonal
RhoGDI	Rabbit	Abcam	Ab133248	1:1000	Monoclonal
WWP2 WB	Rabbit	Abcam	Ab86544	1:500	Polyclonal

2.1.9.2 Secondary antibodies

HRP conjugated anti-mouse (raised in Goat), anti-rabbit (raised in Goat), anti-rat (raised in Rabbit) and anti-goat (raised in rabbit) were all from Sigma-Aldrich and used at a dilution of 1:10000 in 5% milk and PBS-T.

All secondary antibodies Cy2, Cy3 and Cy5 (raised in Donkey) for immunocytochemistry were from Jackson ImmunoResearch and used at 1:400 in 3% BSA in PBS.

2.1.10 Plasmid constructs

Plasmid constructs generated are listed in table below.

Table 2-3 List of plasmid constructs used.

Protein	Species	Backbone	Tag	Cloning Sites
ADAR2 WT	Rat	pcDNA3.1	HA	5'KpnI 3'XbaI
ADAR2 T32A	Rat	pcDNA3.1	HA	5'KpnI 3'XbaI
ADAR2 T32D	Rat	pcDNA3.1	HA	5'KpnI 3'XbaI
shADAR2 Complete	Rat, mouse	pSuper-neo-GFP	GFP	5'BglII 3'XhoI
shADAR2 Partial	Rat, mouse, Human	pSuper-neo-GFP	GFP	5'BglII 3'XhoI
shADAR2 Complete	Rat, mouse	pXLG3-100bp stuffer	GFP	5'KpnI 3'KpnI
shADAR2 Partial	Rat, mouse, Human	pXLG3-100bp stuffer	GFP	5'KpnI 3'KpnI
shADAR2 Complete	Rat, mouse	pXLG3-Wpre	GFP	5'PacI 3'XhoI
ADAR2 rescue	Rat	pXLG3-Wpre	HA	5'SpeI 3'BamHI
ADAR2 T32A rescue	Rat	pXLG3-wpre	HA	5'SpeI 3'BamHI

ADAR2 T32D rescue	Rat	pXLG3-wpre	HA	5'SpeI 3'BamHI
GluK2 621Q *	Rat	pcDNA3.1	YFP Myc	
GluK2 621R *	Rat	pcDNA3.1	YFP Myc	
shGluK2*	Rat	pXLG3-100bp stuffer	GFP	5'KpnI 3'KpnI
Pin1	Rat	peGFP-N1	GFP	5'EcoRI 3'BamHI
Wwp2	Rat	pcDNA3.1	HA	5'KpnI 3'XbaI
shwwp2 1	Rat, mouse	pSuper-neo-GFP	GFP	5'BglII 3'XhoI
shwwp2 2	Rat, mouse, human	pSuper-neo-GFP	GFP	5'BglII 3'XhoI
shwwp2 1	Rat, mouse	pXLG3-wpre	GFP	5'PacI 3'XhoI
shwwp2 2	Rat, mouse, human	pXLG3-wpre	GFP	5'PacI 3'XhoI

*GluK2 621Q was made by Dr. Stephane Martin (Martin, Nishimune et al. 2007) and GluK2 621R was made by Dr. Ash Evans by using Quickchange Mutagenesis. shGluK2 was prepared by Dr. K.A.Willkinson.

2.1.11 Drugs

Following drugs were used for various experiments:

Table 2-4: List of drugs used throughout the project.

Drug	Stock Concentration	Final Concentration	Diluted in	Supplier
Bicuculline (Bic)	40mM	40µM	DMSO	Sigma
Bortezomib (BTZ)	10mM	1µM	DMSO	Cell Signalling
Cycloheximide (CHX)	100mg/ml	25-50µg/ml	DMSO	Sigma
GYKI53655	10mM	40µM	ddH_2O	Abcam
Kainate (KA)	20mM	10µM	ddH_2O	Sigma
N-methyl-D-Aspartate (NMDA)	50mM	25µM	ddH_2O	Tocris Bioscience
Tetrodotoxin (TTX)	1mM	0.5-1µM	ddH_2O	Tocris Bioscience

2.2 Molecular biology methods

2.2.1 Polymerase Chain Reaction (PCR)

High fidelity Hot KOD polymerase, purified from *Thermococcus kodakaraensis,* were used for conventional PCR. Each PCR reaction was made in 50µl volume with following ingredients and mixed by pipetting:

Table 2-5: List of components added to the PCR reaction mixture

Components	Volume (µl)	Stock concentration	Final concentration
10x Buffer	5	10x	1x
dNTP mix	5	2mM	0.2mM
$MgSO_4$	3	25mM	1.5mM
Forward primer	1.5	10µM	0.3µM
Reverse primer	1.5	10µM	0.3 µM
Template DNA	10	1ng/µl	0.2ng/µl
ddH_2O	20.5		
DMSO	2.5		
KOD Hot Start Polymerase	1	1unit/µl	0.02unit/µl
	Total = 50µl		

PCR was then performed using a thermal cycler with the following settings:

Table 2-6: PCR reaction thermocycler setup

Polymerase activation	**95°C for 2 minutes (mins)**			
Denature DNA	95°C for 20 seconds			
Annealing primers	55°C for 10 seconds			
Polymerase extension	<500bp 70°C 10 s/kb	<1000bp 70°C 15 s/kb	<3000bp 70°C 20 s/kb	3000bp< 70°C 25 s/kb
Repeat Cycles	Repeat steps 2-4, 25 times			
Final extensions	70°C for sec/min (per step 4)			
Cooling	10°C for 10 mins			

Site Directed Mutagenesis (SDM) was used to introduce point mutations. For this, long primers were designed which were oppositely coded and annealed to the region of interest with desired point mutation. The desired mutation site was kept in the middle during primer design with complementary 21bp added

either side. PCR was then performed to copy the whole plasmid. PCR was performed with mostly **Table 2-6** settings, except polymerase extension at 70ºC 25s/kb (length of whole vector + insert) and repeat steps 2-4 were performed 18-22 times.

2.2.2 Agarose gel electrophoresis

Agarose gels were prepared by mixing either 0.8% or 1.5% agarose with 0.5x TAE buffer (40mM Tris acetate, 1mM EDTA) and heated to dissolve the agarose. The mixture is then cooled (but not set) and ethidium bromide (0.5µl/ml) was added, swirled to mix and poured into mould with the well setting combs added beforehand. The gels were then allowed to set.

In a Mupid®-eXu gel tank, the agarose gels were submerged in 0.5x TAE. Samples were mixed with 6x loading dye (ThermoScientific) and loaded into the agarose gel wells. Typically, 5µl of sample would be mixed with 1µl loading due to load 6µl total volume. 5µl of 1kb Hyperladder (Bioline) was also loaded to identify the DNA size. Electrophoresis was run at 135 volts (V) for 20 minutes to allow the DNA to resolve and gels were imaged using a UV transilluminator.

2.2.3 PCR purification

A GeneJET^{TM} Gel extraction kit was used to purify the PCR products. Binding buffer was added in a ratio of 5 times the volume of the product to be purified, vortexed briefly and added to a purification column. The column was spun at 16100g for 1 min on a bench-top centrifuge. The flow-through was discarded. Wash buffer was added to the column and spun at max speed for 1 min on bench-top centrifuge. Flow through was discarded and wash step repeated, after which the column was spun again to discard residual wash buffer from the column. The column was transferred into a fresh 1.5ml Eppendorf tube and 50µl ddH_2O was added to the column and incubated for 2 mins before spinning at 16100g for 2 mins.

2.2.4 Restriction enzyme digestion

50µl of purified PCR product and 5µg of vector DNA were digested with 20units of restriction endonucleases in appropriate NEB buffer and made up to a final

volume of 100µl with ddH_2O. For vector DNA digestion, 20 units of Calf Intestinal Alkaline phosphatase (CIP) was also added to remove the 5' phosphate groups and prevent vector re-ligation. The digest mixture reactions were incubated at 37^oC for 2 hours and purified using GeneJET^{TM} Gel Extraction kit as explained in section 2.1.3.6.

For SDM, PCR product was not purified and digested straight using DpnI restriction endonuclease for 2 hours at 37^oC. DpnI is used to digest methylated DNA to remove the original template DNA and not the PCR product. After digestion, the mutated vector was purified again (see section 2.2.3) and eluted twice using the same 10µl volume of ddH_2O.

2.2.5 DNA ligation

The digested and purified DNA and vector were run on an agarose gel (see section 2.1.3.5) to ensure the vector was linearised and help determine vector:insert molar ratio. The vector DNA was diluted in appropriate volume of ddH_2O to obtain 3:1 molar ratio with the insert when mixed in 1:1 ratio. 1µl of insert DNA was then mixed with 1µl diluted vector DNA along with 2µl T4 ligase solution 1 (Takara). Control ligation was set up where ddH_2O was used instead of insert to determine the amount of vector-ligation. The ligation mixture was left at room temperature (rt) for 30 mins.

2.2.6 Bacterial transformation

Chemically competent E.coli were grown in lab and aliquots stored in -80^oC. DH5α E.coli were used for general transformation and amplification while XL1-Blue E.coli was specifically used for pXLG3 based transformation and amplification for lentivirus purposes due to their low recombinase activity.

The 4µl of ligation mixture added to 40µl of E.coli (thawed on ice) in a 1.5ml Eppendorf tube and incubated on ice for 20 mins.

Agar plates containing the appropriate antibiotics was pre-warmed in the 37^oC bacterial incubator. Cells were heat shocked for 90 seconds in 42^oC waterbath and transferred on ice for 2 mins. For commercial XL1-Blue, the cells were heat shocked for only 45 seconds. After 2 mins, 100µl of warm LB broth was added to the bacteria. The bacterial cells were then added to the agar plate

and spread evenly using a sterile hockey spreader stick. For kanamycin resistance genes, 200µl of LB broth was added to the E.coli after heat-shock and incubated for an hour at 37ºC to allow for expression of genes before plating on the agar plate. The agar plate was then incubated at 37ºC overnight with the lid facing down so that the condensation does not drip onto the plate and disrupt growing bacteria. For site-directed mutagenesis, the 10µl of purified digested product was added to 40µl of E.coli and above protocol was followed.

2.2.7 Bacterial amplification and plasmid DNA purification

Single colonies on LB agar plates were picked and cultured in 3ml of LB Broth overnight supplemented with the appropriate antibiotics in a 37ºC shaking incubator. Plasmid DNA was extracted and purified the next day using GeneJET™ Plasmid Miniprep Kit according to the manufacturer's instructions and eluted in 50µl of elution buffer. DNA concentrations were measured using a NanoDrop ND-1000 (LabTech) at an absorbance wavelength of 260nm. The successful colonies were PCR screened and sent for sequencing.

The correct miniprep DNA were amplified using Midiprep for transfection purposes. For this, bacterial transformation was carried as section 2.2.6, where 1µl of miniprep DNA was transformed in 10µl of E.Coli and plated on appropriate antibiotic coated agar plate overnight at 37ºC to pick clonal population. The next day, single colony was picked and grown in 100ml of LB Broth supplemented with appropriate antibiotic in a shaking incubator at 37ºC. The following day DNA was extracted and purified using a GeneJET™ Plasmid Midiprep kit according to manufacturer's instructions (following the high-speed protocol) and was eluted in 500µl of elution buffer. DNA concentration was measured and stored at -20ºC till use.

2.2.8 Colony screening

After single bacteria clones were amplified using Miniprep kit, they were PCR screened to test for positive colonies with the desired insert. Appropriate forward and reverse primers were used to perform PCR with same methods as mentioned before. However, the PCR volume was scaled down to 10µl

instead of 50µl volume and all the product was run on an agarose gel and PCR products visualised to confirm ligation.

The positive preps were then sent for full sequencing to MWG Eurofins using appropriate primers either available from MWG or using pre-made primers.

2.2.9 shRNA synthesis

Forward and reverse complementary oligonucleotides consisting of the full shRNA hairpin sequence with 5' BamHI and 3' XhoI overhangs were ordered from Sigma-Aldrich. The oligonucleotides were diluted to 100µM in 1x TE buffer (10mM Tri-HCl, 1mM EDTA, pH 8). 2µl of each oligonucleotide were mixed together in an Eppendorf tube and heated to 95^{o}C in a heat block for 4 mins and left to cool after for 30 mins at rt to allow annealing to occur. The annealed oligonucleotides were diluted to 250µl with ddH_2O. 1µl of diluted oligonucleotide was ligated with 1µl pSUPER-neo-GFP (cut with BglII and XhoI minus the CIP), transformed and plated onto ampicillin-containing LB agar plates.

Once successfully cloned pSUPER was identified, the shRNA including the H1 promoter from pSUPER was subcloned into lentiviral vector pXLG-3 (Demaison, Parsley et al. 2002). For the knockdown vector, flanking KpnI restriction sites were introduced via primers. For knockdown rescue vectors (pXLG3-wpre), flanking 5' PacI and 3' XhoI was introduced via primers to ligate the shRNA cassette. Ligation, transformation and screening was performed as mentioned before.

Table 2-7: shRNA target sequences for protein knockdown

shRNA	Backbone	Target sequence
shADAR2 Complete	pXLG3-100bp stuffer pXLG3 wpre	AAGAACGCCCTGATGCAGCTG
shADAR2 Partial	pXLG3-100bp stuffer	AACAAGAAGCTTGCCAAGGCC
shGluK2	pXLG3-100bp stuffer	GCCGTTTATGACACTTGGA
shwwp2 1	pXLG3-wpre	TGCCCAATGGGCGTGTCTATT
shwwp2 2	pXLG3-wpre	GCAGCACTTCAGCCAAAGATT

wpre: Woodchuck Hepatitis Virus (WHP) Posttranscriptional Regulatory Element

*shGluK2 was designed and prepared by Dr. K.A Wilkinson.

2.2.10 Lentivirus production

HEK293T cells for lentivirus production was grown using Complete Sigma DMEM media (Plain Sigma DMEM ((with L-glutamine) and supplemented with 10% FBS) and all transfections were also performed using this media.

2.2.10.1 Plating HEK293T cells

HEK293T cells were cultured in Complete DMEM media and passaged as described in section 2.3.1 and 2.3.2. 6.5 x 10^6 cells were plated in a 10cm cell culture dish (not pre-treated with PLL) containing 7ml of Sigma complete DMEM media. The cells were incubated overnight to allow them to adhere and grow.

2.2.10.2 HEK293T cell transfection

The next day, the HEK293T cells were transfected. For this, required amount of plain DMEM media was sterile filtered using 0.2µM syringe filter. For knockdown vector, 20µl of XLG viral vector containing the shRNA under H1 promoter (pXLG3-100bp stuffer) and promoter was mixed with 5µg pDMD2.G packaging vector (Addgene) and 15µg of p8.91 helper vector (Addgene) into a sterile bijou vile containing 2.5ml of sterile filtered Sigma plain DMEM media.

In a 15ml falcon tube, 2.5ml of plain DMEM media was mixed 4.8% 1mg/ml polyethylenimide (PEI) by inverting several times. The PEI mixture solution was sterile filtered using 0.2µM syringe filter into a fresh 15ml falcon tube, left to stand in rt for 2-3 mins and inverted to mix several times again. The PEI-DMEM mixture was then added to the bijou vile containing the earlier prepped DNA mixture, inverted to mix several times and left to stand in rt for 30 mins.

During this incubation period, the plated HEK293T cells were carefully washed with 6ml of plain DMEM media twice. After second wash the media was aspirated and the 5ml of transfection solution was slowly added to the cells and incubated at 37^{o}C for 4 hours. After the incubation, the transfection mixture media was aspirated from cells and replaced with 7ml of neuronal feeding media (sterile filtered with 0.2µM filter and warmed to 37^{o}C). The cells were the placed back in the 37^{o}C incubator.

For pXLG3-wpre vector (for knockdown and rescues) above protocol was used for HEK293T transfection with slight variances in concentrations of vectors and PEI:

- 10µg of viral vector was added to 2.5µg pDMD2.G and 7.5µg of p8.91 vector.
- 2.4% 1mg/ml PEI was added to make the transfection mixture.
- After 4 hours of incubation, 7ml of complete DMEM was added to the HEK293T cells instead of the feeding media.

2.2.10.3 Lentivirus harvesting

60-72h post-transfection, the virus containing media was collected into 15ml falcon tube and centrifuged at 3000g for 10 minutes at 4^{o}C to pellet any remaining dead cells in the media. The supernatant was syringe filtered (0.45µM) into a fresh 15ml falcon tube. The syringe filter was pre-wetted with neuronal plating media beforehand. The sterile filtered virus containing media was then aliquoted to required volume (500µl to 1ml) before being stored at -80^{o}C.

For XLG-wpre vector (knockdown under H1 promoter but rescue/GFP under SFFV promoter), the virus-containing media was harvested 40-48 hours post-

transfection and the syringe filter was pre-wetted with complete DMEM media. Otherwise, the protocol was same as above.

2.2.11 RNA extraction and cDNA synthesis

RNA extraction was performed using Qiagen RNeasy Mini Kit as per manufacturer's instructions. The surface and all required equipment for this process were sprayed and wiped with RNAseZap™ RNase decontamination solution (Invitrogen™) spray. RNAse free 1.5ml microcentrifuge tubes and filter pipette tips were used throughout the process and the whole process was carried out in rt.

Briefly, after required treatments 350µl of buffer RLT supplemented with β-mercaptoethanol (β-ME) 1:100 were added per 1 million cells. Cells were scraped and collected in a RNAse free 1.5ml microcentrifuge tube. The solution was spun at 16100g in a benchtop centrifuge to remove any undissolved pellet. The supernatant was transferred in to a fresh tube and the RNA was precipitated using 70% ethanol, pipetted to mix and transferred onto the RNeasy Mini Spin Column. Wash steps were followed per manufacturer's instructions and the RNA was eluted into a fresh RNAse free microcentrifuge with 25µl of RNase-Free water. RNA concentration was measured using Nanodrop at 260nm wavelength.

cDNA synthesis was performed using RevertAid First Strand cDNA synthesis kit (Thermo Scientific) following manufacturer's instructions. 1µg of extracted RNA was used along with oligo(dT)$_{18}$ primer and other components shown in Table 2-8 below:

Table 2-8: Components of the reaction mixture for cDNA synthesis.

Components	Volume	Stock Concentration	Final concentration
Template RNA	- As needed	1µg	0.05µg/µl
Primer	1µl	100µM	5µM
Water, nuclease-free	To make to 12ul with template RNA and Primer		-
Reaction Buffer	4µl	5x	1x
RiboLock RNase Inhibitor	1µl	20units/µl	1unit/µl
dNTP Mix	2µl	10mM	1mM
RevertAid M-MuLV Reverse Transcriptase (RT)	1µl	200units/µl	10units/µl
	Total = 20µl		

The mixture was pipetted to mix, spun down briefly and then heated at 42^{o}C on a heatblock for an hour before heating at 70^{o}C for 5 mins to inactivate the reverse polymerase enzyme.

No RT control and ddH_2O control was also prepared to ensure no genomic DNA contamination occurred.

2.2.12 BbvI restriction enzyme assay and analysis

For BbvI restriction enzyme Assay, once cDNA was synthesised per condition, primers spanning the TMII region of GluK2 and GluA2 were used as follows to perform PCR.

GluK2 F: 5’-GGTATAACCCACACCCTTGCAACC-3’
GluK2 R: 5’-TGACTCCATTAAGAAAGCATAATCCGA-3’

GluA2 F: 5’-GTGTTTGCCTACATTGGGGTC-3’
GluA2 R: 5’-TCCTCCTACACGGCTAACTTA-3’

To set up PCR, 6µl of cDNA synthesised was used per condition with the same set up as **Table 2-5**, but ddH_2O volume adjusted to make up to 50µl total volume. PCR amplification set up was the same as described in **Table 2-6**, except the repeat steps 2-4 were performed for 35 times. The resultants PCR product was purified as described in section 2.1.3.6 and eluted in 25µl of ddH_2O.

For BbvI digestion, the 15µl of the purified PCR product was incubated with 20 units of BbvI enzyme (NEB) and 2µl of CutSmart Buffer (NEB) made up to 20µl volume with ddH_2O and incubated at 37^oC for 2 hours. All the 20µl of digested product was run on a 4% agarose gel and the ethidium bromide stained bands were imaged using UV transilluminator and quantified using FIJI ImageJ (NIH). Densitometry was calculated using the Gel Analysis Tool in FIJI ImageJ (NIH). The relative pixel intensity was calculated as the area under each peak and the percentage of editing was determined as below:

For GluK2;

[Intensity of 376(edited)/(Intensity of (376 (edited)+269(unedited))] * 100.

The band at 76bp present in both edited and unedited products allowed to determine equal loading.

The above protocol for GluK2 was adapted from (Bernard, Ferhat et al. 1999).

For GluA2;

[Intensity of 231 (edited)/Intensity of 131 (unedited)] * 100.

2.2.13 Obtaining sequencing chromatographs

To obtain sequence chromatographs to highlight the dual peaks at the region of editing, the 2µl of purified PCR product was diluted in 13µl of ddH_2O and sent for sequencing to MWG Eurofins. The resultant chromatographs were downloaded from the Eurofins webpage and opened and imaged using the free version of Chromas (Technelysium, version 2.6.2).

2.2.14 Genotyping and PCR

Ear Notch samples from mice (rough 2mm volume) were received from Animal Unit Breeding Team as requested. KAPA Mouse Genotyping Kit (Sigma) was

used to extract the genomic DNA following manufacturer's protocol. DNA extraction was performed per extraction in 100µl volume with 88µl PCR-grade water, 10µl 10x KAPA Express extract Buffer and 1U/µl KAPA Express Extract Enzyme added to the mouse tissue in a 1.5ml Eppendorf tube. The mixture was pipetted up and down to mix the solution and heated to 75^{O}C for 10 minutes on a heat block for lysis followed by enzyme inactivation at 95^{O}C for 5 mins. The samples were centrifuged briefly to pellet cellular debris. The supernatant (DNA) was moved to a fresh 1.5ml Eppendorf tube and diluted 10-fold with 10mM Tris-HCl pH 8.0 (crude extract).

To set up PCR, following components were mixed per individual PCR tube and mixed well.

Table 2-9: PCR Reaction Set up for genotyping.

Component	Volume (µl)	Stock Conc.	Final Conc.
PCR-grade water	7.75	N/A	N/A
2xKAPA2G Fast (HotStart) Genotyping Mix with dye	12.5	2x	1x
Forward Primer	1.25	10µM	0.5µM
Reverse Primer	1.25	10µM	0.5µM
Reverse Primer 2	1.25	10µM	0.5µM
Template DNA	1µl of crude extract	N/A	N/A
	Total=25µl		

Following PCR cycling settings were used.

Table 2-10: PCR cycling protocol for genotyping samples.

Polymerase activation	95ºC for 3 mins
Denature DNA	95ºC for 15 seconds
Annealing primers	60ºC for 15 seconds
Polymerase extension	72ºC for 30 seconds
Repeat Cycles	Repeat steps 2-4, 30 times
Final extensions	72ºC for 2 mins
Cooling	10ºC for 10 mins

The PCR products were run on a 4% agarose gel and visualised using UV transilluminator.

2.3 Cell culture methods

All cell culture work was performed under sterile hood conditions and all the cells were incubated at 37ºC, 5% CO_2 and 95% O_2.

2.3.1 Culturing HEK293T cells

HEK293T cells stored in liquid nitrogen cryostore (10% DMSO in DMEM media) were thawed in 37ºC waterbath before mixing them with 10ml Complete DMEM media (Plain DMEM supplemented with 10% FBS, 1% L-glutamine and 1% Penicillin/Streptomycin) in a 15ml falcon tube. The cells were resuspended and centrifuged at 1500g for 2 minutes at rt. The suspension media was removed, and the cell pellet was resuspended in 1ml of Complete DMEM to remove any DMSO. The resuspended cells were transferred to a T25 flask along with additional 5ml of complete media and incubated overnight. The cells were passaged the next day into T75 flask containing 15ml complete DMEM media. Cells in culture were regularly passaged for experimental use.

2.3.2 Passaging HEK293T cells

The HEK293T cells were passaged regularly when 70-90% confluency was reached. In a T75 flask, cells were gently washed with 10ml of 1x PBS (10x

PBS (Gibco) diluted in sterile cell culture grade water (Hyclone™ HyQPAK)) before adding 1ml of 0.05% typsin-EDTA to the cells. The cells were incubated for 2-3 mins at 37ºC to allow the adherent cells to detach from the flask. The trypsin was deactivated by adding 10ml of Complete DMEM to the flask and collecting the cells in to a 15ml falcon tube. The cells were centrifuged at 1500g for 2 minutes at rt. The supernatant was aspirated, and the cell pellet was resuspended in 10ml of complete DMEM media by triturating with a 10ml serological pipette. 1ml of the cell suspension was added to a new T75 flask containing 15ml of complete DMEM media and incubated till the next passage.

2.3.3 Plating HEK293T cells

To plate HEK293T cells for experiments, wells of a cell culture 6-well dish or 3cm dishes were coated with PLL to aid cell adhesion to the dish. For this, PLL diluted to 0.1mg/ml in sterile cell culture grade water was added to cover the wells/dish, incubated at 37ºC for at least 1 hour and washed three times with 2ml of sterile cell culture grade water before adding 2ml of transfection DMEM media (Plain DMEM media supplemented with 10% FBS and 1% L-glutamine). Cells in a T75 flask was passaged and counted using haemocytometer. 200,000 cells per well of a 6 well dish was added or 1 million cells per 3 cm dish was added and incubated overnight to allow them to adhere.

2.3.4 Counting cells

To count cells, the resuspended cells were diluted 1:10 in 0.4% Trypan Blue solution (Gibco). The trypan blue-cell mixture was pipetted into a haemocytometer and counted to determine concentration of cells in million per ml.

2.3.5 Transfecting HEK293T cells

For transfection, appropriate amount of DNA (as per the experiment) was added to 100µl of plain DMEM media in a 1.5ml Eppendorf tube. In another 1.5ml Eppendorf tube, 1.5µl of Lipofectamine® 2000 per µg of DNA was added to another 100µl of plain DMEM media. The solutions were vortexed briefly and left to incubate in rt for 5 minutes. The Lipofectamine® tube was added to the DNA tube and vortexed briefly again and allowed to incubate in rt for 25 mins. After 25 mins, the tubes with the transfection mixtures were vortexed

again and added to the wells/dishes in dropwise manner. The transfection was left to incubate for either 48 hours for overexpression constructs or 72 hours for knockdown constructs before lysing the cells. If both overexpression and knockdown constructs were used at the same time, the transfection was left on for 72 hours.

2.4 Primary neuronal cell culture

2.4.1 Preparation of glass coverslips

25mm glass coverslips (~50) were placed in a large glass beaker, submerged in nitric acid and incubated overnight with gentle agitation at rt. The next day, the nitric acid was removed carefully, and the coverslips were washed with distilled water (3 quick washes followed by 3 x 30 mins washes). The coverslips were then transferred to 140mm plastic cell culture dish and sterilised in 70% ethanol for at least 2 hours with gentle agitation at rt. After the incubation, the coverslips were given three quick washes and 3 x 30 minutes washes with sterile cell culture grade water. All the washes after ethanol incubation were done in sterile laminar flow hood. The coverslips were then stored in cell culture grade water at rt.

2.4.2 Preparation of sterile borate buffer

To prepare borate buffer, required grams of Borax and Boric acid powders was added to a 50ml falcon tube to achieve a final concentration of 10mM Borax and 50mM Boric acid in 500ml volume. 50ml sterile cell culture grade water was added to the powder mixture under sterile laminar flow hood and left to dissolve on a rotating wheel at rt for 2 hours. The dissolved borax and boric acid were then sterile filtered using vacuum filtration system with 0.2µM pore membrane and made up to volume of 500ml with sterile cell culture grade water. The sterile borate buffer was then stored at rt for future use.

2.4.3 Coating glass coverslips and plastic plates with Poly-L-lysine (PLL)

To prepare dishes were cell culture, the plastic wells of 6-well dish were coated with 0.5mg/ml PLL diluted in sterile borate buffer. Prepared glass coverslips

were placed in 35mm plastic dishes and washed three times with sterile cell culture grade water before adding 1mg/ml PLL diluted in sterile borate buffer. Plates and dishes were left to incubate overnight in a 37ºC incubator, after which they were washed three times with sterile cell culture grade water and replaced with 2ml of plating media (Neurobasal® medium supplemented with 5% Horse serum, 2% B27 and 1% Glutamax) and stored in a 37ºC incubator until needed.

2.4.4 Rat embryonic dissection

All dissection tools and work place were cleaned with 70% ethanol in distilled water before use. Pregnant E18 Han Wistar rats were anaesthetised using isoflurane with pure oxygen flow and humanely sacrificed using cervical dislocation under Home Office Schedule 1 regulations. The skin of the animal was sterilised with 70% ethanol in distilled water and cut through to extract embryos from the womb. The embryos were kept in Hank's Buffered Salt Solution (HBSS) (Gibco) at rt once extracted and throughout the dissection. Embryos were immediately removed from their sacks and decapitated. Under a dissection microscope, the brains were removed from severed heads using sharp forceps. The left and right brain hemispheres were separated, and the cerebellum, midbrain and meninges were removed and discarded. The hippocampus was excised from each hemisphere to prepare hippocampal cultures while the rest was kept for cortical cultures.

2.4.5 Tissue dissociation, plating and feeding neurones

After dissection, the rest of the procedures mentioned here were carried out in a sterile laminar flow hood using aseptic techniques. The dissected hippocampi and cortices were transferred to sterile 15ml and 50ml falcon tubes respectively. The cortical tissues were cut into smaller pieces using sterile scalpel blade. Both the tissues were washed three times with HBSS (10ml HBSS for hippocampi and 30ml HBSS for cortices). Hippocampi were the incubated in 10ml HBSS containing 0.005% trypsin-EDTA for 9 minutes and cortices in 30ml HBSS containing 0.005% trypsin-EDTA for 15 minutes at 37ºC. The trypsinised tissues were washed three times in HBSS volumes mentioned before and washed once with 1ml and 5ml plating media for

hippocampi and cortices respectively. The hippocampal cell suspension was pipetted up and down several times using 1ml pipette to dissociate hippocampal cells while the cortices were triturated with 5ml serological pipette. The hippocampal cell suspension was diluted with 4ml plating media and the cortical cell suspension was diluted in 25ml plating media.

The cells were counted and for biochemistry 500,000 cortical or hippocampal cells per well of a 6 well dish were plated. For imaging, 200,000 cells per 25mm coverslips were plated and incubated at 37^{o}C incubator overnight.

24 hours after plating, the plating media was replaced with 3 ml of feeding media (Neurobasal® medium supplemented with 2% B27 and 1% Glutamax) and replaced in 37^{o}C incubator until use.

2.4.6 Transfecting neurones

Hippocampal neurones on 25mm coverslips were transfected around DIV 9-10. For each transfection, appropriate amount of DNA (as per the experiment) was added to 100µl of plain Neurobasal® media in a 1.5ml Eppendorf tube. In another 1.5ml Eppendorf tube, 2µl of Lipofectamine® 2000 per µg of DNA was added to another 100µl of plain Neurobasal® media. The solutions were vortexed briefly and left to incubate in rt for 5 mins. The Lipofectamine® tube was added to the DNA tube and vortexed briefly again and allowed to incubate in rt for 30 mins.

Meanwhile, hippocampal neurones on the coverslips were rinsed in warm (37^{o}C) plain Neurobasal® media in a 10cm dish and transferred onto a 6-well dish containing 1ml of feeding media. After 30 mins incubation of the transfection mixture, the tubes were vortexed again and added to the neurones on coverslips in a dropwise manner. The transfection was left to incubate at 37^{o}C for 1.5 hours after which the coverslips were rinsed again in warm (37^{o}C) plain Neurobasal® media in a 10cm dish and transferred back to their original 35mm dish containing the pre-conditioned media. The transfected neurones were placed back into the 37^{o}C incubator and treated as appropriate and immunostained at DIV 14-15.

2.4.7 Viral transduction of neurones

For viral transduction, lentivirus and sindbis aliquots stored at -80ºC were thawed at rt. The appropriate volume (as optimised) of virus were added to the cortical or hippocampal neurones. Sindbis virus was used for GFP overexpression to label cell outline and was produced by Dr. K. A. Wilkinson. Appropriate amount of sindbis expressing GFP were added to hippocampal cultures on coverslips 18h before NMDA and Kainate (KA) treatments. Lentivirus for knockdown and knockdown-rescue studies were added to neurones at DIV 9 and left to incubate for 5-6 days respectively before the stated use.

2.5 Biochemical methods

2.5.1 Subcellular fractionation

All the steps were performed on ice with ice-cold buffers unless stated otherwise. Following stated treatments, the cells were washed with 1x PBS followed by addition of 250µl of Buffer 1 (150mM NaCl, 50mM HEPES pH 7.4, 25µg/ml Digitonin (Sigma) and 1x protease inhibitors) per well of a 6-well dish, incubated for 20 mins, scraped, homogenised, transferred into a 1.5ml Eppendorf tube and centrifuged at 16100g for 30 mins at 4ºC. For each condition, three wells of cells (500,000 per well) were pooled together. The supernatant consisted of the cytosolic proteins and was transferred into a new 1.5ml Eppendorf tube, while the pellet was resuspended in 40µl of Buffer 2 (Buffer 1 with 1% triton), incubated for 20 mins and again centrifuged at 16100g for 30 mins at 4ºC. The supernatant consisted of mitochondrial proteins and was discarded, while the pellet was resuspended in 40µl of Buffer 3 (150mM NaCl, 50mM HEPES pH 7.4, 0.5% sodium deoxycholate, 0.1% SDS, 1x protease inhibitors and 0.5% triton), incubated for 1 hour on a wheel at 4ºC and centrifuged at 16100g for 30 mins at 4ºC. The supernatant was discarded and the pellet, consisting of nuclear proteins, was resuspended in 40µl of buffer 3. The cytosolic supernatant was transferred into a 15ml falcon tube and concentrated using 4 volumes of acetone (kept at -20ºC), incubated at -20ºC for 1 hour and spun for 20 minutes at 3000g and resuspended in 40µl of buffer 3. BCA assay was then performed to determine protein

concentrations to allow equal loading. The workflow is summarised in **Figure 2-1**.

2.5.2 BCA assay

BCA Assay was performed using Pierce™ BCA Protein Assay Kit (Pierce, Thermo Scientific) as per manufacturer's instructions in a clear flat 96-well plate. Following 30 minutes incubation with the required mixture at 37°C, the samples were read using a plate reader (Versamax Microplate reader, Molecular devices) at wavelength of 562nm. The samples were diluted 1:10 in the lysis used to lyse the cells initially. Each sample reads were tested in triplicates. For blank control, a well with just the lysis buffer and no lysate was used to get background read. This was subtracted from other reads. A series of dilutions of known concentrations of BSA (included in the kit) (2µg to 0.0625µg diluted in the lysis buffer) were also prepared and assayed alongside the unknown samples to help determine the unknown concentration.

The values from known BSA concentrations were plotted in an excel sheet and best fit straight line was determined to be used as the standard curve.

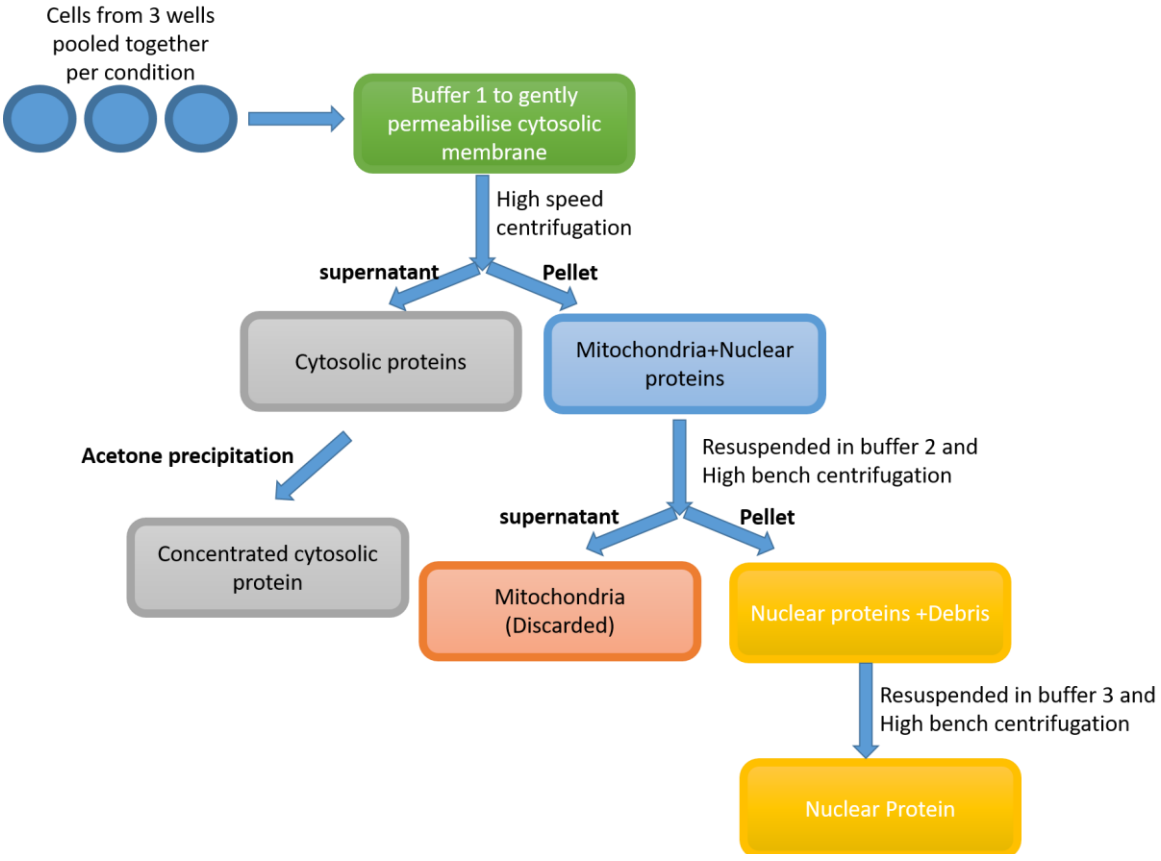

Figure 2-1 Schematic of workflow of subcellular fractionation protocol applied.

Straight-line equation was applied (y=mx+c) to determine the slope (m) and the y-intercept (c) from the standard curve. This was then used to determine the concentration of the unknown samples (x). Once determined and the dilutions were accounted for, the concentrations of each sample were calculated, and equal µg of sample was diluted in 2x sample buffer per condition and loaded on to an SDS-PAGE gel.

2.5.3 Cell lysis for sample preparation

To study the total levels of proteins from cells, the cells were lysed straight into 1x sample buffer (2% SDS, 5% glycerol, 5% β-mercaptoethanol (β-ME), 0.002% bromophenol blue, 0.0625M Tris-HCl pH6.4) or in ice cold lysis buffer (150mM NaCl, 25mM Tris-HCL pH 7.4, 1% Triton-X 100, 0.01% SDS and 1x protease inhibitors (PI)).

1x Laemmli Sample buffer: After required treatments, the cell media was aspirated and 250µl of 1x sample buffer were added into each well of a 6-well dish for cortical and hippocampal neurones. For HEK293T cells, 400µl of 1x sample buffer were added to each well of a 6-well dish. The cells were scraped and transferred into a 1.5ml Eppendorf tube, vortexed briefly and heated at 95^{o}C on a rotating heat block. After this, the samples were spun down briefly and stored at -20^{o}C till used for western blotting purposes.

Lysis buffer: 250µl of lysis buffer were added to neuronal cells in a well per 6 well-dish, scraped and transferred into an Eppendorf tube, then incubated on ice for 30 minutes and centrifuged at 20,000g at 4^{o}C for 20 mins to pellet insoluble debris. Supernatants were dilute 1:1 with 2x Laemmli sample buffer (4% SDS, 10% 2-β-mercaptoethanol (β-ME), 10% glycerol, 125mM Tris-HCl pH 6.4, 0.004% bromophenol blue). Heating and storing of samples were carried out as above.

2.5.4 Cell surface biotinylation and streptavidin pull down

All steps were performed at 4^{o}C with ice-cold buffers unless stated otherwise. Live hippocampal neurones on 6-well dishes post stated treatments, were cooled on ice to prevent any further trafficking events before being washed

twice in 2ml of 1xPBS (10xPBS (Gibco) diluted in ddH_2O). Surface proteins were live-labelled with 1.5ml of membrane impermeable Sulfo-NHS-SS biotin (0.3mg/ml diluted in 1x PBS) for 10 mins with gentle agitation every 2 minutes and washed thrice with 2ml of 1x PBS. 1.5ml of 100mM NH_4CL diluted in 1x PBS was added to quench free biotin-reactive groups for two minutes. The cells were washed twice with 2ml of 1x PBS. Cells were then lysed in lysis buffer (50mM Tris pH 7.4, 150mM NaCl, 1% triton X-100, 0.1% SDS, Protease Inhibitor (X1) in ddH_2O) and scraped onto a 1.5ml Eppendorf tube. The lysates were vortexed briefly and incubated on ice for 30 mins and centrifuged at 20,000g, 4^oC for 20 mins to get rid of cell debris. A 20µl input sample was taken and added to an equal volume of 2x Laemmli sample buffer.

For pulldown, 30µl Pierce^{TM} Streptavidin UltraLink^{TM} Resin beads per pulldown was washed twice with 500µl wash buffer (same as the lysis buffer without the protease inhibitor) by centrifuging at 1500g for 2 minutes at rt and aspiring the supernatant. 100µl of lysates were added to the beads and rotated on a wheel for 90 mins at 4^oC. Following three washes with 500µl wash buffer, the supernatant was aspirated and resuspended in 40µl 2 x Laemmli sample buffer. The input and bead samples in the sample buffer were boiled at 95^oC on a rotating heat block for 10 mins for western blotting analysis.

2.5.5 SDS PAGE

Sodium dodecyl sulphate-polyacrylamide gel electrophoresis (SDS-PAGE) was used to separate proteins based on their molecular weight (MW). 1.5mm glass plates were filled with 10% of acrylamide resolving gel solution (375mM Tris-HCL pH 8.8, 10% acrylamide, 0.1% SDS, 0.1% APS and 0.01% TEMED) and topped with 100% ethanol to ensure even polymerisation of the gel. After resolving gel was polymerised, 100% ethanol was washed off with excess double distilled water (ddH_2O). The resolving gel was stacked with 5% stacking gel (125mM Tris-HCL pH 6.8, 5% acrylamide, 0.1% SDS, 0.1% APS, 0.01% TEMED) and 1.5mm 15-well comb was inserted.

The polymerised gels were assembled into an electrode and inserted into an electrophoresis tank of appropriate size. The tank's reservoirs were filled with SDS-PAGE running buffer (25mM Tris, 250mM glycine and 0.1% SDS in

ddH_2O). Gel loading tips were used to load samples in Laemmli sample buffer on to the wells of the gel along with 4µl protein MW marker. The electrophoresis was carried out initially at 100V to allow the samples to stack onto the stacking gel and were increased up to 150V to allow the proteins to separate.

The separated proteins in the acrylamide gel were then transferred to an Immobilin-PVDF membrane. The membrane was cut into appropriate gel sizes and activated in 100% methanol for 30 seconds and left to equilibrate in the transfer buffer (50mM Tris, 40mM glycine and 20% methanol in ddH_2O) for at least 10 mins. The membrane, gel, cellulose chromatography papers (cut into appropriate gel sizes) and sponges were soaked in transfer buffer and assembled in a wet transfer cassette according to manufacturer's instructions and run at 400mA. The acrylamide gel was removed from the glass plates and stacking gels were discarded. The sponges and the chromatography papers were used to sandwich the gel and the activated membrane. The assembled cassette was then placed into the electrode with the membrane facing the anode and the gel facing the cathode, which was then transferred into a tank filled with transfer buffer. The wet transfer was carried out at 400mA for 70 mins with constant stirring and cooling with ice packs.

2.5.6 Western blotting

2.5.6.1 Immunoblotting

Once the transfer was completed, the membrane was removed from the wet transfer cassette and blocked in 5% non-fat milk powder in PBS-T (PBS (recipe: 0.137M NaCl, 2.7mM KCl, 10mM Na_2HPO_4, 2mM K_2HPO_4, pH to 7.4 with HCl) + 0.001% Tween-20) for an hour at rt. The membrane was then incubated with primary antibody diluted to appropriate concentration in 2.5% milk in PBS-T (see **Table 2-2**) overnight at 4^oC on a shaker. Following incubation, the membrane was washed three times with PBS-T for 5 minutes at rt on to remove any excess unbound primary antibody. The membrane was then incubated with the respective secondary antibodies diluted 1:10,000 in 5% milk in PBS-T in rt for an hour. Again, the membrane was washed three

times with PBS-T for 5 mins each to remove excess unbound secondary antibodies at rt on a shaker.

2.5.6.2 Chemiluminescence detection

For protein visualisation, the membrane was incubated for 2 mins at rt with one of the following substrates in order of increasing sensitivity:

- SuperSignal® West Pico Enhanced Chemiluminescence (ECL)
- Luminata™ Crescendo
- Luminata™ Forte
- West Femto ECL

Once the excess ECL was removed, the membrane was placed on an Odyssey Fc detection system tray and placed in the machine. The ECL substrate signal was detected using the chemiluminescence channel for 2-5 mins and the marker was detected using the 700-fluorescence channel.

If the machine detection system was not sensitive enough, ECL-incubated membrane was sandwiched between sheets of acetate in a developing cassette. The ECL substrate signal was then detected in a dark room by exposing the X-ray film of appropriate sizes to the membrane (for required amount of time) and developing the film in an automatic medical X-ray film processor.

2.5.7 Membrane stripping

The membranes were stripped and reprobed with different primary antibodies as well when needed. For this, the membrane was given three quick washes with PBS-T and incubated with 5ml of Restore™ Stripping buffer (Thermo Scientific) for 15 minutes at 65^{o}C and washed three times with PBS-T quickly and one 15 mins wash with PBS-T on a shaker at rt. The membrane was then re-blocked for 30 mins before incubating with another primary antibody.

2.5.8 Quantification and analysis of immunoblots

Western blot data from the Odyssey Fc detection system was quantified as pixel signal intensity per protein bands using ImageStudio Lite Version 5.2 (LI-COR). Data on the X-ray film was scanned using a scanner and analysed by

measuring densitometry using the Gel Analysis Tool in FIJI ImageJ (NIH). The relative pixel intensity was calculated as the area under each peak. The values obtained with both systems were transferred to Microsoft Excel and normalised to the appropriate bands and statistical significance measured [See section 2.10].

For all surface biotinylation analysis, the surface pulldown fraction and input (total) lysates were always run on the same gel and visualised using LI-COR on the same membrane. The pixel signal intensity per protein band was determined for both surface and total fraction. Surface/Total ratio was then determined by dividing the surface signal values with that of the total.

2.6 Fixed cell imaging

2.6.1 Immunocytochemistry

For fixed cell imaging, hippocampal neurones were plated at 200,000 per 25mm glass coverslips. After required transfection [see section 2.4.6] or transduction [see section 2.4.7], the cells were fixed in 1ml warm to 37ºC 4% PFA (16% PFA diluted 1:4 in 1 x PBS and 5% sucrose) for 10 minutes at rt. All steps after this stage was also carried out in rt unless stated otherwise. After 10 mins fixation, the coverslips were washed three times in 2ml of 1x PBS (10x PBS diluted in ddH_2O). Then, 1ml of 100mM glycine was used to quench the PFA for 2 minutes. The coverslips were then washed three times with 2ml of 1x PBS again. Neurones were permeabilised and blocked with 0.1% triton in 3% BSA in 1xPBS for 30 mins. The primary antibodies were diluted to appropriate concentration as described in section 2.1.9.1 in 3% BSA in 1xPBS. After blocking, neurones were incubated in primary antibody for 1 hour. For this, the 90µl of the antibody mix was pipetted onto a Parafilm and the coverslip was flipped over with cell side down on to the mixture. The coverslips were transferred back to their dishes and washed again three times in 2ml of 1xPBS for 5 mins each on a gentle shaker. Secondary antibodies were then diluted 1:400 in 3% BSA in 1xPBS and the coverslips were incubated in it for 45 minutes (same protocol as the primary incubation). After three x 5 minutes washes to remove excess secondaries, the coverslips were

washed once with ddH_2O and mounted on a glass microscope slides using 40µl of Fluoromount-G™ with DAPI (Thermo Fisher) and left to dry at rt overnight before storing them at 4°C before imaging.

2.6.2 Image acquisition

The coverslips were imaged using Leica SP5-II confocal laser scanning microscope attached to a Leica DMI 6000 inverted epifluorescence microscope. The confocal images were captured under 63x HCxPL APO CS oil-immersion objective, with 1024x1024 pixel resolution and 1x optical zoom at 400Hz. Frame average of 2 was taken with a Z-stack of 6-8 Z-planes with 0.5µM interval. DAPI was excited using a 50 mW 405nm diode laser, Cy2 was excited using 150mW Ar laser (488nm), Cy3 using 20mW solid state yellow laser (561nm) and Cy5 using a 20mW Red He/Ne (633nm). All the parameters with excitation and gain were kept constant for a complete set of experiments. Number of neurones imaged are quantified in the figure legends and the neurones were acquired from at least three independent dissections as stated.

2.7 Scaling protocol

Dyas in Vitro (DIV) 14-15 hippocampal neurones plated for coverslips or biochemistry were treated with 1µM TTX (Tocris Bioscience, 1mM stock in ddH_2O and stored at 4°C) for 24 hours to induce up-scaling process.

For down-scaling protocol, DIV 16-17 hippocampal neurones were treated with 40µM bicuculline (bic) (Sigma, 40mM stock in DMSO, aliquoted and stored at -20°C). The control cells were treated with the equal volume of DMSO for the longest length of time.

2.8 Cycloheximide assay

For cycloheximide assay, cycloheximide (CHX) (Sigma, stored at 4°C) could thaw at rt and 25µg/ml was added to cortical neurones and 50µg/ml was added to HEK293T cells for the stated lengths of time.

2.9 Developmental time-course

For neuronal developmental time course, neurones at indicated Days in vitro (DIVs) were washed once with 2ml of 1x PBS at rt. The cells were plated at 1 million per 35mm cell culture dish. Cells up to DIV 7 were lysed in 150µl of lysis buffer and cells between DIV 7-12 were lysed in 250µl volume of lysis buffer. Following the lysis buffer protocol, BCA Assay was performed to measure protein concentration. Equal amount of protein per DIV was mixed with 2x Laemmli Sample Buffer to prepare for western blotting analysis. For RNA extraction, RNA extraction protocol was followed as above at the indicated DIVs.

2.10 Statistical analysis and figures

Statistical Analysis was performed using Graphpad Prism version 7.0. All statistical tests are labelled per figure with n (number of cells) or N (number of dissections) values along with the p-values and error bars. All the graphs were prepared using Graphpad Prism version 7.0 and the results images and cartoon schematics were prepared using Microsoft Powerpoint 2013. The original figures that were adapted into figures and schematics are cited accordingly and copyright permission were obtained for figures taken from sources online as indicated.

Chapter 3. ROLES OF KAINATE RECEPTORS IN VARIOUS FORMS OF SYNAPTIC PLASTICITY

3.1 Introduction

Previous studies have shown kainate receptor (KAR) involvement in various forms of plasticity. More specifically, as set out below KARs have been shown to be able to induce synaptic plasticity and undergo plasticity themselves.

3.1.1 KAR surface expression is bidirectionally regulated in response to activity

KARs can signal through both ionotropic and metabotropic pathways. This pertussis-toxin sensitive non-canonical metabotropic signalling from KARs has been reported to be involved in its trafficking. Sustained activation of KARs decreases surface expressed postsynaptic KARs in a Ca^{2+} and PKA independent but PKC-dependent manner (Martin and Henley 2004). The surface GluK2-KARs are internalised and are targeted for lysosomal degradation. Similarly, NMDA activation also induces KAR internalisation in a Ca^{2+}, PKA and PKC dependent manner but are then recycled back to the plasma membrane (Martin and Henley 2004).

On the other hand, transient/mild agonist stimulation increases postsynaptic KARs surface expression, which is thought to enhance synaptic activity and promote network development and stabilisation (Martin, Bouschet et al. 2008). The kainate evoked increase in surface KARs is dependent on its metabotropic signalling, which results in increased recycling of KARs via Rab-11 dependent, transferrin-positive endosomes to synapses (Gonzalez-Gonzalez and Henley 2013). This positive KAR feedback system potentially allows the adjustment of neuronal responsiveness according to the stimulus intensity.

3.1.2 KARs regulate AMPAR synaptic plasticity

While NMDAR mediated LTP is the best characterised form of LTP, NMDAR independent forms of LTP have also been shown to occur. Hippocampal mossy fibre-CA3 synapses, which expresses both pre-and post-synaptic KARs, express a NMDAR independent form of LTP (Bortolotto, Clarke et al. 1999, More, Nistico et al. 2004), which is mediated by the activation of pre-synaptic KAR signalling facilitating glutamate release (Lauri, Bortolotto et al. 2001). Initially this was reported to be a GluK1 containing KAR mediated

signalling mechanism, but subsequent studies revealed that the metabotropic action of GluK2 containing KARs is essential to mediate this form of LTP (Contractor, Swanson et al. 2000, Breustedt and Schmitz 2004). Thus, although the precise KAR subunit/combination of subunits responsible is still a point of debate, it is clear that KARs can mediate LTP at these MF-CA3 synapses. Activation of pre-synaptic KARs by agonist kainate have also been shown to decrease glutamate release at CA3-CA1 pyramidal cell synapses resulting in decrease in pre-synaptic Ca^{2+} influx (Chittajallu, Vignes et al. 1996, Kamiya and Ozawa 1998). Moreover, the KAR mediated depression of glutamate release was shown to be mediated via direct metabotropic action of pre-synaptic KARs (Frerking, Schmitz et al. 2001).

More recently, it has been shown that following transient/mild activation of KARs at CA1 synapses, functional AMPA receptor (AMPAR) synaptic expression increases, driven by increased AMPAR-receptor recycling. This novel form of KAR-dependent, NMDAR-independent LTP at CA1 synapses is mediated via metabotropic action of GluK2-containing KARs and subsequent activation of G protein, PKC and PLC (Petrovic, Viana da Silva et al. 2017) [**Figure 3-1**]. Moreover, GluK2-/- mice lacked this form of LTP further establishing GluK2 to be the important subunit for this novel form of LTP (Petrovic, Viana da Silva et al. 2017).

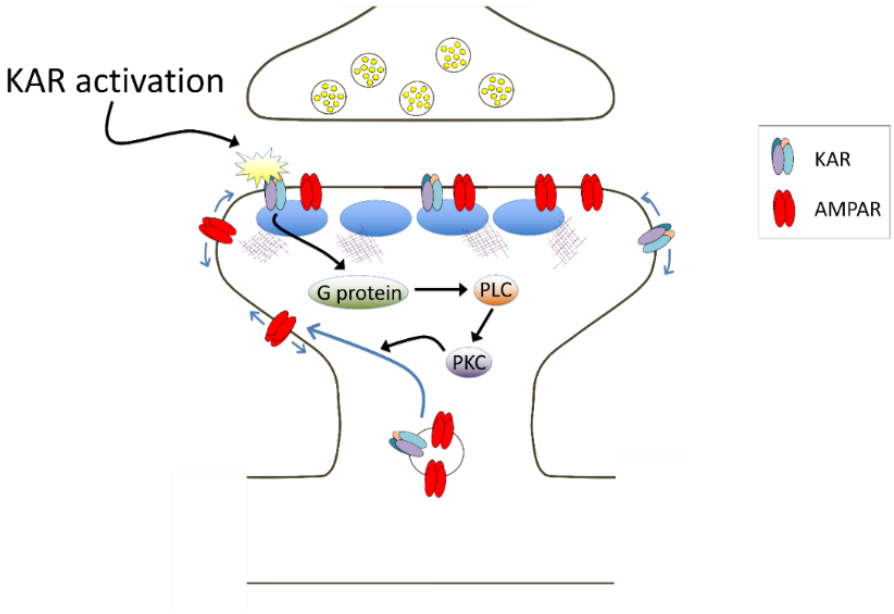

Figure 3-1: KAR_{AMPAR}-LTP mechanism at CA3-CA1 synapses.

Stimulation of postsynaptic GluK2 containing KARs leads to the downstream metabotropic signalling activating pertussis toxin sensitive G-protein, PLC and PKC pathway; leading to increased AMPAR exocytosis from the recycling endosomes. Figure taken from (Evans, Gurung et al. 2017).

In addition, GluK2 Q/R editing deficient mice also displayed a form of NMDAR-independent LTP at the medial perforant path-dentate gyrus synapse. When NMDAR activity was inhibited, the Ca^{2+} influx through unedited GluK2-containing KARs were enough to induce NMDAR independent LTP (Vissel, Royle et al. 2001). This further shows the importance of KARs in synaptic plasticity.

Together, these findings indicate that KARs play key roles in the induction of synaptic plasticity.

3.1.3 KARs can exhibit plasticity themselves

Post synaptic GluK2 and GluK5 containing KARs at mossy fibre synapses can also undergo LTD (KAR-LTD), which was experimentally induced using low frequency stimulation (LFS) (Selak, Paternain et al. 2009) or post-synaptic depolarisation (Chamberlain, Gonzalez-Gonzalez et al. 2012). In terms of mechanism, SUMOylation of GluK2 at K886 triggered by GluK2 phosphorylation by PKC was shown to lead to activity dependent KAR-LTD (Chamberlain, Gonzalez-Gonzalez et al. 2012). Interestingly, phosphorylation

at S846 by PKC promotes recycling of GluK2-KARs back to the plasma membrane in the absence of SUMOylation while phosphorylation at S868 in combination with K886 SUMOylation results in endocytosis of KARs leading to KAR-LTD as such SUMOylation is thought to act as a molecular switch that regulates this KAR-LTD (Martin and Henley 2004, Martin, Bouschet et al. 2008, Nasu-Nishimura, Jaffe et al. 2010, Konopacki, Jaafari et al. 2011). GluK5 internalisation was also shown to be required for KAR-LTD at mossy fibre-CA3 synapses, which was regulated by its interaction with SNAP-25 (Selak, Paternain et al. 2009). It was thus proposed that during LTD, KARs containing both GluK2 and GluK5 are removed from the synapses (Chamberlain, Gonzalez-Gonzalez et al. 2012).

While KARs synaptic responses in mossy fibres are only the minor component of mossy fibre-Excitatory Post Synaptic Potentials (EPSPs), it was shown that KAR-LTD relieves the inhibition of the slow afterhyperpolarisation (sAHP) mediated by KAR metabotropic function (Melyan, Wheal et al. 2002) [section 1.2.2.8], thus allowing KAR plasticity to regulate cellular excitability (Chamberlain, Sadowski et al. 2013).

3.1.4 KARs in homeostatic scaling

The role of AMPARs and NMDARs in homeostatic scaling in response to chronic suppression and enhancement of synaptic activity is well established and characterised (Turrigiano 2012) while very limited reports of KAR scaling exists. A study in cerebellar mossy fibre-granule cell synapses showed that the loss of synaptic AMPARs increased KAR-mediated synaptic transmission. This increase in post synaptic KAR activity was shown to be mediated by the increased expression of high affinity GluK5 subunit of KAR (Yan, Yamasaki et al. 2013). This indicated a potential role of KARs in homeostatic scaling response in the absence of AMPAR signalling.

Recently, a proteome study in which newly synthesised proteins were metabolically labelled, captured and identified during homeostatic scaling, GluK2 synthesis was shown to be up-regulated during scaling-up and downregulated during scaling-down (Schanzenbächer, Sambandan et al. 2016). However, while this study captured changes in *de novo* protein

synthesis during scaling, it does not account for changes in other cellular processes such as recycling or degradation that also play key roles in regulating protein levels during activity. Nevertheless, these initial studies suggest KARs may be subject to homeostatic scaling.

3.1.5 KAR assembly and trafficking regulates their surface expression

KARs are thought to favourably oligomerise as heteromers over forming homomeric assemblies. Studies on GluK2/GluK5 receptors have shown them to initially assemble as heterodimers thus favouring heteromeric assembly (Kumar, Schuck et al. 2011, Reiner, Arant et al. 2012). Moreover, high affinity subunits GluK4 and GluK5 are only functional as heteromers with low affinity subunits GluK1-3 (Ayalon and Stern-Bach 2001). For instance, GluK2 assembly with GluK5 disrupts the ER retention of GluK5 by reducing its binding to COPI thus allowing GluK5 to exit the ER efficiently and express on the surface. Increased association of GluK5 with 14-3-3 is also thought to contribute to their increased surface expression (Vivithanaporn, Yan et al. 2006). Interestingly, GluK1 and GluK2 but not necessarily GluK3 is thought to predominantly regulate GluK5 surface expression in the hippocampus (Darstein, Petralia et al. 2003, Christensen, Paternain et al. 2004, Ruiz, Sachidhanandam et al. 2005). However, GluK1-/- mice did not have altered GluK5 surface expression, suggesting GluK2 to be the partnering subunit of GluK5 (Ball, Atlason et al. 2010). Furthermore, GluK2 Q/R editing that occurs in the channel pore region also regulates the surface expression of KAR, potentially acting as a rate limiting factor of KAR ER exit whilst also favouring heteromeric assembly with GluK5 (Ball, Atlason et al. 2010). In addition, GluK2 homomers have also been shown to exist alongside GluK2/GluK5 heteromers (Barberis, Sachidhanandam et al. 2008, Ma-Hogemeier, Korber et al. 2010). Thus, both subunit composition and editing status of subunits can regulate membrane delivery of KARs, which could have implications during activity mediated trafficking.

3.1.6 Objectives

As many lines of evidence point towards the role of KARs in various forms of plasticity, my initial objective was to confirm and validate KAR plasticity and then investigate the underlying mechanisms. I restricted analysis to GluK2 containing KARs because GluK2, along with GluK5, are the predominant KAR subunits expressed in hippocampal neurones and almost uniquely among the KAR subunits high quality GluK2 antibodies are available. Previous studies in this lab, on which my work builds, also focused on GluK2 containing KARs. Some of my work has also focused on GluK5 containing KARs. More specifically, my objectives were to address the following questions:

1. Can transient KARs stimulation increase AMPAR surface expression (LTP)? If so, what are the possible mechanisms?
2. Can sustained KARs stimulation decrease AMPAR surface expression (LTD)? If so, what are the possible mechanisms?
3. Can KARs themselves undergo homeostatic scaling?

3.2 Materials and methods

3.2.1 Pharmacological stimulation

3.2.1.1 Solutions

- HEPES-buffered Saline (HBS) Buffer

Table 3-1: Components in HBS Buffer.

Components	Concentration (mM)
NaCl	137
D-glucose	5
KCl	15
HEPES	25
$CaCl_2$	1.5
$MgSO_4$	1.5

pH was adjusted to 7.4 with NaOH and osmolarity adjusted to match the cellular media. Osmolarity was measured with an osmometer (Model 3320, Advanced Instruments, Inc). The solutions were warmed to 37^{o}C before experiments.

3.2.1.2 Transient kainate (KA) and NMDA stimulation

The protocol for transient kainate (KA) stimulation was adapted from (Martin, Bouschet et al. 2008, Gonzalez-Gonzalez and Henley 2013, Petrovic, Viana da Silva et al. 2017). Following one wash with 1.5ml HBS buffer, DIV 15 cortical neurones were pre-incubated in 1.5ml of HBS containing 0.5µM TTX for 15 minutes (mins) at 37^{o}C. The cells were then treated with 1.5ml HBS either containing 10µM kainate (KA) or 25µM NMDA or no drugs (control cells) for 3 mins, all in the presence of TTX. The drugs were washed off with 1.5ml of HBS+TTX twice and cells were incubated with 1.5ml of HBS+TTX media for further 20 mins at 37^{o}C to allow AMPAR trafficking. After 20 mins, the cells were allowed to cool on ice for 2-3 mins to stop any further trafficking and surface biotinylation was performed (see section 2.5.4).

3.2.1.3 Sustained kainate (KA) stimulation

For sustained KA stimulation, the protocol was adapted from (Martin and Henley 2004, Martin, Bouschet et al. 2008). The HBS buffer consisted of 0.5µM TTX and 40µM GYKI throughout the protocol. The cells were preincubated as above for 15 mins and the cells were then treated with HBS buffer containing 10µM KA or no KA at 37^{o}C for 10 or 20 mins. For the 10 mins treatment, the cells were treated with KA for the last 10 mins of incubation. Surface biotinylation was then performed for both 10- and 20-mins stimulation together.

3.2.2 Live immunolabelling and surface staining

Imaging experiments were also performed after transient KA and NMDA stimulation. Before the stimulation, the cells were incubated with 10µl of GFP Sindbis* virus overnight (no more than 24 hours) to fill the cell with GFP and outline the cell structure for imaging. Following stimulation, live cells on 25mm coverslips (150,000) were incubated with the N-terminal targeted GluA2 (Millipore, 1:70) and GluA1 antibody (Millipore, 1:100) for the last 15 mins of incubation at 37^{o}C post 3 mins stimulation. The antibodies were diluted in the HBS+TTX buffer and 100µl of the antibody solution were placed on a parafilm on heated tray and the coverslips were placed on the top with the cell-side down.

Following 15 mins incubation, cells were returned to their dishes and washed 5 times with 2ml of 1x PBS at room temperature. The cells were then fixed with warmed 1ml of 4% paraformaldehyde (16% PFA diluted 1:4 in 1x PBS and 5% sucrose) for 10 mins and washed three times with 2ml of 1x PBS, quenched with 1ml of 100mM glycine made up in PBS for 2 mins and washed again three times with 2ml of 1x PBS. Anti-mouse Cy5 secondary (diluted 1:400 in 3% Bovine Serum Albumin (BSA in 1x PBS)) was added for 45 mins. 100µl of diluted secondary antibody was added to parafilm and cells were placed on top with cell-side down. The coverslips were returned to their dishes after 45 mins and washed three times with 1x PBS and once with distilled water. The cells were then mounted on glass slides using Fluoromount-G^{TM} with DAPI (Thermo Fisher) with the cell side facing down. The slides were left to dry at room temperature overnight and stored at 4^{o}C till imaging. **Figure 3-2**

is a schematic depicting timeline at which different stages of drug treatment and live immunolabelling was performed.

*Sindbis-GFP virus was prepared by Dr. K.A. Wilkinson.

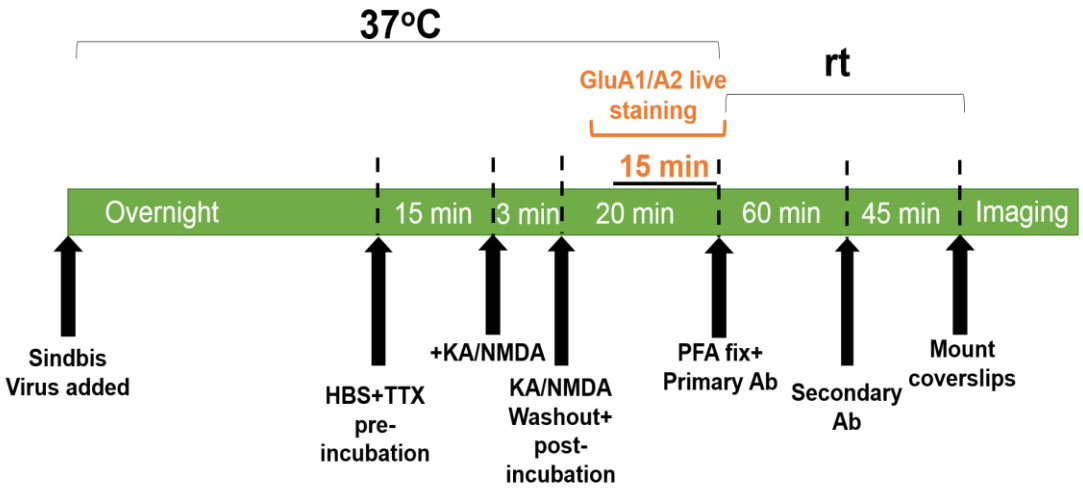

Figure 3-2: Timeline of live immunolabelling with drug stimulation.

The cells were treated with GFP expressing Sindbis virus overnight (~18h) to help outline the cell structure before performing the drug (KA or NMDA) stimulation and live immunolabelling with N-terminal targeted GluA1 or GluA2 antibody during the last 15 minutes of post-treatment incubation. The cells were then fixed and immunolabelled with the secondary antibodies before mounting.

3.2.3 Image acquisition and analysis

Image acquisition was performed as per section 2.6.2.

The cells were chosen for imaging using 488 channel (GFP) to avoid bias. The images were analysed using FIJI ImageJ (NIH). Rectangular boxes were drawn at dendrites and GFP channel was used to draw an outline around the dendritic structure (Region of Interest (ROI)). Mean intensity per selected area (ROI) was determined. Three dendritic regions per neuron were analysed and averaged to get the surface intensity per cell (n value). Cells from at least 3 independent dissections were analysed.

3.2.4 Electrophysiology

All electrophysiology experiments were performed by Dr. Ellen Braksator.

3.2.4.1 Materials

- Sucrose Solution

Table 3-2: Components in Sucrose Solution

Components	Concentration (mM)
Sucrose	189
D-glucose	10
$NaHCO_3$	26
KCl	3
$MgSO_4$	5
$CaCl_2$	1
NaH_2PO_4	1.25

- Artificial cerebrospinal fluid (aCSF)

Table 3-3: Components in aCSF solution.

Components	Concentration (mM)
NaCl	124
$NaHCO_3$	26
KCl	3
NaH_2PO_4	1
$MgSO_4$	1
D-glucose	10
$CaCl_2$	2

- Patch-clamp electrode solution

Table 3-4: Components in Patch-clamp electrode solution.

Components	Concentration (mM)
$CsMeSO_4$	130
NaCl	8
Mg-ATP	4
NA-GTP	0.3
EGTA	0.5
HEPES	10
QX-314-Cl	5

pH was adjusted to 7.2.

3.2.4.2 Acute slice preparation

Postnatal day 13-15 male and female Han Wistar rats were anaesthetised with 4% isoflurane and decapitated. Brains were rapidly removed and placed in 4^{o}C oxygenated (95% O_2, 5% CO_2) sucrose solution. Parasagittal hippocampal slices 400µm thick were prepared using a vibratome (7000smz-2, Campden Instruments). Slices were kept in a slice holder containing artificial cerebrospinal fluid (aCSF) and incubated for 30 mins at 35^{o}C and then for a further 30 mins at room temperature before use.

3.2.4.3 Electrophysiology and analysis

Hippocampal slices were placed in a submerged holding chamber and perfused with 30^{o}C oxygenated aCSF at 2ml.min^{-1}. Excitatory post-synaptic currents (EPSCs) of AMPA transmission were evoked at -70mV by stimulating the Schaffer collateral pathway and recorded from CA1 pyramidal neurons. Pyramidal neurons were patch-clamped in the whole-cell configuration using borosilicate glass (Harvard Apparatus) electrodes with a resistance of 2-5 MΩ and were backfilled with electrode solutions. The CA3 area of the hippocampal slices was removed using a scalpel blade to minimise epileptic activity. D-AP5 (50 µM) and picrotoxin (50 µM) were bath applied to isolate AMPA-mediated EPSCs. Cells in which the series resistance changed above 20 MΩ or deviated by 20% were discarded.

After a 10 mins stable baseline was achieved, 1µM kainate (KA) was bath applied for 10 mins followed by a 30 mins washout period.

Signals were low-pass filtered at 2 kHz and digitised at 10 kHz using a Axopatch 200B amplifier (Molecular Devices) and WinLTP v1.11 acquisition software (Anderson and Collingridge 2007).

3.2.4.4 Statistical analysis

For statistical analysis GraphPad Prism 7 was used (GraphPad Software, Inc.). Results are expressed as mean ± SEM and Student's t-test was used to assess statistical significance.

3.3 Results

3.3.1 Transient kainate (KA) stimulation did not alter surface levels of GluK2-KARs or GluA1- and GluA2-AMPARs

To study the role of KARs in LTP I first attempted to recapitulate previously published work, which showed transient stimulation of KARs increased the surface expression of AMPARs. I performed surface biotinylation experiments on cortical neurones following 3 mins 10µM kainate (KA) stimulation. However, I did not detect any changes in the surface expression of either GluA1 or GluA2 containing AMPARs or GluK2 containing KARs [**Figure 3-3** A, B, C and D]. As a control, NMDA mediated LTD was induced in parallel to ensure neuronal health was not compromised, which could have resulted in the lack of activity induction. NMDA application significantly decreased the surface expression of both GluA1 and GluA2-containing AMPARs as expected (Luthi, Chittajallu et al. 1999, Beattie, Carroll et al. 2000) and also decreased the surface expression of GluK2 containing KARs, which has been shown previously (Martin and Henley 2004). Hence, my results showed lack of change in the surface expression of AMPARs following kainate (KA) application. EGFR, which did not respond to the KA stimulation [**Figure 3-3** A and E], was used as a non-glutamate surface receptor control to ensure the effect of treatment is specific to the surface expression of glutamate receptors.

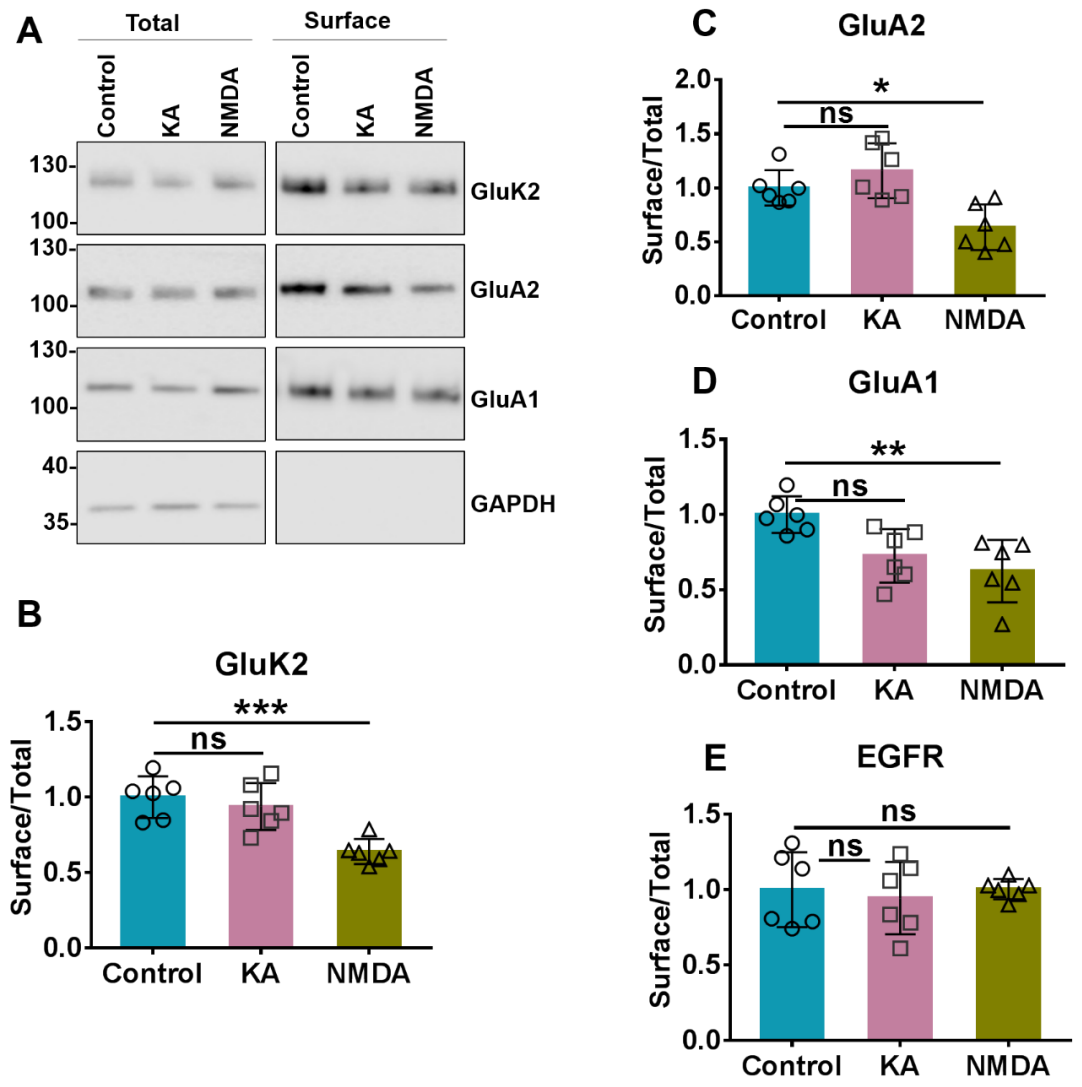

Figure 3-3: Transient KA stimulation did not change GluA1, GluA2 and GluK2 surface expression. Surface biotinylation was performed on DIV 15 cortical neurones following 3 mins transient stimulation with KA (10μM) and 3 mins NMDA (25μM) stimulation to isolate surface proteins and determine surface/total ratio by western blotting.

A. Representative western blot images of surface and total levels of GluK2, GluA2, GluA1 and EGFR post KA or NMDA treatment. EGFR was used as a surface expressed non-glutamate receptor control that should not respond to stimulation. GAPDH was used as an internal control to determine no internal proteins were biotinylated.

B-E. Quantification of surface to total ratio of GluK2 (B), GluA2 (C), GluA1 (D) and EGFR (E) shown in A. N=6 independent dissections, ns $p>0.05$, *$p<0.05$, **$p<0.01$, ***<0.001; One-way ANOVA with Dunnett's multiple post comparisons correction; error bars=S.D.

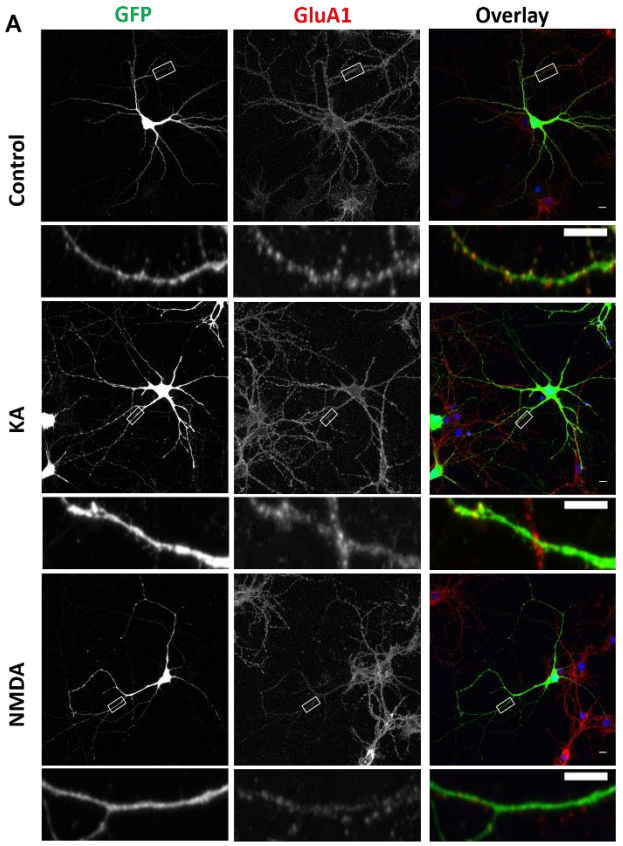
A
GFP
GluA1
Overlay
Control
KA
NMDA

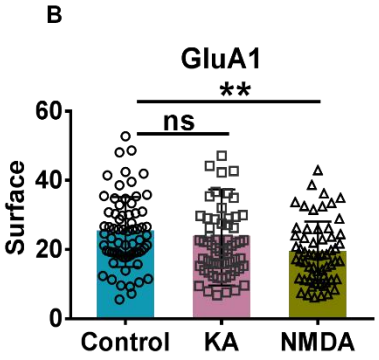
B
GluA1
**
ns
Surface
60
40
20
0
Control
KA
NMDA

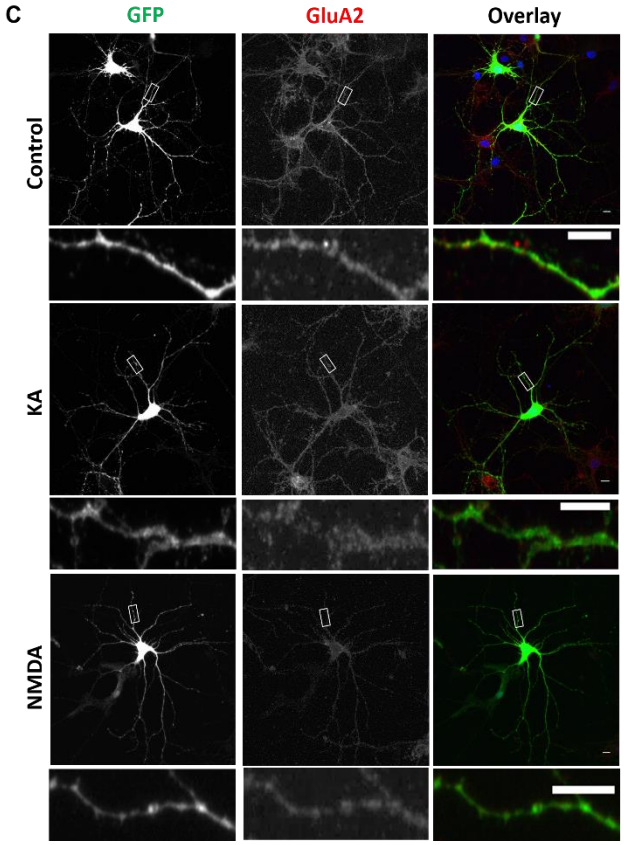
C
GFP
GluA2
Overlay
Control
KA
NMDA

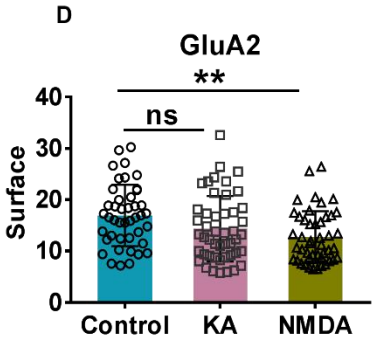
D
GluA2
**
ns
Surface
40
30
20
10
0
Control
KA
NMDA

Figure 3-4: Transient KA stimulation did not change GluA1 or GluA2 surface expression. Live cell immunolabelling was performed on DIV 15 hippocampal neurones following 3 mins transient stimulation with KA (10µM) and 3 mins NMDA (25µM) stimulation to determine surface levels of GluA1 and GluA2.

A. Representative images of surface GluA1 (Cy3-red) on GFP labelled neurones. White boxes represent regions of interest, zoom panel underneath each image within dendritic regions that were analysed for surface intensity. Scale bar=10µm.

B. Quantification of surface intensity of GluA1 shown in (A). Intensity within three regions of interest within dendrites per cell was measured and averaged to get a red per cell. n=60-68 cells, N= 3 independent dissections. ns p>0.05, **p<0.01; One-way ANOVA with Dunnett's multiple post comparisons correction; error bars=S.D.

C. Representative images of surface GluA2 (Cy3-red) on GFP labelled neurones. White boxes represent regions of interest, zoom panel underneath each image within dendritic regions that were analysed for surface intensity. Scale bar=10µm.

D. Quantification of surface intensity of GluA2 shown in (C). Intensity within three regions of interest within dendrites per cell was measured and averaged to get a red per cell. n=43-47 cells, N= 3 independent dissections; ns p>0.05, **p<0.01; One-way ANOVA with Dunnett's multiple post comparisons correction; error bars=S.D.

Surface biotinylation can only measure changes in the whole surface area of neurones, which may mask compartment restricted changes. To assess potential compartment specific changes in surface expression of AMPARs, I also performed imaging experiments to assess the effects of KA stimulation in hippocampal neurones, focusing on regions of interest (ROIs) within dendrites [**Figure 3-4**]. However, I was again unable to see an increase in GluA1 or GluA2-containing AMPARs post transient KA stimulation. Similar to the surface biotinylation experiments, I did see a decrease in surface levels of GluA1 and GluA2 post 3 mins NMDA stimulation. Because there is no reliable and effective N-terminal GluK2 antibody available to monitor surface staining I could not study the surface levels of GluK2 containing KARs in parallel.

3.3.2 Sustained KA stimulation alters the surface levels of GluK2-KARs and GluA1- and GluA2-AMPARs

Because I was unable to repeat the previously reported KAR_{AMPAR}-LTP studies, I started investigating potential role of KARs in AMPAR-LTD. Here, cortical neurones were incubated with 10µM KA for 10 or 20 mins in presence of 40µM GYKI53655 (an AMPAR antagonist) (Partin and Mayer 1996) and

surface biotinylation was performed. In this case I did successfully recapitulate previous findings where following 20 mins stimulation surface expression of GluK2 containing KARs decreased [**Figure 3-5** A and B] (Martin and Henley 2004). In addition, this change in surface expression of KARs was also followed by significant decrease in the surface expression of GluA2-containing AMPARs post 20 mins treatment [**Figure 3-5** A and C]. Post 10 mins stimulation, an apparent decrease was observed for both GluK2 and GluA2 containing AMPARs, although this change was not significant. As these experiments were performed in the presence of AMPAR inhibitor (GYKI53655), these observations suggest that changes in AMPAR surface expression is most likely being regulated by KAR signalling. As expected EGFR did not respond to the KA stimulation [**Figure 3-5** A and D].

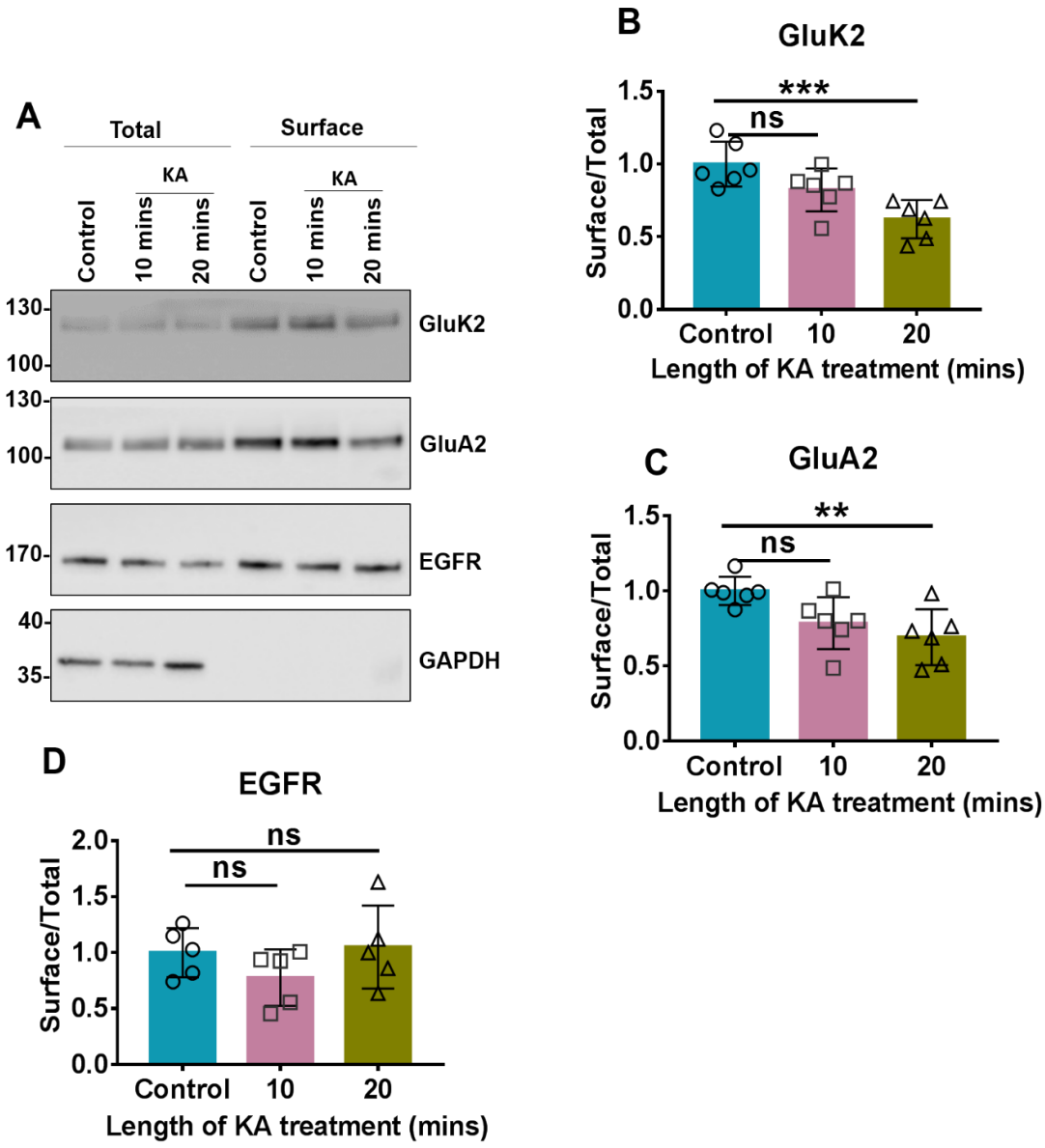

Figure 3-5: Sustained KA (10μM) stimulation in presence of AMPAR inhibitor (GYKI53655) 40μM decreases surface expression of GluK2 and GluA2. Surface biotinylation was performed on DIV 15 cortical neurones following 10 or 20 mins of sustained KA stimulation to isolate surface proteins and determine surface/total ratio by western blotting.

A. Representative western blot images of surface and total levels of GluK2, GluA2 and EGFR post 10 and 20 mins KA treatment. EGFR was used as a surface expressed non-glutamate receptor control that should not respond to stimulation. GAPDH was used as an internal control to determine no internal proteins were biotinylated.

B-E. Quantification of surface to total ratio of GluK2 (B), GluA2 (C) and EGFR (D) shown in A. N=5-6 independent dissections, ns $p>0.05$, ** $p<0.01$, *** <0.001; One-way ANOVA with Dunnett's multiple post comparisons correction; error bars=S.D.

3.3.3 Sustained KA stimulation evokes initial AMPAR-EPSC depression in CA1 hippocampal slices

Since sustained KA stimulation showed a potential role of KARs in AMPAR-LTD, we decided to follow this study using electrophysiology in CA1 hippocampal slices. All the electrophysiology studies in this chapter were performed and analysed by Dr. Ellen Brakastor.

During 10 mins application of 1µM KA, we observed an initial depression of evoked AMPAR-Excitatory Post Synaptic Currents (EPSCs). Following a 30 mins washout period, responses remained significantly depressed compared to the pre-KA application baseline in the same slice (baseline 100.3 ± 0.27% vs KA 73.62 ± 5.67%; p=0.0003). However, a run-down of response was observed in the vehicle control group in the last 10 mins of the recording and therefore no significant difference was observed between the control slices and those treated with KA (vehicle control 85.03 ± 2.55% (n = 10) vs KA 73.62 ± 5.67% (n = 17); p=0.1503) [**Figure 3-6** A, B and C].

UBP310 compound was synthesised as an inhibitor of ionotropic function of GluK1 and GluK3 subunit containing KARs (Dolman, More et al. 2007, Perrais, Pinheiro et al. 2009) but was later shown to also antagonise ionotropic functions of GluK2 and GluK5 containing KARs (Pinheiro, Lanore et al. 2013, Petrovic, Viana da Silva et al. 2017) while not affecting the AMPA or NMDA receptors (Pinheiro, Lanore et al. 2013). We therefore used UBP310 to determine if the changes we observed with the KA application were mediated through KAR ionotropic function. When KA was applied in the continuous presence of UBP310 (10µM), the initial reduction in AMPAR EPSCs (average of first 10 mins washout) was significantly less compared to KA treatment alone (KA + UBP310 65.46 ± 6.98% (n = 9) vs KA alone 44.64 ± 3.32 (n = 18); (p = 0.0051) but there was no significant difference in AMPA-EPSCs amplitude when comparing to the last 10 mins (KA + UBP310 92.2 ± 9.48% vs KA alone 73.62 ± 5.67%; P = 0.0860) [**Figure 3-6** A, D, E and F]. We interpret these results to suggest that the initial KA-evoked AMPAR EPSCs depression is mediated via KAR ionotropic function, but it seems the changes are not

sustained long-term (last 10 mins post stimulation), perhaps suggesting this to be a form of short-term plasticity (STP).

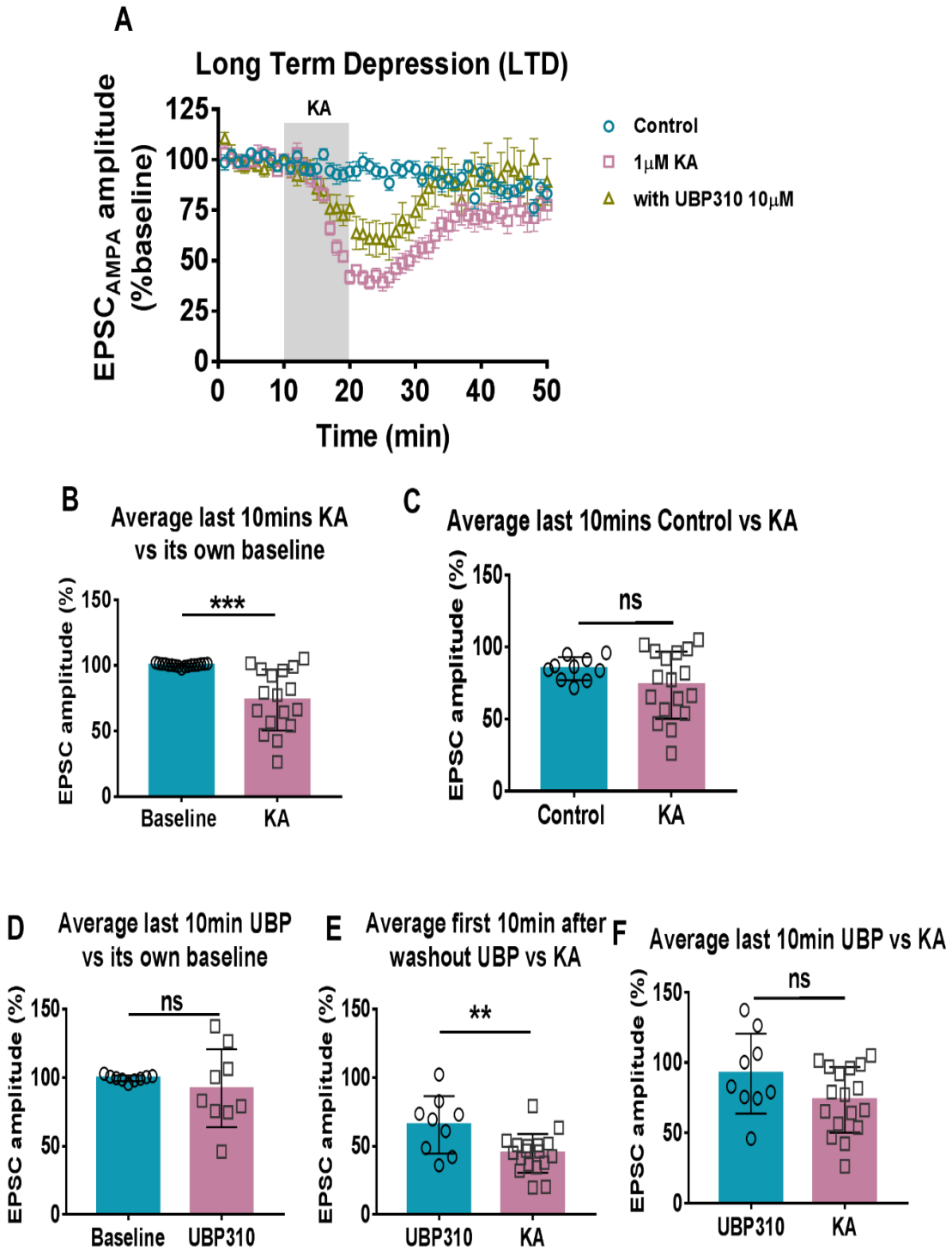

Figure 3-6: 10 mins of 1μM KA application in acute CA1 slices induced initial depression of evoked AMPA-EPSCs which was partially inhibited by KAR ionotropic inhibitor UBP310.

A. Graph showing effects of 1μM KA on normalised evoked EPSC amplitudes to the baseline (first 10 mins) and sample traces in presence of D-AP5 (50μM) and picrotoxin (50μM) from CA1 neurones in rat hippocampal slices. N=9-14 cells from different animals; error bar=S.E.M.

B. Quantification of averaged EPSC amplitudes comparing baseline (first 10 mins reads pre-treatment) to the last 10 mins read in KA treated samples shown in A. N=17; Paired t-test, ***p<0.001; error bar = S.D.

C. Quantification of averaged EPSC amplitudes comparing the last 10 mins post KA washout amplitudes between control and KA treated samples shown in A. N=10-17; unpaired t-test; error bar=S.D.

D. Quantification of averaged EPSC amplitudes comparing baseline (first 10 mins reads pre-treatment) to the last 10 minutes read in UBP310 treated samples shown in A. N=9; paired t-test; error bar=S.D.

E. Quantification of averaged EPSC amplitudes comparing the first 10 mins amplitude reads between UBP310 and KA treated samples shown in A. N=9-18; unpaired t-test, **p<0.01; error bar=S.D.

F. Quantification of averaged EPSC amplitudes comparing the last 10 mins amplitude reads between UBP310 and KA treated samples shown in A. N=9-17; unpaired t-test; error bar=S.D.

3.3.4 Pre-synaptic KARs mediate initial AMPA-EPSC depression

KARs are present at both pre- and postsynaptic sites (Lerma and Marques 2013) so to assess if the initial depression of AMPAR-EPSCs caused by KA application is of presynaptic origin, the paired pulse ratio (PPR) was measured. For this, two stimuli are applied with a 50ms interval and the ratio of amplitude of the second response to that of the first is determined. This is used as a measure of glutamate release probability, where PPR is inversely related to the release probability (Manabe, Wyllie et al. 1993, Debanne, Guerineau et al. 1996, Dobrunz and Stevens 1997) and is thought to be of pre-synaptic origin (Zucker and Regehr 2002, Xu-Friedman and Regehr 2004).

After a 10 mins KA application, the paired pulse ratio (PPR) significantly increased from 1.62 ± 0.07 (baseline levels) to 2.42 ± 0.15 ($p< 0.0001$) [**Figure 3-7** A]. This means there is a decrease in the glutamate release probability which would result in the decreased EPSCs amplitude observed post 10 mins

KA stimulation. The paired pulse ratio (PPR) returned to baseline levels 10 mins following KA washout, reaching levels similar to that of the control [**Figure 3-7** B]. These results suggest that the AMPAR-EPSC depression is mediated by a presynaptic mechanism, most likely a pre-synaptic KAR signalling function.

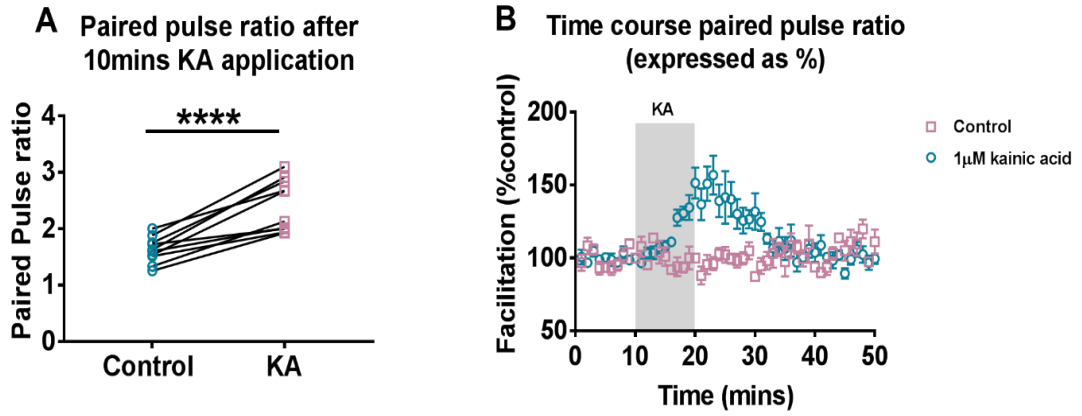

Figure 3-7: Initial AMPA-EPSC depression is mediated via pre-synaptic KARs.

A. Graph of PPR comparing control to KA treated cells (post 10 mins treatment). N=10 independent experiments; Paired t-test, ****p<0.0001.

B. Graph showing timecourse up to 30 mins post KA washout of PPR expressed as percentage of the control (100%). N=5-9 cells. Error Bar= SE.M.

3.3.5 Chronic suppression of network activity increases surface expression of GluK2 and GluK5 containing KARs

Another fascinating but not as well studied aspect of KAR plasticity is whether KARs have a role in homeostatic scaling. I initially wanted to determine if KARs can alter their surface expression in response to changes in synaptic activity. I performed surface biotinylation experiments to investigate KAR surface expression in cultured hippocampal neurones subjected to 1μM tetrotodoxin (TTX) treatment for 24 hours (h). TTX when added to the culture inhibits firing of action potential by blocking the sodium channels, resulting in chronic suppression of network activity (O'Brien, Kamboj et al. 1998, Johnston 2013). In response to decreased synaptic activity following TTX treatment (O'Brien, Kamboj et al. 1998), there is a significant and robust increase in the surface

expression (up-scaling) of both GluK2 and GluK5 containing KARs after 24 h [**Figure 3-8** A, B C]. As expected, this TTX induced suppression of activity also increased the surface expression of GluA2 and GluA1 containing AMPARs, which were used as a control of scaling response (O'Brien, Kamboj et al. 1998, Turrigiano, Leslie et al. 1998) [**Figure 3-8** D and E]. In contrast, Epidermal growth factor receptor (EGFR), which is widely expressed at synapses (Faundez, Krauss et al. 1992), was not affected by TTX treatment [**Figure 3-8** F]. GAPDH was used as a negative control to ensure only surface proteins were labelled with biotin.

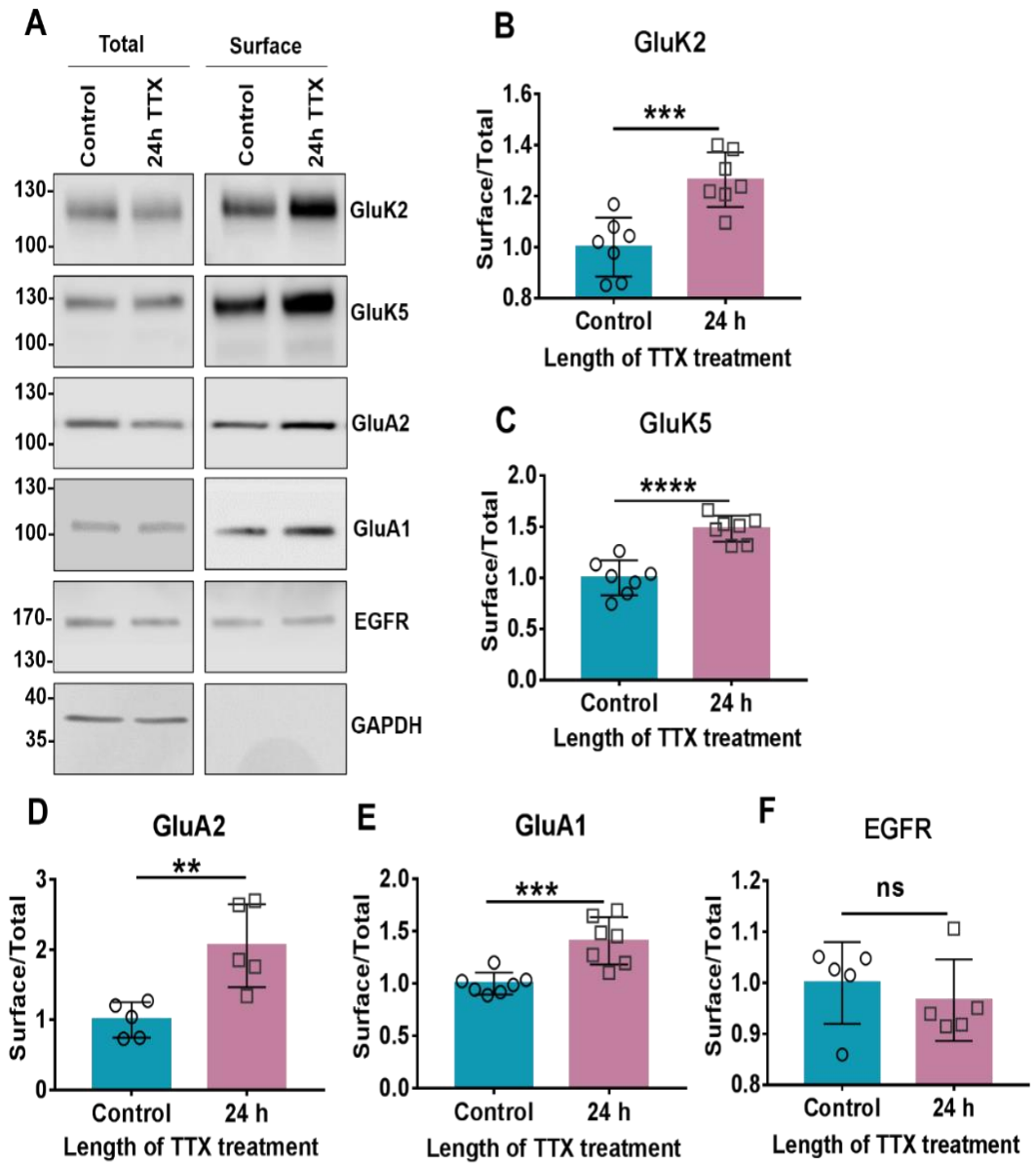

Figure 3-8: Chronic Suppression of network activity following 1µM tetrodotoxin (TTX) treatment for 24 h increases surface expression of GluK2 and GluK5 containing KARs. Surface biotinylation was performed on DIV 15 hippocampal neurones following TTX treatment to isolate surface proteins and determine surface/total ratio by western blotting.

A. Representative western blot images of surface and total levels of GluK2, GluK5, GluA2, GluA1 and EGFR post 24 h TTX treatment. EGFR was used as a surface expressed non-glutamate receptor control that should not respond to stimulation. GAPDH was used as an internal control to determine no internal proteins were biotinylated.

B-F. Quantification of surface to total ratio of GluK2 (B), GluK5 (C), GluA2 (D), GluA1 (E) and EGFR (F) shown in A. N=5-7 independent dissections, ns $p>0.05$, ** $p<0.01$, *** $p<0.001$, **** $p<0.0001$; Unpaired t-test; error bars=S.D.

3.3.6 Chronic enhancement of network activity decreases surface expression of GluK2 and GluK5 containing KARs

I also investigated KAR responses to chronic enhancement in network activity using 40µM bicuculline treatment for 24 or 48 h. Bicuculline is an antagonist of inhibitory $GABA_A$ receptors and its addition on neurones results in chronic enhancement of network activity (Johnston 2013). In response to both 24 and 48 h bicuculline treatment, there was a significant decrease (down-scaling) in the surface expression of both GluK2 and GluK5 containing KARs [**Figure 3-9** A, B and C]. On the other hand, while GluA1 containing AMPARs showed similar decrease to KARs, GluA2 containing AMPARs only showed a robust decrease after 48h [**Figure 3-9** A, D and E]. It seems KAR responses are more robust compared to the AMPARs. EGFR, as expected, did not respond to changes in synaptic activity [**Figure 3-9** A and F].

These results show for the first time that KARs can both upregulate and down regulate in response to chronic suppression and enhancement of network activity.

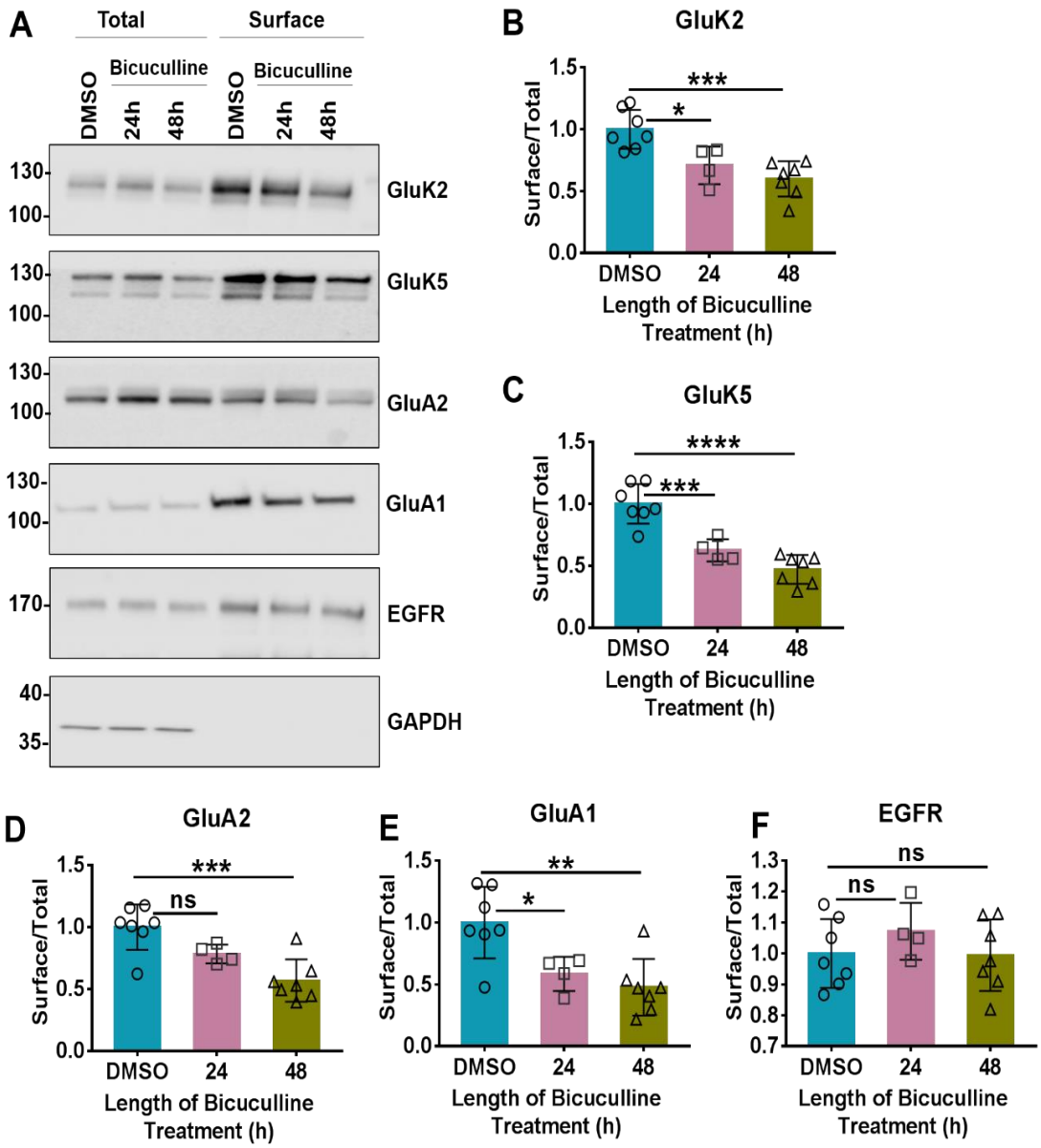

Figure 3-9: Chronic Enhancement of network activity following 40µM bicuculline treatment for 24 and 48 h decreases surface expression of GluK2 and GluK5 containing KARs. Surface biotinylation was performed on DIV 15 hippocampal neurones following bicuculline treatment to isolate surface proteins and determine surface/total ratio by western blotting.

A. Representative western blot images of surface and total levels of GluK2, GluK5, GluA2, GluA1 and EGFR post 24h and 48h bicuculline treatment. EGFR was used as a surface expressed non-glutamate receptor control that should not respond to stimulation. GAPDH was used as an internal control to determine no internal proteins were biotinylated.

B-F. Quantification of surface to total ratio of GluK2 (B), GluK5 (C), GluA2 (D), GluA1 (E) and EGFR (F) shown in A. N=4-7 independent dissections, ns $p>0.05$, *$p<0.05$, **$p<0.01$, ***<0.001, ****$p<0.0001$; One-way ANOVA with Dunnett's multiple post comparisons correction; error bars=S.D.

3.3.7 Q/R editing of KARs are altered in response to changes in the network activity

I next wanted to determine the mechanisms behind TTX and bicuculline mediated GluK2 scaling. For this I studied the potential role of Q/R editing which has been previously shown to affect the GluK2 subunit assembly and trafficking (Ball, Atlason et al. 2010). I performed BbvI digestion analysis (Bernard, Ferhat et al. 1999) [see section 2.2.12] post 24 h TTX treatment, which showed significantly decreased GluK2 Q/R editing [**Figure 3-10**]. This can also be observed in the representative chromatographs where there is an increase in the A peak for treated samples compared to the control at the site of editing following 24 h TTX treatment **[Figure 3-10** D].

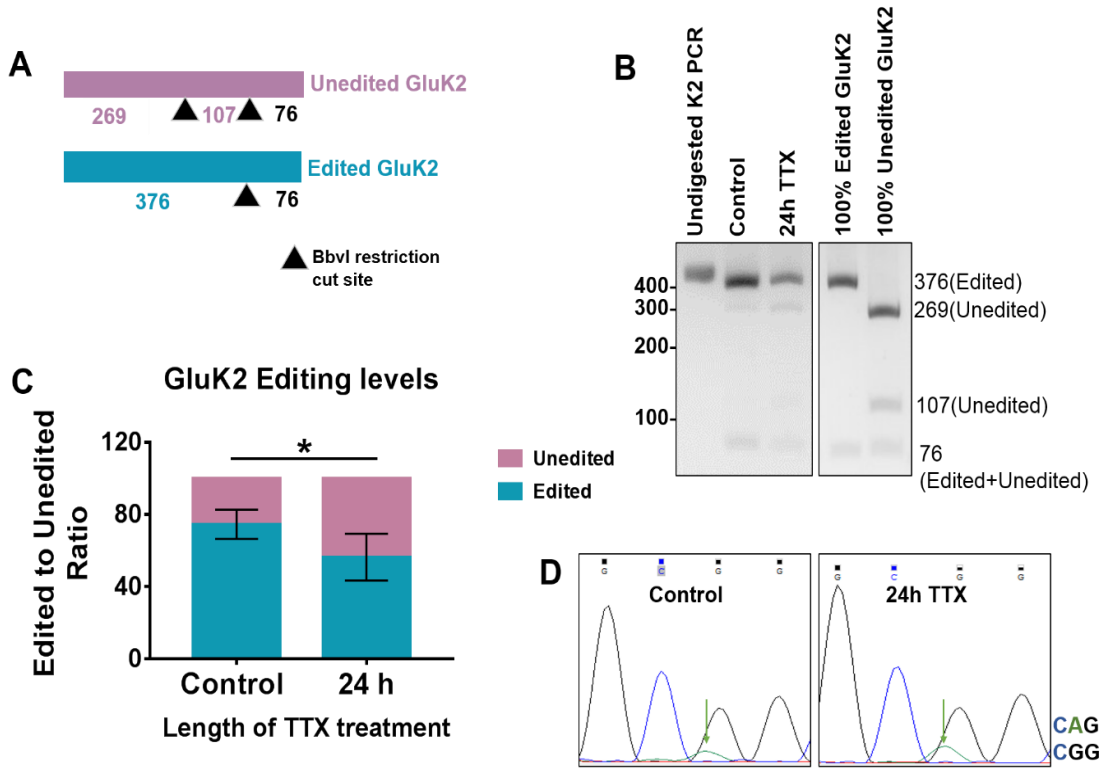

Figure 3-10: Chronic Suppression of network activity following 1µM tetrodotoxin (TTX) treatment for 24 h decreases Q/R editing of GluK2 subunit of KARs. Post 24 h TTX treatment, RNA was extracted from the cells and cDNA was synthesised to perform PCR assays.

A. Cartoon description of BbvI restriction enzyme cut assay used to determine GluK2 editing. PCR product of 452bp length were amplified using primers targeted to the M2 region of GluK2 consisting of the Q/R editing site. The PCR products were then digested using endonuclease BbvI restriction enzyme. PCR products unedited at the site of Q/R (CAG) codes for 2 BbvI restriction sites giving fragmented products of lengths 269, 107 and 76bp post digestion. The edited PCR products (CGG) only codes for 1 restriction site giving fragmented products of lengths 376 and 76bp post digestion.

B. Representative image of the PCR products separated on a 4% agarose gel post BbvI digestion to determine edited to unedited GluK2 ratio post 24 h TTX treatment. 100% edited and unedited GluK2 constructs were used as a control to ensure BbvI cut activity and validity of the assay.

C. Quantification of percentage of edited to unedited ratio of GluK2 population present after 24 h TTX treatment as shown in B. N=5 independent dissections; *p<0.05; Unpaired t-test; error bars=S.D.

D. Representative chromatographs of PCR products comparing control to 24 h TTX treated samples. The undigested PCR products were also sent for sequencing to determine changes in the dual peaks obtained at the site of editing as indicated by the green arrow. A peak (green) represents the unedited base while the G peak (black) represents the edited base. The image is representative of 3 repeats.

Similar analysis was also performed on bicuculline treated samples, which resulted in higher Q to R editing compared to DMSO treated for 48 h (vehicle control added at the same volume as that of bicuculline) treated samples [**Figure 3-11**]. These results strongly suggest a role of GluK2 Q/R editing in KAR scaling.

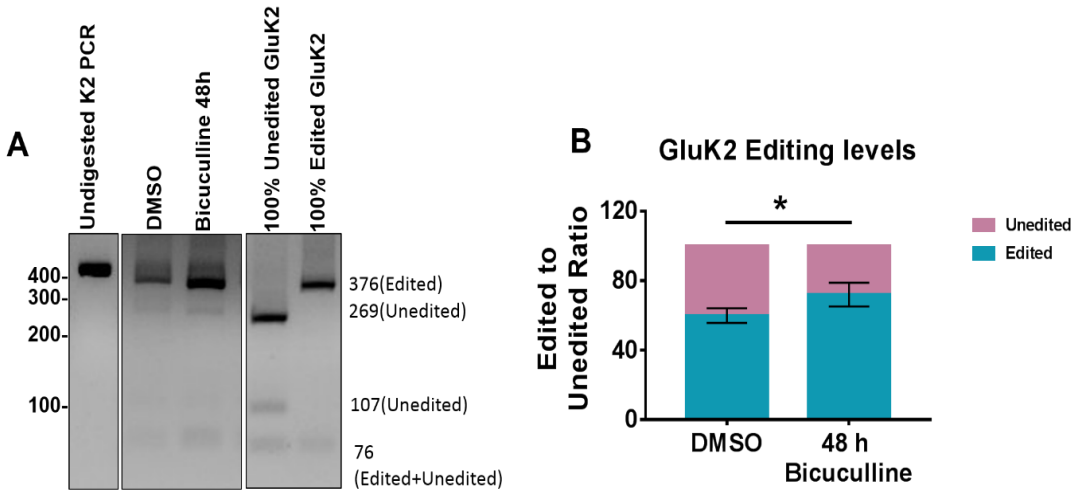

Figure 3-11: Chronic enhancement of network activity following 40µM bicuclline for 48 h increases Q/R editing of GluK2 subunit of KARs**.** Post 48 h bicuculline treatment, RNA was extracted from the cells and cDNA was synthesised to perform PCR assays.

A. Representative images of the PCR products separated on a 4% agarose gel post BbvI digestion to determine edited to unedited GluK2 ratio post 48 h bic treatment. 100% edited and unedited GluK2 constructs were used as a control to ensure BbvI cut activity and validity of the assay.

B. Quantification of percentage of edited to unedited ratio of GluK2 population present after 48 h TTX treatment as shown in B. N=5 independent dissections; *p<0.05; Unpaired t-test; error bars=S.D.

3.3.8 Q/R editing of GluA2 is not altered during chronic changes in the network activity

GluA2 subunit of AMPARs are also known to undergo this Q/R editing process (Sommer, Kohler et al. 1991, Kuner, Beck et al. 2001) and GluA2 themselves can undergo both up-scaling [**Figure 3-8**] and down-scaling process [**Figure 3-9**]. So, I wanted to determine if GluA2 editing levels were also altered in TTX treated samples. Using similar BbvI restriction enzyme assay, I observed no changes in the editing status of GluA2 [**Figure 3-12**]. Furthermore,

chromatographs data further validate these results where no A peak at the site of editing can be detected in either conditions **Figure 3-12** C].

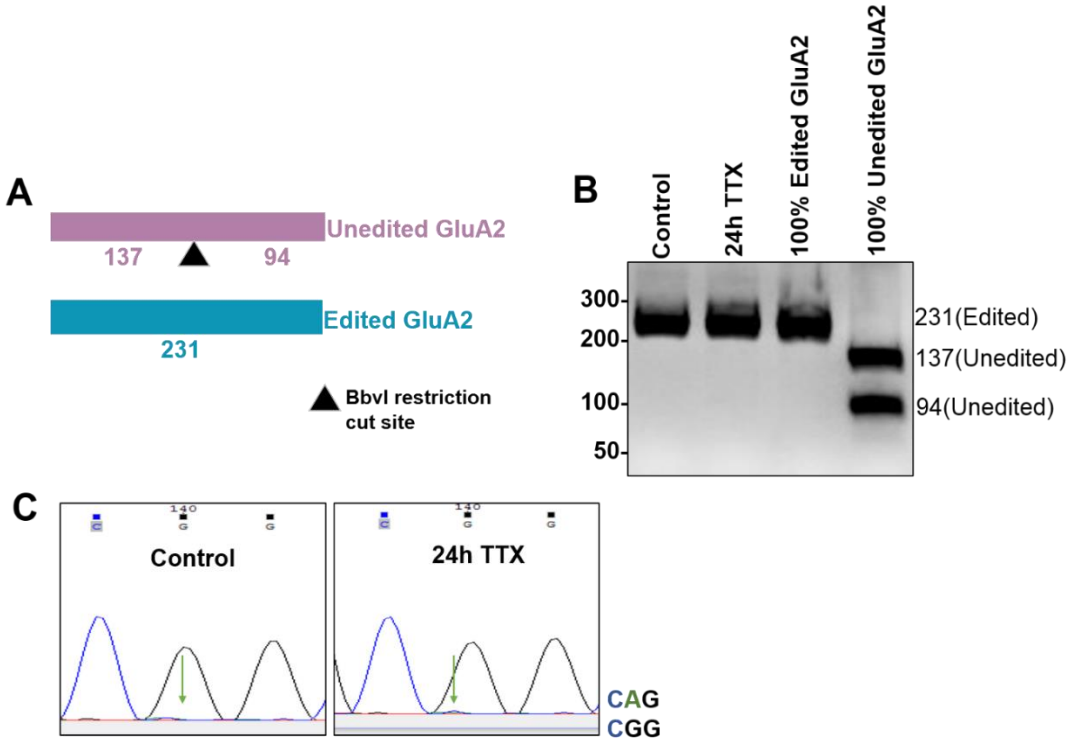

Figure 3-12: Chronic Suppression of network activity following 1µM TTX treatment for 24 h does not alter the Q/R editing of GluA2 subunit of AMPARs. Post 24 h TTX treatment, RNA was extracted from the cells and cDNA was synthesised to perform PCR assays.

A. Cartoon description of BbvI restriction enzyme cut assay used to determine GluA2 editing. PCR product of 231bp length were amplified using primers targeted to the M2 region of GluA2 consisting of the Q/R editing site. The PCR product was then digested using endonuclease BbvI restriction enzyme. PCR products unedited at the site of Q/R (CAG) codes for 1 BbvI restriction site giving fragmented products of lengths 137 and 94bp post digestion. The edited PCR products does not code for any BbvI restriction sites giving intact product of 231bp post digestion.

B. Representative image of the PCR products separated on a 4% agarose gel post BbvI digestion. 100% edited and unedited GluA2 constructs were used as a control to ensure BbvI cut activity and validity of the assay.

C. Representative chromatographs of PCR products of GluA2 comparing control to 24 h TTX treated samples at the editing site. The undigested PCR products were sent for sequencing to determine any changes in the dual peaks obtained at the site of editing as indicated by the green arrow. A peak (green) represents the unedited base while the G peak (black) represents the edited base. The image is representative of 3 repeats.

GluA2 unlike that of GluK2 is almost fully edited (>99%) by birth (Paschen and Djuricic 1995, Hamad, Ma-Hogemeier et al. 2011). So, unedited GluA2 was

not detected in either the BbvI or the chromatograph assays. With this in mind, I did not expect to see any further increase in GluA2 editing during the down-scaling process with bicuculline and therefore did not pursue this line of investigation.

Taken together these data indicate that Q/R editing changes during scaling selectively alters the GluK2 KAR subunit compared to GluA2 subunit of AMPAR.

3.3.9 GluK5 levels are not affected by GluK2 loss

GluK5 unlike GluK2 cannot form homomers and needs to oligomerise with one of the low affinity KAR subunits (GluK1, GluK2 or GluK3) to be released from the ER and express on the surface (Hayes, Braud et al. 2003, Ma-Hogemeier, Korber et al. 2010). As the surface expression of GluK5 containing KARs were also changed in response to the changes in synaptic activity [**Figure 3-8** and **Figure 3-9**], I speculated if changes in GluK2 surface expression leads to the changes in GluK5 surface expression by forming GluK2/GluK5 heteromeric receptors.

To test this hypothesis, I initially performed shRNA GluK2 knockdowns (KD) in my cultures to study the effect of loss of GluK2 on GluK5 expression. As shown in **Figure 3-13** A, B and C, endogenous surface and total GluK2 was reduced by >50% with the GluK2 KD. However, this loss of GluK2 did not affect the surface or the total levels of GluK5 [**Figure 3-13** A, D and E]. These results seem to suggest that GluK2 loss does not necessarily affect the surface expression of GluK5 in my cultures. This could potentially be due to compensation from other high affinity KAR subunits i.e. GluK1 and GluK3.

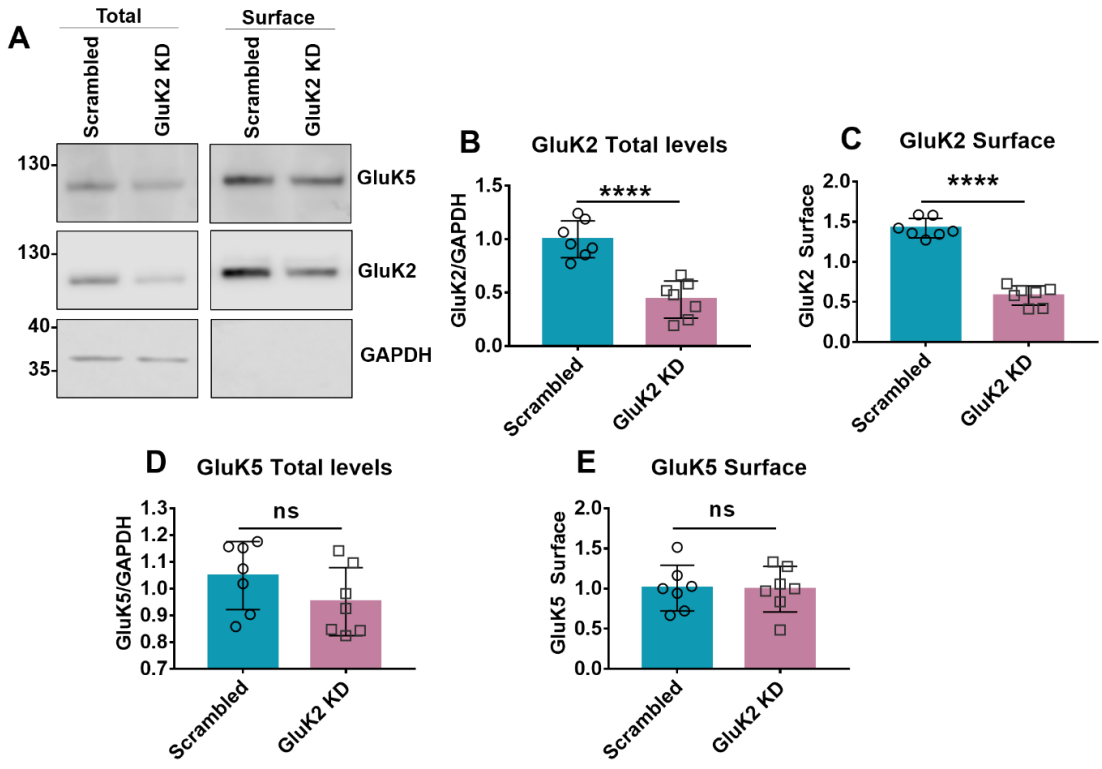

Figure 3-13: Loss of total and surface GluK2 does not alter the total or surface levels of GluK5. Surface biotinylation was performed on DIV 15 hippocampal neurones post 5 days GluK2 KD to isolate surface proteins and determine surface and total GluK2 and GluK5 levels by western blotting.

A. Representative western blot images of surface and total levels of GluK2 and GluK5 post 5 days GluK2 KD. GAPDH was used as an internal control to determine no internal proteins were biotinylated.

B-E. Quantification of separate surface and total protein levels of GluK2 total (B), GluK2 surface (C), GluK5 total (D) and GluK5 surface (E) shown in A. The total levels of proteins were normalised to respective GAPDH levels. Surface/Total ratio was determined to obtain surface reads. N=7 independent dissections, ns $p>0.05$, ****$p<0.0001$; Unpaired t-test; error bars=S.D.

3.4 Discussion

3.4.1 Transient KAR stimulation did not induce AMPAR-LTP

The initial aim of my PhD was to extend previous studies and define the mechanisms behind KAR mediated increase in synaptic AMPARs, and hence KAR_{AMPAR}-LTP (Petrovic, Viana da Silva et al. 2017). I started by attempting to replicate the data where increased AMPAR surface expression was shown following transient KA stimulation. Unfortunately, I could not replicate this [**Figure 3-3**] even though the control, NMDA mediated long term depression

(LTD), was induced in parallel to ensure neuronal health was not compromised, which could have resulted in the lack of activity induction. NMDA application significantly decreased the surface expression of both GluA1 and GluA2-containing AMPARs, thus inducing AMPAR-LTD (Beattie, Carroll et al. 2000). Interestingly, NMDA application also resulted in the decrease of surface expression of GuK2-containing KARs. This is in agreement with a previous report showing decrease in the surface expression of KARs following NMDA application (Martin and Henley 2004).

I reasoned that measuring whole surface changes using surface biotinylation may mask neuronal compartment restricted changes. In order to assess compartment specific changes in surface expression of AMPARs, imaging experiments in hippocampal neurones were also performed, focusing on potential alterations within dendrites. However, I was again unable to replicate previous data [**Figure 3-4**]. Hence, in my hands, these results suggested lack of change in the surface expression of AMPA receptors following transient KAR activation.

While the precise reasons for this remain elusive, possible explanations for this lack of reproducibility of KAR_{AMPAR}-LTP in my hands include subtle differences in experimental protocols, variability in the health and responsiveness of the primary neurones, issues with different batches of KA and/or the possibility that the KA-evoked changes were too erratic and small to reliably detect any changes. Regardless of the reasons, after several months of concerted effort and systematically changing variables, the lack of replicability led me to discontinue these experiments and develop new, but closely related, lines of investigation.

3.4.2 Sustained KAR stimulation decreased AMPAR and KAR surface expression

It was shown previously that following sustained stimulation of KARs, their surface expression decreases. I set out to determine if this change in KARs surface expression also resulted in changes in surface expression of AMPARs.

While there was a decreasing trend in the surface expression of GluK2 containing KARs after both 10 and 20 mins of KA application, the surface levels decreased significantly after 20 mins application [**Figure 3-5**]. Interestingly, the surface biotinylation data also showed a decrease in GluA2-containing AMPARs post 20 mins treatment but not in EGFRs, suggesting this change to be selective for glutamate receptors. Following published protocols, KA concentration of 10μM was chosen for these experiments (Martin, Bouschet et al. 2008, Petrovic, Viana da Silva et al. 2017). However, because AMPARs can be activated by KA at concentrations above 3μM (Bureau, Bischoff et al. 1999), we inhibited AMPAR activation using the well characterised AMPAR antagonist GYKI53655 (Donevan, Yamaguchi et al. 1994, Partin and Mayer 1996). Therefore, our data suggest the changes in AMPAR surface expression are specifically mediated by alterations in KAR signalling. Together our results indicate that KARs can directly regulate AMPAR surface expression which has striking implications for the, as yet almost completely unexplored, roles of KARs in the induction and regulation of AMPAR-mediated synaptic plasticity.

3.4.3 Potential role of pre-synaptic KARs in initial AMPA EPSCs depression

Electrophysiology experiments were carried out to investigate the effects of KA application on hippocampal slices on AMPAR EPSCs in the CA1 region [**Figure 3-6**]. As we were measuring AMPAR EPSCs, we could not use GYKI53655 to inhibit AMPAR signal. So, we instead used KA at concentration of 1μM, a concentration at which KA effect is shown to be selective to KARs (Bureau, Bischoff et al. 1999). Following 10 mins KA application, there was an initial depression in the AMPAR EPSCs compared to the control slices. Moreover, following 30 mins washout period, the reads were significantly depressed compared to its own baseline within individual KA treated slices. However, confusingly, KA-treated slices were not significantly different to non-KA-treated control slices because there was a marked run-down in AMPAR-EPSCs in the vehicle control group after 30 mins, perhaps suggesting the health of the slices were compromised by the long stimulation protocol.

We also used UBP310 compound to specifically inhibit ionotropic function of KARs. It should be noted that there is a controversy around whether this compound inhibits GluK1 (Dolman, More et al. 2007), GluK2/GluK5 KARs (Pinheiro, Lanore et al. 2013) or all KAR compositions. Nevertheless, the application of UBP310 significantly inhibited the extent of initial depression caused by KA application. This suggests that the initial AMPAR EPSC depression observed with KA stimulation is partly mediated by KAR ionotropic function. However, these changes are not sustained over 30 mins.

Furthermore, there was also a decrease in the release probability of glutamate release as shown by the increase in the paired pulse ratio (PPR) following 10 mins of KA application [**Figure 3-7**]. This low release of glutamate can lead to decreased AMPAR-EPSCs observed thus suggesting that the initial depression is potentially caused by pre-synaptic KARs.

Because KARs occur at both pre- and post-synapses (Lerma, Paternain et al. 2001), these results are most consistent with a role of pre-synaptic KAR function. Indeed, there is evidence of functional pre-synaptic KARs mediating NMDAR-independent form of AMPAR-LTP (Bortolotto, Clarke et al. 1999, Lauri, Bortolotto et al. 2001). It is also evident that presynaptic KARs can bidirectionally regulate to either inhibit (Kidd, Coumis et al. 2002) or facilitate (Contractor, Swanson et al. 2001) glutamate release. Moreover, activation of presynaptic KARs has been shown to result in long lasting inhibition of glutamate release, resulting in depression of excitatory transmission (Frerking, Schmitz et al. 2001). Thus, the simplest explanation of our electrophysiology experiments is that at CA1 synapses, pre-synaptic KARs facilitate transmission inhibition potentially leading to pre-synaptic LTD/short-term plasticity (STP). However, while potentially interesting my main focus was on determining the roles and regulation of postsynaptic GluK2-containing KARs, so I did not pursue these observations further into my PhD.

3.4.4 Novel role of GluK2 and GluK5 containing KARs in homeostatic scaling

The study and analysis of neuronal circuits and network activity is an emergent and extensively studied area of neuroscience. At a molecular level, changes

in networks rely on the modification, connectivity and different forms of synaptic plasticity. In particular, synaptic scaling is important to maintain neuronal network integrity and is critical for neuronal circuit development (Contractor, Mulle et al. 2011). As there were very limited reports of KAR in homeostatic scaling [see section 3.1.4], I next decided to study if KARs respond to chronic alterations in network activity. Here I show that GluK2 and GluK5 containing KARs can both up-scale and down-scale in response to chronic suppression (TTX) and enhancement (bicuculline) of synaptic activity as shown by the alterations in their surface expression [**Figure 3-8** and **Figure 3-9**]. Interestingly, to some extent these changes parallel changes in AMPARs surface expression. However, if these occur within same synapses is not known. Indeed, it is not clear if AMPARs and KARs colocalise at the same post synapses (Sheng, Shi et al. 2015). Nevertheless, our data demonstrate that KARs undergo up- and down-scaling in response to changes in synaptic firing rates indicating that they are finely tuned in response to overall network activity.

3.4.5 Chronic changes in synaptic activity alters GluK2 editing status

To establish a mechanism for these activity dependent changes in postsynaptic KARs we investigated Q/R editing within the M2 channel pore region of GluK2 (621aa). Q/R editing has been shown to play a role in GluK2-containing KAR channel conductance and ion channel properties (Egebjerg and Heinemann 1993). Moreover, it was also shown that this GluK2 editing influences KAR assembly, ER exit and delivery to cell surface. More specifically, edited GluK2(R) is more likely to form monomer/dimer and be ER retained (Ball, Atlason et al. 2010, Evans, Gurung et al. 2017). Here, I show that changes in Q/R editing of GluK2 can be activity dependently regulated. Following 24 h TTX treatment, there is a decrease in the Q to R editing of GluK2 while the 48 h bicuculline treatment increased this editing activity [**Figure 3-10** and **Figure 3-11]**. A similar concept of RNA editing regulating activity dependent receptors delivery to surface has also been reported for NMDARs where its mRNA splicing event at the C2/C2’ site of NR1 subunit

was shown to be activity dependently regulated during homeostatic scaling (Mu, Otsuka et al. 2003).

This mechanism to regulate the amount of KARs reaching the cell surface likely plays a key role in controlling neuronal excitability.

3.4.6 Chronic changes in synaptic activity does not alter GluA2 editing status

I also speculated if GluA2 upscaling can be mediated via changes in their Q/R editing status as previous findings have shown unedited GluA2 (Q) at 607aa site to result in its rapid release from ER causing their increased surface expression (Greger, Khatri et al. 2002, Greger, Khatri et al. 2003). Interestingly, GluA2 upscaling response seems to be independent to that of its Q/R editing as TTX treatment did not affect their Q/R editing ratio [**Figure 3-12**]. Previous reports suggests that TTX mediated change in ADAR2 levels altered the R/G site editing of GluA2 subunits (Balik, Penn et al. 2013), which has not been investigated here. Moreover, this also suggests that GluA2 Q/R editing is more tightly regulated than that of GluK2. Furthermore, various reports have linked changes in Q/R editing status of GluA2 (mediated via changes in ADAR2 levels) and hence increased Ca^{2+} permeability during excitotoxicity (Mahajan, Thai et al. 2011) and diseases such as ALS (Hideyama, Yamashita et al. 2012) and ischaemia (Peng, Zhong et al. 2006) as such ensuring maintenance of GluA2 editing status is important for cell survival. This shows the need for maintaining GluA2 editing status i.e. ensure GluA2 is completely edited at the Q/R site.

3.4.7 GluK5 surface expression is not altered following GluK2 loss

Both TTX and bicuculline treatment showed decrease in GluK2 and GluK5 containing KARs [**Figure 3-8** and **Figure 3-9**]. As it is also known that GluK5 is only functional as a heteromeric complex and needs to form heteromers with GluK1/2/3 to traffic out of the ER (Hayes, Braud et al. 2003), I hypothesised if changes in GluK5 are mediated due to its oligomerisation with GluK2. Moreover, GluK5 has higher ligand affinity than that of GluK1-3 (Herb, Burnashev et al. 1992). Perhaps, increasing or decreasing surface expression

of GluK5 allows increased sensitivity of KARs in response to the dampening or enhancement of synaptic activity.

To test this, I initially performed GluK2 KD to determine if loss of GluK2 can decrease GluK5 surface levels. I hypothesised that the lack of GluK2 would result in GluK5 not being able to form heteromeric assemblies, causing them to build up in the ER and potentially get degraded. So, I also tested whether total GluK5 levels post GluK2 KD is altered. However, loss of GluK2 did not alter either GluK5 surface or total levels [**Figure 3-13**]. This was surprising as GluK2 and GluK5 are the most abundant KAR subunit composition in the brain (Petralia, Wang et al. 1994, Kumar, Schuck et al. 2011, Evans, Gurung et al. 2017). Possible explanations could be the lack of complete removal of endogenous GluK2 with the shRNA target used. Only ~50% loss of total GluK2 levels compared to scrambled was achieved and the remaining GluK2 could still be enough for GluK5 to heteromerise with and traffic out of the ER. Secondly, there may be other KAR subunits (GluK1 and GluK3) present in our cultures that can oligomerise with GluK5 and this could be compensating for the lack of GluK2. As the tools to study these subunits are limited, it is difficult to determine this. Finally, the antibody I used can recognise both GluK2 and GluK3, so the remaining GluK2 signal I see post knockdown could potentially be GluK3 in our cultures, which can also oligomerise with GluK5.

With all this in mind, it is not fully conclusive if changes in GluK2 surface levels post activity treatment can lead to subsequent changes in GluK5 surface. So, the rest of my PhD focused on unravelling mechanisms behind GluK2 scaling.

3.5 Conclusions

In conclusion, my initial investigation could not repeat published work showing changes in KAR mediated AMPAR-LTP. Though, KAR could be mediating AMPAR-LTD however, this seems to be potentially mediated by pre-synaptic KARs and more likely to be a form of short term plasticity (STP).

Finally, I show novel KAR scaling responses. GluK2 and GluK5 containing KARs surface expression can increase or decrease in response to chronic changes in network activity like that of AMPARs and NMDARs. Moreover, the

Q/R editing of GluK2 is a potential selective mechanism of GluK2 scaling. Given these intriguing results I subsequently focused on studying the role of Q/R editing in GluK2 containing KARs scaling and the enzyme known to regulate this post-transcriptional editing process.

Chapter 4. ROLE OF ADAR2 MEDIATED Q/R EDITING IN HOMEOSTATIC SCALING OF GLUK2- KARS

4.1 Introduction

ADAR2 is the enzyme that deaminates adenosine to inosine (A-to-I), which is then read as guanosine by the cellular machinery. This results in change in the codon read from glutamine (Q) (CAG) to arginine (R) (CGG) when translated, which affects the functional properties and subcellular distribution of the resultant proteins. Moreover, such editing mediated changes have also been shown to occur during neuronal activity.

4.1.1 Activity dependent regulation of A-to-I RNA editing

It is becoming increasingly evident that RNA editing can be regulated during changes in the neuronal network activity. Initial evidence of this involved the serotonin 2C (5-HT2C) receptor that can be A-to-I edited in a serotonin dependent manner, in early life stress and also following application of antidepressant fluoxetine (Gurevich, Englander et al. 2002, Englander, Dulawa et al. 2005, Bhansali, Dunning et al. 2007). Subsequent genome wide studies on cortical neuronal cultures revealed various RNA editing sites that were regulated by synaptic activity (Sanjana, Levanon et al. 2012). Interestingly, the majority of these changes were shown to occur in ADAR substrates including the GluK2 Q/R editing site which decreased following 6 h potassium (60mM) treatment and following suppression of synaptic activity (Sanjana, Levanon et al. 2012). Interestingly, editing of the AMPAR subunit GluA2 Q/R was not altered with either of the treatments. This study did, however, identify alterations in the GluA2 R/G editing, which was also supported by another independent study showing similar changes in cultured hippocampal slices (Balik, Penn et al. 2013). These changes were shown to be cell-type specific, occurring in the CA1 region of the hippocampus but not the CA3. These observations were also accompanied with concurrent changes in ADAR2 transcript levels but not of any other ADARs, showing the specific importance of ADAR2 in neuronal activity dependent RNA editing (Sanjana, Levanon et al. 2012, Balik, Penn et al. 2013).

4.1.2 Q/R editing of KARs and AMPARs regulate their surface expression

As detailed in the Introduction section 1.5, Q/R editing occurs in the GluK1 and GluK2 subunit of KARs and GluA2 subunit of AMPARs. Having either edited or unedited forms of these subunits is a key determinant of their ionotropic functional properties. In addition, this Q/R editing also affects the surface delivery of the resultant multimeric complex.

4.1.2.1 Evidence that Q/R editing of GluA2 regulates AMPAR assembly and expression

The role of Q/R editing in the surface delivery of glutamate receptors was initially shown for GluA2 containing AMPARs (Greger, Khatri et al. 2002). While GluA1 containing AMPARs could exit the ER and traffic to the surface efficiently, a pool of GluA2 subunits of AMPARs were retained in the ER. Most of this retention was attributed to the Q/R editing of GluA2 subunit since reverting to the unedited version of GluA2 (R607Q) led to rapid release of GluA2 from the ER. This also resulted in their increased surface expression. Consistent with this, another study also showed higher surface expression of unedited forms of GluA2 compared to the edited form (Ma-Hogemeier, Korber et al. 2010). Interestingly, mutating corresponding Glutamine in GluA1 to Arginine (Q600R) also reduced the mutant GluA1 surface expression (Greger, Khatri et al. 2002), further strengthening the role of editing in trafficking.

4.1.2.2 Evidence that Q/R editing of GluK2 regulates KAR assembly and expression

Studies on the GluK2-containing KARs showed differential subunit assembly and subcellular distribution of the edited (R) and unedited (Q) forms of GluK2, like that for GluA2 in AMPARs. The unedited forms of GluK2 were more likely to assemble as tetramers allowing them to be released from the ER whereas the edited form of GluK2 accumulated primarily as monomer/dimer causing them to be predominantly ER retained (Ball, Atlason et al. 2010).

However, another study reported no such differences with either the edited or unedited forms of GluK2 (Ma-Hogemeier, Korber et al. 2010). These opposing observations could be due to the differences in sensitivity of the assays applied

as changes in GluK2 containing KAR oligomerisation and trafficking are relatively moderate compared to GluA2. It should also be noted that these studies were performed in an over-expressed system over 72 h time course. So, changes in the ER assembly and export are more likely to be prominent in the earlier timepoints (24 h) to prevent saturation of the system which may mask the Q/R effect on assembly and trafficking (Ball, Atlason et al. 2010). Equally, EndoH assays used to mark the intracellular immature proteins in both GluK2 and GluA2 Q/R editing studies, has also been questioned in a recent study where it was shown that EndoH-sensitive proteins can be abundant at the neuronal surface as well (Hanus, Geptin et al. 2016).

Nevertheless, in line with the studies showing differential expression of edited and unedited GluK2, recent study from our lab also showed unedited form of GluK2 to have higher surface expression compared to the edited form (Evans, Gurung et al. 2017).

4.1.2.3 Proposed model of Q/R editing regulation of surface delivery

The Q/R editing of both GluA2 and GluK2 occurs in its transmembrane II (TMII) region which lines the channel pore forming loop [see section 1.5]. AMPARs studies have shown oligomerisation of ionotropic glutamate receptors to be a two-step process: dimerisation of dimers (Kuusinen, Abele et al. 1999, Armstrong and Gouaux 2000, Ayalon and Stern-Bach 2001, Mansour, Nagarajan et al. 2001, Sun, Olson et al. 2002). Likewise, KAR assembly also involves an initial dimerisation process mediated by their N-terminal Domains (NTD) (Ayalon and Stern-Bach 2001, Kumar, Schuck et al. 2011). Forming tetrameric assembles would require these pore regions of the subunits to come in close proximity to each other. Having positively charged arginine group in the pore region potentially brings charge repulsion and/or steric hindrances disfavouring multimeric assemblies, in particular homomeric assemblies (Greger, Khatri et al. 2003, Greger, Ziff et al. 2007).

It has also been previously proposed, using separate studies on ATP-sensitive K+ channel trafficking, that the properties of ion channels may act as functional checkpoints in the ER to regulate the export of complexes out of the ER (Zerangue, Schwappach et al. 1999). The reduced channel conductance of

edited subunits (Swanson, Feldmeyer et al. 1996, Burnashev and Rozov 2000, Cull-Candy, Kelly et al. 2006) may act as a disadvantage in ensuring efficiency of synaptic transmission. Favouring this hypothesis, it has been reported that downstream checkpoints potentially exists in ER which allows sensing of gating motions to prevent ER export of glutamate receptor channels with blocked desensitisation (Priel, Selak et al. 2006). However, the identity of these checkpoints is as of yet not known.

Hence, charge repulsion, steric hindrance and/or ER checkpoints are all potentially contributing to the altered surface delivery of Q/R edited and unedited receptors.

4.1.3 Q/R editing role in regulation of protein expression and stability

Beyond their role in trafficking and ion channel properties, Q/R editing has also been shown to regulate protein expression via an interplay between GluA2 Q/R editing and splicing. GluA2 editing was reported to be positively coupled to the pre-mRNA splicing efficiency. The edited GluA2 pre-mRNA transcripts were preferentially spliced compared to the unedited transcripts (Brusa, Zimmermann et al. 1995), which is thought to act as a 'safe-guard' mechanism to ensure high-editing of GluA2 is maintained basally and also during periods of ADAR2 fluctuations (Schoft, Schopoff et al. 2007, Hideyama, Yamashita et al. 2012, Penn, Balik et al. 2013). Furthermore, this splicing regulation of editing provides a mechanism to ensure tight regulation of GluA2 Q/R editing because unedited GluA2 pre-mRNA transcripts are less likely to be successfully transcribed and expressed. Supporting this, ADAR2 knockout mice showed nuclear accumulation of incompletely spliced GluA2 pre-mRNA transcripts and reduced GluA2 expression levels (Higuchi, Maas et al. 2000).

If this is also the case for GluK2 is not known, although GluK2 Q/R assembly studies have shown an increased degradation of edited form of GluK2 (Ball, Atlason et al. 2010). The build-up of intracellular edited GluK2 subunits due to their lack of ability to form heteromeric complexes was thought to lead to increased degradation of these unassembled edited GluK2 subunits. This

suggests that Q/R editing at least indirectly can alter the protein stability and hence the levels of GluK2 containing KARs.

4.1.4 Objectives

It is becoming increasingly evident that changes in neuronal activity regulates RNA editing, in particular ADAR2 mediated RNA editing, that can result in changes in receptor properties. Q/R editing of GluK2 and GluA2, in addition to affecting their ionotropic functional properties, also changes their assembly, ER export and their surface delivery.

My work in Chapter 3 showed novel role of KAR receptors in homeostatic scaling. Chronic suppression and enhancement of network activity resulted in up-scaling and down-scaling of GluK2-containing KARs as demonstrated by their increase and decrease in surface expression following 24 h tetrodotoxin (TTX) treatment and 48 h bicuculline treatment respectively. Furthermore, suppression of network activity decreased Q/R editing of GluK2 leading to an increase in unedited GluK2 (Q) population and *vice-versa* with enhancement in the network activity.

This led to my hypothesis that changes in ADAR2 mediated Q/R editing of GluK2 plays a key role in GluK2 scaling response. So, my objectives for the next phase of my project were to:

1. Determine if ADAR2 levels alter in response to chronic changes in network activity.
2. Apply ADAR2 KD strategies to comparatively test ADAR2 regulation of GluK2 and GluA2 Q/R editing.
3. Apply ADAR2 KD strategies to determine if ADAR2 can induce KAR scaling.

4.2 Materials and methods

All techniques used in this section are covered in the general Materials and methods section.

4.3 Results

4.3.1 ADAR2 but not ADAR1 total levels decrease post 24 h TTX treatment

To investigate the role of ADAR2 mediated GluK2 Q/R editing in KAR scaling I tested the effects of chronic suppression of network activity with 24 h TTX treatment on ADAR2 levels (Higuchi, Maas et al. 2000). As shown in **Figure 4-1** A and B, incubation with TTX for 24 h decreased total ADAR2 levels by ~50% compared to the untreated control. Q/R site editing in glutamate receptors are predominantly mediated by ADAR2 (Higuchi, Maas et al. 2000). However, ADAR1 can also to an extent edit Q/R sites (Dabiri, Lai et al. 1996, Herb, Higuchi et al. 1996) and is the only other functionally active enzyme (Melcher, Maas et al. 1996) in this family so I also probed for ADAR1 levels to determine if it too is regulated by synaptic activity. Following 24 h TTX treatment, ADAR1 levels were unchanged [**Figure 4-1** C and D]. Both bands obtained for ADAR1 were quantified here as ADAR1. These data indicate that ADAR2 is preferentially lost following chronic suppression of network activity.

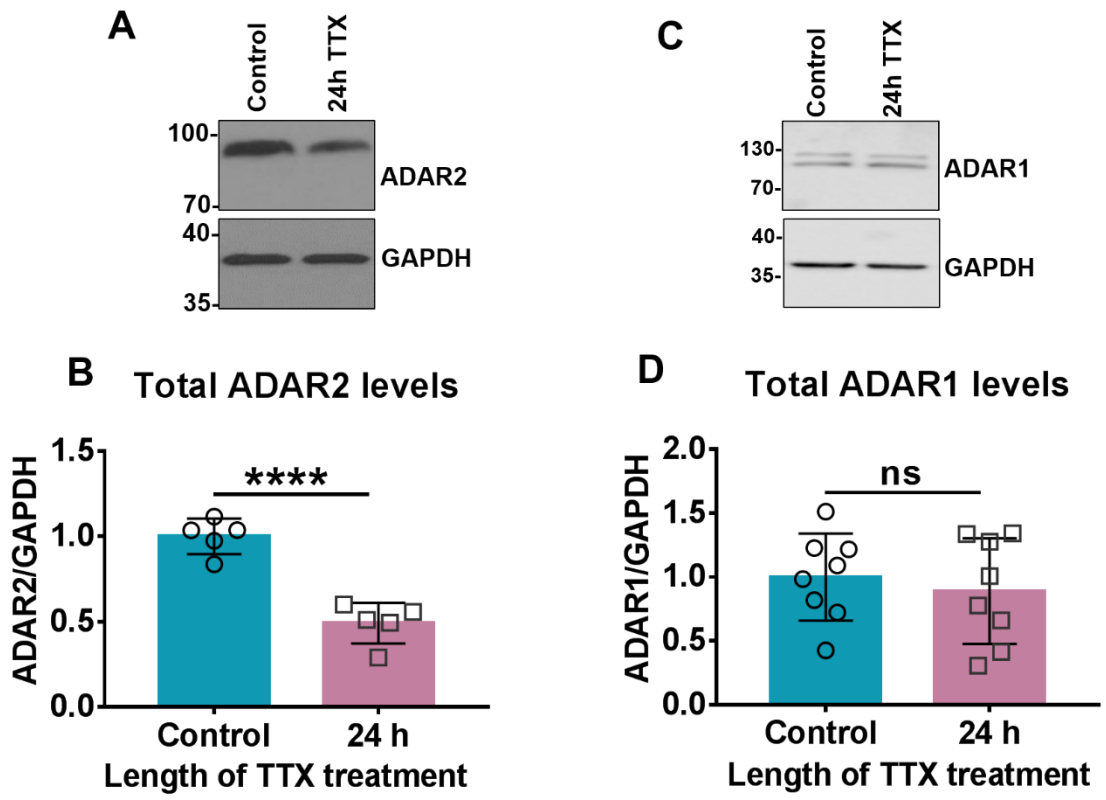

Figure 4-1: ADAR2 but not ADAR1 total levels decrease post 24h 1µM TTX treatment.

A. Representative western blot images of total levels of ADAR2 and GAPDH levels post 24h TTX treatment.

B. Quantification of total ADAR2 levels normalised to GAPDH levels post 24h TTX treatment shown in A. N=5 independent dissections, Unpaired t-test; ****p<0.0001, error bar=S.D.

C. Representative western blot images of total levels of ADAR1 and GAPDH levels post 24h TTX treatment.

D. Quantification of total ADAR1 levels normalised to GAPDH post 24h TTX treatment shown in C. Both bands were quantified. N=8 independent dissections, Unpaired t-test; ns p>0.05, error bar=S.D.

4.3.2 Both ADAR1 and ADAR2 total levels are unchanged post bicuculline treatment

GluK2 containing KARs are susceptible to chronic enhancement of synaptic activity following both 24 h and 48 h bicuculline treatment. As the Q/R editing of GluK2 also increased significantly following bicuculline treatment, I next determined if either ADAR1 or ADAR2 levels were also altered. In contrast to the TTX treatment, ADAR2 levels remained unchanged [**Figure 4-2** A and B]

following both 24 and 48 h of bicuculline treatment. Similarly, ADAR1 levels also remained unchanged [**Figure 4-2** C and D].

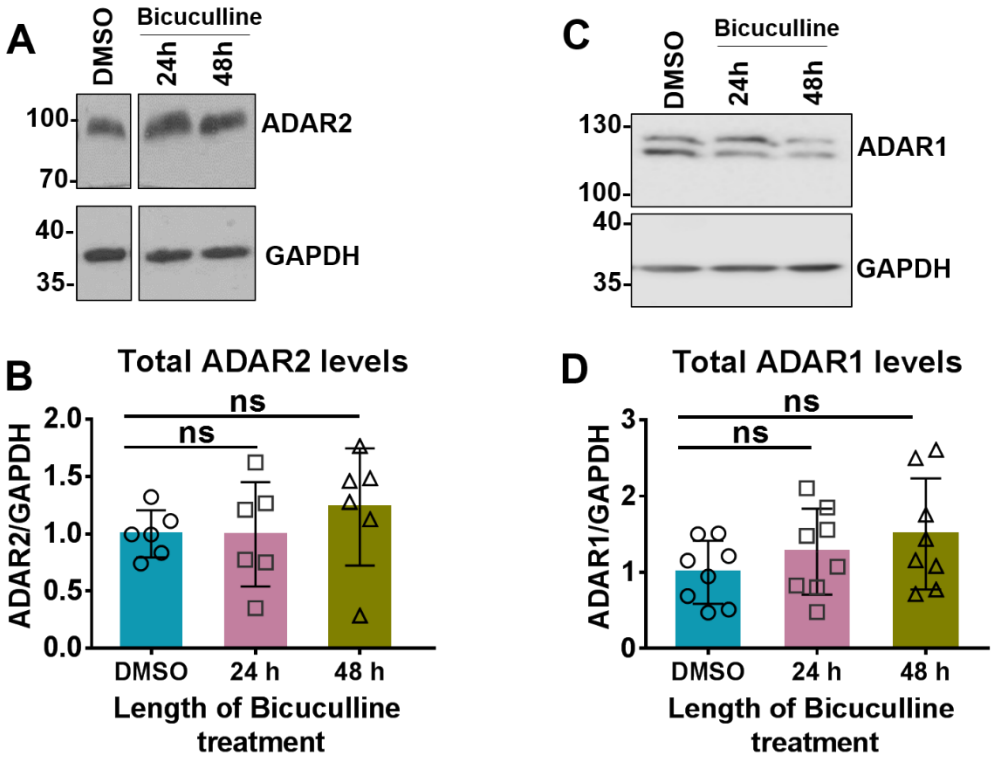

Figure 4-2: Both ADAR2 and ADAR1 total levels are unchanged post 24 and 48 h 40µM bicuculline treatment.

A. Representative western blot images of total levels of ADAR2 and GAPDH levels post 24h and 48h bicuculline treatment.

B. Quantification of total ADAR2 levels normalised to GAPDH post 24h and 48h bicuculline treatment shown in A. N=6 independent dissections, Unpaired t-test; ns p>0.05, error bar=S.D.

C. Representative western blot images of total levels of ADAR1 and GAPDH levels post 24h and 48h TTX treatment.

D. Quantification of total ADAR1 levels normalised to GAPDH post 24h and 48h bicuculline treatment shown in C. Both bands were quantified. N=8 independent dissections, Unpaired t-test; ns p>0.05, error bar=S.D.

These results indicate that in contrast to TTX-evoked up-scaling, the levels of ADAR2 are not altered during bicuculline-evoked down-scaling, suggesting that other mechanism(s) potentially regulates GluK2 Q/R editing during KAR downscaling. I therefore focused on the role of ADAR2 during GluK2 up-scaling.

4.3.3 Longer exposure to TTX does not decrease ADAR2 levels further

I next wanted to determine if ADAR2 levels are altered in a time-dependent manner by TTX treatment. Studies using TTX to mediate suppression of network activity have varied from 6 to 48 h (Craig, Jaafari et al. 2012, Schanzenbächer, Sambandan et al. 2016, Schaukowitch, Reese et al. 2017). Therefore, I treated hippocampal neurones with 1µM TTX for 6, 12, 24, 36 and 48 h and determined ADAR2 levels. While there was a decreasing trend in ADAR2 levels following 12 h TTX treatment, there was significant reduction only after 24h, with no further significant decrease in ADAR2 levels at 36 or 48h [**Figure 4-3**]. This suggests basal level of ADAR2 must be maintained throughout long-term suppression of synaptic activity to ensure editing of other ADAR2 substrates including that of GluA2.

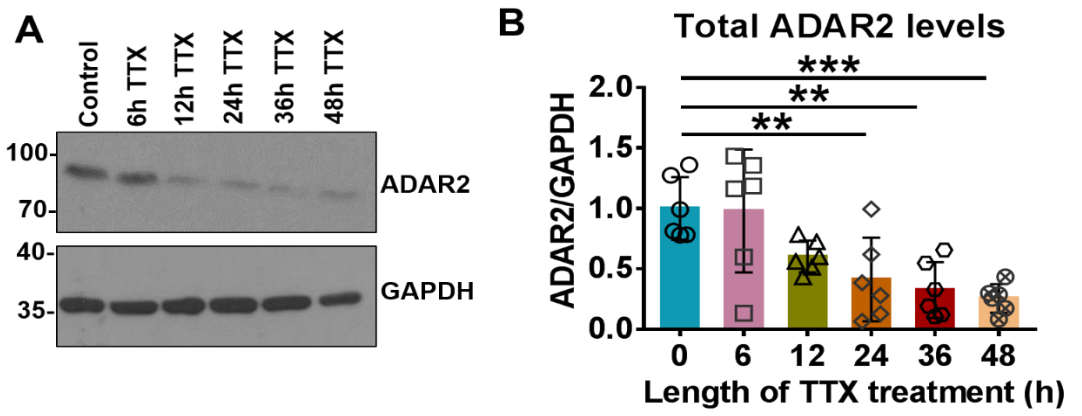

Figure 4-3: Longer lengths of 1µM TTX treatment do not decrease total ADAR2 levels further.

A. Representative western blot images of total levels of ADAR2 and GAPDH levels post 6, 12, 24, 24, 36 and 48 h TTX treatments.

B. Quantification of total ADAR2 levels normalised to GAPDH post stated lengths of TTX treatment shown in A. N=6 independent dissections, One-way ANOVA with Dunnett's multiple post comparisons correction; **p<0.01, ***p<0.001, error bar=S.D.

4.3.4 ADAR2 is localised in the nucleus and the nuclear levels are decreased following TTX treatment

ADAR2 is a nuclear protein (Desterro, Keegan et al. 2003, Sansam, Wells et al. 2003) where it interacts with its dsRNA substrates (Higuchi, Single et al. 1993, Herb, Higuchi et al. 1996, Wahlstedt and Ohman 2011). I first confirmed that ADAR2 is expressed in the nucleus in my neuronal cultures and then determined the effect of 24 h TTX treatment within the nucleus. As expected, subcellular fractionation of neuronal cultures shows that ADAR2 is entirely expressed in the nucleus [**Figure 4-4**] and that TTX treatment decreased levels of ADAR2 in the nucleus by ~50%, consistent with the total ADAR2 decrease observed.

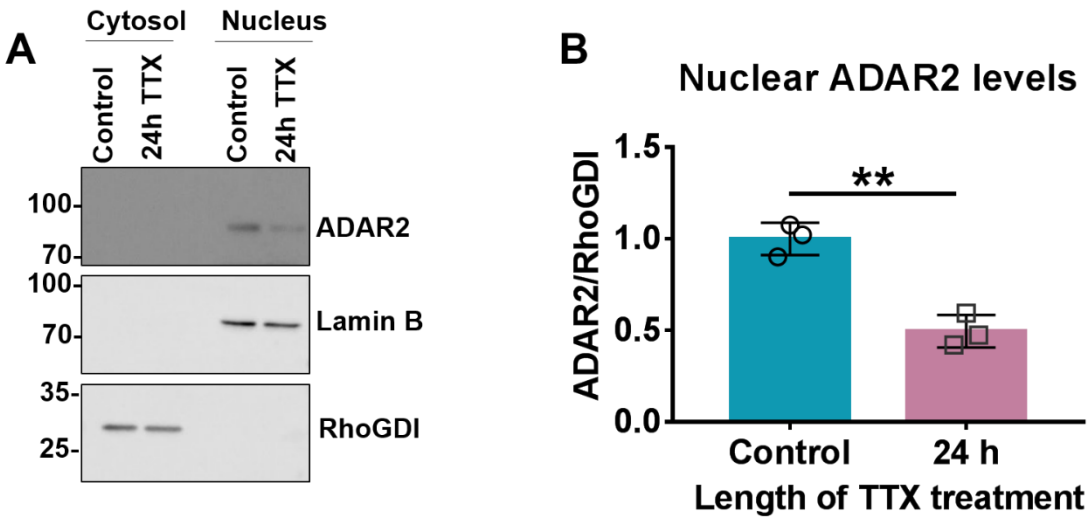

Figure 4-4: Subcellular fractionation show nuclear localisation of ADAR2 which is decreased following 24 h 1µM TTX treatment. Cytosolic and nuclear compartments were isolated to determine ADAR2 localisation and levels post 24 h TTX treatment.

A. Representative western blot images of levels of ADAR2 in the cytosol and the nucleus post 24 h TTX treatment. RhoGDI was used as a cytosolic marker (Maurya, Sundaram et al. 2009) and Lamin B as a nuclear marker (Olins, Rhodes et al. 2010).

B. Quantification of nuclear ADAR2 levels normalised to Lamin B post 24 h TTX treatment shown in A. N=3 independent dissections, Unpaired t-test; **p<0.01; error bar=S.D.

To further confirm the data obtained from subcellular fractionation, I also performed fixed immunocytochemistry experiments. DAPI was used to stain the nucleus and the cells to be imaged were selected under this channel to avoid bias. Fibrillarin, a nucleolar RNA methyltransferase, was used as a

nucleolar specific marker (Lafontaine and Tollervey 2000, Shubina, Musinova et al. 2016) as ADAR2 has been reported to predominantly localise within the nucleolus (Desterro, Keegan et al. 2003, Sansam, Wells et al. 2003). Consistent with previous studies ADAR2 in hippocampal neurones were localised in the fibrillarin positive nucleoli structures. Moreover, 24h TTX treatment caused a decrease in the overall nuclear ADAR2 signal [**Figure 4-5** A and B].

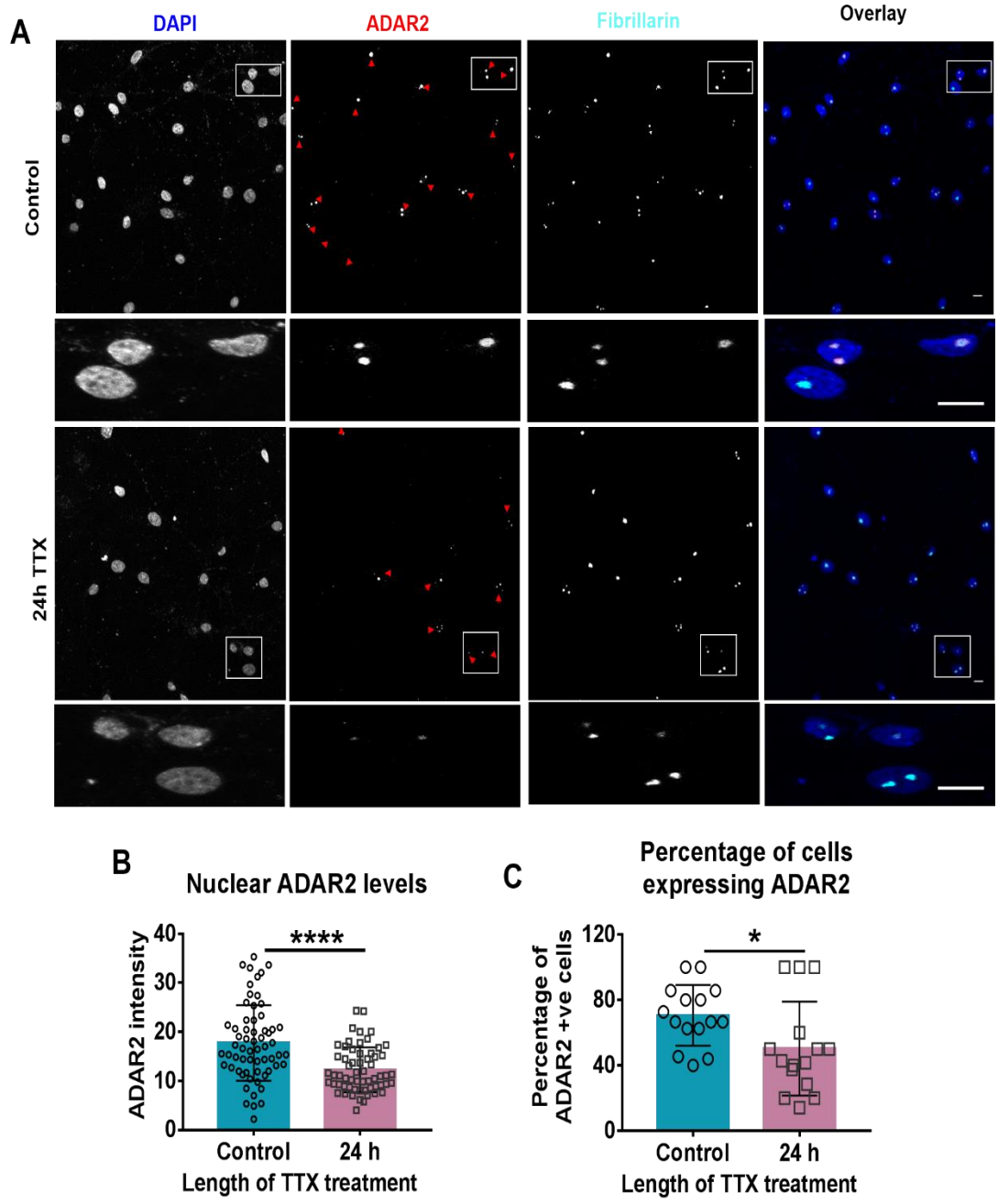

Figure 4-5: Fixed immunolabelling show nucleolar localisation of ADAR2. The intensity of ADAR2 signal and the percentage of cells expressing ADAR2 were both decreased following 24h 1µM TTX treatment.

A. Representative images showing predominantly nucleolar localisation of ADAR2 in the nucleus stained with DAPI (blue) and imaged for ADAR2 (red-Cy3) and fibrillarin (cyan-Cy5, nucleolar marker). White boxes in the top panel represent zoomed images below showing decreased ADAR2 intensity and red arrows show cells positive for ADAR2 expression. Scale bar=10µm.

B. Quantification of nuclear intensity of ADAR2 following 24h TTX treatment shown in A. DAPI channel was used to draw regions of interest around the nucleus and average intensity was calculated. n=60-62 cells, N= 3 independent dissections, Unpaired t-test; ****p<0.0001, error bar=S.D.

C. Quantification of percentage of cells expressing ADAR2 post 24h TTX treatment per field of view as shown in A (red arrows). N=15 fields of view, Unpaired t-test; *p<0.05, error bar=S.D.

Surprisingly not all cells expressed ADAR2 with approximately 80% of cells within a field of view positive for ADAR2 signal (indicated by red arrows). Dispersed neuronal cultures are thought to possess predominantly CA1 pyramidal cell properties (Lerma, Morales et al. 1997, IM, FA et al. 2011). Previous work has suggested that the CA1 does not express ADAR2 as highly as the CA3 hippocampal region (Balik, Penn et al. 2013). This may explain why ~20% of cells do not express ADAR2. Other possibilities include that the ADAR2-lacking cells are non-neuronal e.g. glial cells, which do not highly express ADAR2 (Jacobs, Fogg et al. 2009). It may also be the case that these cells express isoforms of ADAR2 (Dracheva, Lyddon et al. 2009) not detected by our antibody. While further investigation will be needed to distinguish between these possibilities, TTX treatment also caused the percentage of cells expressing ADAR2 to decrease significantly from ~80% to ~50% [**Figure 4-5** A and C].

4.3.5 Creating and validating knockdown tools against ADAR2

I reasoned that the decrease in ADAR2 following 24h TTX treatment was a causal factor in reduced GluK2 Q/R editing. To test this hypothesis, I generated lentiviruses expressing either shRNAs targeted to ADAR2 or non-specific scrambled shRNA control. I synthesised two different shRNAs against

ADAR2. Serendipitously, one shRNA completely removed endogenous ADAR2, which I named ‘Complete’ ADAR2 KD whereas second shRNA reduced ADAR2 levels to ~50% of the scrambled control, which I named ‘Partial’ ADAR2 KD [**Figure 4-6** A and B].

Fixed imaging analysis also showed absolute loss of ADAR2 signal when infected with ‘Complete’ ADAR2 KD. On the other hand, the ‘Partial’ ADAR2 KD had significantly reduced ADAR2 intensity signal along with significantly reduced percentage of cells expressing ADAR2, similar to those elicited by TTX treatment [**Figure 4-6** C, D and E].

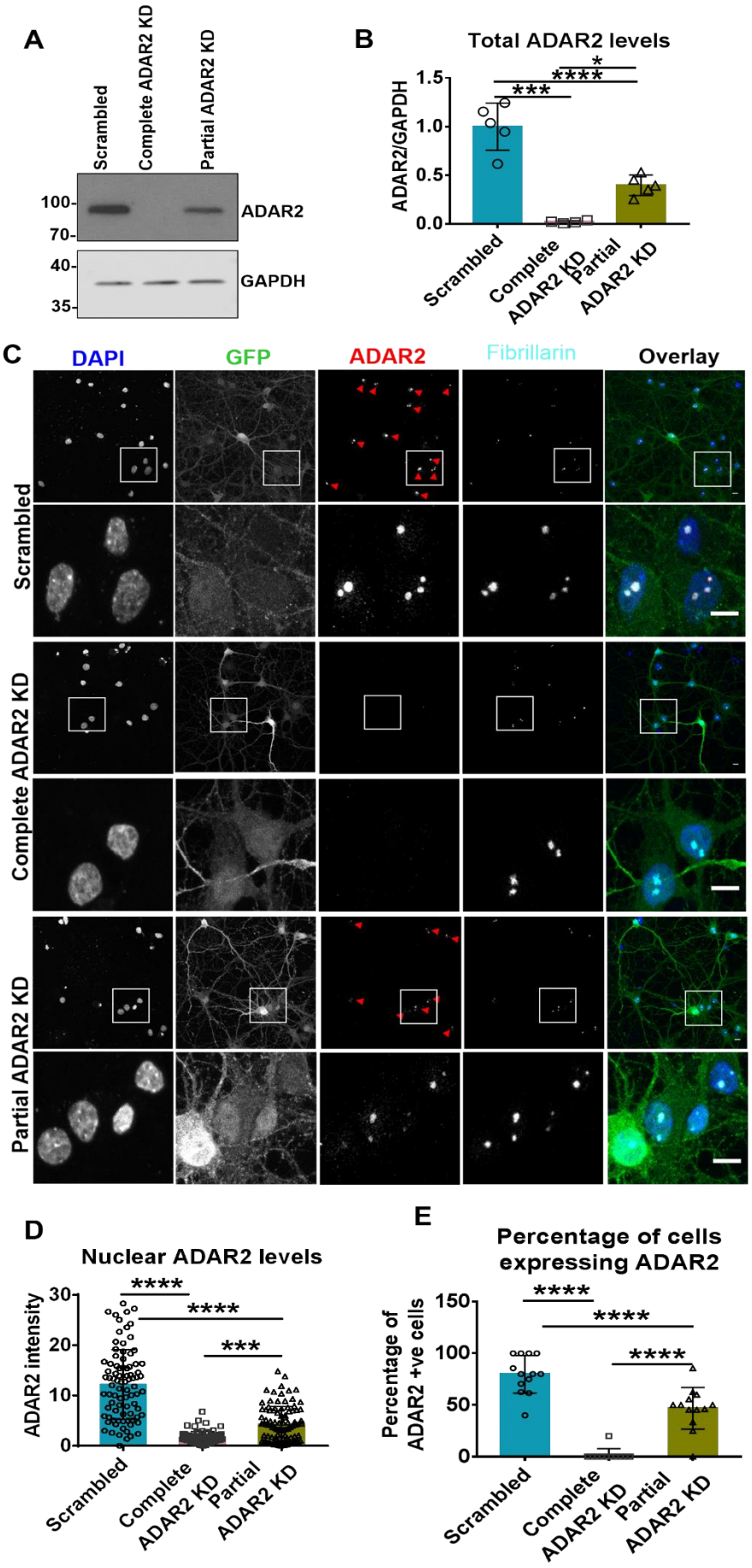
A
Scrambled
Complete ADAR2 KD
Partial ADAR2 KD
100
70
40
35
ADAR2
GAPDH
B
Total ADAR2 levels
ADAR2/GAPDH
1.5
1.0
0.5
0.0
*
****
***
Scrambled
Complete ADAR2 KD
Partial ADAR2 KD
C
DAPI
GFP
ADAR2
Fibrillarin
Overlay
Scrambled
Complete ADAR2 KD
Partial ADAR2 KD
D
Nuclear ADAR2 levels
ADAR2 intensity
30
20
10
0
****
****
***
Scrambled
Complete ADAR2 KD
Partial ADAR2 KD
E
Percentage of cells expressing ADAR2
Percentage of ADAR2 +ve cells
150
100
50
0
****
****
****
Scrambled
Complete ADAR2 KD
Partial ADAR2 KD

Figure 4-6: Validating knockdown tools against ADAR2. Lentiviral delivery system was used to target two different shRNAs against ADAR2**.** 'Complete ADAR2 KD' completely removes endogenous ADAR2 whereas 'Partial ADAR2 KD' removes 50% of the endogenous ADAR2 compared to the scrambled.

A. Representative western blot images of ADAR2 and GAPDH levels post 5 days infection with either Complete ADAR2 KD or Partial ADAR2 KD.

B. Quantification of total ADAR2 levels normalised to GAPDH shown in A. N=5 independent dissections, One-way ANOVA with Tukey's multiple post comparisons correction; *p<0.05, **p<0.01, ***p<0.001, ****p<0.0001; error bar=S.D.

C. Representative images of ADAR2 levels post 5 days infection with either Complete ADAR2 KD or Partial ADAR2 KD. The cells were stained with DAPI (blue) and imaged for GFP (green-Cy2), ADAR2 (red-Cy3) and fibrillarin (cyan-Cy5, nucleolar marker). White boxes in the top panel represent zoomed images below showing decreased ADAR2 intensity and red arrows show cells positive for ADAR2 expression. Scale bar=10µm.

D. Quantification of nuclear intensity of ADAR2 shown in C. DAPI channel was used to draw regions of interest around the nucleus and average intensity was calculated. n=75-99 cells, N=3 independent dissections, One-way ANOVA post Tukey's multiple post comparisons correction; ***p<0.001, ****p<0.0001; error bar=S.D.

E. Quantification of percentage of cells expressing ADAR2 per field of view as shown in C (red arrows). n=11-13 fields of view; N=3 independent dissections, One-way ANOVA post Tukey's multiple post comparisons correction; ****p<0.0001; error bar=S.D.

4.3.6 Complete and Partial ADAR2 knockdown differentially alter GluK2 editing

I next tested if removing endogenous ADAR2 reduces the GluK2 Q/R editing. As expected, 'Complete' ADAR2 KD reduced GluK2 editing by over 60% whereas 'Partial' ADAR2 KD reduced GluK2 editing by ~20% compared to the scrambled control [**Figure 4-7** A and B]. Consistent with this, chromatographs of neurones treated with 'Complete' ADAR2 KD showed a dramatic change in the base read of the editing site to A (unedited) rather than G (edited). In contrast, the editing site in the neurons treated with the 'Partial' ADAR2 KD predominantly read G but had an increased peak read for A and decreased peak read for G compared to the scrambled control [**Figure 4-7** C].

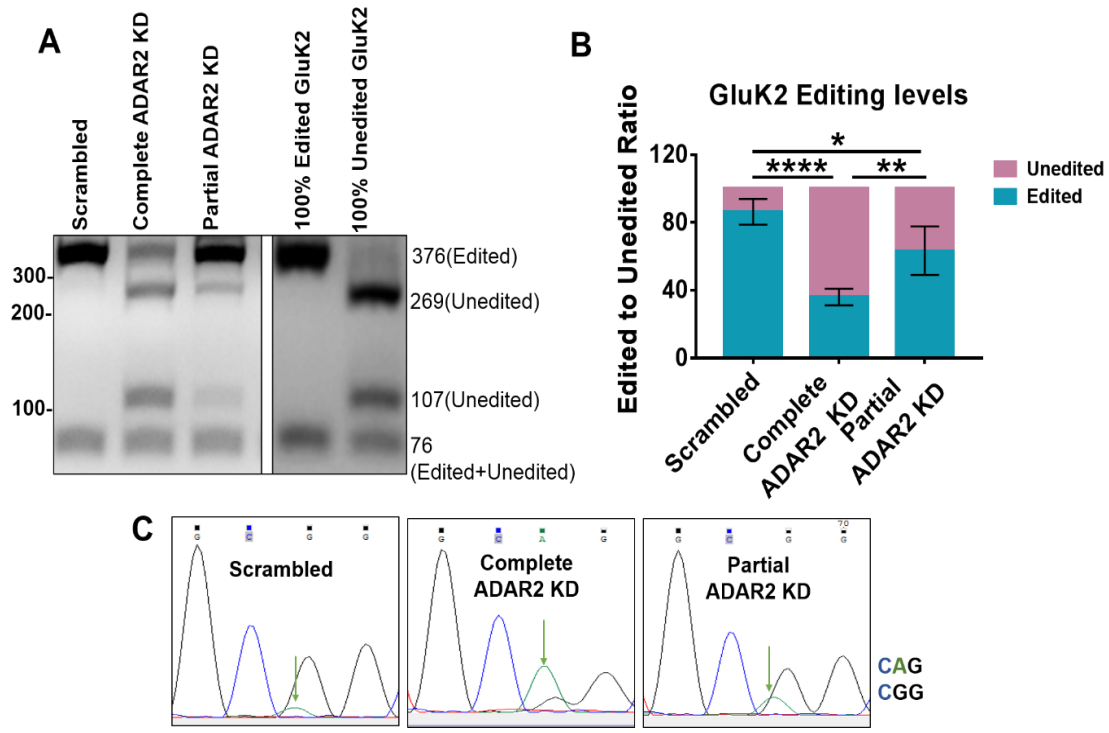

Figure 4-7: Complete and Partial removal of ADAR2 differentially alters GluK2 editing. 5 days after knockdown virus infection, RNA was extracted from the cells and cDNA was synthesised to perform PCR assays.

A. Representative images of the PCR products separated on a 4% agarose gel post BbvI digestion to determine edited to unedited GluK2 ratio after knockdowns infection. 100% edited and unedited GluK2 constructs were used as a control to ensure BbvI cut activity and validity of the assay.

B. Quantification of percentage of edited to unedited ratio of GluK2 population present after 24 h TTX treatment as shown in A. n=4 independent dissections; One way ANOVA with Tukey's multiple post comparisons correction; *p<0.05, **p<0.01, ****p<0.0001; error bars=S.D.

C. Representative chromatographs of PCR products comparing scrambled infected cells with the knockdowns infected cells at the Q/R editing site. The undigested PCR products were sent for sequencing to determine changes in the dual peaks obtained at the site of editing as indicated by the green arrow. A peak (green) represents the unedited base while the G peak (black) represents the edited base. The image is representative of 3 repeats.

4.3.7 Complete and Partial ADAR2 knockdown differentially alter GluA2 editing

ADAR2 KO mice are deficient in both GluA2 and GluK2 editing (Higuchi, Maas et al. 2000) and the majority of the functional studies on ADAR2 mediated Q/R editing have focused on the GluA2 AMPAR subunit. With this in mind, I wanted

to determine the effect of the two ADAR2 shRNA knockdowns on GluA2 editing.

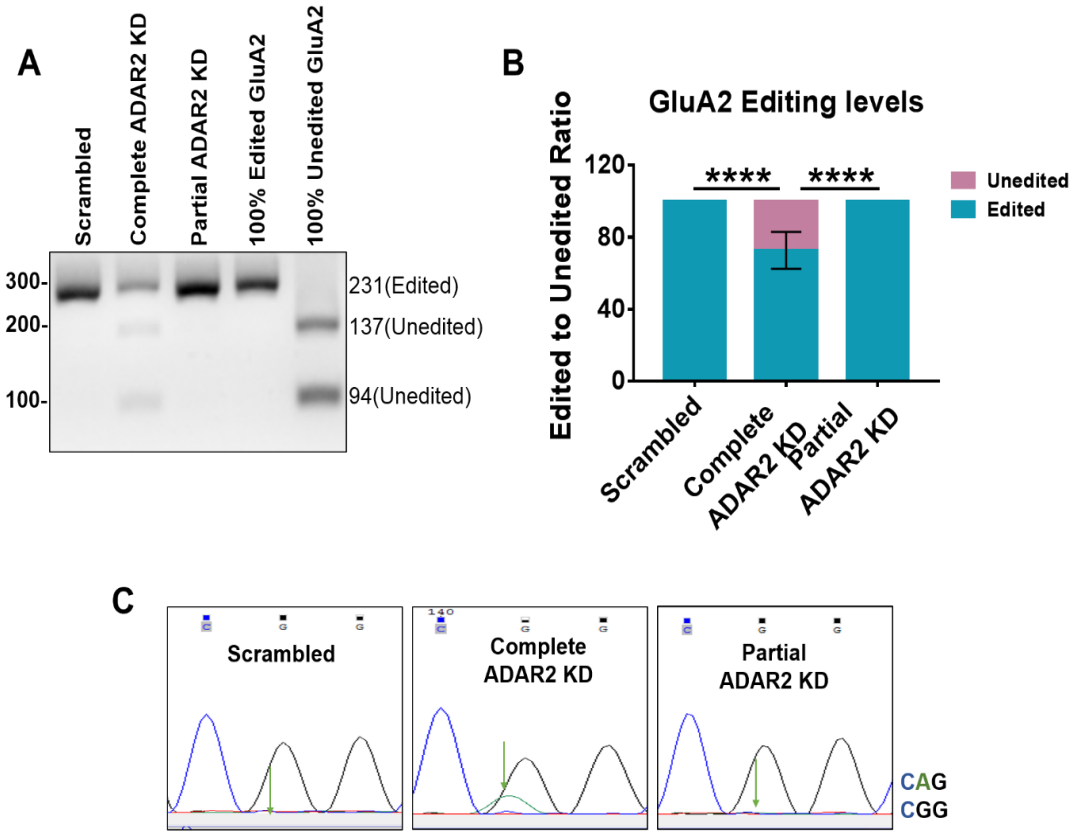

Figure 4-8: Complete and Partial knockdown of ADAR2 differentially alters GluA2 editing. 5 days after knockdown virus infection, RNA was extracted from the cells and cDNA was synthesised to perform PCR assays.

A. Representative images of the PCR products separated on a 4% agarose gel post BbvI digestion to determine edited to unedited GluA2 ratio. 100% edited and unedited GluA2 constructs were used as a control to ensure BbvI cut activity and validity of the assay.

B. Quantification of percentage of edited to unedited ratio of GluA2 population present after 24 h TTX treatment as shown in A. n=4 independent dissections; One way ANOVA with Tukey's multiple post comparisons correction; ****p<0.0001; error bars=S.D.

C. Representative chromatographs of PCR products comparing scrambled infected cells with the knockdowns infected cells at the Q/R editing site. The undigested PCR products were sent for sequencing to determine changes in the dual peaks obtained at the site of editing as indicated by the green arrow. A peak (green) represents the unedited base while the G peak (black) represents the edited base. The image is representative of 3 repeats.

Interestingly, 'Complete' ADAR2 KD only reduced GluA2 editing by ~30% while the 'Partial' ADAR2 KD did not have any effect on the Q/R editing of the AMPAR subunit GluA2 [**Figure 4-8** A and B]. The changes are also visible in

the chromatographs where in scrambled control there is no dual peak at the editing site (green arrow), consistent with GluA2 being edited over 99% pre-birth (Jacobs, Fogg et al. 2009). This remains unchanged with the 'Partial' ADAR2 KD however, with the 'Complete' ADAR2 KD, there is an increased A to G peak ratio [**Figure 4-8** C].

4.3.8 ADAR2 knockdown can be rescued by lentiviral infection

Removing endogenous ADAR2 reduced the editing status of both GluK2 and GluA2 to varying degrees. I next determined if this editing deficiency could be rescued by expression of exogenous shRNA insensitive WT ADAR2 rescue construct to confirm the specificity of the ADAR2 KD and establish proof of concept for rescue with mutant forms of ADAR2. I generated two separate lentiviruses using the same backbone vector; one contained the 'Complete' ADAR2 KD shRNA expressing GFP and another consisted of the N-terminally HA tagged shRNA insensitive WT ADAR2 rescue. The knockdown virus (250µl) completely ablated endogenous ADAR2 while adding (100µl) of HA tagged ADAR2 rescue virus alongside the knockdown restored ADAR2 to levels comparable to the control [**Figure 4-9** A]. Both viruses were added to the cells on the same day. Moreover, adding two separate viruses successfully infected same cells as shown by colocalization of GFP and HA markers in the rescue panel in [**Figure 4-9** B].

I also wanted to ensure there were comparable number of cells expressing ADAR2 with the volume of rescue virus used. Fixed imaging analysis [**Figure 4-9** B and C] showed that ~80% of cells expressed exogenous ADAR2 after knockdown and rescue, similar to the percentage of cells expressing endogenous ADAR2 in the scrambled control. Hence, I determined the optimum volume of viruses to obtain rescue at comparable levels to the endogenous.

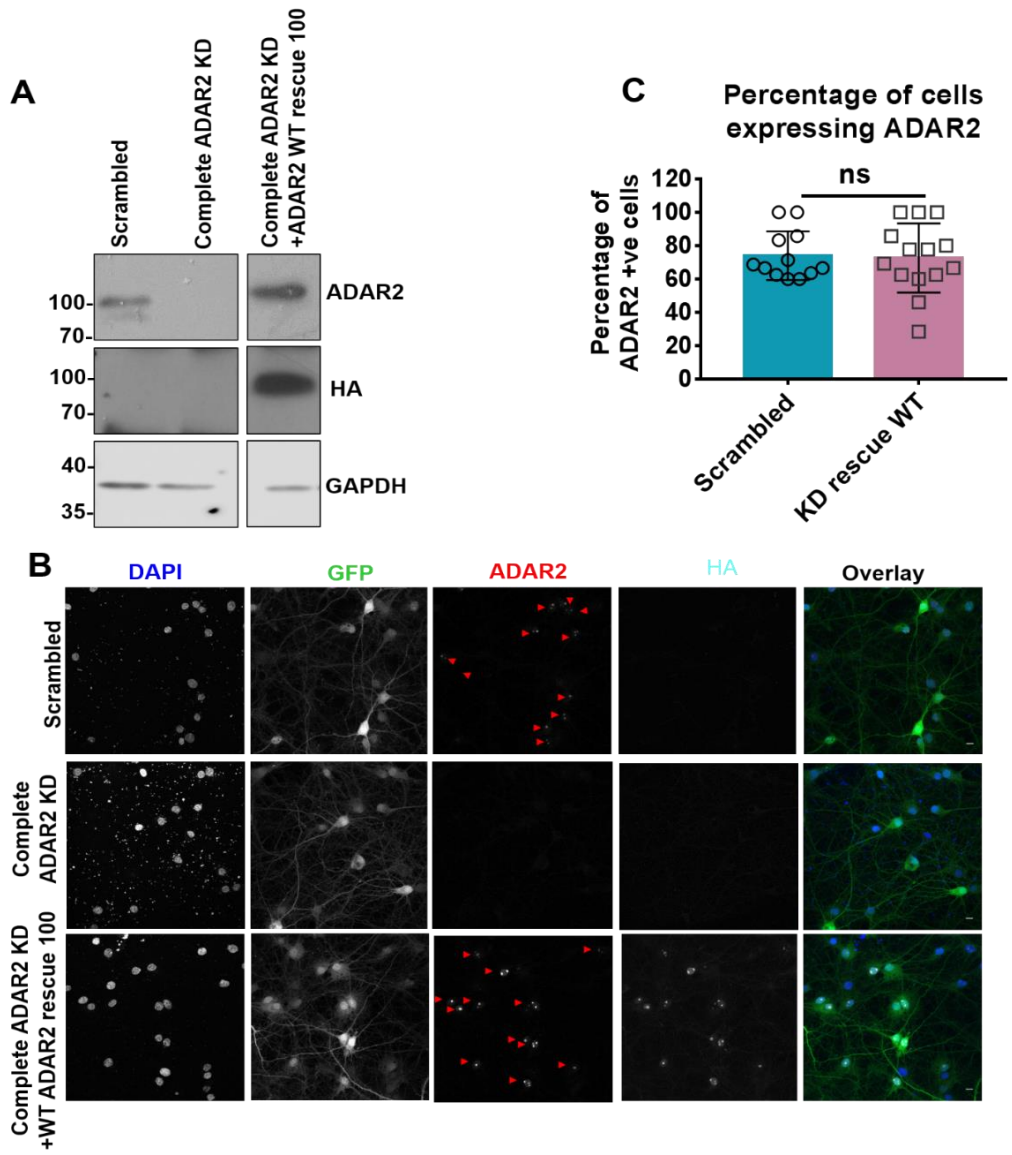

Figure 4-9: ADAR2 loss can be rescued by lentiviral overexpression after complete ADAR2 knockdown in hippocampal neuronal cultures.

A. Representative western blot images of ADAR2, HA and GAPDH levels of cells infected with either scrambled, Complete ADAR2 KD or complete ADAR2 KD with WT HA-ADAR2 at DIV 9 for 6 days.

B. Representative images of cells stained with DAPI (blue) and imaged for GFP (green-Cy2), ADAR2 (red-Cy3) and fibrillarin (cyan-Cy5). The cells were infected with either scrambled, Complete ADAR2 KD or Complete ADAR2 KD with WT HA-ADAR2 at DIV 9 for 6 days. Thus, the GFP panels shows cells expressing knockdown while HA and ADAR2 panels show the cells expressing the rescue constructs. Red arrows show cells positive for ADAR2 expression. Scale bar=10µm.

C. Quantification of percentage of cells expressing ADAR2 per field of view as shown in B (red arrows). n=12-14 fields of view; N=3 independent dissections, Unpaired t-test; ns $p>0.05$; error bar=S.D.

4.3.9 ADAR2 rescue restores the editing deficiency following ‘Complete’ and ‘Partial’ ADAR2 KDs

With the rescue system in place, I determined if the editing deficiency observed with ADAR2 loss was rescued when ADAR2 levels are rescued. Following 6 days of knockdown and rescue, I performed RNA extraction and cDNA synthesis and analysed the editing ratio. As shown in **Figure 4-10** A and B, GluK2 editing was significantly rescued for both ‘Complete’ and ‘Partial’ ADAR2 KDs.

GluA2 editing was unaffected by ‘Partial’ ADAR2 knockdown but the increase in unedited GluA2 population following ‘Complete’ ADAR2 KD was reversed by rescue with expression of shRNA insensitive WT ADAR2 rescue [**Figure 4-10** D and E]. This data confirms GluK2 and GluA2 editing deficiency is a direct consequence of the loss of ADAR2.

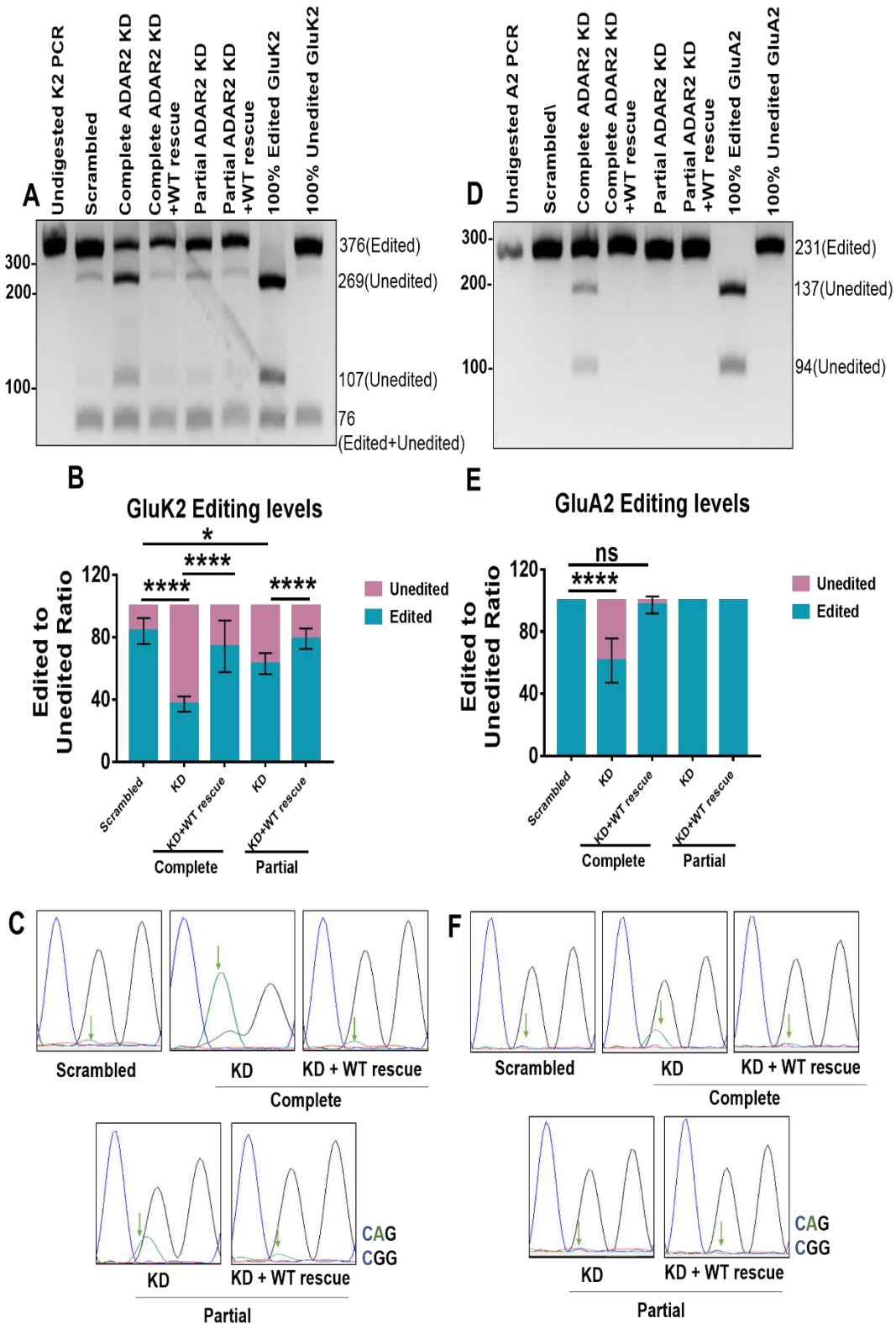
A
Undigested K2 PCR
Scrambled
Complete ADAR2 KD
Complete ADAR2 KD +WT rescue
Partial ADAR2 KD
Partial ADAR2 KD +WT rescue
100% Edited GluK2
100% Unedited GluK2
300
200
100
376(Edited)
269(Unedited)
107(Unedited)
76 (Edited+Unedited)
D
Undigested A2 PCR
Scrambled\
Complete ADAR2 KD
Complete ADAR2 KD +WT rescue
Partial ADAR2 KD
Partial ADAR2 KD +WT rescue
100% Edited GluA2
100% Unedited GluA2
300
200
100
231(Edited)
137(Unedited)
94(Unedited)
B
GluK2 Editing levels
Edited to Unedited Ratio
120
80
40
0
*
****
****
****
Unedited
Edited
Scrambled
KD
KD+WT rescue
KD
KD+WT rescue
Complete
Partial
E
GluA2 Editing levels
Edited to Unedited Ratio
120
80
40
0
ns
****
Unedited
Edited
Scrambled
KD
KD+WT rescue
KD
KD+WT rescue
Complete
Partial
C
Scrambled
KD
KD + WT rescue
Complete
KD
KD + WT rescue
CAG
CGG
Partial
F
Scrambled
KD
KD + WT rescue
Complete
KD
KD + WT rescue
CAG
CGG
Partial

Figure 4-10: Rescuing ADAR2 levels rescues editing levels of GluK2 and GluA2 following Complete and Partial ADAR2 KD. 6 days after knockdown and rescue virus infections, RNA was extracted from the hippocampal cells and cDNA was synthesised to perform PCR assays.

A. Representative images of the PCR products separated on a 4% agarose gel post BbvI digestion to determine edited to unedited GluK2 ratio. 100% edited and unedited GluK2 constructs were used as a control to ensure BbvI cut activity and validity of the assay.

B. Quantification of percentage of edited to unedited ratio of GluK2 population present as shown in A. N=4 independent dissections; One way ANOVA with Tukey's multiple post comparisons correction; *p<0.05, **p<0.01, ****p<0.0001; error bars=S.D.

C. Representative chromatographs of PCR products comparing scrambled infected cells with the knockdowns and knockdown rescue infected cells at the Q/R editing site of GluK2. The undigested PCR products were sent for sequencing to determine changes in the dual peaks obtained at the site of editing as indicated by the green arrow. A peak (green) represents the unedited base while the G peak (black) represents the edited base. The image is representative of 3 repeats.

D. Representative images of the PCR products separated on a 4% agarose gel post BbvI digestion to determine edited to unedited GluA2 ratio. 100% edited and unedited GluA2 constructs were used as a control to ensure BbvI cut activity and validity of the assay.

E. Quantification of percentage of edited to unedited ratio of GluA2 population present as shown in A. N=4 independent dissections; One way ANOVA with Tukey's multiple post comparisons correction; ns p>0.05, ****p<0.0001; error bars=S.D.

F. Representative chromatographs of PCR products comparing scrambled infected cells with the knockdowns and knockdown rescue infected cells at the Q/R editing site of GluA2. The undigested PCR products were sent for sequencing to determine changes in the dual peaks obtained at the site of editing as indicated by the green arrow. A peak (green) represents the unedited base while the G peak (black) represents the edited base. The image is representative of 3 repeats.

4.3.10 Complete and Partial ADAR2 KD differentially alter total GluA2 and GluK2 levels

As loss of ADAR2 editing function has been suggested to lead to eventual loss of total protein expression at least in case of GluA2 (Higuchi, Maas et al. 2000), I next tested if the ADAR2 KDs affected the total protein expression of GluK2 and GluA2. Interestingly, 'Complete' ADAR2 KD decreased the total protein levels of both GluA2 and GluK2. 'Partial' ADAR2 KD also significantly decreased total GluA2 levels although to a lesser extent than 'Complete'

ADAR2 KD. On the other hand, total protein levels of GluK2 were unaffected [**Figure 4-11**]. Thus, 'Partial ADAR2 KD' does not affect total GluK2 levels.

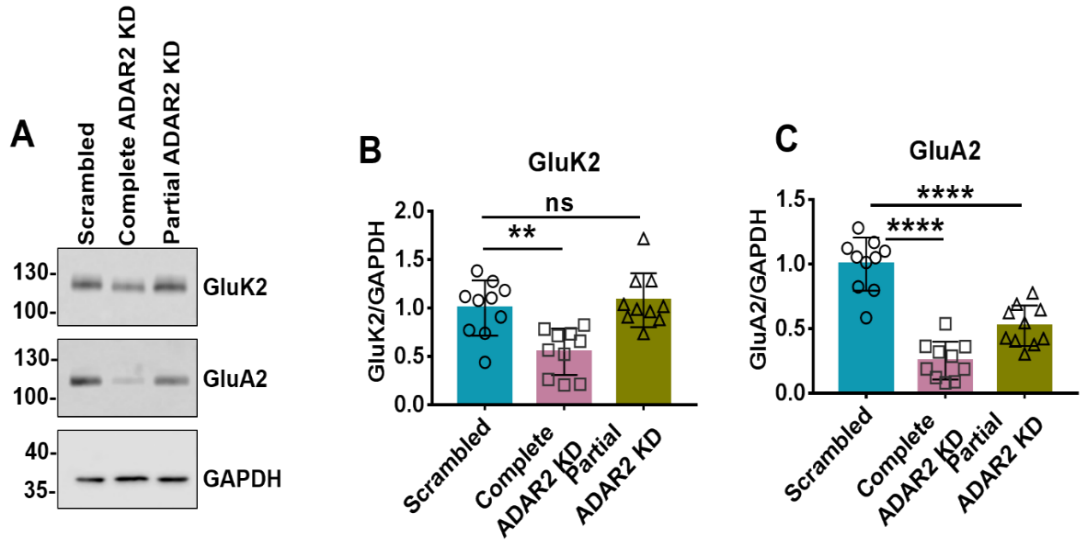

Figure 4-11: Complete and Partial knockdown of ADAR2 differentially alter GluA2 and GluK2 total levels. 5 days after knockdown virus infection, cells were harvested and analysed using western blotting.

A. Representative western blot images of total levels of GluK2 and GluA2 post 5 days infection with complete and partial ADAR2 KD.

B-C. Quantification of GluK2 (B) and GluA2 (C) normalised to GAPDH shown in A. N=10 independent dissections. One-way ANOVA with Tukey's multiple post comparisons correction; ns $p>0.05$, **$p<0.01$, ****$p<0.0001$; error bars=S.D.

4.3.11 Partial ADAR2 KD phenocopies and occludes GluK2 scaling

Intriguingly, the levels of ADAR2 loss observed with Partial ADAR2 KD were comparable to the levels obtained following 24 h TTX treatment. The shift in proportions of edited to unedited GluK2 were also similar. Moreover, 'Partial' ADAR2 KD did not affect the total expression of GluK2 unlike the 'Complete' ADAR2 KD.

I therefore determined if 'Partial' loss of ADAR2 is enough to mediate GluK2 up-scaling. As shown in **Figure 4-12** A and B, 24 h TTX treated neurones and neurones infected with Partial ADAR2 KD, both significantly increased GluK2 surface expression compared to the neurones infected with scrambled shRNA, with no effect on the EGFR surface expression [**Figure 4-12** A and

C]. However, TTX treatment in combination with Partial ADAR2 KD had no additive effects consistent with partial ADAR2 loss phenocopying and occluding GluK2 up-scaling.

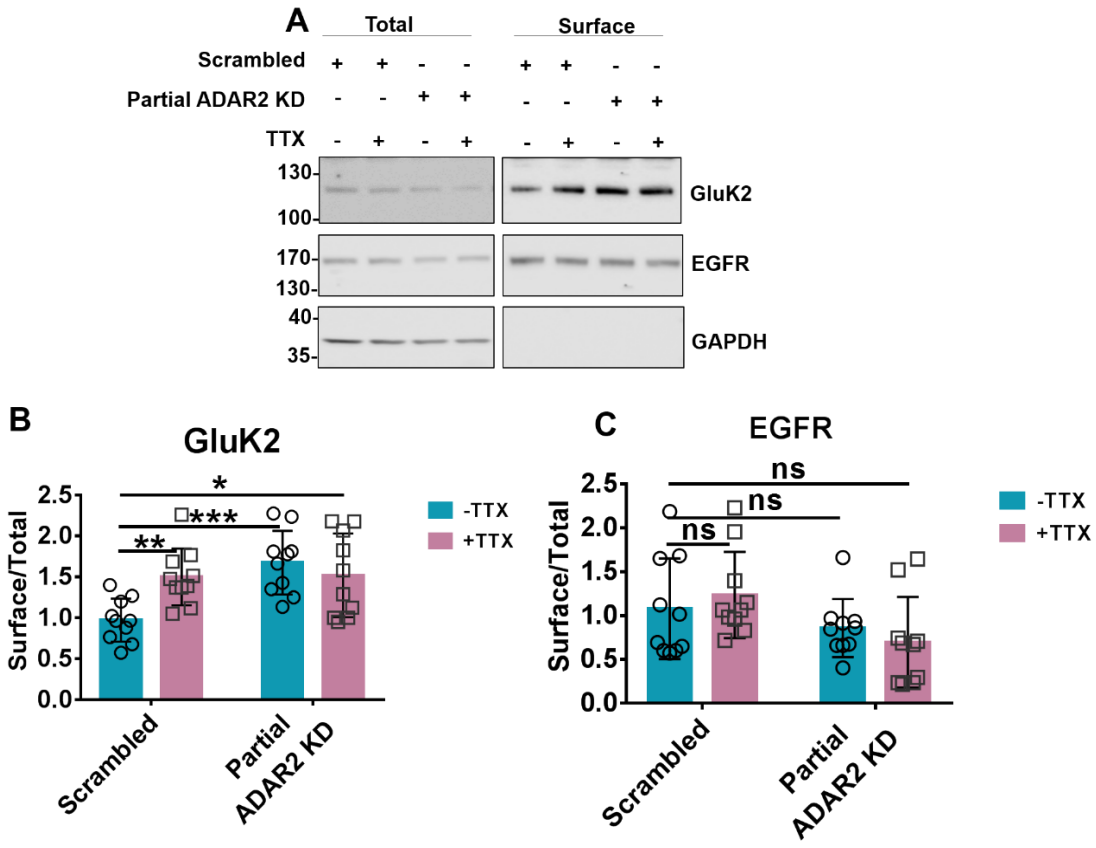

Figure 4-12: Partial ADAR2 KD phenocopies and occludes GluK2 scaling. Surface biotinylation was performed on DIV 15 hippocampal neurones following infections with either scrambled or Partial ADAR2 KD for 5 days with or without 24 h TTX treatment to isolate surface proteins and determine surface/total ratio by western blotting.

A. Representative western blot images of surface and total levels of GluK2 and EGFR. EGFR was used as a surface expressed non-glutamate receptor control that should not respond to the stimulation. GAPDH was used as an internal control to determine no internal proteins were biotinylated.

B-C. Quantification of surface to total ratio of GluK2 (B) and EGFR (C) shown in A. N=10 independent dissections. One-way ANOVA with Tukey's multiple post comparisons correction; ns $p>0.05$, *$p<0.05$, **$p<0.01$, ***<0.001; error bars=S.D.

Interestingly, however, in 'Partial ADAR2 KD' neurons treated with 24 h TTX there was a further decrease in ADAR2 levels [**Figure 4-13**], indicating that even when already depleted, ADAR2 levels are still subject to activity-dependent regulation.

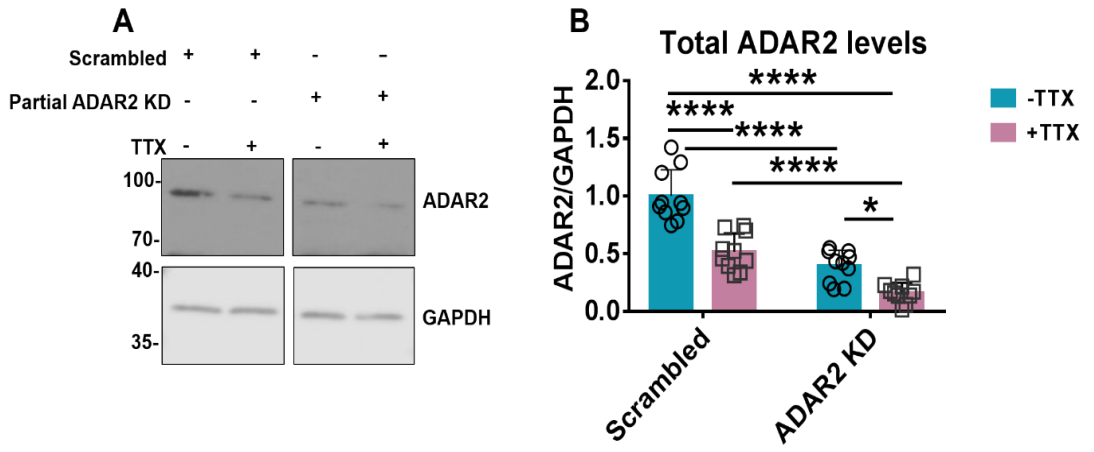

Figure 4-13: Partial ADAR2 KD combined with 24 h TTX treated elicits further decrease in ADAR2 levels. DIV 15 hippocampal neurones following infected with either scrambled or Partial ADAR2 KD for 5 days with or without 24h TTX treatment were blotted for total ADAR2 levels.

A. Representative western blot images of total levels of ADAR2 and GAPDH.

B. Quantification of ADAR2 normalised to GAPDH shown in A shown in A. N=10 independent dissections. One-way ANOVA with Tukey's multiple post comparisons correction; *p<0.05, ****p<0.0001; error bars=S.D.

4.3.12 No further reduction in GluK2 editing in neurones treated with both Partial ADAR2 KD and TTX

As there was further loss of ADAR2 when cells were infected with 'Partial ADAR2 KD' and treated with 24 h TTX, I tested if GluK2 editing was also decreased further in this condition. As shown in **Figure 4-14**, despite the summative decrease in ADAR2 levels, Partial ADAR2 KD combined with 24 h TTX treatment did not further decrease GluK2 Q/R editing compared to either treatment alone, consistent to no additive increase in GluK2 surface expression in combined TTX and ADAR2 KD condition.

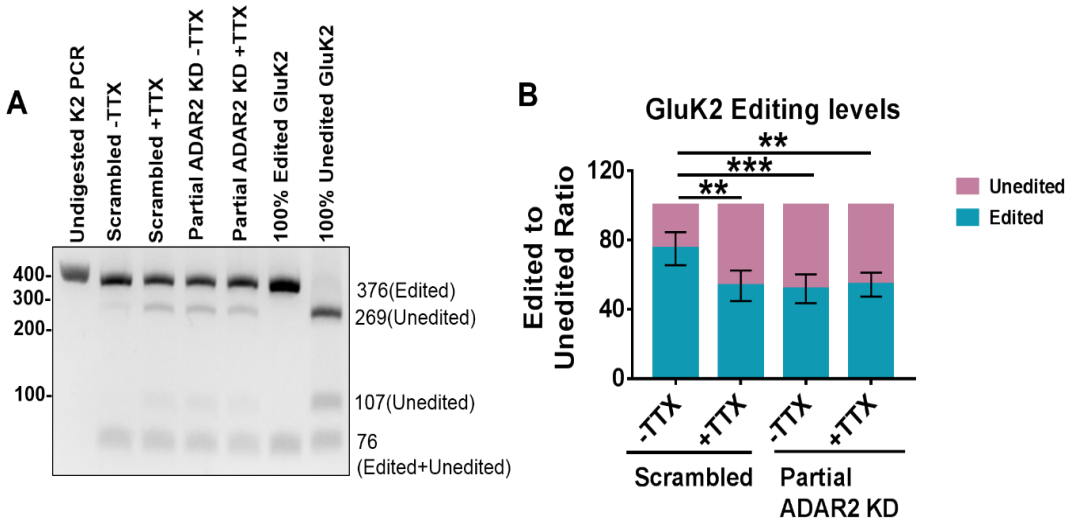

Figure 4-14: No further reduction in GluK2 editing in neurones treated with both Partial ADAR2 KD and 24 h TTX.

A. Representative images of the PCR products separated on a 4% agarose gel post BbvI digestion to determine edited to unedited GluK2 ratio in cells treated with either scrambled or partial ADAR2 KD or 24 h TTX or both partial KD and 24 h TTX. 100% edited and unedited GluK2 constructs were used as a control to ensure BbvI cut activity and validity of the assay.

B. Quantification of percentage of edited to unedited ratio of GluK2 population present as shown in A. N=5 independent dissections; One way ANOVA with Tukey's multiple post comparisons correction; **p<0.01, ***p<0.001; error bars=S.D.

4.3.13 Decreased stability of unedited GluK2 (Q) compared to the edited GluK2 (R)

It has been previously suggested that edited GluK2 is less stable than the unedited GluK2 (Ball, Atlason et al. 2010). Therefore, I determined if exogenously expressed tagged unedited (Q) and edited (R) GluK2 (YFP-myc tagged in the N-terminus) have altered stability. Edited and unedited forms of GluK2 were overexpressed in HEK293T cells for 24 h and then subjected to cycloheximide (CHX) treatment, which blocks translation (Schneider-Poetsch, Ju et al. 2010). Cycloheximide was added for 0, 4 or 8 h to measure the GluK2 stability.

In contrast to published findings, my results show the total protein levels of unedited GluK2 (Q) were decreased significantly by 8 h of CHX addition

suggesting decreased stability. In contrast, the edited form of GluK2 (R) was stable even after 8 h of CHX addition [**Figure 4-15**].

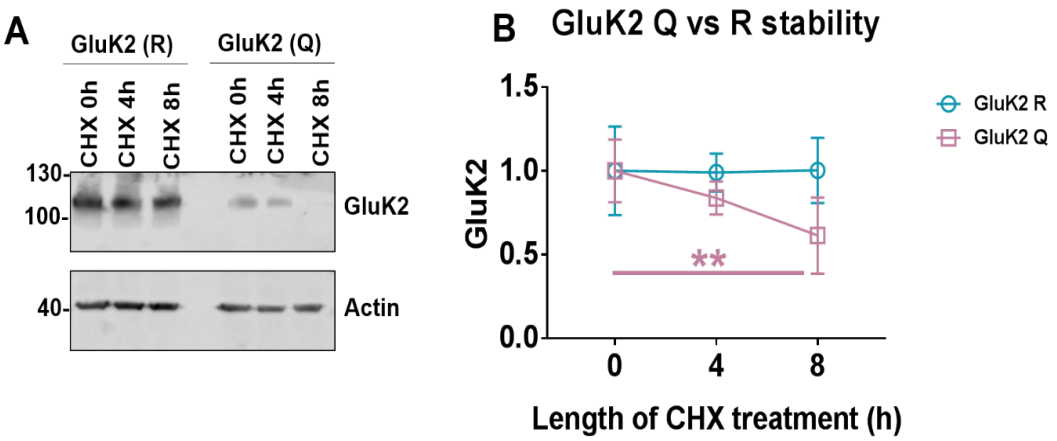

Figure 4-15: Unedited GluK2 (Q) showed less stability than edited GluK2 (R). HEK293T cells transfected with either edited or unedited forms of GluK2. 24h after transfection to overexpress GluK2, cells were treated with translation blocker cycloheximide (CHX) for 0h (same volume of DMSO as CHX for 8h), 4h and 8h and then lysed to determine total GluK2 levels by western blotting.

A. Representative western blot images of the total GluK2 and actin levels after 0, 4 and 8 h CHX treatment. 0 h CHX treated cells were treated with same volume DMSO for 8 h.

B. Quantification of edited or unedited GluK2 as shown in A. Each GluK2 constructs were normalised to their respective 0h control. N=5 independent passages; One way ANOVA with Tukey's multiple post comparisons correction; **p<0.01; error bars=S.D.

4.4 Discussion

4.4.1 ADAR2 levels are not regulated bi-directionally during chronic suppression and enhancement of synaptic activity

Reports in the literature have indicated that ADAR2 levels are susceptible to both acute and chronic changes in synaptic activity (Sanjana, Levanon et al. 2012, Balik, Penn et al. 2013). Here I show that ADAR2, but not ADAR1, protein levels decrease following chronic suppression of synaptic activity with 24 h TTX treatment [**Figure 4-1**]. Subcellular fractionation and imaging data confirmed the nuclear localisation of these proteins [**Figure 4-4** and **Figure 4-5]**. Following 24 h TTX treatment along with the intensity, the percentage of

cells expressing ADAR2 also decreased. Moreover, longer durations of TTX treatment (up to 48 h) did not further decrease ADAR2 levels.

Surprisingly, chronic enhancement of network activity with 48 h bicuculline treatment did not increase ADAR2 or ADAR1 protein levels [**Figure 4-2]**. While ADAR1 has been shown to be unresponsive to changes in the synaptic activity, ADAR2 levels have been reported to be susceptible to both up-scaling and down-scaling of network activity (Sanjana, Levanon et al. 2012, Balik, Penn et al. 2013). While further analysis will be required, we speculate that these different findings could be due to the use of different experimental systems and outcome measures. In particular, both studies monitored alterations in ADAR2 transcripts levels rather than the protein levels, as I have done here. RNA transcripts are not necessarily a true indication of the total protein levels. Furthermore, the genome-wide studies were performed in cerebral cortical cultures (Sanjana, Levanon et al. 2012) whereas my studies were performed in hippocampal neurones. It may be that hippocampal neurones respond differently to cortical cultures. Consistent with this another study reporting changes in response to bicuculline treatment were region specific favouring CA1 to CA3 (Balik, Penn et al. 2013). My studies were performed on dispersed cultures which are generally thought to have a more CA1 phenotype however mixture of various hippocampal subtypes in dispersed cultures could mask subtle changes.

Nonetheless, I did observe increase in GluK2 editing following bicuculline treatment [see section 3.3.7]. Perhaps either ADAR2 (or even ADAR1) could have had increased editing ability. This could be due to changes in their activity domains (deaminase domain) or changes in their ability to bind their substrates either due to lesser substrate sequestration or changes in enzyme subcellular localisation. While interesting, this was not pursued any further.

Perhaps most interestingly, my observation that ADAR2 levels are altered in up-scaling but not in down-scaling shows that opposing changes in network activity are likely governed by distinct underlying mechanisms. Thus, my results suggest that ADAR2 levels are not bi-directionally regulated during chronic suppression and enhancement of network activity.

4.4.2 Differential sensitivity of GluK2 and GluA2 to alterations in ADAR2 levels

Following 24 h TTX treatment, I observed robust up-scaling of both KARs (GluK2) and AMPARs (GluA2). Moreover, I detected a significant decrease in GluK2 Q/R editing, most likely due to the loss of ADAR2 levels. However, no such editing changes were observed in GluA2 AMPARs following TTX treatment. This suggested a specific role of Q/R editing in GluK2 up-scaling.

To study this further, I created two different knockdown tools for ADAR2, one that completely removed endogenous ADAR2 'Complete ADAR2 KD' and another that partially removed endogenous ADAR2 'Partial ADAR2 KD' [**Figure 4-6**]. This allowed me to study the comparative effects of varying levels of ADAR2 in both GluK2 and GluA2 and determine if ADAR2 can selectively alter GluK2 editing.

Complete loss of ADAR2 decreased GluA2 editing by ~30% and GluK2 editing by >60%, whereas partial ADAR2 loss decreased editing of GluK2 by ~20% but had no discernible impact on the editing of AMPAR subunit GluA2 [**Figure 4-7** and **Figure 4-8**]. Furthermore, editing deficiencies for both GluK2 and GluA2 is rescued upon expression of shRNA insensitive WT ADAR2 rescue, showing specificity of ADAR2 role in Q/R editing for both GluK2 and GluA2 [**Figure 4-10**].

These findings suggest that GluA2 is preferentially and almost completely edited at Q/R site, even when only low levels of ADAR2 are available. GluK2 mRNA, on the other hand, is more sensitive to fluctuations in ADAR2 levels. It has been reported that GluA2 Q/R editing is robustly regulated by maintaining less efficient splicing of unedited GluA2 mRNA transcripts (Penn, Balik et al. 2013). Thus, it seems that GluA2 editing is protected and maintained at 'all costs' since failure to edit GluA2 is lethal. This is exemplified by the observation that expression of edited GluA2 in ADAR2 KO mice rescues their lethality (Higuchi, Maas et al. 2000). This infers that control of GluA2 is less nuanced than the regulation of GluK2 by changes in ADAR2 levels.

Interestingly, the ADAR2 KO mice had a build-up of unedited GluA2 pre-mRNA transcripts resulting in the reduction of total GluA2 protein levels

(Higuchi, Maas et al. 2000). In line with this, following even partial loss of ADAR2 there is a decrease in total GluA2 levels [**Figure 4-11**]. This is probably due to the accumulation of immature unedited transcripts that are not spliced efficiently. Hence there is a lack of detectable unedited GluA2 population with 'Partial' ADAR2 KD. The loss of total GluA2 is further amplified with total loss of ADAR2. Thus, rather than express excess amounts of unedited GluA2 neurons compensate by reducing total levels of GluA2. I also speculate that the lack of further loss of ADAR2 with longer times of TTX treatment is a mechanism to ensure that sufficient numbers of edited GluA2 are maintained to constrain AMPAR Ca^{2+} permeability and ensure cell survival **[Figure 4-3**]. Interestingly, with the complete loss of ADAR2, there is 30% increase in the unedited mature GluA2 transcripts. This suggests that while coupling editing with splicing acts as a 'safeguard' mechanism to ensure editing levels of GluA2 are maintained, some of the unedited transcripts can still be spliced to form mature transcripts.

In contrast, partial loss of ADAR2 did not decrease GluK2 levels which suggests that the neurones have higher tolerance to unedited GluK2 compared to GluA2. The fact that only 85% GluK2 population are edited in adults compared to 99.9% in GluA2 further supports the higher tolerance of neurones to unedited GluK2 (Paschen and Djuricic 1995, Bernard, Ferhat et al. 1999). However, there was a significant loss of total GluK2 protein levels following complete loss of ADAR2. This begs the question if the unedited GluK2 can also undergo similar safeguard mechanism to that of GluA2 at higher levels. While GluK2 transcript and total levels were not mentioned in the ADAR2 KO mice, the GluK2 editing deficient mice did not show such phenotype. Therefore, it is not known the mechanism behind the loss of GluK2 total levels following decrease in its editing.

Taken together, my studies show that Q/R editing of GluK2 is more flexible and responsive to changes in ADAR2 levels compared to GluA2. This explains how GluK2 editing, but not GluA2, changes following ADAR2 loss after TTX treatment. In summary, I interpret these data to indicate that the Q/R editing of KARs is more dynamically and activity-dependently regulated than

AMPARs, and reason that this provides a rapidly tunable system to control KAR forward trafficking and scaling.

4.4.3 Selective ADAR2 mediated Q/R editing of GluK2 containing KARs regulates their up-scaling

One of the main aims of my project was to determine if ADAR2 loss mediated decrease in Q/R editing plays a role in GluK2 up-scaling. Partial ADAR2 KD mimicked the decrease in ADAR2 levels observed after TTX induced scaling and importantly did not alter GluA2 editing. Moreover, this knockdown tool did not alter total GluK2 levels compared to complete knockdown of ADAR2. I therefore used this tool to further study the role of ADAR2 mediated changes in GluK2 editing in inducing GluK2 up-scaling in response to TTX treatment.

Here I show that the partial loss of ADAR2 is sufficient to induce an increase in GluK2 surface expression mimicking the surface levels achieved post 24h TTX treatment [**Figure 4-12**]. Further addition of 24 h TTX in partial ADAR2 knockdown treated neurones however, did not increase the surface expression any further. Interestingly in Partial ADAR2 knockdown neurons, TTX treatment did elicit a further decrease in ADAR2 levels, indicating that even when already depleted, ADAR2 levels are still subject to activity-dependent regulation [**Figure 4-13**]. However, despite the summative decrease in ADAR2 levels, GluK2 editing status did not decrease any further [**Figure 4-14**], which perhaps explains the occlusive effect of 'Partial' ADAR2 loss on TTX treatment and strongly suggests that reduced KAR editing underpins KAR up-scaling. EGFR used a negative control in this instance was not significantly affected in their surface expression with the 'Partial' knockdown or TTX treatment.

Hence, I conclude that the 'Partial' loss of ADAR2 phenocopies and occludes GluK2 scaling. Taken together, my data is consistent with the activity-dependent loss of ADAR2 leading to the alterations in KAR editing which, in turn, directly mediates KAR up-scaling as unedited GluK2(Q) has been shown to increase KAR assembly and ER exit compared to edited GluK2(R) (Ball, Atlason et al. 2010, Evans, Gurung et al. 2017).

4.4.4 Potential role of Q/R editing in GluK2 stability

A particularly interesting observation was the loss of GluK2 following complete loss of ADAR2. To investigate the mechanisms involved I tested if unedited GluK2 is less stable than edited GluK2. Following 8 h cycloheximide treatment, the unedited GluK2 transfected in HEK293T cells for 24h were degraded at a significantly higher rate compared to the edited GluK2, consistent with increased rapid turnover of unedited GluK2 [**Figure 4-15**]. As more unedited GluK2 would exit the ER and express on the surface, there is likely a higher turnover and degradation from the surface. However, this contrasts with a previous report suggesting that the edited GluK2 are more likely to be degraded rapidly than unedited GluK2 due to their ER build up and lack of ability to form homomers (Ball, Atlason et al. 2010). Further work will be required to resolve this apparent discrepancy. As both these studies are performed in isolation (overexpressed in HEK293T cells, which do not express any KARs), the kinetics may be different in presence of other KAR subunits.

Therefore, my preliminary work here suggests that the Q/R editing may play a role in GluK2 containing KARs stability.

4.5 Conclusion

In summary of this chapter, I have shown ADAR2 levels are regulated during chronic suppression of network activity leading to a selective decrease in GluK2 Q/R editing but not that of GluA2 editing. This allows more unedited GluK2 to be formed which assembles into tetramers and exits the ER more efficiently leading to an increase in their surface expression and hence GluK2 containing KARs up-scaling. However, similar mechanism does not seem to exist for bicuculline mediated chronic enhancement of network activity.

Chapter 5. STUDYING MECHANISMS REGULATING ADAR2 LEVEL AND FUNCTION DURING SCALING

5.1 Introduction

For the final part of my PhD I wanted to determine the possible mechanisms behind ADAR2 loss during 24 h TTX mediated suppression of synaptic activity. The changes in ADAR2 levels could be due to alterations in mRNA transcription, translation or protein degradation. While not much is known about ADAR2 regulation, here I have summarised the factors that are thought to regulate ADAR2 levels and function.

5.1.1 Transcription

As discussed in section 4.1, ADAR2 transcript levels are susceptible to changes in both the acute and chronic changes in synaptic activity.

5.1.1.1 CREB

One of the potential regulators of ADAR2 transcription is cAMP-response - element-binding protein (CREB). It was reported that during transient ischemic insults, ADAR2 gene expression can be regulated in a CREB dependent manner, where ADAR2 transcription and gene expression was positively regulated by constitutively active CREB expression (Peng, Zhong et al. 2006). Complementing this, ADAR2 promoter region consists of CREB binding site that regulates ADAR2 expression in pancreatic cells in response to glucose uptake via JNK-1 kinase pathway (Yang, Huang et al. 2012). It has also been suggested that Ca^{2+} signalling through L-type voltage-gated Ca^{2+} channels can regulate activity-dependent ADAR2 expression (Wheeler, Barrett et al. 2008). Interestingly, this signalling can also activate nuclear CREB pathway which could be mediating alterations in ADAR2 levels (Balik, Penn et al. 2013).

5.1.1.2 Epigenetic Regulation

Studies in neuronal SH-SY5Y cells suggested ADAR2 mRNA expression can be differentially regulated by epigenetic modifying enzymes DNA methyltransferase (DNMT) and histone deacetylase (HDAC). Inhibiting either of these epigenetic modifying enzymes elicited an increase in ADAR2 mRNA expression. Furthermore, blocking transcription using actinomycin D, prevented the mRNA increase in ADAR2, suggesting these epigenetic modifying enzymes regulate ADAR2 expression by regulating ADAR2 transcription (Uchida and Ito 2015).

5.1.2 Auto-editing

ADAR2 is an interesting protein as it can self-regulate its own expression levels by editing itself. ADAR2 self-edits its own pre-mRNA leading to alternative splicing at various sites. This can generate several ADAR2 alternatively spliced variants, though functional consequences for all the identified forms of auto-edited transcript variants are not known (Li, Tian et al. 2015, Fu, Zhao et al. 2016) [see section 1.4.3].

One such editing event occurs between the exons 1 and 2 of ADAR2 which results in the addition of 47 nucleotides (nt) at the 5' end of exon 2 during subsequent splicing [**Figure 5-1**]. The resultant alternatively spliced ADAR2 variant codes for a premature stop codon giving rise to truncated 9kDa ADAR2 protein which lacks both the dsRNA binding domain and the deaminase domain and is hence non-functional (Rueter, Dawson et al. 1999). The auto-editing at this site has been shown to increase during development in both rat and mouse brains and in cortical cultured neurones (Hang, Tohda et al. 2008, Wahlstedt, Daniel et al. 2009, Behm, Wahlstedt et al. 2017). Moreover, transgenic mice lacking this autoregulation were shown to have increased ADAR2 protein expression at several tissues and had subsequent increase in the editing of various ADAR2 substrates such as the R/G editing of GluA2 (Feng, Sansam et al. 2006).

Moreover, auto-editing of ADAR2 at this site has also been shown to be altered during various cellular insults. Thiamine (vitamin B1) deficiency (TD) in cortical cultured neurones and brain tissue resulted in decreased ADAR2 auto-editing (Lee, Yang et al. 2010). This was regulated by stress-activated protein kinase c-Jun N-terminal kinases (JNK1) and inhibiting this pathway resulted in decreased ADAR2 auto-editing (Yang, Huang et al. 2012). On the other hand, elevated self-editing was observed following glucose stimulation in INS-1 β-cells (Gan, Zhao et al. 2006). Furthermore, less ADAR2 self-editing after 48 h activity-deprivation with TTX has also been shown and the opposite was observed with enhanced network activity (Balik, Penn et al. 2013), however functional consequences of these changes in auto-editing are not known. Hence, ADAR2 auto-editing at this site can act as a potential mechanism to regulate ADAR2 levels and function during neuronal activity.

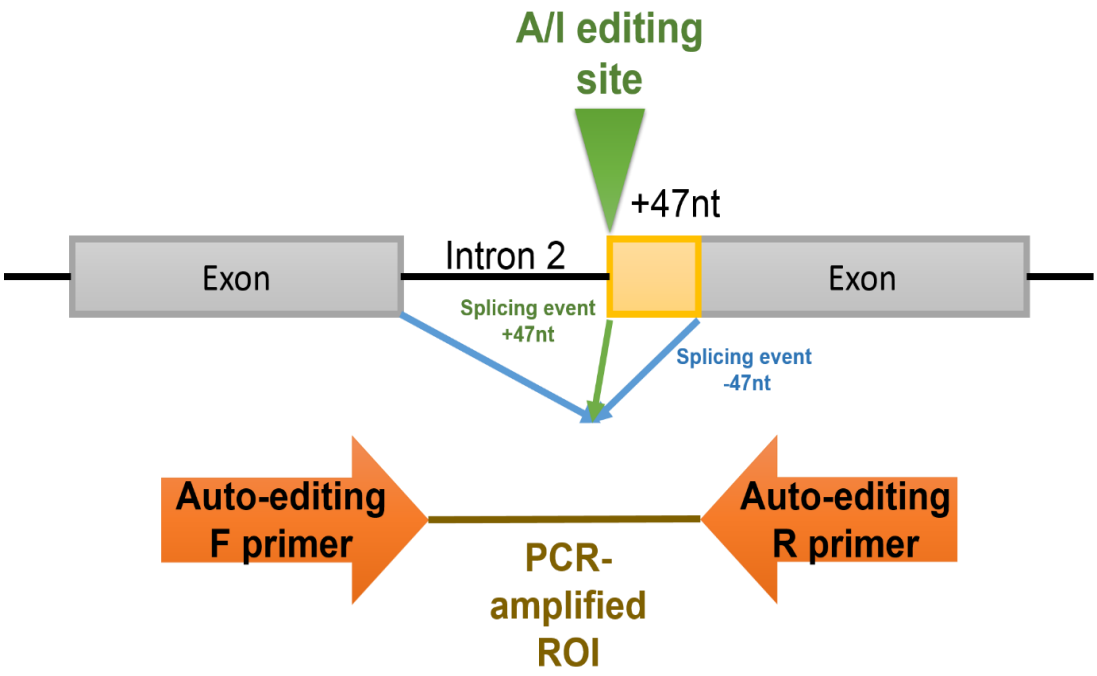

Figure 5-1: ADAR2 can edit its own pre-mRNA.

This generates a new 3' splice site extending the second coding exon by 47 nucleotides (nt). This then results in a frameshift coding for a premature stop codon. This self-editing process can be tested by designing forward and reverse primers spanning the adjacent exons to intron 2 and performing PCR amplification of the region of interest (ROI). The resultant PCR products produces two bands when separated by agarose gel electrophoresis.

5.1.3 Subcellular Localisation

The subcellular localisation of ADAR2 can also regulate ADAR2 function and activity. ADAR2 import into the nucleus is regulated by the family of alpha importins; karyopherin subunit alpha 1 (KPNA1) and 3 (KPNA 3) (Maas and Gommans 2009). Moreover, it was shown that importin alpha-4 (KPNA3) levels increase during neuronal maturation in cultured cortical neurones and increasingly associate with ADAR2, enhancing their import into the nucleus thus contributing to the editing efficiency of ADAR2 (Behm, Wahlstedt et al. 2017).

Interestingly, ADAR2 activity can be regulated in the nucleus via functional sequestration of ADARs in the nucleolus. While the editing is thought to occur mostly in the nucleoplasm where ADAR2 can be present, ADAR2 are predominantly concentrated in the nucleolus (Desterro, Keegan et al. 2003, Sansam, Wells et al. 2003). It has been suggested that ADAR2 can shuttle in

and out of nucleolus to the nucleoplasm, which is regulated by substrate availability and specificity. This functional sequestration by the nucleolus potentially occurs through binding of abundant dsRNA structures associated with small nucleolar RNAs. Moreover, inhibiting ribosomal RNAs increased translocation of ADAR2 to nucleoplasm and resulted in increased substrate editing (Desterro, Keegan et al. 2003). However, a separate study showed that ADAR2 can be functionally active in the nucleolus as well and that specific nucleolar specific mechanisms exists to limit ADAR2 activity there (Sansam, Wells et al. 2003). Taken together, nucleolar sequestration adds another level of cellular mechanism to prevent accidental editing activity in nucleoplasm for ADAR2.

5.1.4 Pin1 mediated ADAR2 phosphorylation

Peptidyl-prolyl isomerase NIMA interacting protein 1 (Pin1) is a phosphorylation dependent peptidyl-prolyl cis/trans isomerase. The WW domain, 38 to 40 amino acid (aa) residues in a triple-stranded β-sheets (Lu, Hanes et al. 1996), present in Pin1 mediates protein-protein interactions by binding to a phosphorylated serine (S) or threonine (T) preceding a proline residue in the target substrates. They catalyse the cis/trans isomerisation of the substrate's peptide bond altering substrate stability, subcellular localisation and/or catalytic activity (Lu, Zhou et al. 1999, Lu and Zhou 2007).

ADAR2 was shown to be post-translationally regulated by Pin1. This binding occurs via phosphorylation of the threonine 32 (T32) residue on the N-terminus of ADAR2. Pin1 binding to ADAR2 regulates ADAR2 nuclear localisation, stability and hence editing activity (Marcucci, Brindle et al. 2011) [**Figure 5-2**]. Further to this, another study in mouse cortical cultured neurones also showed the Pin1 and ADAR2 interaction to be important during development. More specifically, this interaction was important in maintaining ADAR2 stability after its import into the nucleus (Behm, Wahlstedt et al. 2017). This allowed increased editing of ADAR2 substrates during neuronal maturation.

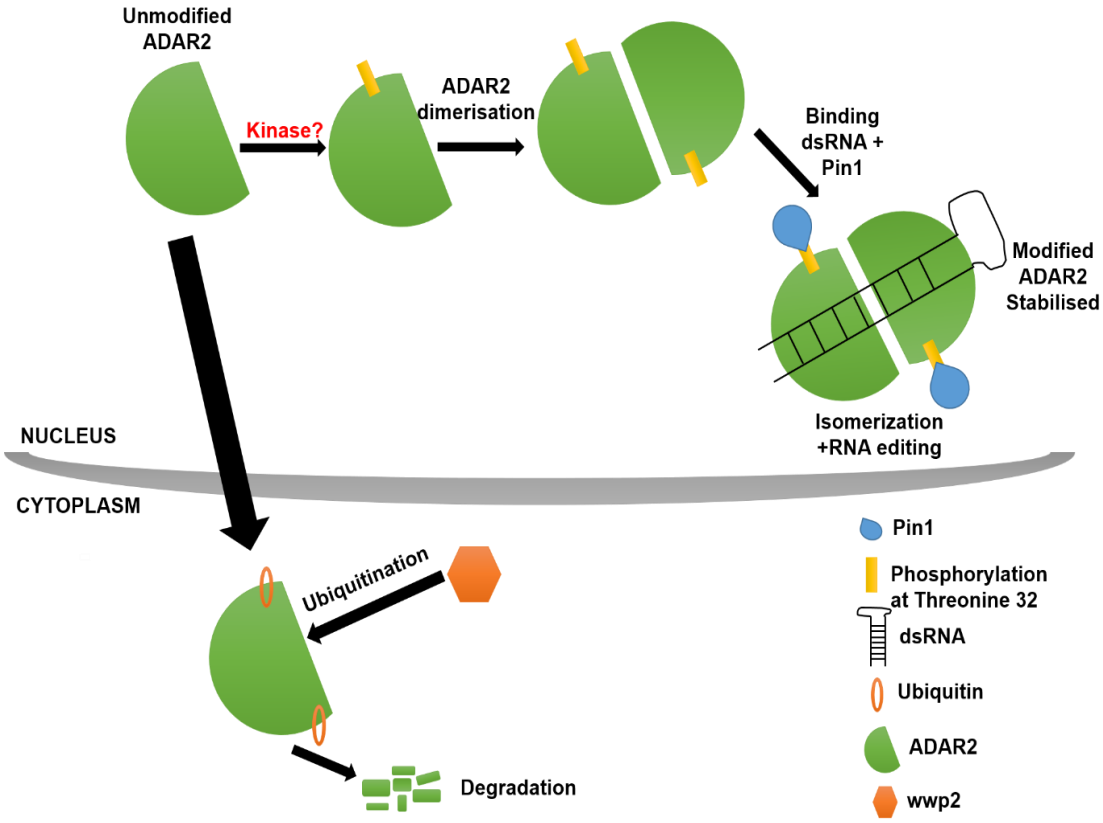

Figure 5-2: Pin1 and WWP2 mediated regulation of ADAR2.

Cartoon diagram of potential Pin1 mediated regulation of ADAR2, altering the stability and activity of ADAR2 within the nucleus. This interaction is phosphorylation mediated where phosphorylated ADAR2 dimerises and binds to the dsRNA. Pin1 binds at the phosphorylated site at Threonine 32 (T32) and stabilises ADAR2 in the nucleus. Upon lack of this phosphorylation mediated interaction, ADAR2 is exported out of nucleus into the cytoplasm, where it is targeted for ubiquitination by WWP2 and hence proteasomal degradation.

5.1.5 WWP2 mediated ADAR2 degradation

WWP2; a HECT (homologous to the E6-AP C terminus) is an E3 ubiquitin ligase (Pirozzi, McConnell et al. 1997) and was shown to bind and negatively regulate ADAR2 levels and activity. It binds to ADAR2 via a conserved PPxY motif in both amino- and carboxyl terminus of ADAR2 resulting in ADAR2 poly-ubiquitination. This targets them for proteasomal degradation in the cytosol, hence acting as another post-translational regulator of ADAR2 (Marcucci, Brindle et al. 2011) [**Figure 5-2**]. However, physiological relevance of this interaction is not known yet.

5.1.6 Other ADAR2 regulators

5.1.6.1 AIMP2

Aminoacyl tRNA synthase complex-interacting multifunctional protein 2 (AIMP2) was recently identified as a negative regulator of A-to-I editing. AIMP2 is a scaffolding component of the aminoacyl t-RNA synthetase complex required for the complex assembly and stability (Kim, Kang et al. 2002). AIMP2 interacted with both ADAR1 and ADAR2 and overexpression of AIMP2 protein decreased both ADAR1 and ADAR2 protein levels without affecting their transcript levels (Desterro, Keegan et al. 2003). This indicated a non-translational role of AIMP2 in ADAR regulation. Interestingly, AIMP2 has been shown to have a non-canonical function in regulating protein stability by mediating ubiquitination of target proteins for degradation (Kim, Park et al. 2003). Thus, AIMP2 could potentially be playing a role in post-translational modification of ADAR2 via ubiquitination targeted degradation of ADAR2.

5.1.6.2 FMRP

Fragile-X-Mental Retardation Protein (FMRP) is an RNA binding protein which can regulate RNA metabolism by altering mRNA translation (Napoli, Mercaldo et al. 2008). However, evidence is accumulating to suggest that FMRP can further regulate post-transcriptional modifications by interacting with ADAR proteins. Studies in drosophila initially showed dFMRP1 can interact with dADAR in the nucleus and alter their editing ability on several common RNA targets (Bhogal, Jepson et al. 2011). Following this, studies in zebrafish (Shamay-Ramot, Khermesh et al. 2015) and fmr1 KO mice (Filippini, Bonini et al. 2017) have shown an interplay between FMRP and ADAR2 enzymes, implying FMRP's negative role in ADAR2 editing function. It is thought that ADAR2 and FMRP can also potentially interact in an RNA independent manner and can co-localise in the nucleus (Filippini, Bonini et al. 2017). However, it is not fully understood how FMRP can regulate ADAR2 function.

5.1.6.3 ADAR3

Unlike other ADARs, ADAR3 is expressed exclusively in the brain (Melcher, Maas et al. 1996) but it has not been shown to have any catalytic activity (Chen, Cho et al. 2000). Nonetheless, it consists of both single and double-

stranded RNA binding domains so ADAR3 can bind to other ADAR family targets and potentially sequester them, thereby altering the availability of substrates and playing a regulatory role in ADAR2 function. Consistent with this, ADAR3 was shown to inhibit activities of ADAR2 *in vitro* (Chen, Cho et al. 2000). A recent study also reported ADAR3 as an important regulator of GluA2 Q/R editing in glioblastoma tumours by directly competing with ADAR2 for substrate binding (Oakes, Anderson et al. 2017). However, a recent study in ADAR3 deficient mice showed no considerable differences in editing of target substrates of ADAR1 or ADAR2 (including the R/G and Q/R site of GluA2), suggesting lack of significant inhibitory function of ADAR3 on other functional ADARs *in vivo* (Mladenova, Barry et al. 2018). Hence, the role of ADAR3 in the brain is a mystery.

5.1.6.4 SRSF9

Serine and Arginine Rich Splicing Factor 9 (SRSF9), which belongs to family of pre-mRNA splicing factors rich in serine/arginine, has also been shown to repress ADAR2 editing activity (Tariq, Garncarz et al. 2013, Shanmugam, Zhang et al. 2018). In particular, SRSF9 has been shown to interact with ADAR2 in the nucleus in the presence of RNA substrate and interfere with ADAR2 editing function by disrupting ADAR2 dimerisation. Moreover, this inhibition of ADAR2 function was highly enriched in the brain specific sites (Shanmugam, Zhang et al. 2018).

5.1.7 Objectives

The results in Chapter 4 showed that ADAR2 levels are modulated by changes in synaptic activity. In this chapter I investigated how loss of ADAR2 levels and hence its function is mediated during chronic suppression of network activity following 24h TTX treatment. My main objectives were to address the following questions:

1. Is the loss mediated via changes in ADAR2 mRNA transcription?
2. Are there alterations in ADAR2 auto-editing?
3. Is Pin1 mediated ADAR2 stabilisation altered during activity?
4. Is ADAR2 targeted for increased degradation following TTX treatment?

5.2 Materials and Methods

5.2.1 RT-qPCR

For RT-qPCR, 2µl of the cDNA samples per condition were mixed with PowerUp SYBR green Master Mix ((Life Technologies) containing Dual-Lock™ Taq DNA Polymerase) and forward and reverse primers targeting ADAR2 and GAPDH:

1. PowerUp SYBR green Master Mix: 10µl (Final concentration:1x)
2. Forward + Reverse Primer: 1µl (Final concentration: 0.25 µM each)
3. Sample: 2µl
4. ddH_2O: 7µl

The primers used were:

ADAR2 Forward: 5'- TCCCGCCTGTGTAAGCAC-3'

ADAR2 Reverse: 5'- TGGGCTTGGTGATCTTGG-3'

GAPDH Forward: 5'- CAAGGTCATCCATGACAACTTTG -3'

GAPDH Reverse: 5'- GTCCACCACCCTGTTGCTGTAG -3'

The mixture was then amplified quantitatively using Real Time PCR System (MiniOpticon, BioRAD) for 40 cycles using following conditions:

1. 95^{o}C for 3 minutes to activate the Hot Start Polymerase.
2. 95^{o}C for 20 seconds to break the double strands.
3. 60^{o}C for 30 seconds to anneal the primers.
4. 72^{o}C for 30 seconds for extension.
5. Repeat steps 3-4, 39 times.
6. 95^{o}C for 10 seconds for final extension.
7. 65^{o}C for 5 seconds + 0.5^{o}C every 5 seconds up to 95^{o}C for melt curve.

Ct values were recorded for each reaction. Each reaction was performed in triplicate and average Ct was measured per condition. The values were exported to Microsoft Excel. ADAR2 Ct values were normalised to GAPDH Ct values and ADAR2 mRNA fold difference value of TTX treated conditions was normalised against the untreated control. Melting curve of the primers were

also determined to ensure the specificity of primers used and lack of primer dimer formation. No Reverse Transcriptase control and water only control was also run, and Ct values were compared to ensure there was no genomic DNA contamination.

5.2.2 Auto-editing Assay

For the auto-editing assay, primers were designed using the exonic regions flanking the editing site in ADAR2 as shown in Figure 5-1. Following primers were used:

Forward primer: 5'-GCCAGTCAAGAAGCCCTCAAAAG-3'

Reverse primer: 5'-TGTCCAGATTGCGGTTTTCTTTAAC-3'

The resultant PCR products were run on a 4% agarose gel to separate the two PCR products formed of 150nt (edited to include extra 47nt) and 103nt (unedited). GAPDH was also amplified using PCR and run on a 1.5% agarose gel to produce 496bp PCR product using following primers:

Forward: 5'-CAAGGTCATCCATGACAACTTTG-3'

Reverse: 5'-GTCCACCACCCTGTTGCTGTAG-3'

The agarose gel was visualised under UV transilluminator.

The bands were quantified by measuring densitometry using the Gel Analysis Tool in FIJI ImageJ (NIH). The relative pixel intensity was calculated as the area under each peak. The values obtained were transferred in Microsoft Excel. Both edited and unedited bands were quantified separately and normalised to the GAPDH values.

ADAR2 self-editing percentage calculation:

Total ADAR2= (edited+unedited) / GAPDH

ADAR2 self-editing percentage= (Edited/Total ADAD2) * 100

Statistical significance was then measured.

5.2.3 HEK293T transfection and GFP Trap

HEK293T cells were plated at a density of $1x10^6$ per 10cm dish, and transfected the next day using Lipofectamine^{TM}3000 and the optimised amount (in µg) of each construct to ensure even expression.

All subsequent steps were performed at 4^{o}C on ice using ice-cold buffers. 48h post-transfection, cells were washed with 1x PBS once. 500µl of lysis buffer was added to each dish, scraped and harvested in lysis buffer (20mM Tris pH 7.4, 137mM NaCl, 2mM sodium pyrophosphate, 2mM EDTA, 1% triton X-100, 0.1% SDS, 25mM β-glycerolphosphate, 10% glycerol, protease inhibitors (Roche), phosphatase inhibitor cocktail 2 (1:100, Sigma)). The lysates were left to incubate for 30 mins on ice and centrifuged at 16100g for 20 minutes at 4^{o}C to remove any cell debris. The supernatant was transferred into a fresh 1.5ml tube.

Meanwhile, 5µl of GFP-trap beads per condition was added to separate 1.5ml tubes. The beads were washed twice with 500µl wash buffer (lysis buffer without protease or phosphatase inhibitors) at rt (1500g spin for 2 mins and aspirate the supernatant) (Chromotek). 480µl of the supernatant was then added to the washed beads, incubated on wheel at 4^{o}C for 90 mins. The remaining 20µl of the lysate was mixed with 20µl of 2x Laemmli sample buffer (Input samples). After incubation, the beads were washed 3x with wash buffer. After the last wash, the supernatant was fully aspirated, and the samples were then lysed in 2x Laemmli sample buffer and then heated at 95^{o}C for 10 mins on a rotating heat block (along with the input samples). Samples were then analysed using SDS-PAGE and western blot.

5.2.4 Bortezomib (BTZ) treatment

For proteasomal degradation assay, bortezomib (BTZ) (Cell Signalling, stock in DMSO at 1mM, stored at -20^{o}C) was thawed at rt and was added to the hippocampal neurones to get final concentration of 1µM for 20h. The control cells were treated with equal volume of DMSO for the same length of time. The cells were then either lysed straight into 1x Laemmli sample buffer or surface biotinylation was performed.

5.3 Results

5.3.1 ADAR2 transcription is not altered following 24 h TTX treatment

I first wanted to determine if changes in ADAR2 levels following 24 h TTX treatment were due to changes in the transcription of ADAR2 mRNA. I measured ADAR2 mRNA levels by RT-qPCR and did not see any changes in the overall mature mRNA transcripts post 24 h TTX treatment **[Figure 5-3**]. Hence, in my cultures, ADAR2 transcription is not altered following suppression of synaptic activity. This was surprising as previous studies had shown altered transcript levels following chronic TTX treatment (Sanjana, Levanon et al. 2012, Balik, Penn et al. 2013). I speculate the differences in observations could be due to use of different systems where the genome wide study was performed in cerebral cortical cultures (Sanjana, Levanon et al. 2012) and the second study was performed specifically on the CA1 hippocampal region (Balik, Penn et al. 2013). Nevertheless, my data suggests that ADAR2 loss during TTX treatment is not due to decrease in ADAR2 mRNA transcription.

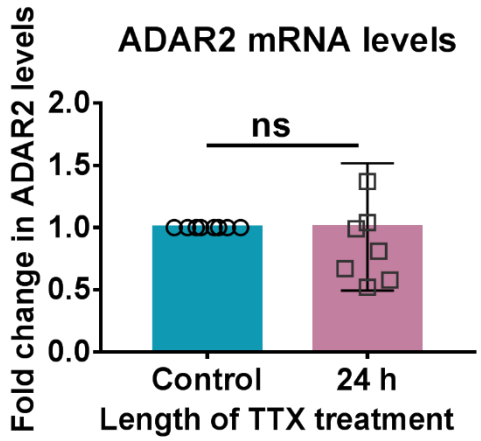

Figure 5-3: ADAR2 transcription is not affected following TTX treatment.

The fold change in mRNA levels of ADAR2 after 24h TTX treatment compared to their respective control treated samples. $\Delta\Delta C_T$ method of analysis was used to measure the fold change in ADAR2 levels. RT-qPCR was used to measure the ADAR2 expression and the reads were normalised to the GAPDH reads. N=7 independent dissections; Unpaired t-test; ns $p>0.05$, error bar=S.D.

5.3.2 ADAR2 self-editing is altered following 24 h TTX treatment

ADAR2 can undergo self-editing process, which acts as a negative feedback mechanism to control ADAR2 expression and activity [See section 5.1.2].

I therefore wanted to determine if ADAR2 self -editing was altered after 24 h TTX treatment. There was a small but significant decrease in the self-editing of ADAR2 [**Figure 5-4** A and B] with no change in ADAR2 total mRNA levels [**Figure 5-4** A and C]. This suggests an increased pool of functional ADAR2 is being translated. While surprising, this may act as a mechanism to counteract the loss of ADAR2 following activity deprivation to prevent the complete loss of ADAR2 levels and function.

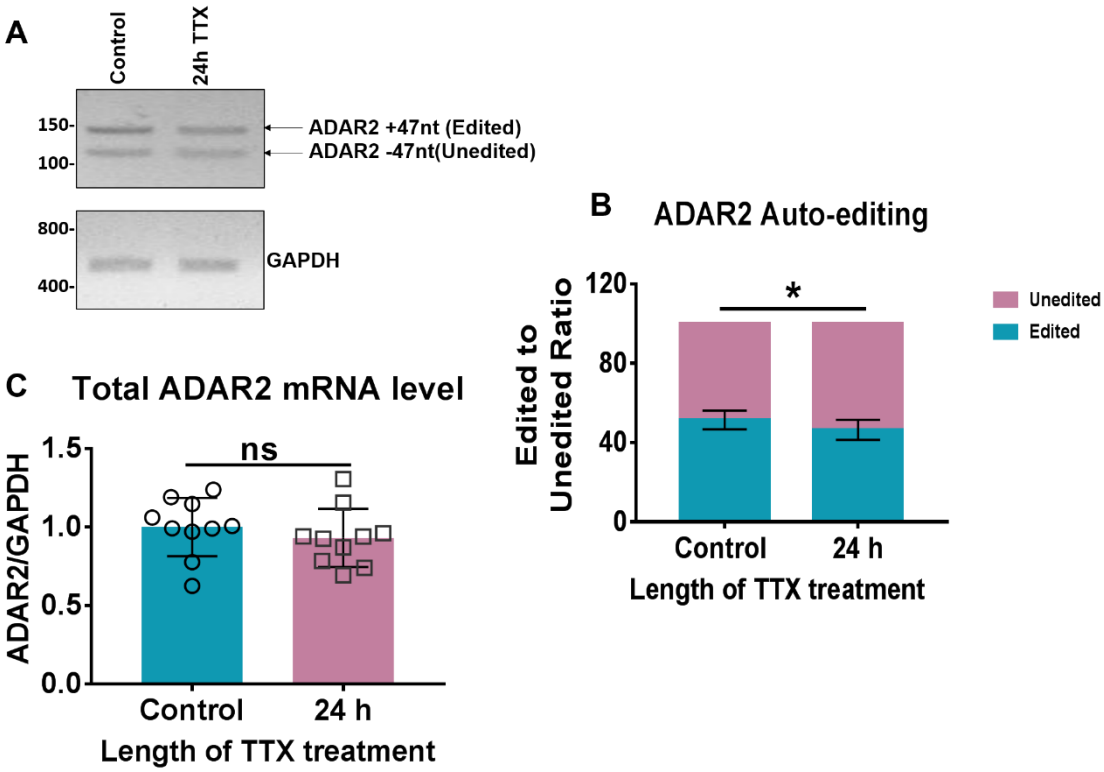

Figure 5-4: ADAR2 auto-editing decreases following 24 h TTX treatment. Post mRNA extraction and cDNA synthesis, the exonic and intronic regions consisting of this 47nt insertion site was amplified and separated on a 4% agarose gel and visualised under UV light.

A. Representative agarose gel image of RT-PCR analysis of alternatively spliced ADAR2 mRNA with or without 47nt insertion as indicated post 24 h TTX treatment.

B. Quantification of edited to unedited ratio of ADAR2 mRNA post 24 h TTX treatment as shown in A. N=10 independent dissections; Unpaired t-test; *p<0.05, error bar=S.D.

C. Quantification of total ADAR2 mRNA levels (edited ADAR2 + unedited ADAR2) and normalised to GAPDH shown in A. N=10 independent dissections, Unpaired t-test; ns p>0.05, error bar=S.D.

5.3.3 Loss of ADAR2 during scaling is not dependent on Pin1 interaction

As neither transcription nor self-editing of ADAR2 contributed to ADAR2 loss, I next determined if post-translational modifications of ADAR2 were altered. I therefore tested if destabilisation of Pin1-ADAR2 interaction underpinned ADAR2 loss [See section 5.1.4].

5.3.3.1 Pin1 levels are unchanged following 24 h TTX treatment

I first studied total Pin1 levels following 24 h TTX treatment as Pin1 loss can alter ADAR2 editing activity (Marcucci, Brindle et al. 2011). However, Pin1 levels were unchanged [**Figure 5-5**] showing that Pin1 is not reduced during synaptic upscaling.

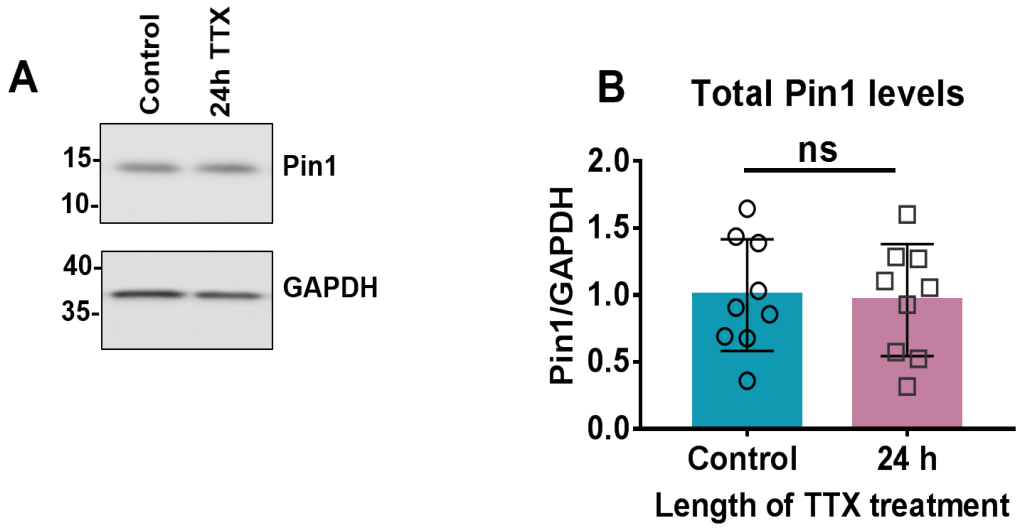

Figure 5-5: Pin levels do not decrease post 24 h TTX treatment.

A. Representative western blot images of total levels of Pin1 and GAPDH levels post 24 h TTX treatment.

B. Quantification of total Pin1 levels normalised to GAPDH post 24 h TTX treatment shown in A. N=9 independent dissections, Unpaired t-test; ns p>0.05, error bar=S.D.

5.3.3.2 GFP-Trap Assays show increased interaction of T32D ADAR2 with Pin1

I next determined if ADAR2 interaction with Pin1 was decreased during TTX treatment. ADAR2 interaction with Pin1 is primarily mediated via

phosphorylation of threonine 32 (T32) site in ADAR2 preceding the proline (P) (Marcucci, Brindle et al. 2011).

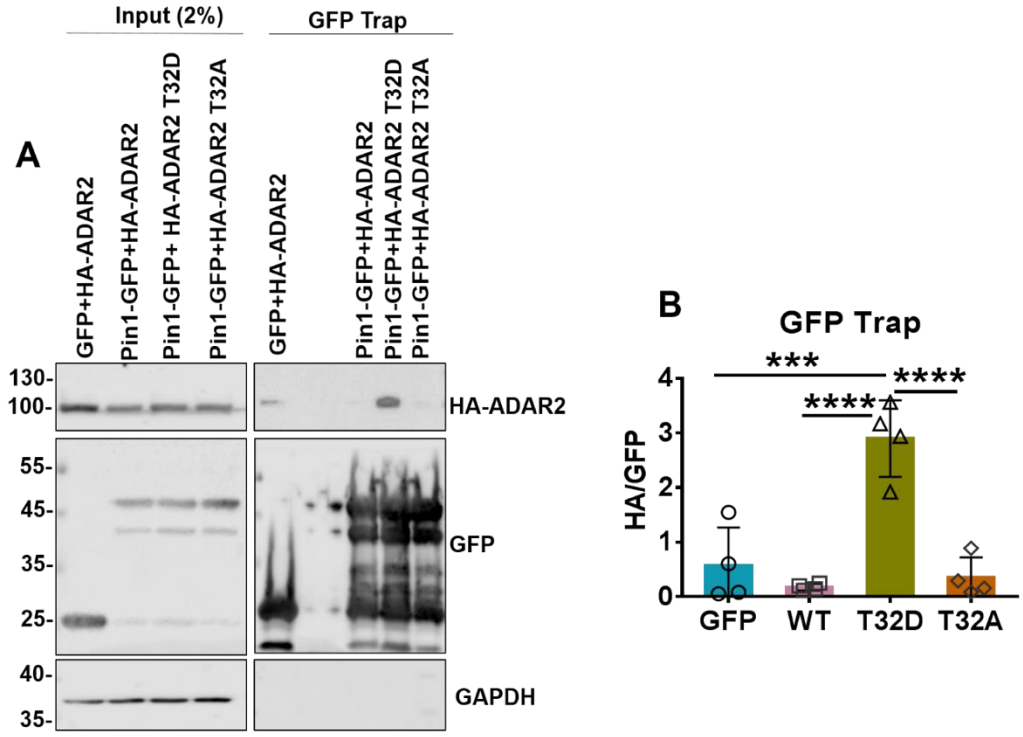

Figure 5-6: Phosphomimetic (T32D) ADAR2 interacts strongly with Pin1. GFP tagged Pin1 (rat construct) was co-transfected with HA tagged WT ADAR2, T32D ADAR2 or T32A ADAR2 (all rat constructs) in HEK293T cells and 48h post transfection GFP-trap assays were performed and analysed using western blotting.

A. Representative western blot images showing strong interaction of T32D ADAR2 to Pin-GFP compared to WT ADAR2 and T32A ADAR2. GFP only control was used to determine any non-specific interactions with the GFP.

B. Quantification of HA-ADAR2 interactions with GFP-Pin1 as shown in A. The HA signal in the GFP trap lanes were normalised to their respective GFP signal. N=4 independent experiments, One way ANOVA with Tukey's multiple post comparisons correction, ***p<0.001, ****p<0.0001, error bar=S.D.

I created N-terminus HA tagged WildType (WT), phosphonull (T32A) and phosphomimetic (T32D) mutant forms of rat ADAR2, co-transfected each of them in HEK293T cells with a C-terminus GFP tagged Pin1 and performed GFP-traps to determine Pin1-ADAR2 interaction. As shown in **Figure 5-6**, phosphomimetic (T32D) version of ADAR2 has significantly stronger interaction with Pin1 compared to the phosphonull (T32A) or WT or GFP only control. Surprisingly, the WT ADAR2 did not show any interaction with Pin1. One possible explanation for this may be that phosphorylation at this site does not occur basally to allow ADAR2 binding to Pin1. Another possibility is that

these experiments were performed in HEK293T cells which may not have the required kinase(s), which are currently unknown, to phosphorylate this threonine site in the rat ADAR2. Nevertheless, when constitutively phosphorylated, ADAR2 showed a strong interaction with Pin1.

5.3.3.3 WT, T32D and T32A ADAR2 are equally sensitive to the 24 h TTX treatment

As phosphomimetic (T32D) ADAR2 showed stronger interaction with Pin1, I performed knockdown rescue experiments in cultured hippocampal neurones to determine if T32D ADAR2 is resistant to TTX mediated loss. For this, I used the knockdown rescue strategy I had already optimised [see section 4.3.8] to remove endogenous ADAR2 and replace with either WT, phosphonull or phosphomimetic ADAR2 (all HA tagged N-terminally and 'complete' shRNA insensitive) and subjected them to further 24 h TTX treatment. Similar to the section 4.3.8, the 'complete' knockdown and the shRNA insensitive ADAR2 rescues were expressed using two separate viruses. Western blot analyses probing for both ADAR2 and HA showed all three WT, T32D and T32A ADAR2 were significantly decreased by TTX treatment [**Figure 5-7**]. These data suggest that Pin1 interaction with ADAR2 does not play a role in loss of ADAR2 during suppression of neuronal activity.

I also performed confocal imaging analysis with the WT and phosphomutants (T32D and T32A) ADAR2. Consistent with the western blot analysis, fixed cell imaging analysis also showed significant loss of ADAR2 intensity and decrease in the percentage of cells expressing ADAR2 following 24 h TTX treatment [**Figure 5-8**]. The intensity was analysed using both ADAR2 and HA signal.

Surprisingly, the nuclear localisation of ADAR2 was not altered with the phoshphonull (T32A) ADAR2. Pin1 is important for ADAR2 nuclear localisation (Marcucci, Brindle et al. 2011) which makes it surprising that in these experiments. ADAR2 nuclear localisation was not altered despite the loss of Pin1 interaction. One potential explanation is that this interaction is important for ADAR2 to be stabilised in the nucleus but not necessarily for it to be imported in the nucleus. The loss of ADAR2 interaction with Pin1 could lead it

to be translocated to the cytosol and degraded rapidly and hence is not observed. Taken together, my results suggest that Pin1 mediated ADAR2 stabilisation does not play a role in activity mediated loss of ADAR2.

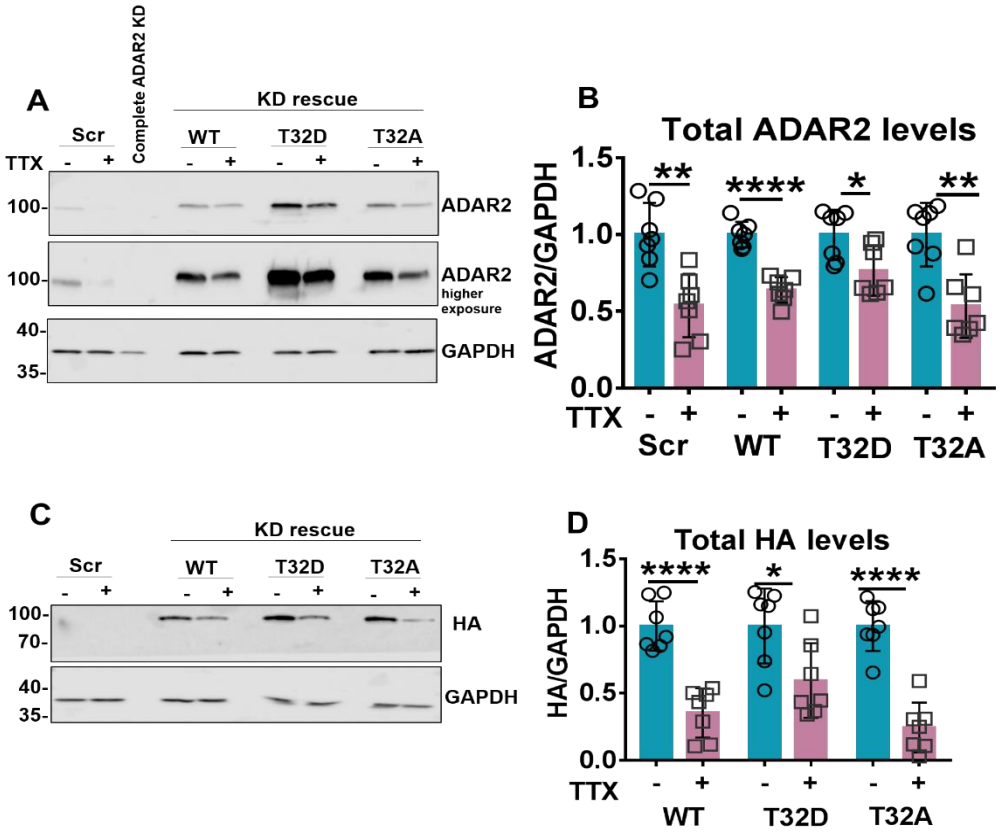

Figure 5-7: WT, T32D and T32A forms of ADAR2 are all equally sensitive to 24 h TTX treatment. Endogenous ADAR2 in hippocampal neurones were replaced with either WT ADAR2 or T32D ADAR2 or T32A ADAR2 using lentiviral knockdown replacement strategy along with scrambled infected control. The cells were then treated with 24 h TTX and lysed and analysed with western blotting. Blue control, pink TTX.

A. Representative western blot images of ADAR2 and GAPDH with or without 24 h TTX treatment.

B. Quantification of ADAR2 normalised to the GAPDH shown in A. Each TTX treated reads were normalised to their respected non-treated controls. N=6 independent dissections, Unpaired t-test for each normalised condition, *p<0.05, **p<0.01, ****p<0.0001, error bar=S.D.

C. Representative western blot images of HA (replaced ADAR2 were tagged with HA) and GAPDH with or without 24 h TTX treatment.

D. Quantification of HA normalised to the GAPDH shown in C. Each TTX treated reads were normalised to their respected non-treated controls. N=6 independent dissections, Unpaired t-test for each normalised condition, *p<0.05, ****p<0.0001, error bar=S.D.

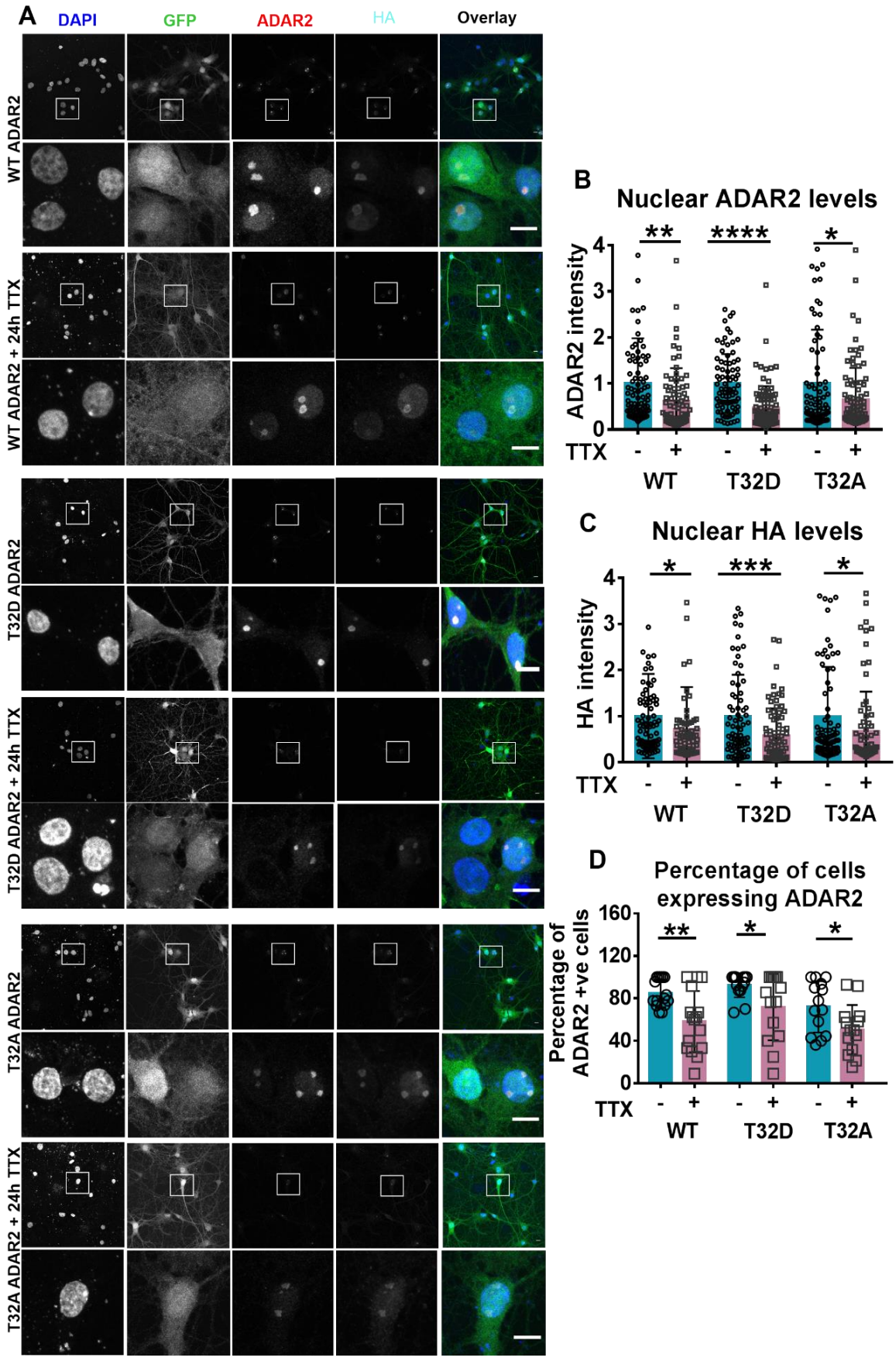
A
DAPI
GFP
ADAR2
HA
Overlay
WT ADAR2
WT ADAR2 + 24h TTX
T32D ADAR2
T32D ADAR2 + 24h TTX
T32A ADAR2
T32A ADAR2 + 24h TTX
B
Nuclear ADAR2 levels
ADAR2 intensity
**
****
*
TTX
WT
T32D
T32A
C
Nuclear HA levels
HA intensity
*
***
*
D
Percentage of cells expressing ADAR2
Percentage of ADAR2 +ve cells
**
*
*

Figure 5-8: Fixed immunolabelling show WT, T32D and T32A forms of ADAR2 are all equally sensitive to 24 h TTX treatment. Endogenous ADAR2 in hippocampal neurones were removed and replaced same as 5-7 and then treated with 24 h TTX, lysed after and analysed with confocal imaging.

A. Representative images labelled with antibodies against GFP (Cy2-green), ADAR2 (Cy3-red) and HA (Cy5-cyan) and stained with DAPI (blue). White boxes in the top panel represent zoomed images below showing decreased ADAR2 intensity and red arrows show cells positive for ADAR2 expression. Scale bar=10µm.

B. Quantification of nuclear intensity of ADAR2 per condition as shown in A. DAPI channel was used to draw regions of interest around the nucleus and average intensity was calculated. Each TTX treated reads were normalised to their respected non-treated controls. n=81-92 cells; N=3 independent dissections, Unpaired t-test for each normalised condition, *p<0.05, **p<0.01, ****p<0.0001, error bar=S.D.

C. Quantification of nuclear intensity of HA per condition as shown in A. DAPI channel was used to draw regions of interest around the nucleus and average intensity was calculated. Each TTX treated reads were normalised to their respected non-treated controls. N=81-92 cells, N=3 independent dissections, Unpaired t-test for each normalised condition, *p<0.05, **p<0.01, ****p<0.0001, error bar=S.D.

D. Quantification of percentage of cells expressing ADAR2 post 24 h TTX treatment per field of view as shown in A. n=14-16 fields of view, N=3 independent dissections, Unpaired t-test; *p<0.05, **p<0.01, error bar=S.D.

5.3.4 Comparing basal stability of phosphomutants ADAR2 to WT ADAR2

While both ADAR2 phosphomutants were equally sensitive to the TTX treatment, I wanted to determine if phosphomimetic ADAR2 has increased basal stability. For this, I again removed endogenous ADAR2 and replaced with shRNA insensitive WT, T32A and T32D ADAR2 rescue constructs in cortical cultured neurones for 5 days and performed cycloheximide time-course assays sampling at 0, 4 and 8 h. Cycloheximide (CHX) is a drug that blocks translation and allows analysis of protein stability/degradation (Schneider-Poetsch, Ju et al. 2010).

Surprisingly, both phosphomimetic (T32D) and phosphonull (T32A) ADAR2 showed decreased stability within 4 h of CHX treatment while WT ADAR2 showed a decreasing trend at 4 h and was significantly decreased by 8 h [**Figure 5-9**]. This suggests that in contrary to previous findings (Marcucci, Brindle et al. 2011) the ADAR2 interaction with Pin1 does not play a role in

ADAR2 stability at basal levels. However, it should be noted that these experiments were performed in rat neuronal cultures whereas previous reports were based on work on human cell lines. Nevertheless, comparing within the rescued groups, phosphomimetic ADAR2 did not show increased stability compared to either WT or phosphonull ADAR2.

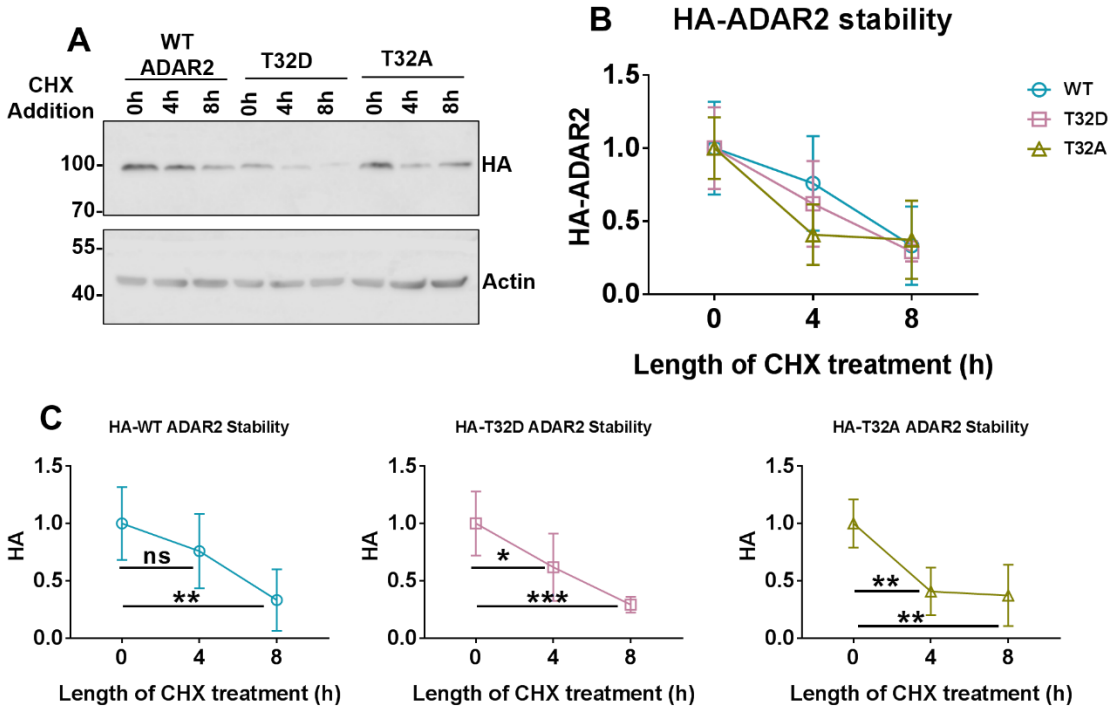

Figure 5-9: All WT, T32A and T32D ADAR2 show comparable level of basal stability. Endogenous ADAR2 in cortical neurones were replaced with either WT ADAR2 or T32D ADAR2 or T32A ADAR2 same as 5-7. Post 6 days of knockdown and replacement translation blocker cycloheximide (CHX) were added to cells for 0 (same volume of DMSO as CHX for 8h), 4 and 8h, were lysed to determine total ADAR2 levels by western blotting.

A. Representative western blot images of the total WT, T32A and T32D HA-ADAR2 and actin levels after 0, 4 and 8h CHX treatment. 0h CHX treated cells were treated with same volume DMSO for 8h.

B. Quantification of conditions shown in A normalised to their respective 0h controls. N=5 independent dissections; error bars=S.D.

C. Same quantifications as B but each ADAR2 mutants shown separately for clarity with the statistical analysis. N=5 independent dissections; One-way ANOVA with Dunnett's multiple post comparisons correction; *p<0.05, **p<0.01, ***p<0.001; error bars=S.D.

5.3.5 All forms of ADAR2 rescue both GluA2 and GluK2 editing equally

Finally, I tested if the ADAR2 phosphomutants (T32A and T32D) had altered ability to edit two key substrates (GluK2 and GluA2) using the BbvI restriction enzyme assay. The ability of ADAR2 to edit was not altered by any of the ADAR2 mutants, equally rescuing both GluK2 and GluA2 editing [**Figure 5-10**] following complete loss of ADAR2. The chromatographs confirm these findings from the BbvI digestion assay [**Figure 5-10** C and F].

While these results contradict previous reports of Pin1 interaction loss leading to loss of ADAR2 editing ability (Marcucci, Brindle et al. 2011), it is entirely consistent with my findings showing that neither the phosphomimetic or phosphonull ADAR2 have altered localisation and can actively edit their substrates in the nucleus.

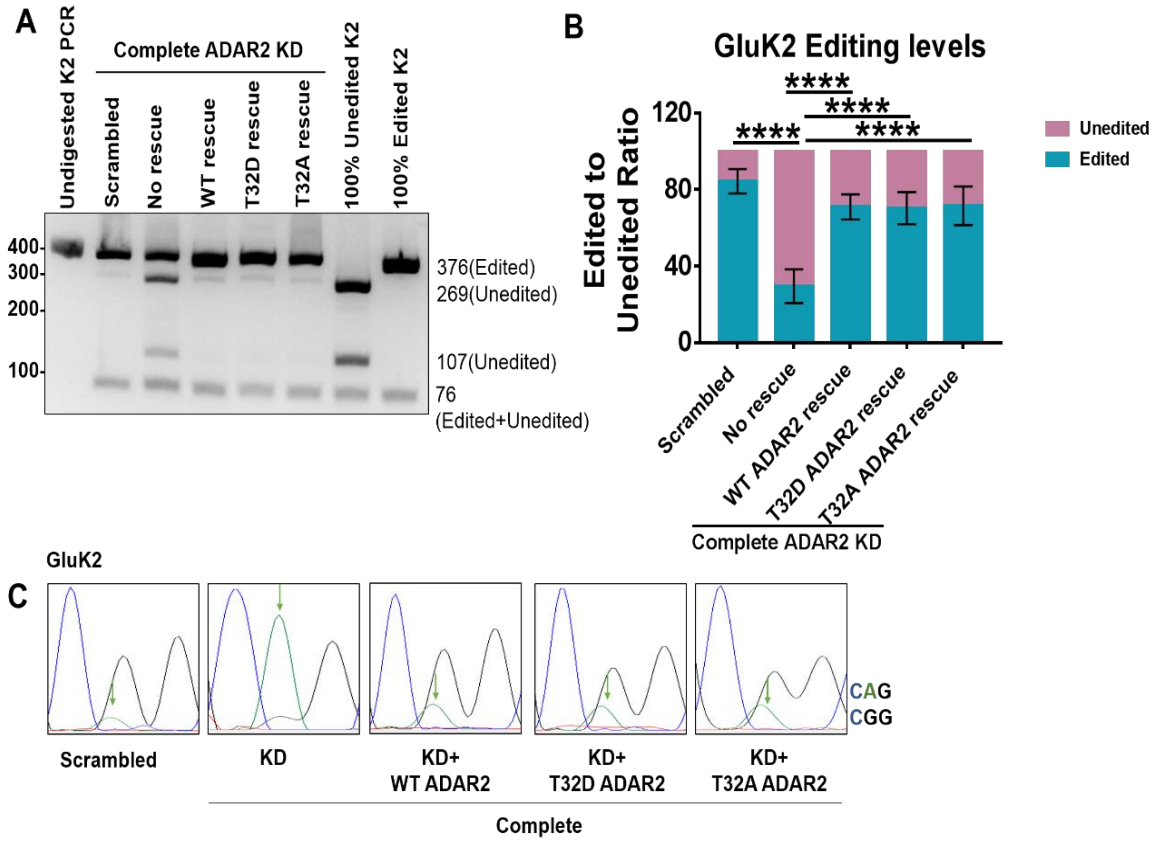
A
Undigested K2 PCR
Complete ADAR2 KD
Scrambled
No rescue
WT rescue
T32D rescue
T32A rescue
100% Unedited K2
100% Edited K2
400
300
200
100
376(Edited)
269(Unedited)
107(Unedited)
76
(Edited+Unedited)
B
GluK2 Editing levels
Edited to Unedited Ratio
120
80
40
0
****
****
****
****
Unedited
Edited
Scrambled
No rescue
WT ADAR2 rescue
T32D ADAR2 rescue
T32A ADAR2 rescue
Complete ADAR2 KD
C
GluK2
CAG
CGG
Scrambled
KD
KD+
WT ADAR2
KD+
T32D ADAR2
KD+
T32A ADAR2
Complete

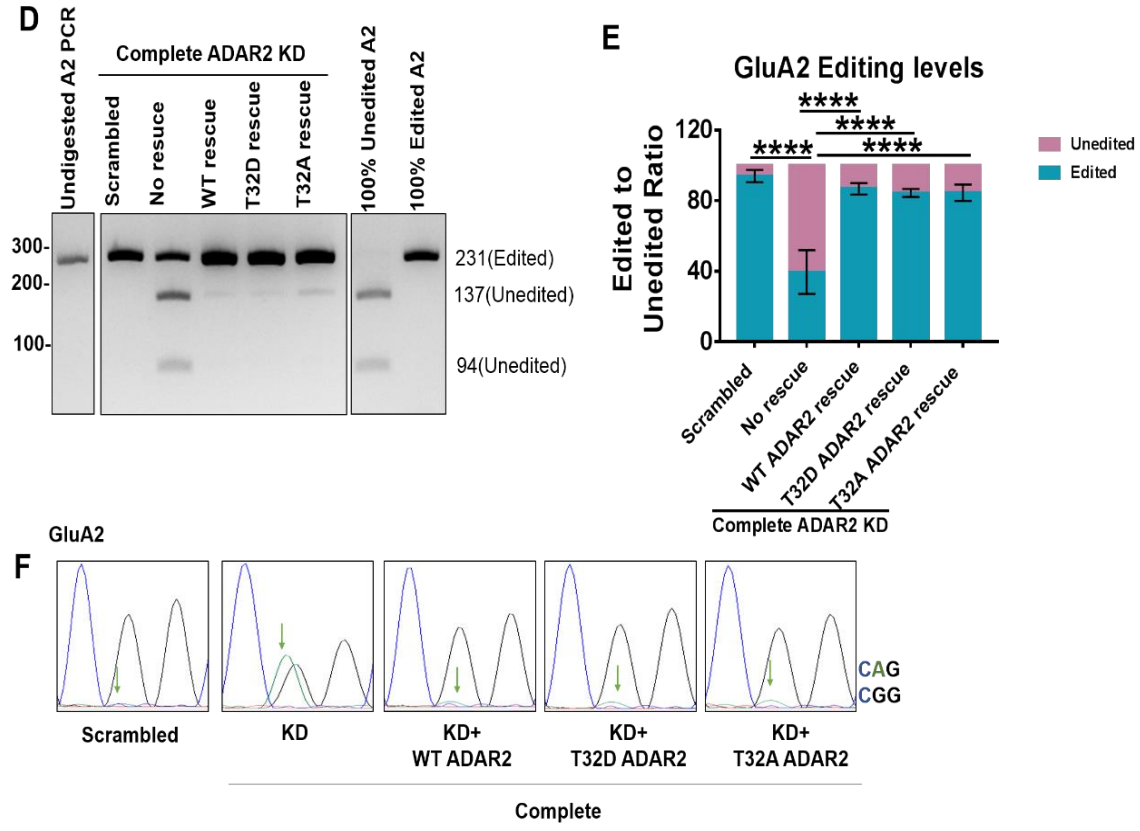
D
Undigested A2 PCR
Complete ADAR2 KD
Scrambled
No resuce
WT rescue
T32D rescue
T32A rescue
100% Unedited A2
100% Edited A2
300
200
100
231(Edited)
137(Unedited)
94(Unedited)
E
GluA2 Editing levels
Edited to Unedited Ratio
120
80
40
0
****
****
****
****
Unedited
Edited
Scrambled
No rescue
WT ADAR2 rescue
T32D ADAR2 rescue
T32A ADAR2 rescue
Complete ADAR2 KD
F
GluA2
CAG
CGG
Scrambled
KD
KD+
WT ADAR2
KD+
T32D ADAR2
KD+
T32A ADAR2
Complete

Figure 5-10: WT, T32A and T32D ADAR2 can rescue both GluK2 and GluA2 editing equally. Endogenous ADAR2 in hippocampal neurones were replaced with either WT ADAR2 or T32D ADAR2 or T32A ADAR2. Post 6 days of knockdown and replacement, RNA was extracted, and cDNA synthesised to perform PCR assays.

A. Representative images of the PCR products separated on a 4% agarose gel post BbvI digestion to determine edited to unedited GluK2 ratio after either scrambled or knockdown and knockdown rescues infection. 100% edited and unedited GluK2 constructs were used as a control to ensure BbvI cut activity and validity of the assay.

B. Quantification of percentage of edited to unedited ratio of GluK2 population shown in A. n=5 independent dissections; One way ANOVA with Tukey's multiple post comparisons corrections; ****p<0.0001; error bars=S.D.

C. Representative chromatographs of PCR products comparing scrambled infected cells with the knockdowns infected cells at the Q/R editing site of GluK2. The undigested PCR products were sent for sequencing to determine changes in the dual peaks obtained at the site of editing as indicated by the green arrow. A peak (green) represents the unedited base while the G peak (black) represents the edited base.

D. Representative images of the PCR products separated on a 4% agarose gel post BbvI digestion to determine edited to unedited GluA2 ratio after either scrambled or knockdown and knockdown rescues infection. 100% edited and unedited GluA2 constructs were used as a control to ensure BbvI cut activity and validity of the assay.

E. Quantification of percentage of edited to unedited ratio of GluA2 population shown in A. n=5 independent dissections; One way ANOVA with Tukey's multiple post comparisons corrections; ****p<0.0001; error bars=S.D.

F. Representative chromatographs of PCR products comparing scrambled infected cells with the knockdowns infected cells at the Q/R editing site of GluA2. The undigested PCR products were sent for sequencing to determine changes in the dual peaks obtained at the site of editing as indicated by the green arrow. A peak (green) represents the unedited base while the G peak (black) represents the edited base.

5.3.6 TTX mediated scaling enhances proteasomal degradation of ADAR2

ADAR2 has been shown to be targeted for ubiquitination mediated proteasomal degradation (Marcucci, Brindle et al. 2011). So, I next wanted to determine if this post-translational modification plays a role in ADAR2 loss during 24 h TTX treatment.

5.3.6.1 ADAR2 loss following TTX treatment can be rescued by inhibiting proteasomes

I used Bortezomib (BTZ) a reversible inhibitor of 26S proteasome (Chen, Frezza et al. 2011) to block proteasomal activity. I tested the effects of 24h TTX up-scaling protocol on ADAR2 stability in the presence or absence BTZ. Accumulation of ubiquitinated products acted as a positive control to show that BTZ worked **[Figure 5-11** A and C]. Consistent with the suppression of synaptic activity leading to enhanced proteasomal degradation (Ehlers 2003), incubation with BTZ prevented the TTX-evoked decrease in ADAR2 levels [**Figure 5-11** A and B].

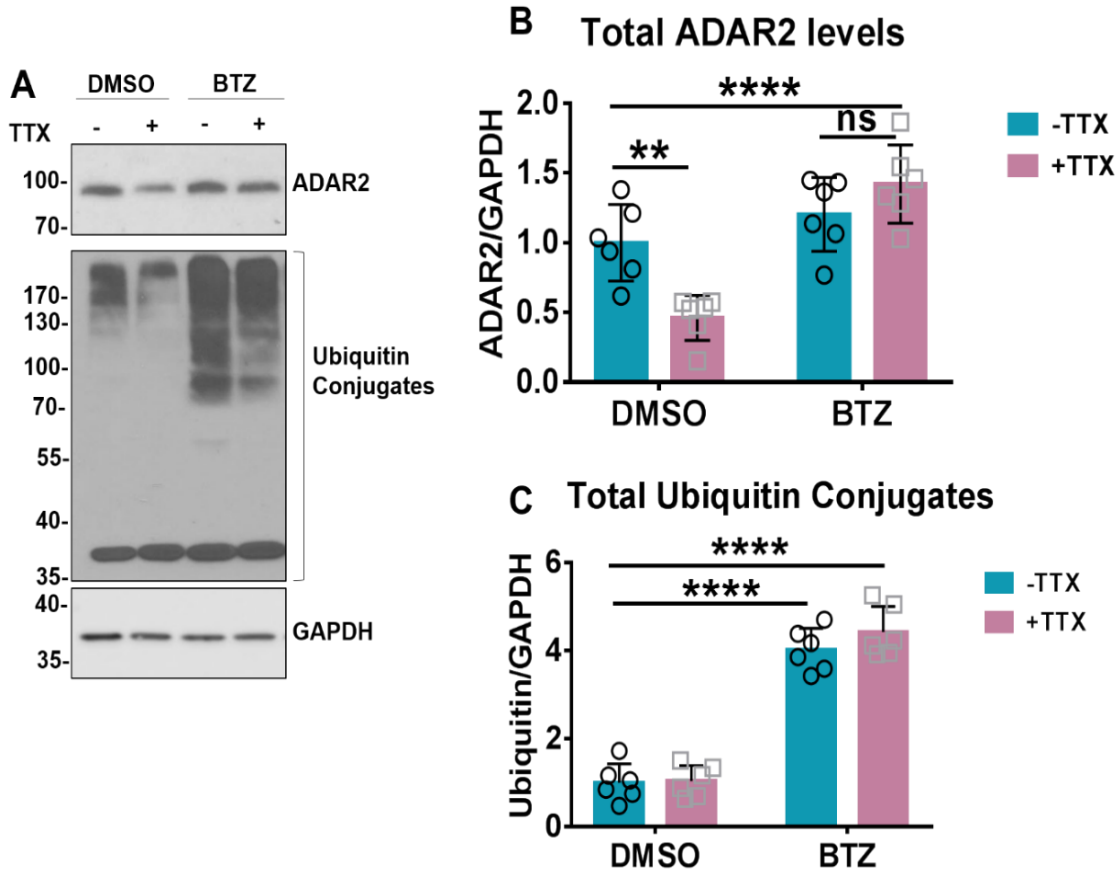

Figure 5-11: ADAR2 loss following 24 h TTX treatment is rescued by inhibiting proteasomes following 20 h 1µM BTZ treatment.

A. Representative western blot images of total levels of ADAR2, ubiquitin conjugates and GAPDH levels post 24h TTX treatment and 20h 1µM BTZ treatment.

B. Quantification of total ADAR2 levels normalised to GAPDH shown in A. N=6 independent dissections, Two-way ANOVA with Tukey's multiple post comparisons correction; ns p>0.05, **p<0.01, ****p<0.0001, error bar=S.D.

C. Quantification of total ubiquitin conjugates normalised to GAPDH shown in A. N=6 independent dissections, Two-way ANOVA with Tukey's multiple post comparisons correction; ns p>0.05, ****p<0.0001, error bar=S.D.

5.3.6.2 ADAR2 is rescued in both the nucleus and the cytosol

I next performed nuclear and cytoplasmic fractionations to determine if ADAR2 is exported from the nucleus for degradation in the cytosol. As expected, in the presence of BTZ the 24h TTX treatment caused ADAR2 to accumulate in the cytosol [**Figure 5-12** A and C]. These data indicate that either ADAR2 is exported in the cytosol to be ubiquitinated or that it is ubiquitinated in the nucleus and exported to the cytosol to be degraded. Moreover, the TTX-induced decrease in the levels of nuclear ADAR2 was prevented by BTZ [**Figure 5-12** A and B], further suggesting that the TTX-induced loss of ADAR2 is mediated by proteasomal degradation of ADAR2.

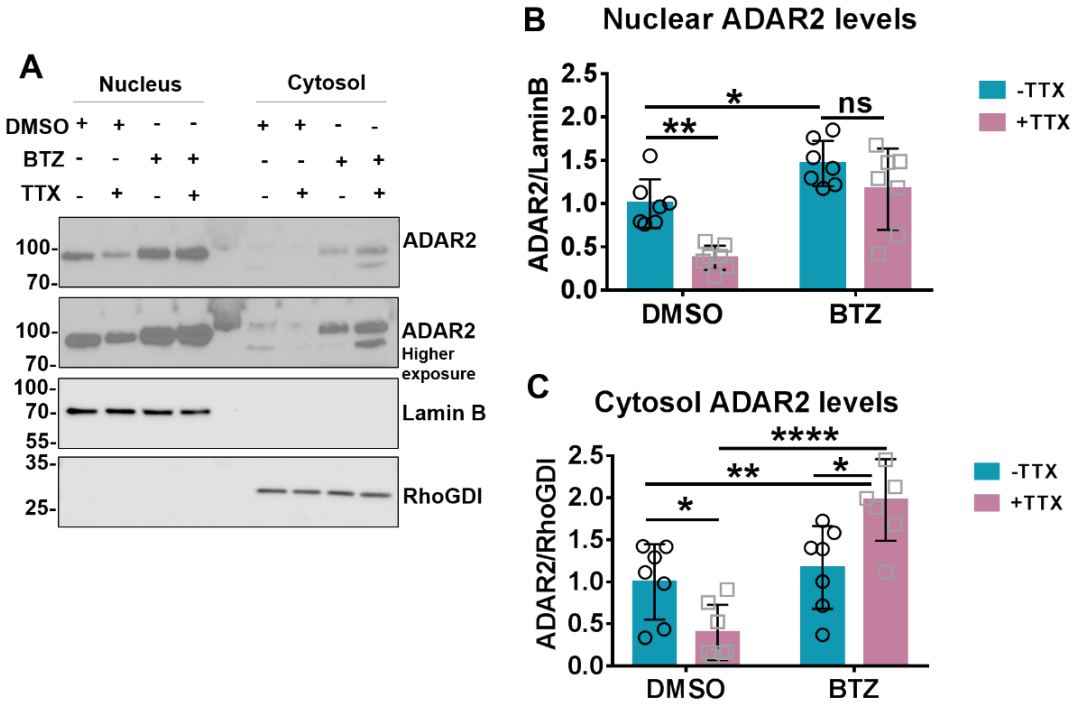

Figure 5-12: ADAR2 loss following 24 h TTX treatment is rescued in both nucleus and cytosol by inhibiting proteasomes following 20h 1µM BTZ treatment. Subcellular fractionation was performed to isolate cytosolic and nuclear compartments to determine ADAR2 localisation and levels.

A. Representative western blot images of levels of ADAR2 in the cytosol and the nucleus. Lamin B was used as a nuclear specific marker while RhoGDI was used as cytosolic marker.

B. Quantification of nuclear ADAR2 levels normalised to Lamin B shown in A. N=6 independent dissections, Two-way ANOVA with Tukey's multiple post comparisons corrections; ns $p>0.05$, *$p<0.05$, **$p<0.01$; error bar=S.D.

C. Quantification of cytosolic ADAR2 levels normalised to RhoGDI shown in A. N=6 independent dissections, Two-way ANOVA with Tukey's multiple post comparisons corrections; ns $p>0.05$, *$p<0.05$, **$p<0.01$, ****$p<0.0001$; error bar=S.D.

5.3.6.3 Preventing ADAR2 loss prevents GluK2 upscaling

Based on these data I hypothesised that, in the presence of BTZ, ADAR2 accumulates in the cytosol. Since it cannot degrade, it undergoes further rounds of nuclear import and export, which results in a functional pool of ADAR2 being maintained in the nucleus. I therefore tested if preventing ADAR2 degradation with BTZ is enough to prevent GluK2 up-scaling with 24h TTX treatment. Consistent with this hypothesis, surface biotinylation showed that blocking ADAR2 proteasomal degradation with BTZ prevents TTX-induced GluK2 upscaling [**Figure 5-13** A and B] with no change in the EGFR

surface levels [**Figure 5-13** A and C].

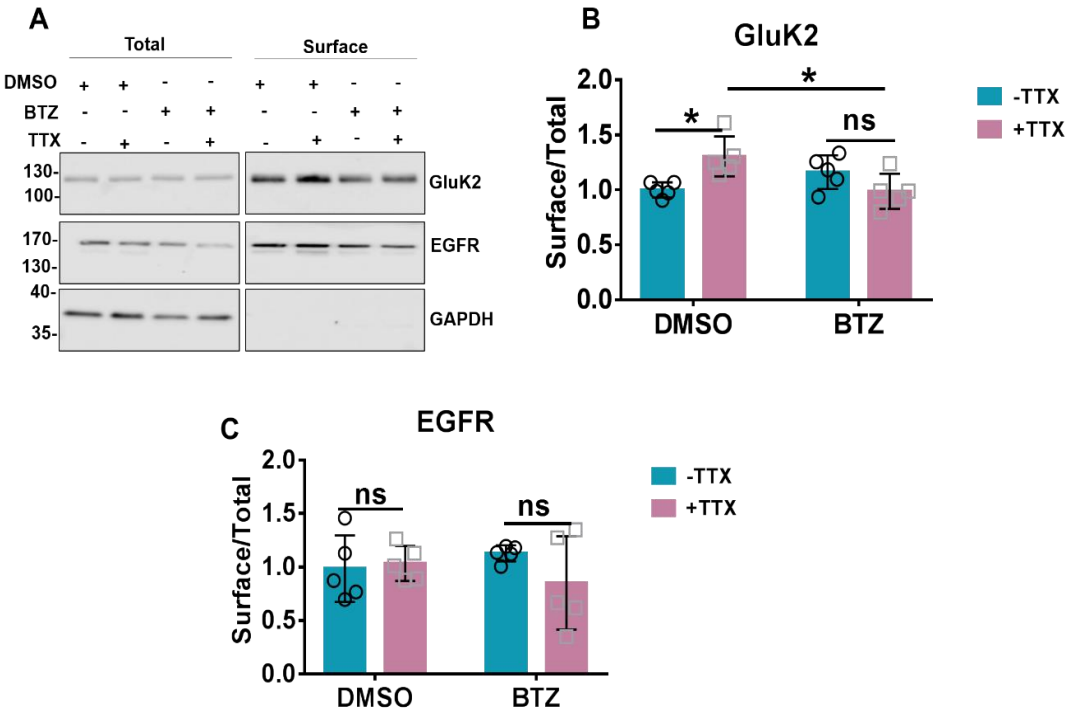

Figure 5-13: Preventing loss of ADAR2 prevents GluK2 upscaling. Partial ADAR2 KD phenocopies and occludes GluK2 scaling. Following 24 h TTX treatment and 20 h 1µM BTZ treatment, surface biotinylation was performed on DIV 15 hippocampal neurones to isolate surface proteins and determine surface/total ratio by western blotting.

A. Representative western blot images of surface and total levels of GluK2, and EGFR. EGFR was used as a surface expressed non-glutamate receptor control that should not respond to stimulation. GAPDH was used as an internal control to determine no internal proteins were biotinylated.

B-C. Quantification of surface to total ratio of GluK2 (B) and EGFR (C) shown in A. N=5 independent dissections; Two-way ANOVA with Tukey's multiple post comparisons corrections; ns $p>0.05$, *$p<0.05$; error bars=S.D.

These results demonstrate that the availability of nuclear ADAR2 mediates upscaling of GluK2 containing KARs.

5.3.7 Creating knockdown tools to study WWP2

WWP2 is an E3 ubiquitin ligase and was previously shown to ubiquitinate ADAR2 (Marcucci, Brindle et al. 2011). I hypothesised if WWP2 mediated ubiquitination plays a role in ADAR2 ubiquitination during TTX treatment. I first generated shRNA knockdown tools to study WWP2 in rat cultures to validate antibodies against WWP2. I cloned rat WWP2 in HA (N-terminally tagged) pcDNA3 vector and co-expressed HA-WWP2 (rat) and shRNA mediated

WWP2 knockdown vectors (pSUPER) in HEK293T cells. I designed shRNA tools against two different sites within the rat WWP2 sequence. This would allow me to validate the knockdown tools against WWP2 and determine if the antibody can recognise rat WWP2. As seen in **Figure 5-14** A, the antibody recognised the overexpressed rat WWP2 construct in HEK293T cells. Moreover, the WWP2 knockdown 1 showed slight loss of overexpressed WWP2 but the knockdown 2 showed robust WWP2 loss.

I then cloned the knockdown shRNA sequences into pXLG3-wpre vector and generated lentiviruses to infect cortical neurones. Firstly, the antibody was able to recognise endogenous WWP2 from cortical neurones. Upon infection with the WWP2 shRNA knockdowns, the knockdown 1 mediated slight loss of endogenous wwp2 while the knockdown 2 showed robust loss of endogenous WWP2 [**Figure 5-14** B]. This was similar to the observations obtained in HEK293T cells.

Interestingly, the antibody showed double bands for WWP2 recognition, both of which seems to be targeted by the knockdowns. I speculate them to potentially be different isoforms of WWP2. With these tools in place, I would next determine whether removing endogenous WWP2 in hippocampal neurones, rescues ADAR2 loss during chronic suppression of network activity and if so, whether GluK2 upscaling is inhibited upon the loss of WWP2. Thus, this will allow me to study the molecular regulators of ADAR2 ubiquitination during up-scaling.

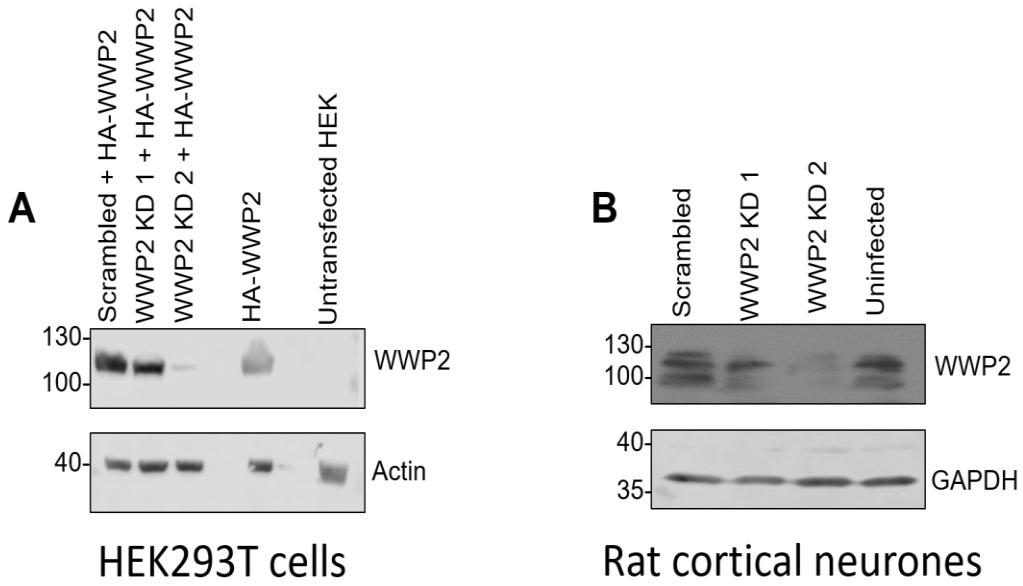

Figure 5-14: Studying and validating tools to study WWP2 in rat neuronal cultures. Validating shRNA mediated knockdown tools and commercial antibody against WWP2 in HEK293T cells and rat neuronal cortical cultures.

A. Representative western blot images of total levels of overexpressed HA-WWP2 and actin. HA-WWP2 (rat) and shRNA against rat WWP2 was co-transfected in HEK293T cells for 3 days and lysed and analysed using western blotting. Levels of WWP2 KD achieved and validity of the antibody were tested.

B. Representative western blot images of total levels of endogenous WWP2 and GAPDH in rat cortical neurones. Two shRNAs against rat WWP2 were added to the cells using lentiviral delivery system. The cells were infected for 6 days and lysed and analysed using western blotting. Levels of WWP2 KD achieved and validity of the antibody were tested.

5.4 Discussion

As ADAR2 transcript levels were not altered post 24 h TTX treatment [**Figure 5-3**], I concluded that the ADAR2 decrease was not occurring at the transcription level. It is also important to note that previous studies on transcript levels of ADAR2 post TTX treatment used 48 h time length of TTX treatment, while my study uses 24 h time length. Whether there could be a difference in responses of loss of ADAR2 depending on the length of activity reduction is not known. Nevertheless, I studied other potential mechanisms by which ADAR2 levels could be altered during scaling.

5.4.1 Self-editing of ADAR2 is altered following 24 h TTX treatment

ADAR2 self-editing has been shown to be a mechanism that can regulate ADAR2 editing activity [See section 5.1.2]. One of these auto-editing process results in a frameshift, coding for an immature stop codon producing a non-functional 9kDa protein (Rueter, Dawson et al. 1999). Thus, increased auto-editing could play a role in ADAR2 loss during activity. However, following 24h TTX treatment I observed a small but significant decrease in ADAR2 self-editing in this region [**Figure 5-4**]. This indicates increased functional ADAR2 is potentially being translated following 24 h TTX treatment.

While surprising, this could perhaps be acting as a regulatory mechanism to prevent any further loss of ADAR2 protein and ADAR2 function. This could allow maintenance of the editing status of other ADAR2 substrates such as GluA2, needed for cellular survival (Higuchi, Maas et al. 2000). I had also previously shown that any further loss of ADAR2 is prevented when TTX is added for longer lengths of time (up to 48 h) [see section 4.3.3]. Hence, this auto-editing process could be acting as a mechanism to maintain threshold ADAR2 levels.

Equally, it can also be argued that the TTX treatment is potentially decreasing ADAR2 enzymatic activity. In other words, loss of ADAR2 is consequentially decreasing its self-editing activity, thus acting as a negative self-regulation mechanism. In line with this, previous studies also showed decrease in ADAR2 self-editing following loss of neuronal activity (Sanjana, Levanon et al. 2012, Balik, Penn et al. 2013). Studying ADAR2 self-editing levels at earlier time-points (6-24 h) could provide initial indication if this is the case.

While the exact role of decreased ADAR2 self-editing in this instance is not fully known, it does not seem to play a causative role in ADAR2 loss during scaling.

5.4.2 Pin1 does not play a role in ADAR2 stability or function during scaling

ADAR2 is functionally active in the nucleus where it has been reported to be stabilised by binding to the protein Pin1. Loss of the ADAR2-Pin1 interaction leads to ADAR2 export into cytosol where it is ubiquitinated and degraded (Marcucci, Brindle et al. 2011). It was also recently reported that this Pin1 mediated stabilisation is important for ADAR2 editing activity during development in cortical neurons (Behm, Wahlstedt et al. 2017). So, I hypothesised this pathway could be altered during TTX mediated loss of ADAR2. While no change in Pin1 levels were observed [**Figure 5-5**], I hypothesised that ADAR2 phosphorylation at T32 site that mediates its interaction with Pin1 [**Figure 5-6**] could be altered either by preventing kinase (identity unknown) activity or increased phosphatase (identity unknown) activity.

However, both phosphonull (T32A) and phosphomimetic (T32D) mutants of ADAR2, which decrease or enhance binding to Pin1 respectively [**Figure 5-6**], were equally susceptible to the TTX mediated loss [**Figure 5-7**]. Furthermore, imaging experiments also showed nuclear localisation of both phosphonull and phosphomimetic ADAR2 and both the intensity of ADAR2 and percentage of cells expressing ADAR2 decreased following TTX treatment for each condition [**Figure 5-8**].

Hence, my experiments suggest that Pin1 mediated ADAR2 stabilisation in the nucleus does not play a role in ADAR2 loss during up-scaling mediated by the suppression of synaptic activity.

5.4.3 Loss of Pin1 interaction did not alter basal stability of ADAR2

While Pin1 mediated stabilisation did not play a role in activity mediated loss of ADAR2, I wanted to determine if basal stability of ADAR2 was altered. Contrary to the previous reports (Marcucci, Brindle et al. 2011, Behm, Wahlstedt et al. 2017), my cycloheximide experiments suggest that the basal stability of ADAR2 is not altered for any of the mutants [**Figure 5-9**]. This was further confirmed by imaging experiments which showed no change in the

localisation of any of these mutants as they were all nuclear localised despite the supposed loss of interaction with Pin1 **[Figure 5-8**].

Similarly, the editing assays also showed all three WT, phosphomimetic and phosphonull ADAR2 can equally rescue both GluK2 and GluA2 editing [**Figure 5-10**]. Thus, the ability of these mutants to interact with and edit its substrates were not affected. Hence, my results contradict previous findings that suggest ADAR2-Pin1 interaction play a role in ADAR2 stability and function.

The published studies were performed by overexpressing human ADAR2 and Pin1 (Marcucci, Brindle et al. 2011) proteins in HEK293T cells. So, the interactions could be different in rat cultured neurones or perhaps there is another Pin1 interaction site in ADAR2. Equally, there may be other ADAR2 protein interactors compensating for the loss of Pin1 interaction to stabilise it in the nucleus. Similarly the reported role of Pin1 mediated nuclear stabilisation of ADAR2 were performed in mouse cortical cultured neurones (Behm, Wahlstedt et al. 2017). However, these studies only showed increased colocalisation of ADAR2 with Pin1 during development. So, to further study this, I would remove endogenous Pin1 in my cultures and see if that does change ADAR2 stability and localisation. I also want to perform colocalisation experiments of these ADAR2 mutants with Pin1 in neuronal cultures to ensure Pin1 interaction is indeed lost with these mutants as suggested by the GFP-trap experiments in HEK293T cells.

Hence, my results so far suggest that Pin1 does not play any role in the basal stability and localisation of ADAR2.

5.4.4 ADAR2 loss during activity is mediated via ubiquitination targeted degradation

I next wanted to determine if ADAR2 loss during activity is mediated by increased degradation of ADAR2 as ADAR2 has been previously suggested to be ubiquitinated in the cytosol. My results show that TTX treatment does induce the degradation of ADAR2 as the loss can be blocked by the proteasome inhibitor BTZ [**Figure 5-11**].

While it is not known whether the ubiquitination occurs in the cytosol or in the nucleus, subcellular fractionation data show that the rescued ADAR2 accumulates in the cytosol. Interestingly, ADAR2 levels are also rescued in the nucleus [**Figure 5-12**]. We speculate that owing to the accumulation of ADAR2 in the cytosol, which cannot be removed due to inhibition of the proteasomes, it can be re-imported into nucleus, maintaining the functional pool of ADAR2. If this is the case, TTX may enhance the overall turnover rate of ADAR2 but the increase in the rate of export and degradation outweighs the increase in translation and nuclear localisation. Interestingly, increased translation of ADAR2 following TTX treatment has been reported (Schanzenbächer, Sambandan et al. 2016).

I also note that blocking general proteasomal function will lead to accumulation of many ubiquitinated products that cannot be degraded. Hence, the rescue of ADAR2 loss following TTX treatment could be indirectly mediated by rescue of potential other interactors of ADAR2 that could target it for import and stability in the nucleus. To study this, I would determine if the rescued ADAR2 following BTZ treatment is indeed ubiquitinated. It would also be interesting to determine if there is increased import of ADAR2 from cytosol into the nucleus in presence of BTZ by increased association with importin alpha-4 (KPNA3), association of which has been shown to be responsible for increased ADAR2 nuclear accumulation during development (Behm, Wahlstedt et al. 2017).

Nevertheless, when ADAR2 degradation is blocked it leads to the maintenance of a functional pool in the nucleus. Consistent with this, blocking proteasomal degradation of ADAR2 prevents TTX induced GluK2 up-scaling [**Figure 5-14**]. Together, these data demonstrate that the loss of ADAR2, and the consequent reduction in GluK2 Q/R editing, are both necessary and sufficient to support homeostatic scaling of GluK2 containing KARs.

5.4.5 Developing and validating tools to study WWP2 role in ADAR2 ubiquitination

My next aim was to determine molecular pathways behind ADAR2 ubiquitination. As mentioned above, WWP2 has been shown to be potentially regulate ADAR2 ubiquitination and I wanted to determine if this played a role

during scaling. For this I created knockdown tools firstly to validate the antibodies as not many tools are available to study this protein in rat cultures. Comparing the two shRNA knockdown tools, knockdown 2 targeted overexpressed rat WWP2 HEK293T cells more robustly than knockdown 1 [**Figure 5-14** A]. However, I struggled to detect endogenous WWP2 in HEK293T cells with the antibody.

Nevertheless, I moved into rat cortical cultures firstly in order to determine if the antibody can recognise endogenous WWP2. The antibody did recognise a band around the height expected (same as that with the overexpressed construct in HEK293T cells) ~110kDa [**Figure 5-14** B]. This band was decreased in the knockdown lanes, suggesting it to be WWP2 specific band. However, the antibody signal was generally very weak which could be due to presence of less WWP2 in my cultures or lack of a good recognition from the antibody.

So, to further study this in future I want to test other commercially available antibodies against rat WWP2. The eventual goal is to see whether WWP2 levels themselves are altered during TTX treatment and/or altering ADAR2 interaction with WWP2 results in altered levels of ADAR2 basally and during activity.

5.5 Conclusion

In conclusion, my work suggests that ADAR2 loss during TTX mediated up-scaling is mediated by targeting ADAR2 for ubiquitination and degradation but not due to loss of Pin1 mediated stability or reduction in transcription or alterations in auto-editing.

Chapter 6. GENERAL DISCUSSION

6.1 Summary of research

I started my PhD with the aim to explore the potential roles of KARs in various forms of synaptic plasticity. I approached this by initially studying AMPAR regulation by KAR signalling in both LTP and LTD. I also determined whether KARs themselves can undergo homeostatic plasticity i.e. scale up and down in response to the chronic changes in network activity. My next aim was to study the molecular mechanisms behind regulation of KARs in these forms of plasticity, adding to the wealth of knowledge that currently exists on activity dependent regulation of KARs expression and function. Below I summarise the main findings from my PhD.

6.1.1 KARs regulation of AMPAR surface expression and plasticity

Previous studies from the lab had shown that along with undergoing plasticity themselves, KARs can also regulate AMPAR surface expression and function. The activity dependent regulation of KAR surface expression following KAR activation can in turn regulate AMPAR surface expression, inducing a novel form of KAR_{AMPAR}-LTP (Martin, Bouschet et al. 2008, Gonzalez-Gonzalez and Henley 2013, Petrovic, Viana da Silva et al. 2017). Furthermore, metabotropic signalling via GluK2 subunit of KARs was shown to mediate AMPAR regulation by KARs. This non-classical form of LTP presented an opportunity for an exciting project and I was keen to extend on these studies and define the downstream signalling pathways and players that mediate this increase in synaptic AMPARs. One particularly interesting aspect of the study would be to determine if NMDAR-LTP and KAR-LTP share common pathways and whether the effect of both forms of LTP would be summative or occlusive. Unfortunately, lack of reproducibility of KAR_{AMPAR}-LTP in cultures in my hands, led me to discontinue this project and develop other avenues of investigation within KAR plasticity.

The idea of KAR_{AMPAR}-LTP was initiated by the findings that the transient stimulation of KAR can increase KAR surface expression (Martin, Bouschet et al. 2008, Gonzalez-Gonzalez and Henley 2013). Based on these data I hypothesised that KAR signalling could also play a role in KAR_{AMPAR}-LTD, as

sustained KAR stimulation was shown to induce KAR endocytosis and degradation (Martin and Henley 2004). Indeed, sustained KAR stimulation not only decreased KAR surface expression but also decreased AMPAR surface expression and electrophysiological studies on CA1 synapses suggested induction of KAR_{AMPAR}-LTD following sustained KAR activation. Further study suggested the pre-synaptic KARs to be responsible for this phenomenon partially through their ionotropic function. Hence, this is more likely to be a form of pre-synaptic LTD/short term plasticity (STP) as the depression in $AMPAR_{EPSCs}$ were not sustained long term. This finding possibly adds to the understanding of the functions of pre-synaptic KARs in plasticity (Jiang, Xu et al. 2001, Andrade-Talavera, Duque-Feria et al. 2013).

Application of the ionotropic KAR inhibitor (UBP310) partially inhibited the initial decrease in $AMPAR_{EPSCs}$. However, since this was only partial block it would be interesting to investigate the potential role of metabotropic signalling from pre-synaptic KARs as pre-synaptic KARs have been shown to modulate GABA release and glutamate release by their metabotropic signalling (Rodriguez-Moreno and Lerma 1998, Frerking, Schmitz et al. 2001). While interesting, I did not pursue this any further as I wanted to study the function and plasticity of postsynaptic GluK2 containing KARs.

Nevertheless, KARs like NMDARs can regulate AMPAR surface expression and function thereby regulating synaptic plasticity itself.

6.1.2 KARs undergo homeostatic scaling in response to chronic activity changes

Homeostatic plasticity maintains network stability and function in response to input-specific changes (Pozo and Goda 2010). The very limited study of the role of KARs in this form of plasticity made this an intriguing area to explore. My study showed that GluK2 and GluK5 containing KARs undergo homeostatic up and down scaling in response to chronic suppression (TTX) and enhancement (bicuculline) of synaptic activity respectively. Intriguingly, TTX treatment decreased, whereas bicuculline treatment increased GluK2 Q/R editing. Oligomerisation, ER exit and surface expression of GluK2 containing KARs are all affected by GluK2 Q/R editing (Ball, Atlason et al.

2010), Therefore, I formulated the hypothesis that Q/R editing of GluK2 regulates KAR surface expression during chronic changes in network activity.

6.1.3 ADAR2 mediated Q/R editing of GluK2-KARs regulates KAR upscaling

Q/R editing of KARs is predominantly regulated by the enzyme ADAR2 (Higuchi, Maas et al. 2000). Furthermore, ADAR2 is activity dependently regulated in neurones (Sanjana, Levanon et al. 2012, Balik, Penn et al. 2013). My data show that following 24 h TTX treatment, ADAR2 levels decrease significantly while the ADAR1 levels remain unchanged. Interestingly, however, levels of ADAR2 did not change following bicuculline treatment, suggesting a mechanism separate to that of upscaling.

To demonstrate that the loss of ADAR2 causes the decrease in Q/R editing of GluK2, I created shRNA targeted knockdown tools against ADAR2. Partial ablation of ADAR2 (50% decrease compared to the scrambled control) caused a ~20% decrease in GluK2 editing, the same levels observed with the TTX treatment. Importantly, total levels of GluK2 remained unchanged. Moreover, replacing endogenous ADAR2 with an exogenously expressed shRNA insensitive mutant (knockdown-rescue) restored GluK2 editing.

The knockdown of 50% of ADAR2 was sufficient to increase the GluK2 surface expression, mimicking the surface levels of GluK2 post TTX treatment. Furthermore, this surface increase following TTX treatment is occluded in the Partial ADAR2 KD cells. Interestingly, while there is further loss of ADAR2 in cells treated with both Partial ADAR2 KD and 24 h TTX, there is no further decrease in the GluK2 editing itself, consistent with the occluding effect.

These data support my hypothesis that the decrease in GluK2 editing following 24 h TTX treatment is mediated by the reduced levels of ADAR2. This in turn causes increased oligomerisation and ER exit of GluK2 containing KARs, resulting in their increased surface expression and upscaling [**Figure 6-1**]. These findings provide a novel functional role of ADAR2 mediated Q/R editing of KARs in synaptic plasticity.

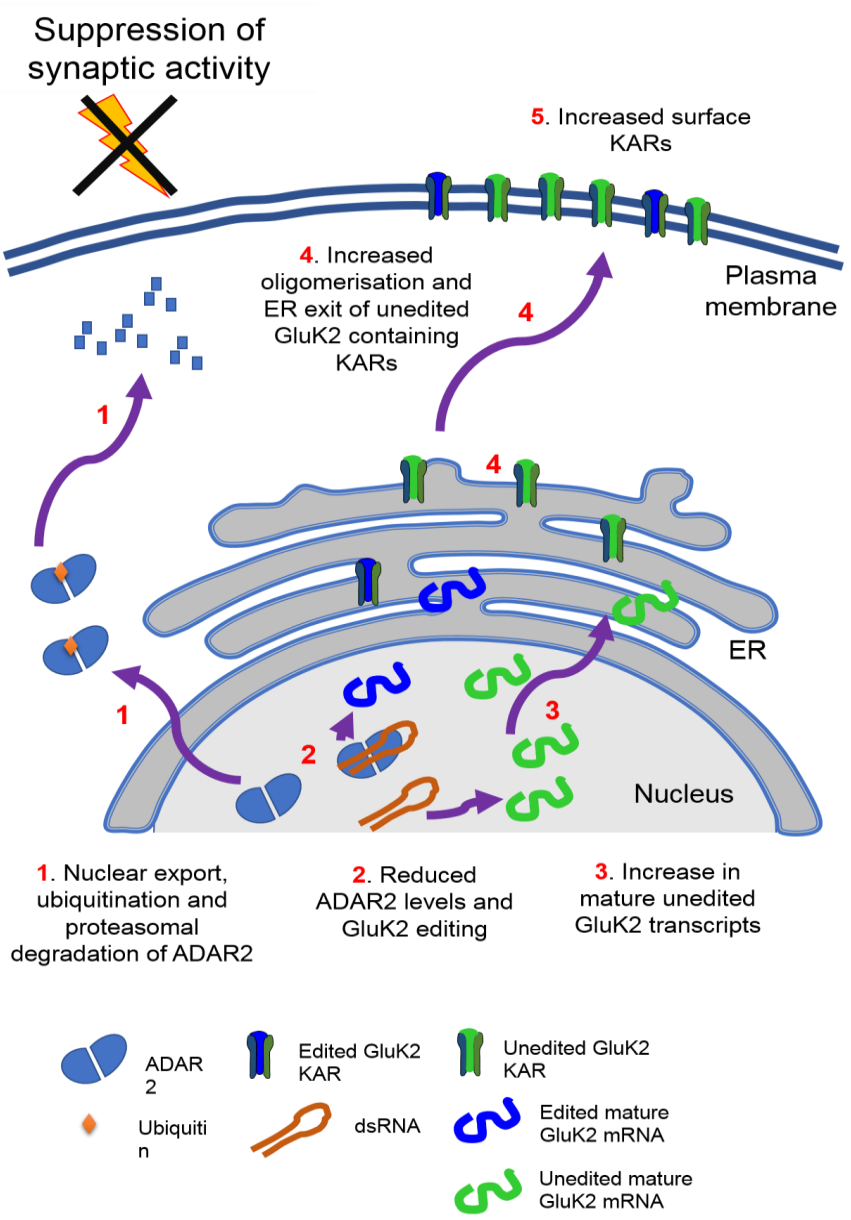

Figure 6-1: Schematic of ADAR2 mediated Q/R editing regulating GluK2 containing KARs homeostatic up-scaling.

Under basal conditions unedited GluK2 transcripts are edited at their Q/R site by ADAR2 enzyme resulting in ~80% edited mature GluK2 transcripts. The resultant edited and unedited GluK2 subunits oligomerise in the ER and traffic into the surface. Under conditions of synaptic activity suppression with TTX treatment, ADAR2 undergoes proteasomal degradation in the cytosol (1). This results in less ADAR2 editing of GluK2 pre-mRNA transcripts (2) and increased levels of unedited GluK2 mature transcripts (3). The subsequent increase in the proportion of unedited GluK2(Q) allows enhanced oligomerisation and ER exit (4) to increase surface expression of GluK2 containing KARs on the surface (5).

6.1.4 Q/R editing of GluK2 and GluA2 by ADAR2 is differentially regulated

Another interesting finding was the differential sensitivity of GluA2 and GluK2 mRNA to varying levels of endogenous ADAR2. ADAR2 KO mice have profound deficits in editing of both GluA2 and GluK2 (Higuchi, Maas et al. 2000). However, my experiments show that only the Q/R editing of GluK2 was altered by the reduced levels of ADAR2 following 24 h TTX treatment. The very high levels of GluA2 Q/R editing were maintained despite the partial ADAR2 loss. These findings were reiterated in the ADAR2 KD experiments, where the partial loss of ADAR2 resulted in the editing loss of GluK2 but not of GluA2. Only after the complete loss of ADAR2, GluA2 unedited status increased by ~30%, while GluK2 unedited population increased by over ~60%. These results suggest that GluA2 is preferentially and almost completely edited at the Q/R site even when low levels of ADAR2 are present.

Complementing this finding, my results also show that ADAR2 levels do not decrease any further when treated for longer times with TTX, suggesting threshold levels of ADAR2 are preserved by the cell to maintain editing status of GluA2. This is likely because editing of GluA2 is essential for neuronal survival.

GluK2, on the other hand, is susceptible to relatively small changes in ADAR2 levels. This is consistent with the observations that a relatively larger proportion of GluK2 remains unedited in adult rat brain (>15%) whereas GluA2 is almost entirely edited, with <1% unedited (Burnashev, Monyer et al. 1992, Bernard, Ferhat et al. 1999). This means that there is a higher tolerance of neurones to unedited GluK2 population than that of GluA2. This is also evident in studies from GluA2 unedited mice and ADAR2 KO mice which, due to presence of significantly higher unedited GluA2 population, are extremely seizure prone and die soon after birth (Higuchi, Maas et al. 2000). GluK2 editing deficient mice, on the other hand, are completely viable and show much subtler changes in phenotype, including their plasticity and have increased susceptibility to induced seizures (Vissel, Royle et al. 2001).

Taken together, my results demonstrate that GluK2 Q/R editing site is regulated by changes in ADAR2 levels, to preferentially regulate GluK2 expression and function in response to alterations in neuronal activity.

6.1.5 Pin1 does not mediate ADAR2 regulation basally or during activity

Pin1 was previously identified as a regulator of ADAR2 localisation and activity (Marcucci, Brindle et al. 2011, Behm, Wahlstedt et al. 2017). Pin1 interacts with ADAR2 in a phosphorylation dependent manner. Phosphorylation of threonine 32 (T32) stabilises ADAR2 in the nucleus and prevents degradation in the cytosol. GFP trap assays in HEK293T cells showed significantly stronger interaction of constitutively phosphorylated (T32D) ADAR2 to Pin1. To determine whether altered ADAR2 interaction with Pin1 resulted in the ADAR2 loss following 24 h TTX treatment I performed knockdown rescue experiments. I determined ADAR2 susceptibility to TTX treatment in WT, phosphomimetic (T32D) or phosphonull (T32A) mutants using knockdown-rescue experiments. Surprisingly, all the mutant forms of ADAR2 were equally vulnerable to the TTX mediated loss. I interpret these data to indicate that the phosphorylation of T32 in ADAR2 does not play a role in the Pin1-ADAR2 interaction and does not regulate ADAR2 stability during homeostatic scaling. Interestingly, immunocytochemistry experiments with the phosphomutants did not show altered localisation of phosphonull ADAR2, which was surprising as it was previously shown that the loss of ADAR2 interaction with Pin1 regulates their nuclear localisation (Marcucci, Brindle et al. 2011, Behm, Wahlstedt et al. 2017). Moreover, WT and both the phosphomutant versions of ADAR2 could equally rescue GluA2 and GluK2 editing. Finally, cycloheximide stability assays showed that WT and both phosphomutant versions of ADAR2 are equally stable as well. Hence, these data suggest that Pin1 does not play a role in ADAR2 stability, localisation or function in neurones both basally or during TTX mediated activity.

6.1.6 ADAR2 ubiquitination could play a role in homeostatic scaling

ADAR2 is targeted for degradation via the ubiquitin-proteasome pathway. I tested to see whether inhibiting the proteasomal pathway would prevent this TTX facilitated ADAR2 loss. Addition of bortezomib (BTZ), a specific inhibitor of the proteasome (Chen, Frezza et al. 2011), caused a build-up of ubiquitinated products following 20 h drug treatment. Interestingly, application of drug alongside 24 h TTX rescued the loss of ADAR2. Moreover, subcellular fractionation experiments showed that ADAR2 is rescued in both nucleus and in the cytosol in presence of BTZ. I speculate that the build-up of ubiquitinated but not degraded ADAR2 results in the nuclear import and export recycling of ADAR2, which maintains a functional pool in the nucleus. In line with this, TTX-induced GluK2 up-scaling is inhibited in the presence BTZ. These data suggest ADAR2 loss following TTX treatment is mediated by its ubiquitination mediated degradation [**Figure 6-1**].

6.2 Future work

The findings outlined above open interesting questions and numerous research avenues, some of which are outlined below.

6.2.1 How does GluK2 Q/R editing lead to KAR upscaling?

Previous studies have shown that unedited GluK2 containing KARs form oligomers more readily than edited GluK2. This means unedited GluK2-containing KARs are more efficiently released from the ER allowing their increased surface expression (Ball, Atlason et al. 2010). However, it is not known, whether there are also variations along the secretory pathway trafficking of unedited KARs and/or recycling and degradation rates between edited and unedited GluK2 due to their altered oligomerisation.

We have shown previously that KAR forward traffic through the secretory pathway is subject to multiple regulatory checkpoints (Evans, Gurung et al. 2017). It would be interesting to study if unedited GluK2 also have increased surface expression due to enhanced KAR forward trafficking. The

cycloheximide assay performed in HEK293T cells suggested that the unedited GluK2 are less stable than the edited GluK2. This begs a question whether unedited KARs have enhanced internalisation from the surface leading to enhanced degradation or do these unedited receptors also have altered recycling rates to the surface. Addressing these questions can provide further understanding as to how Q/R editing leads to KAR upscaling.

Furthermore, using strategies such as removing endogenous GluK2 and replacing with either completely edited and unedited forms of GluK2, would be interesting to determine if unedited GluK2 express more on the surface and whether the cultures expressing completely unedited GluK2 would be insensitive to TTX mediated and partial ADAR2 mediated GluK2 upscaling. This would further emphasise the role of Q/R editing in GluK2 scaling.

6.2.2 Functional relevance of unedited KARs during scaling

What is the functional relevance of increased unedited KARs on surface during synaptic scaling? Co-localisation with post synaptic markers, calcium imaging and electrophysiology experiments can help determine if the increase in GluK2 occurs at synapses. Furthermore, determine the ionic properties of these synaptic KARs and how changes in Q/R editing of the incorporated receptors impacts on Ca^{2+} permeability and synaptic function will be interesting to study.

Moreover, KARs signal via both metabotropic and ionotropic signalling pathways. It is completely unknown, however, whether the increase in surface KARs following scaling/partial ADAR2 loss alters the metabotropic functions of KARs. This is important because synaptic activation of postsynaptic metabotropic KARs can inhibit slow AHP that regulates neuronal excitability (Melyan, Wheal et al. 2002, Chamberlain, Sadowski et al. 2013).

Moreover, metabotropic function of GluK2 have been implicated in KAR-LTP_{AMPAR} (Petrovic, Viana da Silva et al. 2017). Would the increase in GluK2-KARs following scaling/partial ADAR2 loss, affect the threshold for induction of KAR-LTP_{AMPAR}? If the increase in KARs occurs at synapses, would these receptors have altered excitability. Determining such signalling pathways,

could provide profound new insights into the regulation, roles and signalling pathways of KARs.

6.2.3 Crosstalk between other forms of RNA editing

Is ADAR2 loss selectively altering GluK2 Q/R editing over other editing sites of GluK2, GluK1 and GluA2 or this selectiveness is towards KARs in general?

The presence of other potential editing sites in GluK2 (I/V and Y/C sites), which can also be edited by ADAR2, begs the question if these sites are targeted during homeostatic up-scaling. Editing at these sites along with the Q/R site regulates the ion permeability of the GluK2 containing KARs. Together they can alter the channel properties of KARs on synapses following scaling (Köhler, Burnashev et al. 1993, Burnashev, Zhou et al. 1995). Equally, the Q/R editing site at GluK1 could also be altered with ADAR2 loss during scaling.

Future experiments could address whether R/G editing sites in GluA2 are altered by TTX treatment. While R/G editing does not alter the GluA2 trafficking properties, it does affect their desensitisation kinetics (Lomeli, Mosbacher et al. 1994). As GluA2 have been shown to be have increased surface expression during homeostatic upscaling this would help us understand whether the GluA2 expressed on the surface have altered ionic properties.

6.2.4 GluK2 Q/R editing deficient mice

GluK2 Q/R editing deficient mice offer an invaluable *in vivo* and *ex vivo* tool to study functional implications of unedited GluK2 receptors. Only one study on these mice have been published (Vissel, Royle et al. 2001). However, there are many interesting questions that can be addressed in this model, which will shed light into the function and importance of unedited KARs. These mice have recently been shipped to Bristol providing us with an opportunity to work with them. They have deleted ECS region within the intron, resulting in the loss of ability of GluK2 pre-mRNA to be edited [**Figure 6-2]** as dsRNA cannot be formed at the Q/R site for ADAR2 to bind and deaminate the site.

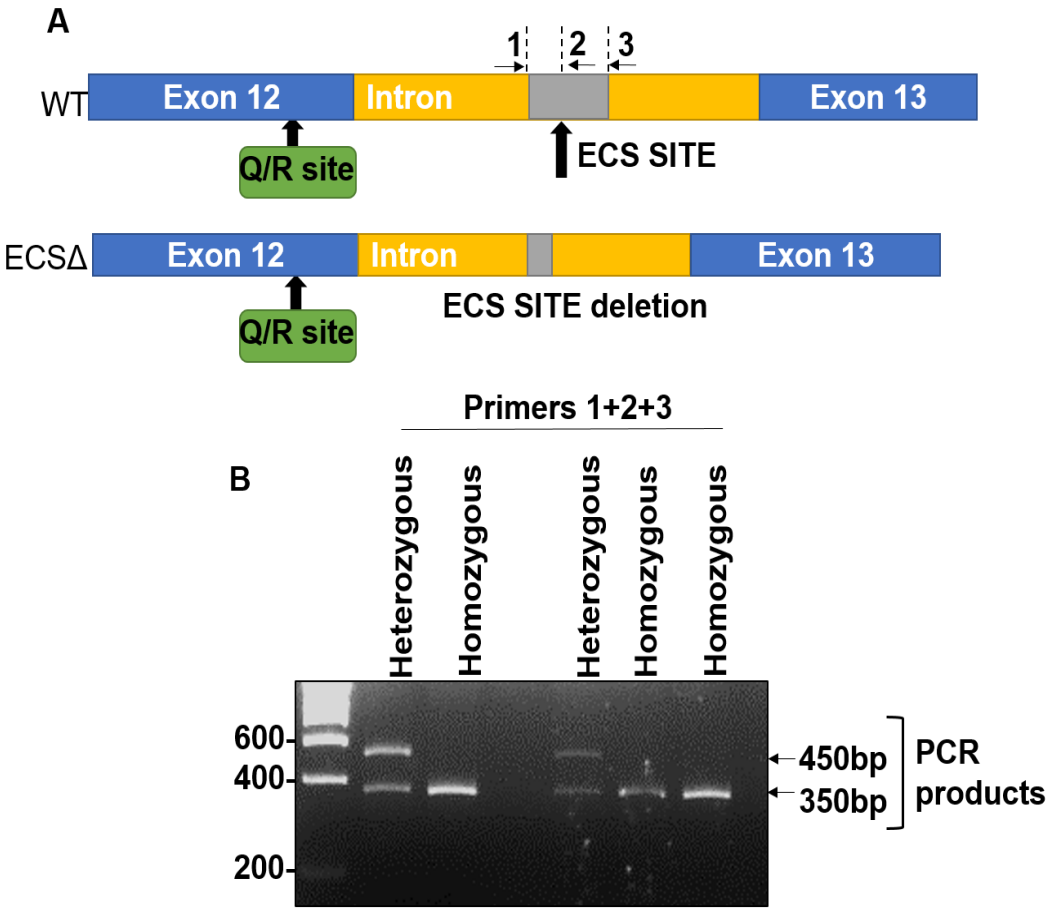

Figure 6-2: Genotyping GluK2 Q/R editing deficient mice.

The Editing site Complementary sequence (ECS) in the adjacent intronic region is ~1900nt downstream of the exonic sequence consisting of the Q/R editing site, between exon 12 and 13 (A). The WT mice have this ECS site intact, while the homozygous ECSΔ mice have 600bp intronic region between exon 12 and 13 deleted which consists of the ECS site. This results in lack of ability of ECS mice to edit its GluK2 pre-mRNA at Q/R site as such all the GluK2 translated are unedited. Mice were genotyped to determine whether they are homozygous, heterozygous or WT using primers targeting the deleted region as shown in (A) indicated by numbers 1, 2 and 3. Figure B shows an example of PCR products obtained. With primers 1, 2 and 3 combined heterozygous genomic DNA gives band at 450bp (PCR product of primers 1 and 2) and 350bp (PCR product of primers 1 and 3) while from homozygous DNA only the at 350bp (PCR products from primers 1 and 3) is obtained. No PCR product is obtained from Primer combinations 1 and 2 from homozygous mouse genomic DNA.

While no alterations in the total GluK2 protein or transcript levels were reported, whether there are changes in overall surface expression of GluK2 and whether there is presence of increased synaptic KARs in these mice has not been studied. Using dissociated cultures, we can perform surface biotinylation experiments and measure KAR mEPSCs using electrophysiology. Region specific changes in GluK2 levels could also be

studied using slice electrophysiology. This can be extended into studying the ionotropic and metabotropic functions of unedited KARs, determining whether the synaptic KARs have altered inhibition of slows AHP and have reduced threshold for KAR_{AMPAR}-LTP. Interestingly, these mice have also been reported to induce a form of LTP in the absence of NMDAR activity. Homeostatic scaling studies can also be performed to determine whether these mice display TTX mediated KAR increase on the surface.

6.2.5 ADAR2 regulators

There have been studies indicating various regulators of ADAR2 function and localisation [summarised in Chapter 5]. While I have shown that ubiquitination mediated degradation of ADAR2 plays a role in scaling, I am keen to define molecular regulators in this activity dependent pathway. Studying the potential role of ubiquitin ligase WWP2 as a mediator of activity dependent ADAR2 regulation (Marcucci, Brindle et al. 2011) will be the starting point as the tools. I have made and validated the relevant tool, and these are ready to use.

If WWP2 is the ligase, we can define the binding sites, design WWP2 non-binding ADAR2 mutants and use knockdown replace strategies to study WWP2 role. If this is not the case, co-immunoprecipitation and proteomics approach can be taken to systematically search for the ubiquitin ligase responsible. This would also allow us to search for unidentified new regulators of ADAR2 while also providing us with an opportunity to explore potential ADAR2 regulators during downscaling process (bicuculline treatment), where ADAR2 function was potentially shown to be increased but not its levels.

6.2.6 GluK2 Q/R editing in development

As unedited KARs are predominant early in life, it is thought that they play an important role during development (Bernard, Ferhat et al. 1999). Moreover, at certain synapses the contribution of KARs to transmission decreases in an activity dependent manner during development and they are replaced by AMPARs (Kidd and Isaac 1999).

Could the increase in GluK2 editing be playing a role in decreased KAR transmission? Is having increased unedited GluK2 during scaling reverting the

neurones to an immature state, perhaps allowing GluK2-KARs to increasingly contribute to the synaptic transmission. Interestingly, my dissociated hippocampal cultures mimic the studies in brain where there is an increased proportion of unedited GluK2 up to DIV5, after which the editing is increased up to DIV 12 to reach a stable level [**Figure 6-3**]. This also correlates with increasing ADAR2 levels, further showing ADAR2 role in GluK2 editing during development. This puts forward an interesting idea if KARs are increasing at the synapses and potentially contributing to the synaptic transmission and whether the increase of both KARs and AMPARs occur at the same synapses during scaling?

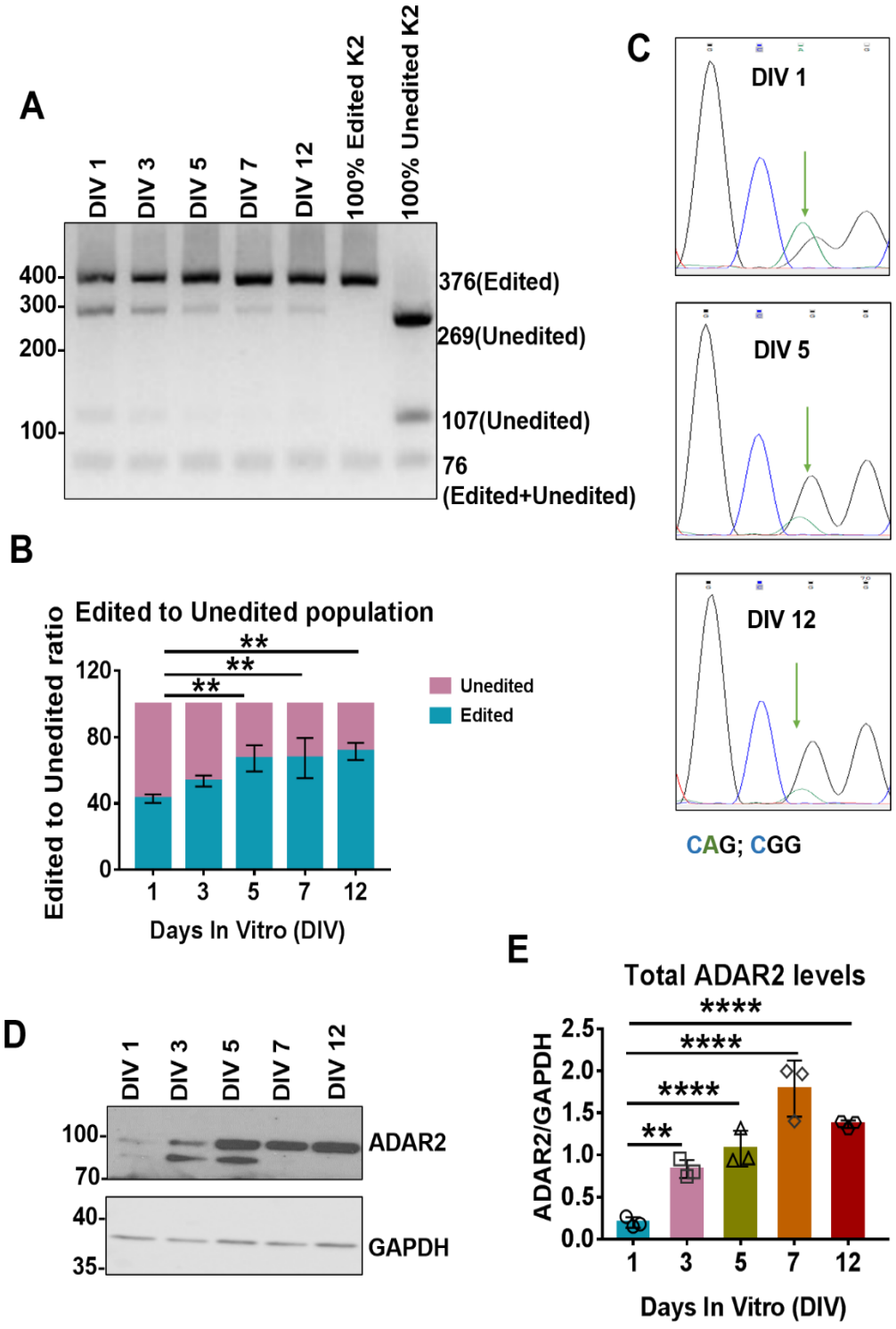
A
DIV 1
DIV 3
DIV 5
DIV 7
DIV 12
100% Edited K2
100% Unedited K2
400
300
200
100
376(Edited)
269(Unedited)
107(Unedited)
76
(Edited+Unedited)
B
Edited to Unedited population
Edited to Unedited ratio
120
80
40
0
**
**
**
Unedited
Edited
1
3
5
7
12
Days In Vitro (DIV)
C
DIV 1
DIV 5
DIV 12
CAG; CGG
D
DIV 1
DIV 3
DIV 5
DIV 7
DIV 12
100
70
40
35
ADAR2
GAPDH
E
Total ADAR2 levels
ADAR2/GAPDH
2.5
2.0
1.5
1.0
0.5
0.0
****
****
****
**
1
3
5
7
12
Days In Vitro (DIV)

Figure 6-3: Developmental increase in ADAR2 levels and GluK2 Q/R editing in hippocampal cultures.

A. Representative images of the PCR products separated on a 4% agarose gel post BbvI digestion to determine edited to unedited GluK2 ratio at indicated Days in vitro (DIV). 100% edited and unedited GluK2 constructs were used as a control to ensure BbvI cut activity and validity of the assay. RNA extraction was performed on hippocampal cells at indicated DIVs, cDNA synthesised, and PCR performed.

B. Quantification of percentage of edited to unedited ratio of GluK2 population as shown in A. N=3 independent dissections; One way ANOVA with Dunnett's multiple post comparisons corrections; **p<0.01, ***p<0.001; error bars=S.D.

C. Representative chromatographs of PCR products comparing hippocampal cells at DIV 1, 5 and 12 at the Q/R editing site. The undigested PCR products were sent for sequencing to determine changes in the dual peaks obtained at the site of editing as indicated by the green arrow. A peak (green) represents the unedited base while the G peak (black) represents the edited base. The image is representative of 3 repeats.

D. Representative western blot images of ADAR2 and GAPDH levels at indicated DIVs. Hippocampal cells were lysed at indicated DIVs, proteins extracted, protein quantification performed, and equal amount was loaded per condition.

E. Quantification of total ADAR2 levels normalised to GAPDH shown in D. N=3 independent dissections, One-way ANOVA with Dunnett's multiple post comparisons corrections; **p<0.01, ****p<0.0001; error bar=S.D.

6.2.7 GluK2 Q/R editing and disease

ADAR2 and GluK2 (including unedited GluK2) have all been implicated in diseases principally in epilepsy (Kortenbruck, Berger et al. 2001, Wondolowski and Dickman 2013). Additionally, the unedited GluK2 transgenic mice were shown to have increased seizure susceptibility compared to the WT mice (Vissel, Royle et al. 2001). Intriguingly, dysregulation of homeostatic synaptic plasticity is thought to play a role in excitation/inhibition imbalances that underlies the pathogenic epileptogenic states, however molecular links for this have been elusive (Wondolowski and Dickman 2013). Perhaps, increases in GluK2 editing during development act as a regulatory mechanism to reduce seizure vulnerability in adults. Hence, it would be of immense interest in the field to test the related questions:

- Does increased unedited GluK2 generate a pathogenic epileptic phenotype?

- Does increasing edited GluK2 provide a mechanism for cells to avoid epileptic states?

Moreover, we have recently received rat brain samples from pilocarpine induced epileptic rat brains extracted at various timepoints of pilocarpine injection and epileptic induction, from collaborators in University of Aston [**Figure 6-4**]. The Reduced Intensity Status Epilepticus (RISE) model of pilocarpine-induced temporal lobe epilepsy (TLE) was used, which features low mortality compared to other forms of epileptic models and allows for detection of subtler changes that is potentially leading to the epileptogenic states (Modebadze, Morgan et al. 2016). This model gives us an opportunity to determine levels of ADARs and KARs and the editing status of both KAR and AMPAR subunits at different stages of epilepsy induction to investigate if they are causative factors of epileptic induction.

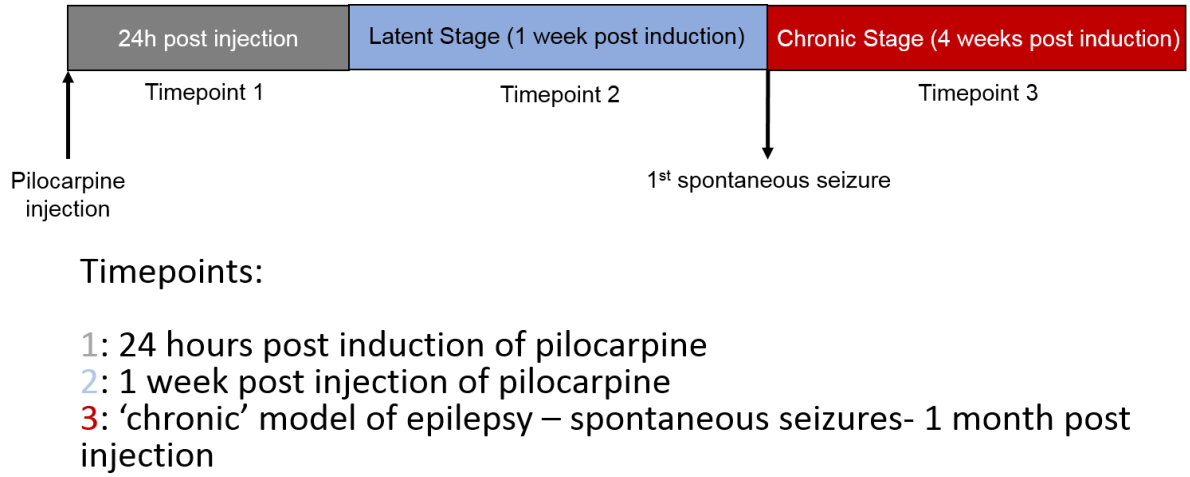

Figure 6-4: Timelines at which rat brains were obtained.

RISE model of epilepsy involved pilocarpine injection at 0h, causing the initial seizure activity. Rat brains were obtained 24 h post injection (Timepoint 1), control brains were subjected to sham injection. The latent phase is 1 week post injection where the rats show no symptoms or seizure activities. Chronic stage (Timepoint 3) is 4 weeks post injection, where the rats have recurrent spontaneous recurrent seizures.

6.2.8 Other potential questions and directions

Along with GluK2 subunit of KARs, GluK5 also scaled up and down. Moreover, removing endogenous GluK2 did not affect GluK5 total or surface expression. This led me to speculate if the involvement of low affinity KAR subunits (such as GluK5) is required to form heteromers to allow their traffic out of ER

(Gallyas, Ball et al. 2003, Vivithanaporn, Yan et al. 2006). This opens many interesting questions such as:

- Do other KAR subunits GluK1, GluK3 and GluK4 also respond to changes in the network activity?
- Are other interacting proteins that are involved in KAR trafficking and that stabilise KARs on the surface and synapses also involved in surface increase of not just GluK5 but also GluK2? (Pahl, Tapken et al. 2014, Evans, Gurung et al. 2017).

While I showed GluK2 editing plays a major role in GluK2 scaling, do processes such as post translational modifications and interactions also contribute to aid and maintain these changes. If so, are these mechanisms shared in both upscaling and downscaling of KARs? Screening for changes that occur during scaling with KAR interactors and/or modifications can allow us to understand mechanisms that are involved in scaling. Furthermore, studying whether similar mechanisms play role in both up-scaling and down-scaling will also be an equally interesting aspect to follow.

Finally, KAR function in inhibitory transmission is becoming increasingly evident with its role in regulating GABA release (Rodriguez-Moreno and Lerma 1998) and regulating KCC2 surface expression (Pressey, Mahadevan et al. 2017). Here I initially explored the role of KARs in both upregulation and downregulation of AMPARs to study their function in excitatory neurotransmission. But following questions are also of interest:

- Do KARs regulate inhibitory transmission by altering surface expression of KCC2 during these transient and sustained KAR activations?
- Do KARs have a role as a mediator of excitation and inhibition signalling?

This would add a new direction to the study of KAR function and further implement KAR importance in synaptic plasticity.

6.3 Conclusion and Significance

There is substantial and increasing evidences for key roles of KARs in certain forms of synaptic plasticity, both by autoregulation of their own plasticity and by regulating the plasticity of AMPARs. In the first part of my PhD, I showed a potential role of pre-synaptic KARs in regulating short term plasticity by regulating AMPAR surface expression. Moreover, I showed a novel role of KARs in homeostatic scaling by demonstrating that KARs can scale up and down on the surface in response to the changes in the network activity. Furthermore, I highlighted the importance of Q/R editing of GluK2 in this upscaling process.

While unedited GluK2 had been shown in the past to be efficiently released from the ER and traffic to the surface, here I establish the physiological relevance of this increased ER export and surface expression of unedited KARs in scaling. With this, I also demonstrate an important role of ADAR2 in neuronal activity, which has been alluded to before. ADAR2 seems to undergo proteasomal degradation following chronic decrease in the network activity, which in turn alters its editing activity. While ADAR2 studies have predominantly focused on its function of regulating GluA2 Q/R and R/G editing, here I have shown that alterations in ADAR2 levels functions to regulate GluK2 upscaling by regulating GluK2 Q/R editing. How ADAR2 is mechanistically regulated during scaling, understanding the functional relevance of upscaling unedited KARs and how the interplay between editing, KAR and homeostatic plasticity can potentially lead to pathological phenotypes will be an important subject for future studies.

Chapter 7. REFERENCES

(2015). Basic Electrophysiological Methods. Oxford University Press, Oxford University Press.

Akbarian, S., M. A. Smith and E. G. Jones (1995). "Editing for an AMPA receptor subunit RNA in prefrontal cortex and striatum in Alzheimer's disease, Huntington's disease and schizophrenia." Brain Res **699**(2): 297-304.

Alberts, B. (2015). Molecular Biology of the cell, New York: Garland Science.

Ancona Esselmann, S. G., J. Diaz-Alonso, J. M. Levy, M. A. Bemben and R. A. Nicoll (2017). "Synaptic homeostasis requires the membrane-proximal carboxy tail of GluA2." Proc Natl Acad Sci U S A **114**(50): 13266-13271.

Anderson, W. W. and G. L. Collingridge (2007). "Capabilities of the WinLTP data acquisition program extending beyond basic LTP experimental functions." J Neurosci Methods **162**(1-2): 346-356.

Andrade-Talavera, Y., P. Duque-Feria, T. S. Sihra and A. Rodriguez-Moreno (2013). "Pre-synaptic kainate receptor-mediated facilitation of glutamate release involves PKA and Ca(2+) -calmodulin at thalamocortical synapses." J Neurochem **126**(5): 565-578.

Anggono, V., R. L. Clem and R. L. Huganir (2011). "PICK1 loss of function occludes homeostatic synaptic scaling." J Neurosci **31**(6): 2188-2196.

Armstrong, N. and E. Gouaux (2000). "Mechanisms for activation and antagonism of an AMPA-sensitive glutamate receptor: crystal structures of the GluR2 ligand binding core." Neuron **28**(1): 165-181.

Athanasiadis, A., D. Placido, S. Maas, B. A. Brown, 2nd, K. Lowenhaupt and A. Rich (2005). "The crystal structure of the Zbeta domain of the RNA-editing enzyme ADAR1 reveals distinct conserved surfaces among Z-domains." J Mol Biol **351**(3): 496-507.

Ayalon, G. and Y. Stern-Bach (2001). "Functional assembly of AMPA and kainate receptors is mediated by several discrete protein-protein interactions." Neuron **31**(1): 103-113.

Bahn, S., B. Volk and W. Wisden (1994). "Kainate receptor gene expression in the developing rat brain." J Neurosci **14**(9): 5525-5547.

Balik, A., A. C. Penn, Z. Nemoda and I. H. Greger (2013). "Activity-regulated RNA editing in select neuronal subfields in hippocampus." Nucleic Acids Res **41**(2): 1124-1134.

Ball, S. M., P. T. Atlason, O. O. Shittu-Balogun and E. Molnar (2010). "Assembly and intracellular distribution of kainate receptors is determined by RNA editing and subunit composition." J Neurochem **114**(6): 1805-1818.

Barberis, A., S. Sachidhanandam and C. Mulle (2008). "GluR6/KA2 kainate receptors mediate slow-deactivating currents." J Neurosci **28**(25): 6402-6406.

Barbon, A. and S. Barlati (2011). "Glutamate receptor RNA editing in health and disease." Biochemistry (Mosc) **76**(8): 882-889.

Barbon, A., F. Fumagalli, L. Caracciolo, L. Madaschi, E. Lesma, C. Mora, S. Carelli, T. A. Slotkin, G. Racagni, A. M. Di Giulio, A. Gorio and S. Barlati

(2010). "Acute spinal cord injury persistently reduces R/G RNA editing of AMPA receptors." J Neurochem **114**(2): 397-407.

Barbon, A., F. Fumagalli, L. La Via, L. Caracciolo, G. Racagni, M. A. Riva and S. Barlati (2007). "Chronic phencyclidine administration reduces the expression and editing of specific glutamate receptors in rat prefrontal cortex." Exp Neurol **208**(1): 54-62.

Barraud, P. and F. H. Allain (2012). "ADAR proteins: double-stranded RNA and Z-DNA binding domains." Curr Top Microbiol Immunol **353**: 35-60.

Bashir, Z. I., Z. A. Bortolotto, C. H. Davies, N. Berretta, A. J. Irving, A. J. Seal, J. M. Henley, D. E. Jane, J. C. Watkins and G. L. Collingridge (1993). "Induction of LTP in the hippocampus needs synaptic activation of glutamate metabotropic receptors." Nature **363**(6427): 347-350.

Bass, B. L. (2002). "RNA editing by adenosine deaminases that act on RNA." Annu Rev Biochem **71**: 817-846.

Bass, B. L. and H. Weintraub (1988). "An unwinding activity that covalently modifies its double-stranded RNA substrate." Cell **55**(6): 1089-1098.

Beattie, E. C., R. C. Carroll, X. Yu, W. Morishita, H. Yasuda, M. von Zastrow and R. C. Malenka (2000). "Regulation of AMPA receptor endocytosis by a signaling mechanism shared with LTD." Nat Neurosci **3**(12): 1291-1300.

Behm, M., H. Wahlstedt, A. Widmark, M. Eriksson and M. Öhman (2017). "Accumulation of nuclear ADAR2 regulates adenosine-to-inosine RNA editing during neuronal development." J Cell Sci **130**(4): 745-753.

Belcher, S. M. and J. R. Howe (1997). "Characterization of RNA editing of the glutamate-receptor subunits GluR5 and GluR6 in granule cells during cerebellar development." Brain Res Mol Brain Res **52**(1): 130-138.

Ben-Ari, Y. and R. Cossart (2000). "Kainate, a double agent that generates seizures: two decades of progress." Trends Neurosci **23**(11): 580-587.

Bernard, A., L. Ferhat, F. Dessi, G. Charton, A. Represa, Y. Ben-Ari and M. Khrestchatisky (1999). "Q/R editing of the rat GluR5 and GluR6 kainate receptors in vivo and in vitro: evidence for independent developmental, pathological and cellular regulation." Eur J Neurosci **11**(2): 604-616.

Bernard, V., P. Somogyi and J. P. Bolam (1997). "Cellular, subcellular, and subsynaptic distribution of AMPA-type glutamate receptor subunits in the neostriatum of the rat." J Neurosci **17**(2): 819-833.

Bettler, B., J. Boulter, I. Hermans-Borgmeyer, A. O'Shea-Greenfield, E. S. Deneris, C. Moll, U. Borgmeyer, M. Hollmann and S. Heinemann (1990). "Cloning of a novel glutamate receptor subunit, GluR5: expression in the nervous system during development." Neuron **5**(5): 583-595.

Bettler, B. and C. Mulle (1995). "Review: neurotransmitter receptors. II. AMPA and kainate receptors." Neuropharmacology **34**(2): 123-139.

Bhansali, P., J. Dunning, S. E. Singer, L. David and C. Schmauss (2007). "Early life stress alters adult serotonin 2C receptor pre-mRNA editing and expression of the alpha subunit of the heterotrimeric G-protein G q." J Neurosci **27**(6): 1467-1473.

Bhattacharyya, S., V. Biou, W. Xu, O. Schluter and R. C. Malenka (2009). "A critical role for PSD-95/AKAP interactions in endocytosis of synaptic AMPA receptors." Nat Neurosci **12**(2): 172-181.

Bhogal, B., J. E. Jepson, Y. A. Savva, A. S. Pepper, R. A. Reenan and T. A. Jongens (2011). "Modulation of dADAR-dependent RNA editing by the Drosophila fragile X mental retardation protein." Nat Neurosci **14**(12): 1517-1524.

Blackman, M. P., B. Djukic, S. B. Nelson and G. G. Turrigiano (2012). "A critical and cell-autonomous role for MeCP2 in synaptic scaling up." J Neurosci **32**(39): 13529-13536.

Bliss, T. V. and G. L. Collingridge (1993). "A synaptic model of memory: long-term potentiation in the hippocampus." Nature **361**(6407): 31-39.

Bliss, T. V. and T. Lomo (1973). "Long-lasting potentiation of synaptic transmission in the dentate area of the anaesthetized rabbit following stimulation of the perforant path." J Physiol **232**(2): 331-356.

Bonini, D., A. Filippini, L. La Via, C. Fiorentini, F. Fumagalli, M. Colombi and A. Barbon (2015). "Chronic glutamate treatment selectively modulates AMPA RNA editing and ADAR expression and activity in primary cortical neurons." RNA Biol **12**(1): 43-53.

Bortolotto, Z. A., V. R. Clarke, C. M. Delany, M. C. Parry, I. Smolders, M. Vignes, K. H. Ho, P. Miu, B. T. Brinton, R. Fantaske, A. Ogden, M. Gates, P. L. Ornstein, D. Lodge, D. Bleakman and G. L. Collingridge (1999). "Kainate receptors are involved in synaptic plasticity." Nature **402**(6759): 297-301.

Bortolotto, Z. A., V. J. Collett, F. Conquet, Z. Jia, H. van der Putten and G. L. Collingridge (2005). "The regulation of hippocampal LTP by the molecular switch, a form of metaplasticity, requires mGlu5 receptors." Neuropharmacology **49 Suppl 1**: 13-25.

Bosch, M., J. Castro, T. Saneyoshi, H. Matsuno, M. Sur and Y. Hayashi (2014). "Structural and molecular remodeling of dendritic spine substructures during long-term potentiation." Neuron **82**(2): 444-459.

Bowie, D. and M. L. Mayer (1995). "Inward rectification of both AMPA and kainate subtype glutamate receptors generated by polyamine-mediated ion channel block." Neuron **15**(2): 453-462.

Bredt, D. S. and R. A. Nicoll (2003). "AMPA receptor trafficking at excitatory synapses." Neuron **40**(2): 361-379.

Breustedt, J. and D. Schmitz (2004). "Assessing the role of GLUK5 and GLUK6 at hippocampal mossy fiber synapses." J Neurosci **24**(45): 10093-10098.

Brusa, R., F. Zimmermann, D. S. Koh, D. Feldmeyer, P. Gass, P. H. Seeburg and R. Sprengel (1995). "Early-onset epilepsy and postnatal lethality associated with an editing-deficient GluR-B allele in mice." Science **270**(5242): 1677-1680.

Bureau, I., S. Bischoff, S. F. Heinemann and C. Mulle (1999). "Kainate receptor-mediated responses in the CA1 field of wild-type and GluR6-deficient mice." J Neurosci **19**(2): 653-663.

Burnashev, N., H. Monyer, P. H. Seeburg and B. Sakmann (1992). "Divalent ion permeability of AMPA receptor channels is dominated by the edited form of a single subunit." Neuron **8**(1): 189-198.

Burnashev, N. and A. Rozov (2000). "Genomic control of receptor function." Cell Mol Life Sci **57**(11): 1499-1507.

Burnashev, N., Z. Zhou, E. Neher and B. Sakmann (1995). "Fractional calcium currents through recombinant GluR channels of the NMDA, AMPA and kainate receptor subtypes." J Physiol **485 (Pt 2)**: 403-418.

Caracciolo, L., F. Fumagalli, S. Carelli, L. Madaschi, L. La Via, D. Bonini, C. Fiorentini, S. Barlati, A. Gorio and A. Barbon (2013). "Kainate receptor RNA editing is markedly altered by acute spinal cord injury." J Mol Neurosci **51**(3): 903-910.

Carta, M., P. Opazo, J. Veran, A. Athane, D. Choquet, F. Coussen and C. Mulle (2013). "CaMKII-dependent phosphorylation of GluK5 mediates plasticity of kainate receptors." Embo j **32**(4): 496-510.

Casimiro, T. M., K. G. Sossa, G. Uzunova, J. B. Beattie, K. C. Marsden and R. C. Carroll (2011). "mGluR and NMDAR activation internalize distinct populations of AMPARs." Mol Cell Neurosci **48**(2): 161-170.

Castillo, P. E., R. C. Malenka and R. A. Nicoll (1997). "Kainate receptors mediate a slow postsynaptic current in hippocampal CA3 neurons." Nature **388**(6638): 182-186.

Catterall, W. A. (1995). "Structure and function of voltage-gated ion channels." Annu Rev Biochem **64**: 493-531.

Cazakoff, B. N. and J. G. Howland (2011). "AMPA receptor endocytosis in rat perirhinal cortex underlies retrieval of object memory." Learn Mem **18**(11): 688-692.

Cenci, C., R. Barzotti, F. Galeano, S. Corbelli, R. Rota, L. Massimi, C. Di Rocco, M. A. O'Connell and A. Gallo (2008). "Down-regulation of RNA editing in pediatric astrocytomas: ADAR2 editing activity inhibits cell migration and proliferation." J Biol Chem **283**(11): 7251-7260.

Chamberlain, S. E., I. M. Gonzalez-Gonzalez, K. A. Wilkinson, F. A. Konopacki, S. Kantamneni, J. M. Henley and J. R. Mellor (2012). "SUMOylation and phosphorylation of GluK2 regulate kainate receptor trafficking and synaptic plasticity." Nat Neurosci **15**(6): 845-852.

Chamberlain, S. E., J. H. Sadowski, L. M. Teles-Grilo Ruivo, L. A. Atherton and J. R. Mellor (2013). "Long-term depression of synaptic kainate receptors reduces excitability by relieving inhibition of the slow afterhyperpolarization." J Neurosci **33**(22): 9536-9545.

Chater, T. E. and Y. Goda (2014). "The role of AMPA receptors in postsynaptic mechanisms of synaptic plasticity." Front Cell Neurosci **8**: 401.

Chen, C. X., D. S. Cho, Q. Wang, F. Lai, K. C. Carter and K. Nishikura (2000). "A third member of the RNA-specific adenosine deaminase gene family, ADAR3, contains both single- and double-stranded RNA binding domains." RNA **6**(5): 755-767.

Chen, D., M. Frezza, S. Schmitt, J. Kanwar and Q. P. Dou (2011). "Bortezomib as the first proteasome inhibitor anticancer drug: current status and future perspectives." Curr Cancer Drug Targets **11**(3): 239-253.

Cherubini, E., M. D. Caiati and S. Sivakumaran (2011). "In the developing hippocampus kainate receptors control the release of GABA from mossy fiber terminals via a metabotropic type of action." Adv Exp Med Biol **717**: 11-26.

Chilibeck, K. A., T. Wu, C. Liang, M. J. Schellenberg, E. M. Gesner, J. M. Lynch and A. M. MacMillan (2006). "FRET analysis of in vivo dimerization by RNA-editing enzymes." J Biol Chem **281**(24): 16530-16535.

Chittajallu, R., M. Vignes, K. K. Dev, J. M. Barnes, G. L. Collingridge and J. M. Henley (1996). "Regulation of glutamate release by presynaptic kainate receptors in the hippocampus." Nature **379**(6560): 78-81.

Cho, D. S., W. Yang, J. T. Lee, R. Shiekhattar, J. M. Murray and K. Nishikura (2003). "Requirement of dimerization for RNA editing activity of adenosine deaminases acting on RNA." J Biol Chem **278**(19): 17093-17102.

Choquet, D. and A. Triller (2013). "The dynamic synapse." Neuron **80**(3): 691-703.

Christensen, J. K., A. V. Paternain, S. Selak, P. K. Ahring and J. Lerma (2004). "A mosaic of functional kainate receptors in hippocampal interneurons." J Neurosci **24**(41): 8986-8993.

Cingolani, L. A., A. Thalhammer, L. M. Yu, M. Catalano, T. Ramos, M. A. Colicos and Y. Goda (2008). "Activity-dependent regulation of synaptic AMPA receptor composition and abundance by beta3 integrins." Neuron **58**(5): 749-762.

Citri, A. and R. C. Malenka (2008). "Synaptic plasticity: multiple forms, functions, and mechanisms." Neuropsychopharmacology **33**(1): 18-41.

Collingridge, G. L., J. T. Isaac and Y. T. Wang (2004). "Receptor trafficking and synaptic plasticity." Nat Rev Neurosci **5**(12): 952-962.

Collingridge, G. L., S. J. Kehl and H. McLennan (1983). "Excitatory amino acids in synaptic transmission in the Schaffer collateral-commissural pathway of the rat hippocampus." J Physiol **334**: 33-46.

Collingridge, G. L., R. W. Olsen, J. Peters and M. Spedding (2009). "A nomenclature for ligand-gated ion channels." Neuropharmacology **56**(1): 2-5.

Conn, P. J. and J. P. Pin (1997). "Pharmacology and functions of metabotropic glutamate receptors." Annu Rev Pharmacol Toxicol **37**: 205-237.

Connors, B. W., R. C. Malenka and L. R. Silva (1988). "Two inhibitory postsynaptic potentials, and GABAA and GABAB receptor-mediated responses in neocortex of rat and cat." J Physiol **406**: 443-468.

Contractor, A., C. Mulle and G. T. Swanson (2011). "Kainate receptors coming of age: milestones of two decades of research." Trends Neurosci **34**(3): 154-163.

Contractor, A., G. Swanson and S. F. Heinemann (2001). "Kainate receptors are involved in short- and long-term plasticity at mossy fiber synapses in the hippocampus." Neuron **29**(1): 209-216.

Contractor, A., G. T. Swanson, A. Sailer, S. O'Gorman and S. F. Heinemann (2000). "Identification of the kainate receptor subunits underlying modulation of excitatory synaptic transmission in the CA3 region of the hippocampus." J Neurosci **20**(22): 8269-8278.

Copits, B. A., J. S. Robbins, S. Frausto and G. T. Swanson (2011). "Synaptic targeting and functional modulation of GluK1 kainate receptors by the auxiliary neuropilin and tolloid-like (NETO) proteins." J Neurosci **31**(20): 7334-7340.

Copits, B. A. and G. T. Swanson (2013). "Kainate receptor post-translational modifications differentially regulate association with 4.1N to control activity-dependent receptor endocytosis." J Biol Chem **288**(13): 8952-8965.

Coussen, F., E. Normand, C. Marchal, P. Costet, D. Choquet, M. Lambert, R. M. Mege and C. Mulle (2002). "Recruitment of the kainate receptor subunit glutamate receptor 6 by cadherin/catenin complexes." J Neurosci **22**(15): 6426-6436.

Craig, T. J., N. Jaafari, M. M. Petrovic, S. C. Jacobs, P. P. Rubin, J. R. Mellor and J. M. Henley (2012). "Homeostatic synaptic scaling is regulated by protein SUMOylation." J Biol Chem **287**(27): 22781-22788.

Cull-Candy, S., L. Kelly and M. Farrant (2006). "Regulation of Ca2+-permeable AMPA receptors: synaptic plasticity and beyond." Curr Opin Neurobiol **16**(3): 288-297.

Dabiri, G. A., F. Lai, R. A. Drakas and K. Nishikura (1996). "Editing of the GLuR-B ion channel RNA in vitro by recombinant double-stranded RNA adenosine deaminase." Embo j **15**(1): 34-45.

Darstein, M., R. S. Petralia, G. T. Swanson, R. J. Wenthold and S. F. Heinemann (2003). "Distribution of kainate receptor subunits at hippocampal mossy fiber synapses." J Neurosci **23**(22): 8013-8019.

Debanne, D., N. C. Guerineau, B. H. Gahwiler and S. M. Thompson (1996). "Paired-pulse facilitation and depression at unitary synapses in rat hippocampus: quantal fluctuation affects subsequent release." J Physiol **491 (Pt 1)**: 163-176.

Demaison, C., K. Parsley, G. Brouns, M. Scherr, K. Battmer, C. Kinnon, M. Grez and A. J. Thrasher (2002). "High-level transduction and gene expression in hematopoietic repopulating cells using a human immunodeficiency [correction of imunodeficiency] virus type 1-based lentiviral vector containing an internal spleen focus forming virus promoter." Hum Gene Ther **13**(7): 803-813.

Denker, A. and S. O. Rizzoli (2010). "Synaptic vesicle pools: an update." Front Synaptic Neurosci **2**: 135.

Desai, N. S., R. H. Cudmore, S. B. Nelson and G. G. Turrigiano (2002). "Critical periods for experience-dependent synaptic scaling in visual cortex." Nat Neurosci **5**(8): 783-789.

Desterro, J. M., L. P. Keegan, M. Lafarga, M. T. Berciano, M. O'Connell and M. Carmo-Fonseca (2003). "Dynamic association of RNA-editing enzymes with the nucleolus." J Cell Sci **116**(Pt 9): 1805-1818.

Diering, G. H., A. S. Gustina and R. L. Huganir (2014). "PKA-GluA1 coupling via AKAP5 controls AMPA receptor phosphorylation and cell-surface targeting during bidirectional homeostatic plasticity." Neuron **84**(4): 790-805.

Diering, G. H., R. S. Nirujogi, R. H. Roth, P. F. Worley, A. Pandey and R. L. Huganir (2017). "Homer1a drives homeostatic scaling-down of excitatory synapses during sleep." Science **355**(6324): 511-515.

Dobrunz, L. E. and C. F. Stevens (1997). "Heterogeneity of release probability, facilitation, and depletion at central synapses." Neuron **18**(6): 995-1008.

Doherty, A. J., M. J. Palmer, Z. A. Bortolotto, A. Hargreaves, A. E. Kingston, P. L. Ornstein, D. D. Schoepp, D. Lodge and G. L. Collingridge (2000). "A novel, competitive mGlu(5) receptor antagonist (LY344545) blocks DHPG-induced potentiation of NMDA responses but not the induction of LTP in rat hippocampal slices." Br J Pharmacol **131**(2): 239-244.

Dolman, N. P., J. C. More, A. Alt, J. L. Knauss, O. T. Pentikainen, C. R. Glasser, D. Bleakman, M. L. Mayer, G. L. Collingridge and D. E. Jane (2007). "Synthesis and pharmacological characterization of N3-substituted willardiine derivatives: role of the substituent at the 5-position of the uracil ring in the development of highly potent and selective GLUK5 kainate receptor antagonists." J Med Chem **50**(7): 1558-1570.

Donevan, S. D., S. Yamaguchi and M. A. Rogawski (1994). "Non-N-methyl-D-aspartate receptor antagonism by 3-N-substituted 2,3-benzodiazepines: relationship to anticonvulsant activity." J Pharmacol Exp Ther **271**(1): 25-29.

Dong, H., R. J. O'Brien, E. T. Fung, A. A. Lanahan, P. F. Worley and R. L. Huganir (1997). "GRIP: a synaptic PDZ domain-containing protein that interacts with AMPA receptors." Nature **386**(6622): 279-284.

Dracheva, S., R. Lyddon, K. Barley, S. M. Marcus, Y. L. Hurd and W. M. Byne (2009). "Editing of serotonin 2C receptor mRNA in the prefrontal cortex characterizes high-novelty locomotor response behavioral trait." Neuropsychopharmacology **34**(10): 2237-2251.

Dudek, S. M. and M. F. Bear (1992). "Homosynaptic long-term depression in area CA1 of hippocampus and effects of N-methyl-D-aspartate receptor blockade." Proc Natl Acad Sci U S A **89**(10): 4363-4367.

Egebjerg, J. and S. F. Heinemann (1993). "Ca2+ permeability of unedited and edited versions of the kainate selective glutamate receptor GluR6." Proc Natl Acad Sci U S A **90**(2): 755-759.

Ehlers, M. D. (2003). "Activity level controls postsynaptic composition and signaling via the ubiquitin-proteasome system." Nat Neurosci **6**(3): 231-242.

Ehlers, M. D., M. Heine, L. Groc, M. C. Lee and D. Choquet (2007). "Diffusional trapping of GluR1 AMPA receptors by input-specific synaptic activity." Neuron **54**(3): 447-460.

Englander, M. T., S. C. Dulawa, P. Bhansali and C. Schmauss (2005). "How stress and fluoxetine modulate serotonin 2C receptor pre-mRNA editing." J Neurosci **25**(3): 648-651.

Evans, A. J., S. Gurung, J. M. Henley, Y. Nakamura and K. A. Wilkinson (2017). "Exciting Times: New Advances Towards Understanding the Regulation and Roles of Kainate Receptors." Neurochem Res.

Evans, A. J., S. Gurung, K. A. Wilkinson, D. J. Stephens and J. M. Henley (2017). "Assembly, Secretory Pathway Trafficking, and Surface Delivery of Kainate Receptors Is Regulated by Neuronal Activity." Cell Rep **19**(12): 2613-2626.

Faundez, V., R. Krauss, L. Holuigue, J. Garrido and A. Gonzalez (1992). "Epidermal growth factor receptor in synaptic fractions of the rat central nervous system." J Biol Chem **267**(28): 20363-20370.

Feldmeyer, D., K. Kask, R. Brusa, H. C. Kornau, R. Kolhekar, A. Rozov, N. Burnashev, V. Jensen, O. Hvalby, R. Sprengel and P. H. Seeburg (1999). "Neurological dysfunctions in mice expressing different levels of the Q/R site-unedited AMPAR subunit GluR-B." Nat Neurosci **2**(1): 57-64.

Feng, Y., C. L. Sansam, M. Singh and R. B. Emeson (2006). "Altered RNA editing in mice lacking ADAR2 autoregulation." Mol Cell Biol **26**(2): 480-488.

Fernandes, D. and A. L. Carvalho (2016). "Mechanisms of homeostatic plasticity in the excitatory synapse." J Neurochem **139**(6): 973-996.

Fernandes, H. B., J. S. Catches, R. S. Petralia, B. A. Copits, J. Xu, T. A. Russell, G. T. Swanson and A. Contractor (2009). "High-affinity kainate receptor subunits are necessary for ionotropic but not metabotropic signaling." Neuron **63**(6): 818-829.

Fievre, S., M. Carta, I. Chamma, V. Labrousse, O. Thoumine and C. Mulle (2016). "Molecular determinants for the strictly compartmentalized expression of kainate receptors in CA3 pyramidal cells." Nat Commun **7**: 12738.

Filippini, A., D. Bonini, E. Giacopuzzi, L. La Via, F. Gangemi, M. Colombi and A. Barbon (2018). "Differential Enzymatic Activity of Rat ADAR2 Splicing Variants Is Due to Altered Capability to Interact with RNA in the Deaminase Domain." Genes (Basel) **9**(2).

Filippini, A., D. Bonini, L. La Via and A. Barbon (2017). "The Good and the Bad of Glutamate Receptor RNA Editing." Mol Neurobiol **54**(9): 6795-6805.

Filippini, A., D. Bonini, C. Lacoux, L. Pacini, M. Zingariello, L. Sancillo, D. Bosisio, V. Salvi, J. Mingardi, L. La Via, F. Zalfa, C. Bagni and A. Barbon (2017). "Absence of the Fragile X Mental Retardation Protein results in defects of RNA editing of neuronal mRNAs in mouse." RNA Biol **14**(11): 1580-1591.

Fisahn, A., S. F. Heinemann and C. J. McBain (2005). "The kainate receptor subunit GluR6 mediates metabotropic regulation of the slow and medium AHP currents in mouse hippocampal neurones." J Physiol **562**(Pt 1): 199-203.

Fitzjohn, S. M., Z. A. Bortolotto, M. J. Palmer, A. J. Doherty, P. L. Ornstein, D. D. Schoepp, A. E. Kingston, D. Lodge and G. L. Collingridge (1998). "The potent mGlu receptor antagonist LY341495 identifies roles for both cloned and novel mGlu receptors in hippocampal synaptic plasticity." Neuropharmacology **37**(12): 1445-1458.

Fitzjohn, S. M., A. E. Kingston, D. Lodge and G. L. Collingridge (1999). "DHPG-induced LTD in area CA1 of juvenile rat hippocampus; characterisation and sensitivity to novel mGlu receptor antagonists." Neuropharmacology **38**(10): 1577-1583.

Frank, C. A., J. Pielage and G. W. Davis (2009). "A presynaptic homeostatic signaling system composed of the Eph receptor, ephexin, Cdc42, and CaV2.1 calcium channels." Neuron **61**(4): 556-569.

Frerking, M. and P. Ohliger-Frerking (2002). "AMPA receptors and kainate receptors encode different features of afferent activity." J Neurosci **22**(17): 7434-7443.

Frerking, M., D. Schmitz, Q. Zhou, J. Johansen and R. A. Nicoll (2001). "Kainate receptors depress excitatory synaptic transmission at CA3-->CA1 synapses in the hippocampus via a direct presynaptic action." J Neurosci **21**(9): 2958-2966.

Fritz, J., A. Strehblow, A. Taschner, S. Schopoff, P. Pasierbek and M. F. Jantsch (2009). "RNA-regulated interaction of transportin-1 and exportin-5 with the double-stranded RNA-binding domain regulates nucleocytoplasmic shuttling of ADAR1." Mol Cell Biol **29**(6): 1487-1497.

Fritzell, K., L. D. Xu, J. Lagergren and M. Ohman (2017). "ADARs and editing: The role of A-to-I RNA modification in cancer progression." Semin Cell Dev Biol.

Fu, Y., X. Zhao, Z. Li, J. Wei and Y. Tian (2016). "Splicing variants of ADAR2 and ADAR2-mediated RNA editing in glioma." Oncol Lett **12**(2): 788-792.

Fukata, Y. and M. Fukata (2010). "Protein palmitoylation in neuronal development and synaptic plasticity." Nat Rev Neurosci **11**(3): 161-175.

Gainey, M. A., J. R. Hurvitz-Wolff, M. E. Lambo and G. G. Turrigiano (2009). "Synaptic scaling requires the GluR2 subunit of the AMPA receptor." J Neurosci **29**(20): 6479-6489.

Gainey, M. A., V. Tatavarty, M. Nahmani, H. Lin and G. G. Turrigiano (2015). "Activity-dependent synaptic GRIP1 accumulation drives synaptic scaling up in response to action potential blockade." Proc Natl Acad Sci U S A **112**(27): E3590-3599.

Gaisler-Salomon, I., E. Kravitz, Y. Feiler, M. Safran, A. Biegon, N. Amariglio and G. Rechavi (2014). "Hippocampus-specific deficiency in RNA editing of GluA2 in Alzheimer's disease." Neurobiol Aging **35**(8): 1785-1791.

Gallo, A., L. P. Keegan, G. M. Ring and M. A. O'Connell (2003). "An ADAR that edits transcripts encoding ion channel subunits functions as a dimer." Embo j **22**(13): 3421-3430.

Gallo, A. and F. Locatelli (2012). "ADARs: allies or enemies? The importance of A-to-I RNA editing in human disease: from cancer to HIV-1." Biol Rev Camb Philos Soc **87**(1): 95-110.

Gallyas, F., Jr., S. M. Ball and E. Molnar (2003). "Assembly and cell surface expression of KA-2 subunit-containing kainate receptors." J Neurochem **86**(6): 1414-1427.

Gan, Z., L. Zhao, L. Yang, P. Huang, F. Zhao, W. Li and Y. Liu (2006). "RNA editing by ADAR2 is metabolically regulated in pancreatic islets and beta-cells." J Biol Chem **281**(44): 33386-33394.

Garcia, E. P., S. Mehta, L. A. Blair, D. G. Wells, J. Shang, T. Fukushima, J. R. Fallon, C. C. Garner and J. Marshall (1998). "SAP90 binds and clusters kainate receptors causing incomplete desensitization." Neuron **21**(4): 727-739.

Gardner, S. M., K. Takamiya, J. Xia, J. G. Suh, R. Johnson, S. Yu and R. L. Huganir (2005). "Calcium-permeable AMPA receptor plasticity is mediated by subunit-specific interactions with PICK1 and NSF." Neuron **45**(6): 903-915.

Gerber, A., M. A. O'Connell and W. Keller (1997). "Two forms of human double-stranded RNA-specific editase 1 (hRED1) generated by the insertion of an Alu cassette." Rna **3**(5): 453-463.

Giese, K. P., N. B. Fedorov, R. K. Filipkowski and A. J. Silva (1998). "Autophosphorylation at Thr286 of the alpha calcium-calmodulin kinase II in LTP and learning." Science **279**(5352): 870-873.

Goel, A., B. Jiang, L. W. Xu, L. Song, A. Kirkwood and H. K. Lee (2006). "Cross-modal regulation of synaptic AMPA receptors in primary sensory cortices by visual experience." Nat Neurosci **9**(8): 1001-1003.

Gonzalez-Gonzalez, I. M. and J. M. Henley (2013). "Postsynaptic kainate receptor recycling and surface expression are regulated by metabotropic autoreceptor signalling." Traffic **14**(7): 810-822.

González-González, I. M., Konopacki, F.A., Rocca, D.L., Doherty, A.J., Jaafari, N., Wilkinson, K.A., Henley, J.M. (2012). "Kainate receptor trafficking." Wiley Interdisciplinary Reviews (WIRES): Membrane Transport and Signaling **1**(1): 31-44.

Grabauskas, G., B. Lancaster, V. O'Connor and H. V. Wheal (2007). "Protein kinase signalling requirements for metabotropic action of kainate receptors in rat CA1 pyramidal neurones." J Physiol **579**(Pt 2): 363-373.

Greger, I. H., L. Khatri, X. Kong and E. B. Ziff (2003). "AMPA receptor tetramerization is mediated by Q/R editing." Neuron **40**(4): 763-774.

Greger, I. H., L. Khatri and E. B. Ziff (2002). "RNA editing at arg607 controls AMPA receptor exit from the endoplasmic reticulum." Neuron **34**(5): 759-772.

Greger, I. H., E. B. Ziff and A. C. Penn (2007). "Molecular determinants of AMPA receptor subunit assembly." Trends Neurosci **30**(8): 407-416.

Griffiths, S., H. Scott, C. Glover, A. Bienemann, M. T. Ghorbel, J. Uney, M. W. Brown, E. C. Warburton and Z. I. Bashir (2008). "Expression of long-term depression underlies visual recognition memory." Neuron **58**(2): 186-194.

Grigorenko, E., S. Glazier, W. Bell, M. Tytell, E. Nosel, T. Pons and S. A. Deadwyler (1997). "Changes in glutamate receptor subunit composition in hippocampus and cortex in patients with refractory epilepsy." J Neurol Sci **153**(1): 35-45.

Grigorenko, E. V., W. L. Bell, S. Glazier, T. Pons and S. Deadwyler (1998). "Editing status at the Q/R site of the GluR2 and GluR6 glutamate receptor subunits in the surgically excised hippocampus of patients with refractory epilepsy." Neuroreport **9**(10): 2219-2224.

Grosenbaugh, D. K., B. M. Ross, P. Wagley and S. A. Zanelli (2018). "The Role of Kainate Receptors in the Pathophysiology of Hypoxia-Induced Seizures in the Neonatal Mouse." Sci Rep **8**(1): 7035.

Gurevich, I., M. T. Englander, M. Adlersberg, N. B. Siegal and C. Schmauss (2002). "Modulation of serotonin 2C receptor editing by sustained changes in serotonergic neurotransmission." J Neurosci **22**(24): 10529-10532.

Guzman, Y. F., K. Ramsey, J. R. Stolz, D. W. Craig, M. J. Huentelman, V. Narayanan and G. T. Swanson (2017). "A gain-of-function mutation in the GRIK2 gene causes neurodevelopmental deficits." Neurol Genet **3**(1): e129.

Hallengren, J., P. C. Chen and S. M. Wilson (2013). "Neuronal ubiquitin homeostasis." Cell Biochem Biophys **67**(1): 67-73.

Hamad, M. I., Z. L. Ma-Hogemeier, C. Riedel, C. Conrads, T. Veitinger, T. Habijan, J. N. Schulz, M. Krause, M. J. Wirth, M. Hollmann and P. Wahle (2011). "Cell class-specific regulation of neocortical dendrite and spine growth by AMPA receptor splice and editing variants." Development **138**(19): 4301-4313.

Hang, P. N., M. Tohda and K. Matsumoto (2008). "Developmental changes in expression and self-editing of adenosine deaminase type 2 pre-mRNA and mRNA in rat brain and cultured cortical neurons." Neurosci Res **61**(4): 398-403.

Hanley, J. G. (2014). "Subunit-specific trafficking mechanisms regulating the synaptic expression of Ca(2+)-permeable AMPA receptors." Semin Cell Dev Biol **27**: 14-22.

Hanus, C., H. Geptin, G. Tushev, S. Garg, B. Alvarez-Castelao, S. Sambandan, L. Kochen, A. S. Hafner, J. D. Langer and E. M. Schuman (2016). "Unconventional secretory processing diversifies neuronal ion channel properties." Elife **5**.

Harms, K. J., K. R. Tovar and A. M. Craig (2005). "Synapse-specific regulation of AMPA receptor subunit composition by activity." J Neurosci **25**(27): 6379-6388.

Hartner, J. C., C. Schmittwolf, A. Kispert, A. M. Muller, M. Higuchi and P. H. Seeburg (2004). "Liver disintegration in the mouse embryo caused by deficiency in the RNA-editing enzyme ADAR1." J Biol Chem **279**(6): 4894-4902.

Hartner, J. C., C. R. Walkley, J. Lu and S. H. Orkin (2009). "ADAR1 is essential for the maintenance of hematopoiesis and suppression of interferon signaling." Nat Immunol **10**(1): 109-115.

Hayashi, Y., S. H. Shi, J. A. Esteban, A. Piccini, J. C. Poncer and R. Malinow (2000). Driving AMPA receptors into synapses by LTP and CaMKII: requirement for GluR1 and PDZ domain interaction. Science. United States. **287:** 2262-2267.

Hayes, D. M., S. Braud, D. E. Hurtado, J. McCallum, S. Standley, J. T. Isaac and K. W. Roche (2003). "Trafficking and surface expression of the glutamate receptor subunit, KA2." Biochem Biophys Res Commun **310**(1): 8-13.

Heidelberger, R., C. Heinemann, E. Neher and G. Matthews (1994). "Calcium dependence of the rate of exocytosis in a synaptic terminal." Nature **371**(6497): 513-515.

Henley, J. M. and K. A. Wilkinson (2016). "Synaptic AMPA receptor composition in development, plasticity and disease." Nat Rev Neurosci **17**(6): 337-350.

Herb, A., N. Burnashev, P. Werner, B. Sakmann, W. Wisden and P. H. Seeburg (1992). "The KA-2 subunit of excitatory amino acid receptors shows widespread expression in brain and forms ion channels with distantly related subunits." Neuron **8**(4): 775-785.

Herb, A., M. Higuchi, R. Sprengel and P. H. Seeburg (1996). "Q/R site editing in kainate receptor GluR5 and GluR6 pre-mRNAs requires distant intronic sequences." Proc Natl Acad Sci U S A **93**(5): 1875-1880.

Herbert, A., J. Alfken, Y. G. Kim, I. S. Mian, K. Nishikura and A. Rich (1997). "A Z-DNA binding domain present in the human editing enzyme, double-stranded RNA adenosine deaminase." Proc Natl Acad Sci U S A **94**(16): 8421-8426.

Heshmati, M. (2009). "Cocaine-induced LTP in the ventral tegmental area: new insights into mechanism and time course illuminate the cellular substrates of addiction." J Neurophysiol **101**(6): 2735-2737.

Heuser, J. E., T. S. Reese, M. J. Dennis, Y. Jan, L. Jan and L. Evans (1979). "Synaptic vesicle exocytosis captured by quick freezing and correlated with quantal transmitter release." J Cell Biol **81**(2): 275-300.

Hideyama, T., T. Yamashita, H. Aizawa, S. Tsuji, A. Kakita, H. Takahashi and S. Kwak (2012). "Profound downregulation of the RNA editing enzyme ADAR2 in ALS spinal motor neurons." Neurobiol Dis **45**(3): 1121-1128.

Higuchi, M., S. Maas, F. N. Single, J. Hartner, A. Rozov, N. Burnashev, D. Feldmeyer, R. Sprengel and P. H. Seeburg (2000). "Point mutation in an AMPA receptor gene rescues lethality in mice deficient in the RNA-editing enzyme ADAR2." Nature **406**(6791): 78-81.

Higuchi, M., F. N. Single, M. Kohler, B. Sommer, R. Sprengel and P. H. Seeburg (1993). "RNA editing of AMPA receptor subunit GluR-B: a base-paired intron-exon structure determines position and efficiency." Cell **75**(7): 1361-1370.

Hilfiker, S., V. A. Pieribone, A. J. Czernik, H. T. Kao, G. J. Augustine and P. Greengard (1999). "Synapsins as regulators of neurotransmitter release." Philos Trans R Soc Lond B Biol Sci **354**(1381): 269-279.

Hirbec, H., J. C. Francis, S. E. Lauri, S. P. Braithwaite, F. Coussen, C. Mulle, K. K. Dev, V. Coutinho, G. Meyer, J. T. Isaac, G. L. Collingridge and J. M. Henley (2003). "Rapid and differential regulation of AMPA and kainate receptors at hippocampal mossy fibre synapses by PICK1 and GRIP." Neuron **37**(4): 625-638.

Hollmann, M., M. Hartley and S. Heinemann (1991). "Ca2+ permeability of KA-AMPA--gated glutamate receptor channels depends on subunit composition." Science **252**(5007): 851-853.

Hollmann, M. and S. Heinemann (1994). "Cloned glutamate receptors." Annu Rev Neurosci **17**: 31-108.

Holz RW, F. S. S. T. I. S. G., Agranoff BW, Albers RW, (1999). Basic Neurochemistry: Molecular, Cellular and Medical Aspects. Philadelphia, Lippincott-Raven

Huganir, R. L. and R. A. Nicoll (2013). "AMPARs and synaptic plasticity: the last 25 years." Neuron **80**(3): 704-717.

Hussain, N. K., G. H. Diering, J. Sole, V. Anggono and R. L. Huganir (2014). "Sorting Nexin 27 regulates basal and activity-dependent trafficking of AMPARs." Proc Natl Acad Sci U S A **111**(32): 11840-11845.

Ibata, K., Q. Sun and G. G. Turrigiano (2008). "Rapid synaptic scaling induced by changes in postsynaptic firing." Neuron **57**(6): 819-826.

IM, G.-G., K. FA, R. DL, D. AJ, J. N, W. KA and H. JM (2011). Kainate receptor trafficking. Wiley Interdisciplinary Reviews: Membrane Transport and Signaling. **1(1):** 31-44.

Inoue, H., H. Nojima and H. Okayama (1990). "High efficiency transformation of Escherichia coli with plasmids." Gene **96**(1): 23-28.

Ishiuchi, S., Y. Yoshida, K. Sugawara, M. Aihara, T. Ohtani, T. Watanabe, N. Saito, K. Tsuzuki, H. Okado, A. Miwa, Y. Nakazato and S. Ozawa (2007). "Ca2+-permeable AMPA receptors regulate growth of human glioblastoma via Akt activation." J Neurosci **27**(30): 7987-8001.

Jaafari, N., J. M. Henley and J. G. Hanley (2012). "PICK1 mediates transient synaptic expression of GluA2-lacking AMPA receptors during glycine-induced AMPA receptor trafficking." J Neurosci **32**(34): 11618-11630.

Jackson, A. C. and R. A. Nicoll (2011). "The expanding social network of ionotropic glutamate receptors: TARPs and other transmembrane auxiliary subunits." Neuron **70**(2): 178-199.

Jacobs, M. M., R. L. Fogg, R. B. Emeson and G. D. Stanwood (2009). "ADAR1 and ADAR2 expression and editing activity during forebrain development." Dev Neurosci **31**(3): 223-237.

Jang, S. S. and H. J. Chung (2016). "Emerging Link between Alzheimer's Disease and Homeostatic Synaptic Plasticity." Neural Plast **2016**: 7969272.

Jaskolski, F., F. Coussen, N. Nagarajan, E. Normand, C. Rosenmund and C. Mulle (2004). "Subunit composition and alternative splicing regulate membrane delivery of kainate receptors." J Neurosci **24**(10): 2506-2515.

Jiang, L., D. Kang and J. Kang (2015). "Potentiation of tonic GABAergic inhibition by activation of postsynaptic kainate receptors." Neuroscience **298**: 448-454.

Jiang, L., J. Xu, M. Nedergaard and J. Kang (2001). "A kainate receptor increases the efficacy of GABAergic synapses." Neuron **30**(2): 503-513.

Jin, Y., W. Zhang and Q. Li (2009). "Origins and evolution of ADAR-mediated RNA editing." IUBMB Life **61**(6): 572-578.

Jo, J., S. Heon, M. J. Kim, G. H. Son, Y. Park, J. M. Henley, J. L. Weiss, M. Sheng, G. L. Collingridge and K. Cho (2008). "Metabotropic glutamate receptor-mediated LTD involves two interacting Ca(2+) sensors, NCS-1 and PICK1." Neuron **60**(6): 1095-1111.

Johnston, G. A. (2013). "Advantages of an antagonist: bicuculline and other GABA antagonists." Br J Pharmacol **169**(2): 328-336.

Johnston, M. V. (1996). "Developmental aspects of epileptogenesis." Epilepsia **37 Suppl 1**: S2-9.

Ju, W., W. Morishita, J. Tsui, G. Gaietta, T. J. Deerinck, S. R. Adams, C. C. Garner, R. Y. Tsien, M. H. Ellisman and R. C. Malenka (2004). "Activity-dependent regulation of dendritic synthesis and trafficking of AMPA receptors." Nat Neurosci **7**(3): 244-253.

Jurado, S., V. Biou and R. C. Malenka (2010). "A calcineurin/AKAP complex is required for NMDA receptor-dependent long-term depression." Nat Neurosci **13**(9): 1053-1055.

Kamboj, S. K., G. T. Swanson and S. G. Cull-Candy (1995). "Intracellular spermine confers rectification on rat calcium-permeable AMPA and kainate receptors." J Physiol **486 (Pt 2)**: 297-303.

Kamiya, H. and S. Ozawa (1998). "Kainate receptor-mediated inhibition of presynaptic Ca2+ influx and EPSP in area CA1 of the rat hippocampus." J Physiol **509 (Pt 3)**: 833-845.

Kamiya, H. and S. Ozawa (2000). "Kainate receptor-mediated presynaptic inhibition at the mouse hippocampal mossy fibre synapse." J Physiol **523 Pt 3**: 653-665.

Kandel, E., Schwartz, J. & Jessell. T. (2000). Principles of Neural Science. New York, McGraw-Hill Professional.

Kask, K., D. Zamanillo, A. Rozov, N. Burnashev, R. Sprengel and P. H. Seeburg (1998). "The AMPA receptor subunit GluR-B in its Q/R site-unedited form is not essential for brain development and function." Proc Natl Acad Sci U S A **95**(23): 13777-13782.

Kauer, J. A., R. C. Malenka and R. A. Nicoll (1988). "NMDA application potentiates synaptic transmission in the hippocampus." Nature **334**(6179): 250-252.

Kawahara, Y., K. Ito, H. Sun, H. Aizawa, I. Kanazawa and S. Kwak (2004). "Glutamate receptors: RNA editing and death of motor neurons." Nature **427**(6977): 801.

Khermesh, K., A. M. D'Erchia, M. Barak, A. Annese, C. Wachtel, E. Y. Levanon, E. Picardi and E. Eisenberg (2016). "Reduced levels of protein recoding by A-to-I RNA editing in Alzheimer's disease." Rna **22**(2): 290-302.

Kidd, F. L., U. Coumis, G. L. Collingridge, J. W. Crabtree and J. T. Isaac (2002). "A presynaptic kainate receptor is involved in regulating the dynamic properties of thalamocortical synapses during development." Neuron **34**(4): 635-646.

Kidd, F. L. and J. T. Isaac (1999). "Developmental and activity-dependent regulation of kainate receptors at thalamocortical synapses." Nature **400**(6744): 569-573.

Kim, C. H., H. J. Chung, H. K. Lee and R. L. Huganir (2001). "Interaction of the AMPA receptor subunit GluR2/3 with PDZ domains regulates hippocampal long-term depression." Proc Natl Acad Sci U S A **98**(20): 11725-11730.

Kim, J. Y., Y. S. Kang, J. W. Lee, H. J. Kim, Y. H. Ahn, H. Park, Y. G. Ko and S. Kim (2002). "p38 is essential for the assembly and stability of macromolecular tRNA synthetase complex: implications for its physiological significance." Proc Natl Acad Sci U S A **99**(12): 7912-7916.

Kim, M. J., B. J. Park, Y. S. Kang, H. J. Kim, J. H. Park, J. W. Kang, S. W. Lee, J. M. Han, H. W. Lee and S. Kim (2003). "Downregulation of FUSE-binding protein and c-myc by tRNA synthetase cofactor p38 is required for lung cell differentiation." Nat Genet **34**(3): 330-336.

Kim, U., Y. Wang, T. Sanford, Y. Zeng and K. Nishikura (1994). "Molecular cloning of cDNA for double-stranded RNA adenosine deaminase, a candidate enzyme for nuclear RNA editing." Proc Natl Acad Sci U S A **91**(24): 11457-11461.

Konopacki, F. A., N. Jaafari, D. L. Rocca, K. A. Wilkinson, S. Chamberlain, P. Rubin, S. Kantamneni, J. R. Mellor and J. M. Henley (2011). "Agonist-induced PKC phosphorylation regulates GluK2 SUMOylation and kainate receptor endocytosis." Proc Natl Acad Sci U S A **108**(49): 19772-19777.

Kortenbruck, G., E. Berger, E. J. Speckmann and U. Musshoff (2001). "RNA editing at the Q/R site for the glutamate receptor subunits GLUR2, GLUR5, and GLUR6 in hippocampus and temporal cortex from epileptic patients." Neurobiol Dis **8**(3): 459-468.

Kumar, J., P. Schuck and M. L. Mayer (2011). "Structure and assembly mechanism for heteromeric kainate receptors." Neuron **71**(2): 319-331.

Kuner, T., C. Beck, B. Sakmann and P. H. Seeburg (2001). "Channel-lining residues of the AMPA receptor M2 segment: structural environment of the Q/R site and identification of the selectivity filter." J Neurosci **21**(12): 4162-4172.

Kuusinen, A., R. Abele, D. R. Madden and K. Keinanen (1999). "Oligomerization and ligand-binding properties of the ectodomain of the

alpha-amino-3-hydroxy-5-methyl-4-isoxazole propionic acid receptor subunit GluRD." J Biol Chem **274**(41): 28937-28943.

Köhler, M., N. Burnashev, B. Sakmann and P. H. Seeburg (1993). "Determinants of Ca2+ permeability in both TM1 and TM2 of high affinity kainate receptor channels: diversity by RNA editing." Neuron **10**(3): 491-500.

Lafontaine, D. L. and D. Tollervey (2000). "Synthesis and assembly of the box C+D small nucleolar RNPs." Mol Cell Biol **20**(8): 2650-2659.

Lai, F., C. X. Chen, K. C. Carter and K. Nishikura (1997). "Editing of glutamate receptor B subunit ion channel RNAs by four alternatively spliced DRADA2 double-stranded RNA adenosine deaminases." Mol Cell Biol **17**(5): 2413-2424.

Lambolez, B., N. Ropert, D. Perrais, J. Rossier and S. Hestrin (1996). "Correlation between kinetics and RNA splicing of alpha-amino-3-hydroxy-5-methylisoxazole-4-propionic acid receptors in neocortical neurons." Proc Natl Acad Sci U S A **93**(5): 1797-1802.

Lanore, F., V. F. Labrousse, Z. Szabo, E. Normand, C. Blanchet and C. Mulle (2012). "Deficits in morphofunctional maturation of hippocampal mossy fiber synapses in a mouse model of intellectual disability." J Neurosci **32**(49): 17882-17893.

Laurencikiene, J., A. M. Kallman, N. Fong, D. L. Bentley and M. Ohman (2006). "RNA editing and alternative splicing: the importance of co-transcriptional coordination." EMBO Rep **7**(3): 303-307.

Lauri, S. E., Z. A. Bortolotto, D. Bleakman, P. L. Ornstein, D. Lodge, J. T. Isaac and G. L. Collingridge (2001). "A critical role of a facilitatory presynaptic kainate receptor in mossy fiber LTP." Neuron **32**(4): 697-709.

Lauri, S. E., Z. A. Bortolotto, R. Nistico, D. Bleakman, P. L. Ornstein, D. Lodge, J. T. Isaac and G. L. Collingridge (2003). "A role for Ca2+ stores in kainate receptor-dependent synaptic facilitation and LTP at mossy fiber synapses in the hippocampus." Neuron **39**(2): 327-341.

Lauri, S. E., M. Segerstrale, A. Vesikansa, F. Maingret, C. Mulle, G. L. Collingridge, J. T. Isaac and T. Taira (2005). "Endogenous activation of kainate receptors regulates glutamate release and network activity in the developing hippocampus." J Neurosci **25**(18): 4473-4484.

Lauri, S. E., A. Vesikansa, M. Segerstrale, G. L. Collingridge, J. T. Isaac and T. Taira (2006). "Functional maturation of CA1 synapses involves activity-dependent loss of tonic kainate receptor-mediated inhibition of glutamate release." Neuron **50**(3): 415-429.

Lee, H. K., K. Kameyama, R. L. Huganir and M. F. Bear (1998). "NMDA induces long-term synaptic depression and dephosphorylation of the GluR1 subunit of AMPA receptors in hippocampus." Neuron **21**(5): 1151-1162.

Lee, H. K., K. Takamiya, K. He, L. Song and R. L. Huganir (2010). "Specific roles of AMPA receptor subunit GluR1 (GluA1) phosphorylation sites in regulating synaptic plasticity in the CA1 region of hippocampus." J Neurophysiol **103**(1): 479-489.

Lee, S., G. Yang, Y. Yong, Y. Liu, L. Zhao, J. Xu, X. Zhang, Y. Wan, C. Feng, Z. Fan, Y. Liu, J. Luo and Z. J. Ke (2010). "ADAR2-dependent RNA editing of GluR2 is involved in thiamine deficiency-induced alteration of calcium dynamics." Mol Neurodegener **5**: 54.

Lee, S. H., L. Liu, Y. T. Wang and M. Sheng (2002). "Clathrin adaptor AP2 and NSF interact with overlapping sites of GluR2 and play distinct roles in AMPA receptor trafficking and hippocampal LTD." Neuron **36**(4): 661-674.

Lee, S. J., Y. Escobedo-Lozoya, E. M. Szatmari and R. Yasuda (2009). "Activation of CaMKII in single dendritic spines during long-term potentiation." Nature **458**(7236): 299-304.

Lehmann, K. A. and B. L. Bass (2000). "Double-stranded RNA adenosine deaminases ADAR1 and ADAR2 have overlapping specificities." Biochemistry **39**(42): 12875-12884.

Leonoudakis, D., P. Zhao and E. C. Beattie (2008). "Rapid tumor necrosis factor alpha-induced exocytosis of glutamate receptor 2-lacking AMPA receptors to extrasynaptic plasma membrane potentiates excitotoxicity." J Neurosci **28**(9): 2119-2130.

Lerma, J. and J. M. Marques (2013). "Kainate receptors in health and disease." Neuron **80**(2): 292-311.

Lerma, J., M. Morales, M. A. Vicente and O. Herreras (1997). "Glutamate receptors of the kainate type and synaptic transmission." Trends Neurosci **20**(1): 9-12.

Lerma, J., A. V. Paternain, A. Rodriguez-Moreno and J. C. Lopez-Garcia (2001). "Molecular physiology of kainate receptors." Physiol Rev **81**(3): 971-998.

Leslie, K. R., S. B. Nelson and G. G. Turrigiano (2001). "Postsynaptic depolarization scales quantal amplitude in cortical pyramidal neurons." J Neurosci **21**(19): Rc170.

Li, I. C., Y. C. Chen, Y. Y. Wang, B. W. Tzeng, C. W. Ou, Y. Y. Lau, K. M. Wu, T. M. Chan, W. H. Lin, S. P. Hwang and W. Y. Chow (2014). "Zebrafish Adar2 Edits the Q/R site of AMPA receptor Subunit gria2alpha transcript to ensure normal development of nervous system and cranial neural crest cells." PLoS One **9**(5): e97133.

Li, J. B., E. Y. Levanon, J. K. Yoon, J. Aach, B. Xie, E. Leproust, K. Zhang, Y. Gao and G. M. Church (2009). "Genome-wide identification of human RNA editing sites by parallel DNA capturing and sequencing." Science **324**(5931): 1210-1213.

Li, Z., Y. Tian, N. Tian, X. Zhao, C. Du, L. Han and H. Zhang (2015). "Aberrant alternative splicing pattern of ADAR2 downregulates adenosine-to-inosine editing in glioma." Oncol Rep **33**(6): 2845-2852.

Lisman, J., R. Yasuda and S. Raghavachari (2012). "Mechanisms of CaMKII action in long-term potentiation." Nat Rev Neurosci **13**(3): 169-182.

Liu, Y., M. Lei and C. E. Samuel (2000). "Chimeric double-stranded RNA-specific adenosine deaminase ADAR1 proteins reveal functional selectivity of

double-stranded RNA-binding domains from ADAR1 and protein kinase PKR." Proc Natl Acad Sci U S A **97**(23): 12541-12546.

Llinas, R., I. Z. Steinberg and K. Walton (1981). "Relationship between presynaptic calcium current and postsynaptic potential in squid giant synapse." Biophys J **33**(3): 323-351.

Lodish H, B. A., Zipursky SL, et al. (2000). Molecular Cell Biology. New York.

Lomeli, H., J. Mosbacher, T. Melcher, T. Hoger, J. R. Geiger, T. Kuner, H. Monyer, M. Higuchi, A. Bach and P. H. Seeburg (1994). "Control of kinetic properties of AMPA receptor channels by nuclear RNA editing." Science **266**(5191): 1709-1713.

Lomeli, H., R. Sprengel, D. J. Laurie, G. Kohr, A. Herb, P. H. Seeburg and W. Wisden (1993). "The rat delta-1 and delta-2 subunits extend the excitatory amino acid receptor family." FEBS Lett **315**(3): 318-322.

Loo, L. S., N. Tang, M. Al-Haddawi, G. S. Dawe and W. Hong (2014). "A role for sorting nexin 27 in AMPA receptor trafficking." Nat Commun **5**: 3176.

Lu, K. P., S. D. Hanes and T. Hunter (1996). "A human peptidyl-prolyl isomerase essential for regulation of mitosis." Nature **380**(6574): 544-547.

Lu, K. P. and X. Z. Zhou (2007). "The prolyl isomerase PIN1: a pivotal new twist in phosphorylation signalling and disease." Nat Rev Mol Cell Biol **8**(11): 904-916.

Lu, P. J., X. Z. Zhou, M. Shen and K. P. Lu (1999). "Function of WW domains as phosphoserine- or phosphothreonine-binding modules." Science **283**(5406): 1325-1328.

Lu, W., H. Man, W. Ju, W. S. Trimble, J. F. MacDonald and Y. T. Wang (2001). "Activation of synaptic NMDA receptors induces membrane insertion of new AMPA receptors and LTP in cultured hippocampal neurons." Neuron **29**(1): 243-254.

Lu, W., Y. Shi, A. C. Jackson, K. Bjorgan, M. J. During, R. Sprengel, P. H. Seeburg and R. A. Nicoll (2009). "Subunit composition of synaptic AMPA receptors revealed by a single-cell genetic approach." Neuron **62**(2): 254-268.

Luscher, C. and K. M. Huber (2010). "Group 1 mGluR-dependent synaptic long-term depression: mechanisms and implications for circuitry and disease." Neuron **65**(4): 445-459.

Luthi, A., R. Chittajallu, F. Duprat, M. J. Palmer, T. A. Benke, F. L. Kidd, J. M. Henley, J. T. Isaac and G. L. Collingridge (1999). "Hippocampal LTD expression involves a pool of AMPARs regulated by the NSF-GluR2 interaction." Neuron **24**(2): 389-399.

Ma-Hogemeier, Z. L., C. Korber, M. Werner, D. Racine, E. Muth-Kohne, D. Tapken and M. Hollmann (2010). "Oligomerization in the endoplasmic reticulum and intracellular trafficking of kainate receptors are subunit-dependent but not editing-dependent." J Neurochem **113**(6): 1403-1415.

Maas, S. and W. M. Gommans (2009). "Identification of a selective nuclear import signal in adenosine deaminases acting on RNA." Nucleic Acids Res **37**(17): 5822-5829.

Maas, S. and W. M. Gommans (2009). "Novel exon of mammalian ADAR2 extends open reading frame." PLoS One **4**(1): e4225.

Macbeth, M. R., H. L. Schubert, A. P. Vandemark, A. T. Lingam, C. P. Hill and B. L. Bass (2005). "Inositol hexakisphosphate is bound in the ADAR2 core and required for RNA editing." Science **309**(5740): 1534-1539.

Mahadevan, V., J. C. Pressey, B. A. Acton, P. Uvarov, M. Y. Huang, J. Chevrier, A. Puchalski, C. M. Li, E. A. Ivakine, M. S. Airaksinen, E. Delpire, R. R. McInnes and M. A. Woodin (2014). "Kainate receptors coexist in a functional complex with KCC2 and regulate chloride homeostasis in hippocampal neurons." Cell Rep **7**(6): 1762-1770.

Mahajan, S. S., K. H. Thai, K. Chen and E. Ziff (2011). "Exposure of neurons to excitotoxic levels of glutamate induces cleavage of the RNA editing enzyme, adenosine deaminase acting on RNA 2, and loss of GLUR2 editing." Neuroscience **189**: 305-315.

Makino, H. and R. Malinow (2009). "AMPA receptor incorporation into synapses during LTP: the role of lateral movement and exocytosis." Neuron **64**(3): 381-390.

Malenka, R. C. and M. F. Bear (2004). "LTP and LTD: an embarrassment of riches." Neuron **44**(1): 5-21.

Malenka, R. C. and R. A. Nicoll (1993). "NMDA-receptor-dependent synaptic plasticity: multiple forms and mechanisms." Trends Neurosci **16**(12): 521-527.

Man, H. Y. (2011). "GluA2-lacking, calcium-permeable AMPA receptors--inducers of plasticity?" Curr Opin Neurobiol **21**(2): 291-298.

Manabe, T., D. J. Wyllie, D. J. Perkel and R. A. Nicoll (1993). "Modulation of synaptic transmission and long-term potentiation: effects on paired pulse facilitation and EPSC variance in the CA1 region of the hippocampus." J Neurophysiol **70**(4): 1451-1459.

Mansour, M., N. Nagarajan, R. B. Nehring, J. D. Clements and C. Rosenmund (2001). "Heteromeric AMPA receptors assemble with a preferred subunit stoichiometry and spatial arrangement." Neuron **32**(5): 841-853.

Maraschi, A., A. Ciammola, A. Folci, F. Sassone, G. Ronzitti, G. Cappelletti, V. Silani, S. Sato, N. Hattori, M. Mazzanti, E. Chieregatti, C. Mulle, M. Passafaro and J. Sassone (2014). "Parkin regulates kainate receptors by interacting with the GluK2 subunit." Nat Commun **5**: 5182.

Marcucci, R., J. Brindle, S. Paro, A. Casadio, S. Hempel, N. Morrice, A. Bisso, L. P. Keegan, G. Del Sal and M. A. O'Connell (2011). "Pin1 and WWP2 regulate GluR2 Q/R site RNA editing by ADAR2 with opposing effects." EMBO J **30**(20): 4211-4222.

Martin, S., T. Bouschet, E. L. Jenkins, A. Nishimune and J. M. Henley (2008). "Bidirectional regulation of kainate receptor surface expression in hippocampal neurons." J Biol Chem **283**(52): 36435-36440.

Martin, S. and J. M. Henley (2004). "Activity-dependent endocytic sorting of kainate receptors to recycling or degradation pathways." Embo j **23**(24): 4749-4759.

Martin, S., A. Nishimune, J. R. Mellor and J. M. Henley (2007). "SUMOylation regulates kainate-receptor-mediated synaptic transmission." Nature **447**(7142): 321-325.

Matsuda, K. (2017). "Synapse organization and modulation via C1q family proteins and their receptors in the central nervous system." Neurosci Res **116**: 46-53.

Matsuda, K., T. Budisantoso, N. Mitakidis, Y. Sugaya, E. Miura, W. Kakegawa, M. Yamasaki, K. Konno, M. Uchigashima, M. Abe, I. Watanabe, M. Kano, M. Watanabe, K. Sakimura, A. R. Aricescu and M. Yuzaki (2016). "Transsynaptic Modulation of Kainate Receptor Functions by C1q-like Proteins." Neuron **90**(4): 752-767.

Matsuda, K., E. Miura, T. Miyazaki, W. Kakegawa, K. Emi, S. Narumi, Y. Fukazawa, A. Ito-Ishida, T. Kondo, R. Shigemoto, M. Watanabe and M. Yuzaki (2010). "Cbln1 is a ligand for an orphan glutamate receptor delta2, a bidirectional synapse organizer." Science **328**(5976): 363-368.

Matthews, M. M., J. M. Thomas, Y. Zheng, K. Tran, K. J. Phelps, A. I. Scott, J. Havel, A. J. Fisher and P. A. Beal (2016). "Structures of human ADAR2 bound to dsRNA reveal base-flipping mechanism and basis for site selectivity." Nat Struct Mol Biol **23**(5): 426-433.

Maurya, D. K., C. S. Sundaram and P. Bhargava (2009). "Proteome profile of the mature rat olfactory bulb." Proteomics **9**(9): 2593-2599.

Mayer, M. L., G. L. Westbrook and P. B. Guthrie (1984). "Voltage-dependent block by Mg2+ of NMDA responses in spinal cord neurones." Nature **309**(5965): 261-263.

Megias, M., Z. Emri, T. F. Freund and A. I. Gulyas (2001). "Total number and distribution of inhibitory and excitatory synapses on hippocampal CA1 pyramidal cells." Neuroscience **102**(3): 527-540.

Melcher, T., S. Maas, A. Herb, R. Sprengel, M. Higuchi and P. H. Seeburg (1996). "RED2, a brain-specific member of the RNA-specific adenosine deaminase family." J Biol Chem **271**(50): 31795-31798.

Melcher, T., S. Maas, A. Herb, R. Sprengel, P. H. Seeburg and M. Higuchi (1996). "A mammalian RNA editing enzyme." Nature **379**(6564): 460-464.

Mellor, J. and R. A. Nicoll (2001). "Hippocampal mossy fiber LTP is independent of postsynaptic calcium." Nat Neurosci **4**(2): 125-126.

Melyan, Z., B. Lancaster and H. V. Wheal (2004). "Metabotropic regulation of intrinsic excitability by synaptic activation of kainate receptors." J Neurosci **24**(19): 4530-4534.

Melyan, Z., H. V. Wheal and B. Lancaster (2002). "Metabotropic-mediated kainate receptor regulation of IsAHP and excitability in pyramidal cells." Neuron **34**(1): 107-114.

Micheau, J., A. Vimeney, E. Normand, C. Mulle and G. Riedel (2014). "Impaired hippocampus-dependent spatial flexibility and sociability represent autism-like phenotypes in GluK2 mice." Hippocampus **24**(9): 1059-1069.

Mladenova, D., G. Barry, L. M. Konen, S. S. Pineda, B. Guennewig, L. Avesson, R. Zinn, N. Schonrock, M. Bitar, N. Jonkhout, L. Crumlish, D. C. Kaczorowski, A. Gong, M. Pinese, G. R. Franco, C. R. Walkley, B. Vissel and J. S. Mattick (2018). "Adar3 Is Involved in Learning and Memory in Mice." Front Neurosci **12**: 243.

Modebadze, T., N. H. Morgan, I. A. Peres, R. D. Hadid, N. Amada, C. Hill, C. Williams, I. M. Stanford, C. M. Morris, R. S. Jones, B. J. Whalley and G. L. Woodhall (2016). "A Low Mortality, High Morbidity Reduced Intensity Status Epilepticus (RISE) Model of Epilepsy and Epileptogenesis in the Rat." PLoS One **11**(2): e0147265.

More, J. C., R. Nistico, N. P. Dolman, V. R. Clarke, A. J. Alt, A. M. Ogden, F. P. Buelens, H. M. Troop, E. E. Kelland, F. Pilato, D. Bleakman, Z. A. Bortolotto, G. L. Collingridge and D. E. Jane (2004). "Characterisation of UBP296: a novel, potent and selective kainate receptor antagonist." Neuropharmacology **47**(1): 46-64.

Morris, R. G. (1999). "D.O. Hebb: The Organization of Behavior, Wiley: New York; 1949." Brain Res Bull **50**(5-6): 437.

Morris, R. G., E. Anderson, G. S. Lynch and M. Baudry (1986). "Selective impairment of learning and blockade of long-term potentiation by an N-methyl-D-aspartate receptor antagonist, AP5." Nature **319**(6056): 774-776.

Mozrzymas, J. W. (2008). "Electrophysiological description of mechanisms determining synaptic transmission and its modulation." Acta Neurobiol Exp (Wars) **68**(2): 256-263.

Mu, Y., T. Otsuka, A. C. Horton, D. B. Scott and M. D. Ehlers (2003). "Activity-dependent mRNA splicing controls ER export and synaptic delivery of NMDA receptors." Neuron **40**(3): 581-594.

Mulkey, R. M., S. Endo, S. Shenolikar and R. C. Malenka (1994). "Involvement of a calcineurin/inhibitor-1 phosphatase cascade in hippocampal long-term depression." Nature **369**(6480): 486-488.

Mulkey, R. M., C. E. Herron and R. C. Malenka (1993). "An essential role for protein phosphatases in hippocampal long-term depression." Science **261**(5124): 1051-1055.

Mulle, C., A. Sailer, I. Perez-Otano, H. Dickinson-Anson, P. E. Castillo, I. Bureau, C. Maron, F. H. Gage, J. R. Mann, B. Bettler and S. F. Heinemann (1998). "Altered synaptic physiology and reduced susceptibility to kainate-induced seizures in GluR6-deficient mice." Nature **392**(6676): 601-605.

Nabavi, S., R. Fox, C. D. Proulx, J. Y. Lin, R. Y. Tsien and R. Malinow (2014). "Engineering a memory with LTD and LTP." Nature **511**(7509): 348-352.

Napoli, I., V. Mercaldo, P. P. Boyl, B. Eleuteri, F. Zalfa, S. De Rubeis, D. Di Marino, E. Mohr, M. Massimi, M. Falconi, W. Witke, M. Costa-Mattioli, N. Sonenberg, T. Achsel and C. Bagni (2008). "The fragile X syndrome protein represses activity-dependent translation through CYFIP1, a new 4E-BP." Cell **134**(6): 1042-1054.

Narahashi, T. (2008). "Tetrodotoxin: a brief history." Proc Jpn Acad Ser B Phys Biol Sci **84**(5): 147-154.

Nasu-Nishimura, Y., H. Jaffe, J. T. Isaac and K. W. Roche (2010). "Differential regulation of kainate receptor trafficking by phosphorylation of distinct sites on GluR6." J Biol Chem **285**(4): 2847-2856.

Naur, P., K. B. Hansen, A. S. Kristensen, S. M. Dravid, D. S. Pickering, L. Olsen, B. Vestergaard, J. Egebjerg, M. Gajhede, S. F. Traynelis and J. S. Kastrup (2007). "Ionotropic glutamate-like receptor delta2 binds D-serine and glycine." Proc Natl Acad Sci U S A **104**(35): 14116-14121.

Negrete-Diaz, J. V., T. S. Sihra, J. M. Delgado-Garcia and A. Rodriguez-Moreno (2006). "Kainate receptor-mediated inhibition of glutamate release involves protein kinase A in the mouse hippocampus." J Neurophysiol **96**(4): 1829-1837.

Negrete-Diaz, J. V., T. S. Sihra, J. M. Delgado-Garcia and A. Rodriguez-Moreno (2007). "Kainate receptor-mediated presynaptic inhibition converges with presynaptic inhibition mediated by Group II mGluRs and long-term depression at the hippocampal mossy fiber-CA3 synapse." J Neural Transm (Vienna) **114**(11): 1425-1431.

Nishikura, K. (2016). "A-to-I editing of coding and non-coding RNAs by ADARs." Nat Rev Mol Cell Biol **17**(2): 83-96.

Nishimune, A., J. T. Isaac, E. Molnar, J. Noel, S. R. Nash, M. Tagaya, G. L. Collingridge, S. Nakanishi and J. M. Henley (1998). "NSF binding to GluR2 regulates synaptic transmission." Neuron **21**(1): 87-97.

Niswender, C. M. and P. J. Conn (2010). "Metabotropic glutamate receptors: physiology, pharmacology, and disease." Annu Rev Pharmacol Toxicol **50**: 295-322.

Noritake, J., Y. Fukata, T. Iwanaga, N. Hosomi, R. Tsutsumi, N. Matsuda, H. Tani, H. Iwanari, Y. Mochizuki, T. Kodama, Y. Matsuura, D. S. Bredt, T. Hamakubo and M. Fukata (2009). "Mobile DHHC palmitoylating enzyme mediates activity-sensitive synaptic targeting of PSD-95." J Cell Biol **186**(1): 147-160.

O'Brien, R. J., S. Kamboj, M. D. Ehlers, K. R. Rosen, G. D. Fischbach and R. L. Huganir (1998). "Activity-dependent modulation of synaptic AMPA receptor accumulation." Neuron **21**(5): 1067-1078.

Oakes, E., A. Anderson, A. Cohen-Gadol and H. A. Hundley (2017). "Adenosine Deaminase That Acts on RNA 3 (ADAR3) Binding to Glutamate Receptor Subunit B Pre-mRNA Inhibits RNA Editing in Glioblastoma." J Biol Chem **292**(10): 4326-4335.

Okuda, T., L. M. Yu, L. A. Cingolani, R. Kemler and Y. Goda (2007). "beta-Catenin regulates excitatory postsynaptic strength at hippocampal synapses." Proc Natl Acad Sci U S A **104**(33): 13479-13484.

Oliet, S. H., R. C. Malenka and R. A. Nicoll (1997). "Two distinct forms of long-term depression coexist in CA1 hippocampal pyramidal cells." Neuron **18**(6): 969-982.

Olins, A. L., G. Rhodes, D. B. Welch, M. Zwerger and D. E. Olins (2010). "Lamin B receptor: multi-tasking at the nuclear envelope." Nucleus **1**(1): 53-70.

Opazo, P., S. Labrecque, C. M. Tigaret, A. Frouin, P. W. Wiseman, P. De Koninck and D. Choquet (2010). "CaMKII triggers the diffusional trapping of surface AMPARs through phosphorylation of stargazin." Neuron **67**(2): 239-252.

Orlandi, C., L. La Via, D. Bonini, C. Mora, I. Russo, A. Barbon and S. Barlati (2011). "AMPA receptor regulation at the mRNA and protein level in rat primary cortical cultures." PLoS One **6**(9): e25350.

Ota, H., M. Sakurai, R. Gupta, L. Valente, B. E. Wulff, K. Ariyoshi, H. Iizasa, R. V. Davuluri and K. Nishikura (2013). "ADAR1 forms a complex with Dicer to promote microRNA processing and RNA-induced gene silencing." Cell **153**(3): 575-589.

Pachernegg, S., Y. Munster, E. Muth-Kohne, G. Fuhrmann and M. Hollmann (2015). "GluA2 is rapidly edited at the Q/R site during neural differentiation in vitro." Front Cell Neurosci **9**: 69.

Pahl, S., D. Tapken, S. C. Haering and M. Hollmann (2014). "Trafficking of kainate receptors." Membranes (Basel) **4**(3): 565-595.

Palacios-Filardo, J., M. I. Aller and J. Lerma (2016). "Synaptic Targeting of Kainate Receptors." Cereb Cortex **26**(4): 1464-1472.

Palmer, M. J., A. J. Irving, G. R. Seabrook, D. E. Jane and G. L. Collingridge (1997). "The group I mGlu receptor agonist DHPG induces a novel form of LTD in the CA1 region of the hippocampus." Neuropharmacology **36**(11-12): 1517-1532.

Partin, K. M. and M. L. Mayer (1996). "Negative allosteric modulation of wild-type and mutant AMPA receptors by GYKI 53655." Mol Pharmacol **49**(1): 142-148.

Paschen, W. and B. Djuricic (1995). "Regional differences in the extent of RNA editing of the glutamate receptor subunits GluR2 and GluR6 in rat brain." J Neurosci Methods **56**(1): 21-29.

Paschen, W., J. Schmitt, C. Gissel and E. Dux (1997). "Developmental changes of RNA editing of glutamate receptor subunits GluR5 and GluR6: in vivo versus in vitro." Brain Res Dev Brain Res **98**(2): 271-280.

Paschen, W., J. Schmitt and A. Uto (1996). "RNA editing of glutamate receptor subunits GluR2, GluR5 and GluR6 in transient cerebral ischemia in the rat." J Cereb Blood Flow Metab **16**(4): 548-556.

Paternain, A. V., M. T. Herrera, M. A. Nieto and J. Lerma (2000). "GluR5 and GluR6 kainate receptor subunits coexist in hippocampal neurons and coassemble to form functional receptors." J Neurosci **20**(1): 196-205.

Patterson, J. B. and C. E. Samuel (1995). "Expression and regulation by interferon of a double-stranded-RNA-specific adenosine deaminase from human cells: evidence for two forms of the deaminase." Mol Cell Biol **15**(10): 5376-5388.

Patterson, M. and R. Yasuda (2011). "Signalling pathways underlying structural plasticity of dendritic spines." Br J Pharmacol **163**(8): 1626-1638.

Pei, W., Z. Huang, C. Wang, Y. Han, J. S. Park and L. Niu (2009). "Flip and flop: a molecular determinant for AMPA receptor channel opening." Biochemistry **48**(17): 3767-3777.

Pelkey, K. A., E. Barksdale, M. T. Craig, X. Yuan, M. Sukumaran, G. A. Vargish, R. M. Mitchell, M. S. Wyeth, R. S. Petralia, R. Chittajallu, R. M. Karlsson, H. A. Cameron, Y. Murata, M. T. Colonnese, P. F. Worley and C. J. McBain (2015). "Pentraxins coordinate excitatory synapse maturation and circuit integration of parvalbumin interneurons." Neuron **85**(6): 1257-1272.

Peng, P. L., X. Zhong, W. Tu, M. M. Soundarapandian, P. Molner, D. Zhu, L. Lau, S. Liu, F. Liu and Y. Lu (2006). "ADAR2-dependent RNA editing of AMPA receptor subunit GluR2 determines vulnerability of neurons in forebrain ischemia." Neuron **49**(5): 719-733.

Penn, A. C., A. Balik and I. H. Greger (2013). "Steric antisense inhibition of AMPA receptor Q/R editing reveals tight coupling to intronic editing sites and splicing." Nucleic Acids Res **41**(2): 1113-1123.

Penn, A. C., C. L. Zhang, F. Georges, L. Royer, C. Breillat, E. Hosy, J. D. Petersen, Y. Humeau and D. Choquet (2017). "Hippocampal LTP and contextual learning require surface diffusion of AMPA receptors." Nature **549**(7672): 384-388.

Peret, A., L. A. Christie, D. W. Ouedraogo, A. Gorlewicz, J. Epsztein, C. Mulle and V. Crepel (2014). "Contribution of aberrant GluK2-containing kainate receptors to chronic seizures in temporal lobe epilepsy." Cell Rep **8**(2): 347-354.

Perrais, D., P. S. Pinheiro, D. E. Jane and C. Mulle (2009). "Antagonism of recombinant and native GluK3-containing kainate receptors." Neuropharmacology **56**(1): 131-140.

Petralia, R. S., Y. X. Wang and R. J. Wenthold (1994). "Histological and ultrastructural localization of the kainate receptor subunits, KA2 and GluR6/7, in the rat nervous system using selective antipeptide antibodies." J Comp Neurol **349**(1): 85-110.

Petrovic, M. M., S. Viana da Silva, J. P. Clement, L. Vyklicky, C. Mulle, I. M. Gonzalez-Gonzalez and J. M. Henley (2017). "Metabotropic action of postsynaptic kainate receptors triggers hippocampal long-term potentiation." Nat Neurosci **20**(4): 529-539.

Petrovic, M. M., S. Viana da Silva, J. P. Clement, L. Vyklicky, C. Mulle, I. M. González-González and J. M. Henley (2017). "Metabotropic action of

postsynaptic kainate receptors triggers hippocampal long-term potentiation." Nat Neurosci **20**(4): 529-539.

Pickard, L., J. Noel, J. K. Duckworth, S. M. Fitzjohn, J. M. Henley, G. L. Collingridge and E. Molnar (2001). "Transient synaptic activation of NMDA receptors leads to the insertion of native AMPA receptors at hippocampal neuronal plasma membranes." Neuropharmacology **41**(6): 700-713.

Pickering, D. S., F. A. Taverna, M. W. Salter and D. R. Hampson (1995). "Palmitoylation of the GluR6 kainate receptor." Proc Natl Acad Sci U S A **92**(26): 12090-12094.

Pin, J. P. and R. Duvoisin (1995). "The metabotropic glutamate receptors: structure and functions." Neuropharmacology **34**(1): 1-26.

Pinheiro, P. and C. Mulle (2006). "Kainate receptors." Cell Tissue Res **326**(2): 457-482.

Pinheiro, P. S., F. Lanore, J. Veran, J. Artinian, C. Blanchet, V. Crepel, D. Perrais and C. Mulle (2013). "Selective block of postsynaptic kainate receptors reveals their function at hippocampal mossy fiber synapses." Cereb Cortex **23**(2): 323-331.

Pinheiro, P. S. and C. Mulle (2008). "Presynaptic glutamate receptors: physiological functions and mechanisms of action." Nat Rev Neurosci **9**(6): 423-436.

Pinheiro, P. S., D. Perrais, F. Coussen, J. Barhanin, B. Bettler, J. R. Mann, J. O. Malva, S. F. Heinemann and C. Mulle (2007). "GluR7 is an essential subunit of presynaptic kainate autoreceptors at hippocampal mossy fiber synapses." Proc Natl Acad Sci U S A **104**(29): 12181-12186.

Pirozzi, G., S. J. McConnell, A. J. Uveges, J. M. Carter, A. B. Sparks, B. K. Kay and D. M. Fowlkes (1997). "Identification of novel human WW domain-containing proteins by cloning of ligand targets." J Biol Chem **272**(23): 14611-14616.

Placido, D., B. A. Brown, 2nd, K. Lowenhaupt, A. Rich and A. Athanasiadis (2007). "A left-handed RNA double helix bound by the Z alpha domain of the RNA-editing enzyme ADAR1." Structure **15**(4): 395-404.

Plant, K., K. A. Pelkey, Z. A. Bortolotto, D. Morita, A. Terashima, C. J. McBain, G. L. Collingridge and J. T. Isaac (2006). "Transient incorporation of native GluR2-lacking AMPA receptors during hippocampal long-term potentiation." Nat Neurosci **9**(5): 602-604.

Poulsen, H., R. Jorgensen, A. Heding, F. C. Nielsen, B. Bonven and J. Egebjerg (2006). "Dimerization of ADAR2 is mediated by the double-stranded RNA binding domain." Rna **12**(7): 1350-1360.

Poulsen, H., J. Nilsson, C. K. Damgaard, J. Egebjerg and J. Kjems (2001). "CRM1 mediates the export of ADAR1 through a nuclear export signal within the Z-DNA binding domain." Mol Cell Biol **21**(22): 7862-7871.

Pozo, K. and Y. Goda (2010). "Unraveling mechanisms of homeostatic synaptic plasticity." Neuron **66**(3): 337-351.

Pressey, J. C., V. Mahadevan, C. S. Khademullah, Z. Dargaei, J. Chevrier, W. Ye, M. Huang, A. K. Chauhan, S. J. Meas, P. Uvarov, M. S. Airaksinen and M. A. Woodin (2017). "A kainate receptor subunit promotes the recycling of the neuron-specific K(+)-Cl(-) co-transporter KCC2 in hippocampal neurons." J Biol Chem **292**(15): 6190-6201.

Priel, A., S. Selak, J. Lerma and Y. Stern-Bach (2006). "Block of kainate receptor desensitization uncovers a key trafficking checkpoint." Neuron **52**(6): 1037-1046.

Rao, A. and A. M. Craig (1997). "Activity regulates the synaptic localization of the NMDA receptor in hippocampal neurons." Neuron **19**(4): 801-812.

Reimers, J. M., J. A. Loweth and M. E. Wolf (2014). "BDNF contributes to both rapid and homeostatic alterations in AMPA receptor surface expression in nucleus accumbens medium spiny neurons." Eur J Neurosci **39**(7): 1159-1169.

Reiner, A., R. J. Arant and E. Y. Isacoff (2012). "Assembly stoichiometry of the GluK2/GluK5 kainate receptor complex." Cell Rep **1**(3): 234-240.

Reymann, K. G. and J. U. Frey (2007). "The late maintenance of hippocampal LTP: requirements, phases, 'synaptic tagging', 'late-associativity' and implications." Neuropharmacology **52**(1): 24-40.

Roberts, R. J. and X. Cheng (1998). "Base flipping." Annu Rev Biochem **67**: 181-198.

Rocca, D. L., S. Martin, E. L. Jenkins and J. G. Hanley (2008). "Inhibition of Arp2/3-mediated actin polymerization by PICK1 regulates neuronal morphology and AMPA receptor endocytosis." Nat Cell Biol **10**(3): 259-271.

Rodriguez-Moreno, A. and J. Lerma (1998). "Kainate receptor modulation of GABA release involves a metabotropic function." Neuron **20**(6): 1211-1218.

Rodriguez-Moreno, A. and T. S. Sihra (2004). "Presynaptic kainate receptor facilitation of glutamate release involves protein kinase A in the rat hippocampus." J Physiol **557**(Pt 3): 733-745.

Rogan, M. T., U. V. Staubli and J. E. LeDoux (1997). "Fear conditioning induces associative long-term potentiation in the amygdala." Nature **390**(6660): 604-607.

Rueter, S. M., T. R. Dawson and R. B. Emeson (1999). "Regulation of alternative splicing by RNA editing." Nature **399**(6731): 75-80.

Ruiz, A., S. Sachidhanandam, J. K. Utvik, F. Coussen and C. Mulle (2005). "Distinct subunits in heteromeric kainate receptors mediate ionotropic and metabotropic function at hippocampal mossy fiber synapses." J Neurosci **25**(50): 11710-11718.

Rutkowska-Wlodarczyk, I., M. I. Aller, S. Valbuena, J. C. Bologna, L. Prezeau and J. Lerma (2015). "A proteomic analysis reveals the interaction of GluK1 ionotropic kainate receptor subunits with Go proteins." J Neurosci **35**(13): 5171-5179.

Safferling, M., W. Tichelaar, G. Kummerle, A. Jouppila, A. Kuusinen, K. Keinanen and D. R. Madden (2001). "First images of a glutamate receptor

ion channel: oligomeric state and molecular dimensions of GluRB homomers." Biochemistry **40**(46): 13948-13953.

Sah, P. (1996). "Ca(2+)-activated K+ currents in neurones: types, physiological roles and modulation." Trends Neurosci **19**(4): 150-154.

Sailer, A., G. T. Swanson, I. Perez-Otano, L. O'Leary, S. A. Malkmus, R. H. Dyck, H. Dickinson-Anson, H. H. Schiffer, C. Maron, T. L. Yaksh, F. H. Gage, S. O'Gorman and S. F. Heinemann (1999). "Generation and analysis of GluR5(Q636R) kainate receptor mutant mice." J Neurosci **19**(20): 8757-8764.

Sakha, P., A. Vesikansa, E. Orav, J. Heikkinen, T. K. Kukko-Lukjanov, A. Shintyapina, S. Franssila, V. Jokinen, H. J. Huttunen and S. E. Lauri (2016). "Axonal Kainate Receptors Modulate the Strength of Efferent Connectivity by Regulating Presynaptic Differentiation." Front Cell Neurosci **10**: 3.

Salinas, G. D., L. A. Blair, L. A. Needleman, J. D. Gonzales, Y. Chen, M. Li, J. D. Singer and J. Marshall (2006). "Actinfilin is a Cul3 substrate adaptor, linking GluR6 kainate receptor subunits to the ubiquitin-proteasome pathway." J Biol Chem **281**(52): 40164-40173.

Sanjana, N. E., E. Y. Levanon, E. A. Hueske, J. M. Ambrose and J. B. Li (2012). "Activity-dependent A-to-I RNA editing in rat cortical neurons." Genetics **192**(1): 281-287.

Sans, N., B. Vissel, R. S. Petralia, Y. X. Wang, K. Chang, G. A. Royle, C. Y. Wang, S. O'Gorman, S. F. Heinemann and R. J. Wenthold (2003). "Aberrant formation of glutamate receptor complexes in hippocampal neurons of mice lacking the GluR2 AMPA receptor subunit." J Neurosci **23**(28): 9367-9373.

Sansam, C. L., K. S. Wells and R. B. Emeson (2003). "Modulation of RNA editing by functional nucleolar sequestration of ADAR2." Proc Natl Acad Sci U S A **100**(24): 14018-14023.

Schanzenbacher, C. T., J. D. Langer and E. M. Schuman (2018). "Time- and polarity-dependent proteomic changes associated with homeostatic scaling at central synapses." Elife **7**.

Schanzenbächer, C. T., S. Sambandan, J. D. Langer and E. M. Schuman (2016). "Nascent Proteome Remodeling following Homeostatic Scaling at Hippocampal Synapses." Neuron **92**(2): 358-371.

Schaukowitch, K., A. L. Reese, S. K. Kim, G. Kilaru, J. Y. Joo, E. T. Kavalali and T. K. Kim (2017). "An Intrinsic Transcriptional Program Underlying Synaptic Scaling during Activity Suppression." Cell Rep **18**(6): 1512-1526.

Schiffer, H. H., G. T. Swanson and S. F. Heinemann (1997). "Rat GluR7 and a carboxy-terminal splice variant, GluR7b, are functional kainate receptor subunits with a low sensitivity to glutamate." Neuron **19**(5): 1141-1146.

Schmitz, D., M. Frerking and R. A. Nicoll (2000). "Synaptic activation of presynaptic kainate receptors on hippocampal mossy fiber synapses." Neuron **27**(2): 327-338.

Schmitz, D., J. Mellor and R. A. Nicoll (2001). "Presynaptic kainate receptor mediation of frequency facilitation at hippocampal mossy fiber synapses." Science **291**(5510): 1972-1976.

Schneider, M. F., J. Wettengel, P. C. Hoffmann and T. Stafforst (2014). "Optimal guideRNAs for re-directing deaminase activity of hADAR1 and hADAR2 in trans." Nucleic Acids Res **42**(10): e87.

Schneider-Poetsch, T., J. Ju, D. E. Eyler, Y. Dang, S. Bhat, W. C. Merrick, R. Green, B. Shen and J. O. Liu (2010). "Inhibition of eukaryotic translation elongation by cycloheximide and lactimidomycin." Nat Chem Biol **6**(3): 209-217.

Schoft, V. K., S. Schopoff and M. F. Jantsch (2007). "Regulation of glutamate receptor B pre-mRNA splicing by RNA editing." Nucleic Acids Res **35**(11): 3723-3732.

Selak, S., A. V. Paternain, M. I. Aller, E. Pico, R. Rivera and J. Lerma (2009). "A role for SNAP25 in internalization of kainate receptors and synaptic plasticity." Neuron **63**(3): 357-371.

Shamay-Ramot, A., K. Khermesh, H. T. Porath, M. Barak, Y. Pinto, C. Wachtel, A. Zilberberg, T. Lerer-Goldshtein, S. Efroni, E. Y. Levanon and L. Appelbaum (2015). "Fmrp Interacts with Adar and Regulates RNA Editing, Synaptic Density and Locomotor Activity in Zebrafish." PLoS Genet **11**(12): e1005702.

Shankar, G. M., S. Li, T. H. Mehta, A. Garcia-Munoz, N. E. Shepardson, I. Smith, F. M. Brett, M. A. Farrell, M. J. Rowan, C. A. Lemere, C. M. Regan, D. M. Walsh, B. L. Sabatini and D. J. Selkoe (2008). "Amyloid-beta protein dimers isolated directly from Alzheimer's brains impair synaptic plasticity and memory." Nat Med **14**(8): 837-842.

Shanmugam, R., F. Zhang, H. Srinivasan, J. L. Charles Richard, K. I. Liu, X. Zhang, C. W. A. Woo, Z. H. M. Chua, J. P. Buschdorf, M. J. Meaney and M. H. Tan (2018). "SRSF9 selectively represses ADAR2-mediated editing of brain-specific sites in primates." Nucleic Acids Res.

Sheng, N., Y. S. Shi, R. M. Lomash, K. W. Roche and R. A. Nicoll (2015). "Neto auxiliary proteins control both the trafficking and biophysical properties of the kainate receptor GluK1." Elife **4**.

Shepherd, J. D. and R. L. Huganir (2007). "The cell biology of synaptic plasticity: AMPA receptor trafficking." Annu Rev Cell Dev Biol **23**: 613-643.

Shepherd, J. D., G. Rumbaugh, J. Wu, S. Chowdhury, N. Plath, D. Kuhl, R. L. Huganir and P. F. Worley (2006). "Arc/Arg3.1 mediates homeostatic synaptic scaling of AMPA receptors." Neuron **52**(3): 475-484.

Shi, S., Y. Hayashi, J. A. Esteban and R. Malinow (2001). "Subunit-specific rules governing AMPA receptor trafficking to synapses in hippocampal pyramidal neurons." Cell **105**(3): 331-343.

Shubina, M. Y., Y. R. Musinova and E. V. Sheval (2016). "Nucleolar Methyltransferase Fibrillarin: Evolution of Structure and Functions." Biochemistry (Mosc) **81**(9): 941-950.

Sigel, E. and M. E. Steinmann (2012). "Structure, function, and modulation of GABA(A) receptors." J Biol Chem **287**(48): 40224-40231.

Sihra, T. S. and A. Rodriguez-Moreno (2013). "Presynaptic kainate receptor-mediated bidirectional modulatory actions: mechanisms." Neurochem Int **62**(7): 982-987.

Silberberg, G., D. Lundin, R. Navon and M. Ohman (2012). "Deregulation of the A-to-I RNA editing mechanism in psychiatric disorders." Hum Mol Genet **21**(2): 311-321.

Slotkin, W. and K. Nishikura (2013). "Adenosine-to-inosine RNA editing and human disease." Genome Med **5**(11): 105.

Snyder, E. M., B. D. Philpot, K. M. Huber, X. Dong, J. R. Fallon and M. F. Bear (2001). "Internalization of ionotropic glutamate receptors in response to mGluR activation." Nat Neurosci **4**(11): 1079-1085.

Soden, M. E. and L. Chen (2010). "Fragile X protein FMRP is required for homeostatic plasticity and regulation of synaptic strength by retinoic acid." J Neurosci **30**(50): 16910-16921.

Soderling, T. R. and V. A. Derkach (2000). "Postsynaptic protein phosphorylation and LTP." Trends Neurosci **23**(2): 75-80.

Sommer, B., N. Burnashev, T. A. Verdoorn, K. Keinanen, B. Sakmann and P. H. Seeburg (1992). "A glutamate receptor channel with high affinity for domoate and kainate." Embo j **11**(4): 1651-1656.

Sommer, B., K. Keinanen, T. A. Verdoorn, W. Wisden, N. Burnashev, A. Herb, M. Kohler, T. Takagi, B. Sakmann and P. H. Seeburg (1990). "Flip and flop: a cell-specific functional switch in glutamate-operated channels of the CNS." Science **249**(4976): 1580-1585.

Sommer, B., M. Kohler, R. Sprengel and P. H. Seeburg (1991). "RNA editing in brain controls a determinant of ion flow in glutamate-gated channels." Cell **67**(1): 11-19.

Stefl, R., M. Xu, L. Skrisovska, R. B. Emeson and F. H. Allain (2006). "Structure and specific RNA binding of ADAR2 double-stranded RNA binding motifs." Structure **14**(2): 345-355.

Steinberg, J. P., K. Takamiya, Y. Shen, J. Xia, M. E. Rubio, S. Yu, W. Jin, G. M. Thomas, D. J. Linden and R. L. Huganir (2006). "Targeted in vivo mutations of the AMPA receptor subunit GluR2 and its interacting protein PICK1 eliminate cerebellar long-term depression." Neuron **49**(6): 845-860.

Steinmetz, C. C. and G. G. Turrigiano (2010). "Tumor necrosis factor-alpha signaling maintains the ability of cortical synapses to express synaptic scaling." J Neurosci **30**(44): 14685-14690.

Stellwagen, D. and R. C. Malenka (2006). "Synaptic scaling mediated by glial TNF-alpha." Nature **440**(7087): 1054-1059.

Stephens, O. M., B. L. Haudenschild and P. A. Beal (2004). "The binding selectivity of ADAR2's dsRBMs contributes to RNA-editing selectivity." Chem Biol **11**(9): 1239-1250.

Storm, J. F. (1990). "Potassium currents in hippocampal pyramidal cells." Prog Brain Res **83**: 161-187.

Straub, C., D. L. Hunt, M. Yamasaki, K. S. Kim, M. Watanabe, P. E. Castillo and S. Tomita (2011). "Distinct functions of kainate receptors in the brain are determined by the auxiliary subunit Neto1." Nat Neurosci **14**(7): 866-873.

Straub, C., Y. Noam, T. Nomura, M. Yamasaki, D. Yan, H. B. Fernandes, P. Zhang, J. R. Howe, M. Watanabe, A. Contractor and S. Tomita (2016). "Distinct Subunit Domains Govern Synaptic Stability and Specificity of the Kainate Receptor." Cell Rep **16**(2): 531-544.

Straughan, D. W., M. J. Neal, M. A. Simmonds, G. G. Collins and R. G. Hill (1971). "Evaluation of bicuculline as a GABA antagonist." Nature **233**(5318): 352-354.

Strehblow, A., M. Hallegger and M. F. Jantsch (2002). "Nucleocytoplasmic distribution of human RNA-editing enzyme ADAR1 is modulated by double-stranded RNA-binding domains, a leucine-rich export signal, and a putative dimerization domain." Mol Biol Cell **13**(11): 3822-3835.

Sun, Q. and G. G. Turrigiano (2011). "PSD-95 and PSD-93 play critical but distinct roles in synaptic scaling up and down." J Neurosci **31**(18): 6800-6808.

Sun, Y., R. Olson, M. Horning, N. Armstrong, M. Mayer and E. Gouaux (2002). "Mechanism of glutamate receptor desensitization." Nature **417**(6886): 245-253.

Sutton, M. A., H. T. Ito, P. Cressy, C. Kempf, J. C. Woo and E. M. Schuman (2006). "Miniature neurotransmission stabilizes synaptic function via tonic suppression of local dendritic protein synthesis." Cell **125**(4): 785-799.

Sutton, M. A., A. M. Taylor, H. T. Ito, A. Pham and E. M. Schuman (2007). "Postsynaptic decoding of neural activity: eEF2 as a biochemical sensor coupling miniature synaptic transmission to local protein synthesis." Neuron **55**(4): 648-661.

Sutton, M. A., N. R. Wall, G. N. Aakalu and E. M. Schuman (2004). "Regulation of dendritic protein synthesis by miniature synaptic events." Science **304**(5679): 1979-1983.

Suzuki, E. and H. Kamiya (2016). "PSD-95 regulates synaptic kainate receptors at mouse hippocampal mossy fiber-CA3 synapses." Neurosci Res **107**: 14-19.

Swann, J. W. and J. M. Rho (2014). "How is homeostatic plasticity important in epilepsy?" Adv Exp Med Biol **813**: 123-131.

Swanson, G. T., D. Feldmeyer, M. Kaneda and S. G. Cull-Candy (1996). "Effect of RNA editing and subunit co-assembly single-channel properties of recombinant kainate receptors." J Physiol **492 (Pt 1)**: 129-142.

Tan, H. L., B. N. Queenan and R. L. Huganir (2015). "GRIP1 is required for homeostatic regulation of AMPAR trafficking." Proc Natl Acad Sci U S A **112**(32): 10026-10031.

Tan, M. H., Q. Li, R. Shanmugam, R. Piskol, J. Kohler, A. N. Young, K. I. Liu, R. Zhang, G. Ramaswami, K. Ariyoshi, A. Gupte, L. P. Keegan, C. X. George, A. Ramu, N. Huang, E. A. Pollina, D. S. Leeman, A. Rustighi, Y. P. S. Goh, A. Chawla, G. Del Sal, G. Peltz, A. Brunet, D. F. Conrad, C. E. Samuel, M. A. O'Connell, C. R. Walkley, K. Nishikura and J. B. Li (2017). "Dynamic landscape and regulation of RNA editing in mammals." Nature **550**(7675): 249-254.

Tariq, A., W. Garncarz, C. Handl, A. Balik, O. Pusch and M. F. Jantsch (2013). "RNA-interacting proteins act as site-specific repressors of ADAR2-mediated RNA editing and fluctuate upon neuronal stimulation." Nucleic Acids Res **41**(4): 2581-2593.

Tashiro, A., A. Dunaevsky, R. Blazeski, C. A. Mason and R. Yuste (2003). "Bidirectional regulation of hippocampal mossy fiber filopodial motility by kainate receptors: a two-step model of synaptogenesis." Neuron **38**(5): 773-784.

Thiagarajan, T. C., M. Lindskog and R. W. Tsien (2005). "Adaptation to synaptic inactivity in hippocampal neurons." Neuron **47**(5): 725-737.

Tomita, S., H. Adesnik, M. Sekiguchi, W. Zhang, K. Wada, J. R. Howe, R. A. Nicoll and D. S. Bredt (2005). "Stargazin modulates AMPA receptor gating and trafficking by distinct domains." Nature **435**(7045): 1052-1058.

Tomita, S. and P. E. Castillo (2012). "Neto1 and Neto2: auxiliary subunits that determine key properties of native kainate receptors." J Physiol **590**(Pt 10): 2217-2223.

Tomita, S., V. Stein, T. J. Stocker, R. A. Nicoll and D. S. Bredt (2005). "Bidirectional synaptic plasticity regulated by phosphorylation of stargazin-like TARPs." Neuron **45**(2): 269-277.

Treiman, D. M. (2001). "GABAergic mechanisms in epilepsy." Epilepsia **42 Suppl 3**: 8-12.

Tsumoto, T. (1993). "Long-term depression in cerebral cortex: a possible substrate of "forgetting" that should not be forgotten." Neurosci Res **16**(4): 263-270.

Turrigiano, G. (2012). "Homeostatic synaptic plasticity: local and global mechanisms for stabilizing neuronal function." Cold Spring Harb Perspect Biol **4**(1): a005736.

Turrigiano, G. G. (2008). "The self-tuning neuron: synaptic scaling of excitatory synapses." Cell **135**(3): 422-435.

Turrigiano, G. G., K. R. Leslie, N. S. Desai, L. C. Rutherford and S. B. Nelson (1998). "Activity-dependent scaling of quantal amplitude in neocortical neurons." Nature **391**(6670): 892-896.

Uchida, H. and S. Ito (2015). "Differential regulation of expression of RNA-editing enzymes, ADAR1 and ADAR2, by 5-aza-2'-deoxycytidine and trichostatin A in human neuronal SH-SY5Y cells." Neuroreport **26**(18): 1089-1094.

Valente, L. and K. Nishikura (2007). "RNA binding-independent dimerization of adenosine deaminases acting on RNA and dominant negative effects of nonfunctional subunits on dimer functions." J Biol Chem **282**(22): 16054-16061.

Vignes, M., V. R. Clarke, M. J. Parry, D. Bleakman, D. Lodge, P. L. Ornstein and G. L. Collingridge (1998). "The GluR5 subtype of kainate receptor regulates excitatory synaptic transmission in areas CA1 and CA3 of the rat hippocampus." Neuropharmacology **37**(10-11): 1269-1277.

Vignes, M. and G. L. Collingridge (1997). "The synaptic activation of kainate receptors." Nature **388**(6638): 179-182.

Vincent, P. and C. Mulle (2009). "Kainate receptors in epilepsy and excitotoxicity." Neuroscience **158**(1): 309-323.

Vissel, B., G. A. Royle, B. R. Christie, H. H. Schiffer, A. Ghetti, T. Tritto, I. Perez-Otano, R. A. Radcliffe, J. Seamans, T. Sejnowski, J. M. Wehner, A. C. Collins, S. O'Gorman and S. F. Heinemann (2001). "The role of RNA editing of kainate receptors in synaptic plasticity and seizures." Neuron **29**(1): 217-227.

Vivithanaporn, P., S. Yan and G. T. Swanson (2006). "Intracellular trafficking of KA2 kainate receptors mediated by interactions with coatomer protein complex I (COPI) and 14-3-3 chaperone systems." J Biol Chem **281**(22): 15475-15484.

Wagner, R. W., J. E. Smith, B. S. Cooperman and K. Nishikura (1989). "A double-stranded RNA unwinding activity introduces structural alterations by means of adenosine to inosine conversions in mammalian cells and Xenopus eggs." Proc Natl Acad Sci U S A **86**(8): 2647-2651.

Wahlstedt, H., C. Daniel, M. Enstero and M. Ohman (2009). "Large-scale mRNA sequencing determines global regulation of RNA editing during brain development." Genome Res **19**(6): 978-986.

Wahlstedt, H. and M. Ohman (2011). "Site-selective versus promiscuous A-to-I editing." Wiley Interdiscip Rev RNA **2**(6): 761-771.

Walsh, D. M. and D. J. Selkoe (2007). "A beta oligomers - a decade of discovery." J Neurochem **101**(5): 1172-1184.

Wang, Y., S. Park and P. A. Beal (2018). "Selective Recognition of RNA Substrates by ADAR Deaminase Domains." Biochemistry **57**(10): 1640-1651.

Watt, A. J., M. C. van Rossum, K. M. MacLeod, S. B. Nelson and G. G. Turrigiano (2000). "Activity coregulates quantal AMPA and NMDA currents at neocortical synapses." Neuron **26**(3): 659-670.

Wenthold, R. J., R. S. Petralia, J. Blahos, II and A. S. Niedzielski (1996). "Evidence for multiple AMPA receptor complexes in hippocampal CA1/CA2 neurons." J Neurosci **16**(6): 1982-1989.

Wheeler, D. G., C. F. Barrett, R. D. Groth, P. Safa and R. W. Tsien (2008). "CaMKII locally encodes L-type channel activity to signal to nuclear CREB in excitation-transcription coupling." J Cell Biol **183**(5): 849-863.

Whitcomb, D. J., E. L. Hogg, P. Regan, T. Piers, P. Narayan, G. Whitehead, B. L. Winters, D. H. Kim, E. Kim, P. St George-Hyslop, D. Klenerman, G. L. Collingridge, J. Jo and K. Cho (2015). "Intracellular oligomeric amyloid-beta rapidly regulates GluA1 subunit of AMPA receptor in the hippocampus." Sci Rep **5**: 10934.

Whitlock, J. R., A. J. Heynen, M. G. Shuler and M. F. Bear (2006). "Learning induces long-term potentiation in the hippocampus." Science **313**(5790): 1093-1097.

Whitney, N. P., H. Peng, N. B. Erdmann, C. Tian, D. T. Monaghan and J. C. Zheng (2008). "Calcium-permeable AMPA receptors containing Q/R-unedited GluR2 direct human neural progenitor cell differentiation to neurons." Faseb j **22**(8): 2888-2900.

Wierenga, C. J., K. Ibata and G. G. Turrigiano (2005). "Postsynaptic expression of homeostatic plasticity at neocortical synapses." J Neurosci **25**(11): 2895-2905.

Wilcox, K. S., J. Buchhalter and M. A. Dichter (1994). "Properties of inhibitory and excitatory synapses between hippocampal neurons in very low density cultures." Synapse **18**(2): 128-151.

Wilkinson, K. A. and J. M. Henley (2010). "Mechanisms, regulation and consequences of protein SUMOylation." Biochem J **428**(2): 133-145.

Wilkinson, K. A., F. Konopacki and J. M. Henley (2012). "Modification and movement: Phosphorylation and SUMOylation regulate endocytosis of GluK2-containing kainate receptors." Commun Integr Biol **5**(2): 223-226.

Wisden, W. and P. H. Seeburg (1993). "Mammalian ionotropic glutamate receptors." Curr Opin Neurobiol **3**(3): 291-298.

Wondolowski, J. and D. Dickman (2013). "Emerging links between homeostatic synaptic plasticity and neurological disease." Front Cell Neurosci **7**: 223.

Wong, S. K., S. Sato and D. W. Lazinski (2001). "Substrate recognition by ADAR1 and ADAR2." Rna **7**(6): 846-858.

Woodin, M. A., K. Ganguly and M. M. Poo (2003). "Coincident pre- and postsynaptic activity modifies GABAergic synapses by postsynaptic changes in Cl- transporter activity." Neuron **39**(5): 807-820.

Wyeth, M. S., K. A. Pelkey, R. S. Petralia, M. W. Salter, R. R. McInnes and C. J. McBain (2014). "Neto auxiliary protein interactions regulate kainate and NMDA receptor subunit localization at mossy fiber-CA3 pyramidal cell synapses." J Neurosci **34**(2): 622-628.

Xu, J., J. J. Marshall, H. B. Fernandes, T. Nomura, B. A. Copits, D. Procissi, S. Mori, L. Wang, Y. Zhu, G. T. Swanson and A. Contractor (2017). "Complete Disruption of the Kainate Receptor Gene Family Results in Corticostriatal Dysfunction in Mice." Cell Rep **18**(8): 1848-1857.

Xu-Friedman, M. A. and W. G. Regehr (2004). "Structural contributions to short-term synaptic plasticity." Physiol Rev **84**(1): 69-85.

Yamazaki, M., K. Araki, A. Shibata and M. Mishina (1992). "Molecular cloning of a cDNA encoding a novel member of the mouse glutamate receptor channel family." Biochem Biophys Res Commun **183**(2): 886-892.

Yan, D., M. Yamasaki, C. Straub, M. Watanabe and S. Tomita (2013). "Homeostatic control of synaptic transmission by distinct glutamate receptors." Neuron **78**(4): 687-699.

Yang, L., P. Huang, F. Li, L. Zhao, Y. Zhang, S. Li, Z. Gan, A. Lin, W. Li and Y. Liu (2012). "c-Jun amino-terminal kinase-1 mediates glucose-responsive upregulation of the RNA editing enzyme ADAR2 in pancreatic beta-cells." PLoS One **7**(11): e48611.

Yasumura, M., T. Yoshida, S. J. Lee, T. Uemura, J. Y. Joo and M. Mishina (2012). "Glutamate receptor delta1 induces preferentially inhibitory presynaptic differentiation of cortical neurons by interacting with neurexins through cerebellin precursor protein subtypes." J Neurochem **121**(5): 705-716.

Yuzaki, M. (2013). "Cerebellar LTD vs. motor learning-lessons learned from studying GluD2." Neural Netw **47**: 36-41.

Yuzaki, M. and A. R. Aricescu (2017). "A GluD Coming-Of-Age Story." Trends Neurosci **40**(3): 138-150.

Zerangue, N., B. Schwappach, Y. N. Jan and L. Y. Jan (1999). "A new ER trafficking signal regulates the subunit stoichiometry of plasma membrane K(ATP) channels." Neuron **22**(3): 537-548.

Zhang, W., F. St-Gelais, C. P. Grabner, J. C. Trinidad, A. Sumioka, M. Morimoto-Tomita, K. S. Kim, C. Straub, A. L. Burlingame, J. R. Howe and S. Tomita (2009). "A transmembrane accessory subunit that modulates kainate-type glutamate receptors." Neuron **61**(3): 385-396.

Zhao, W. Q., F. Santini, R. Breese, D. Ross, X. D. Zhang, D. J. Stone, M. Ferrer, M. Townsend, A. L. Wolfe, M. A. Seager, G. G. Kinney, P. J. Shughrue and W. J. Ray (2010). "Inhibition of calcineurin-mediated endocytosis and alpha-amino-3-hydroxy-5-methyl-4-isoxazolepropionic acid (AMPA) receptors prevents amyloid beta oligomer-induced synaptic disruption." J Biol Chem **285**(10): 7619-7632.

Zhu, J. J., J. A. Esteban, Y. Hayashi and R. Malinow (2000). "Postnatal synaptic potentiation: delivery of GluR4-containing AMPA receptors by spontaneous activity." Nat Neurosci **3**(11): 1098-1106.

Zhu, Q. J., F. S. Kong, H. Xu, Y. Wang, C. P. Du, C. C. Sun, Y. Liu, T. Li and X. Y. Hou (2014). "Tyrosine phosphorylation of GluK2 up-regulates kainate receptor-mediated responses and downstream signaling after brain ischemia." Proc Natl Acad Sci U S A **111**(38): 13990-13995.

Zucker, R. S. and W. G. Regehr (2002). "Short-term synaptic plasticity." Annu Rev Physiol **64**: 355-405.

APPENDIX 1: LIST OF PUBLISHED MATERIALS

1. **Gurung S**, Evans AJ, Wilkinson KA, Henley JM (2018) ADAR2 mediated Q/R editing of GluK2 regulates kainate receptor upscaling in response to suppression of synaptic activity. J Cell Sci. 2018 Dec 17;131(24). pii: jcs222273. doi: 10.1242/jcs.222273.

   Link to the article online:
   http://jcs.biologists.org/content/131/24/jcs222273

2. Evans AJ, **Gurung S**, Henley JM, Nakamura Y, Wilkinson KA (2017) Exciting Times: New Advances Towards Understanding the Regulation and Roles of Kainate Receptors. Neurochem Res. doi: 10.1007/s11064-017-2450-2. PMID: 29270706
3. Luo J*, **Gurung S***, Lee L, Henley JM, Wilkinson KA, Guo C (2017) Increased SUMO-2/3-ylation mediated by SENP3 degradation is protective against cadmium-induced caspase 3-dependent cytotoxicity. J Toxicol Sci. 42(5) 529-538. PMID: 28747609
4. Evans AJ, **Gurung S**, Wilkinson KA, Stephens DJ, Henley JM (2017) Assembly, Secretory Pathway Trafficking, and Surface Delivery of Kainate Receptors Is Regulated by Neuronal Activity. Cell Rep. 19(12) 2613-2626. PMID: 28636947

Neurochemical Research
https://doi.org/10.1007/s11064-017-2450-2

ORIGINAL PAPER

Exciting Times: New Advances Towards Understanding the Regulation and Roles of Kainate Receptors

Ashley J. Evans[1] · Sonam Gurung[1] · Jeremy M. Henley[1] · Yasuko Nakamura[1] · Kevin A. Wilkinson[1]

Received: 23 August 2017 / Revised: 27 November 2017 / Accepted: 7 December 2017

Abstract
Kainate receptors (KARs) are glutamate-gated ion channels that play fundamental roles in regulating neuronal excitability and network function in the brain. After being cloned in the 1990s, important progress has been made in understanding the mechanisms controlling the molecular and cellular properties of KARs, and the nature and extent of their regulation of wider neuronal activity. However, there have been significant recent advances towards understanding KAR trafficking through the secretory pathway, their precise synaptic positioning, and their roles in synaptic plasticity and disease. Here we provide an overview highlighting these new findings about the mechanisms controlling KARs and how KARs, in turn, regulate other proteins and pathways to influence synaptic function.

Keywords Kainate receptors · GluK2 · Trafficking · RUSH · Synaptic transmission · Synaptic plasticity

Introduction

Glutamate is the major excitatory neurotransmitter in the CNS and participates in nearly all aspects of brain function. There are three major subclasses of ionotropic glutamate receptors, kainate receptors (KARs), AMPA receptors and NMDA receptors. KARs are widely distributed throughout the brain and, depending on the cell type in question, they can be localised at pre-, post- and/or extrasynaptic sites. In general, presynaptic KARs modulate both excitatory and inhibitory neurotransmitter release, postsynaptic KARs contribute to excitatory neurotransmission and extrasynaptic KARs play a role in determining neuronal excitability (for reviews of KAR physiology see [1–4]). For reasons that remain unclear, compared to AMPARs and NMDARs, synaptic KAR ionotropic responses are highly restricted to subsets of excitatory synapses. For example, some neurons, including CA1 pyramidal neurons and dispersed hippocampal cultures display robust KAR currents following kainate application [5, 6] but they lack synaptically-evoked ionotropic postsynaptic excitatory post-synaptic currents $KAR_{(EPSCs)}$ [6–8]. Intriguingly, it has been proposed that $KAR_{(EPSCs)}$ are present only at synapses that do not contain $AMPAR_{(EPSCs)}$ [9, 10].

Remarkably, despite their classical ion channel structure, KARs can also signal via a non-canonical G-protein coupled metabotropic cascade [11]. In contrast, postsynaptic metabotropic KAR signalling is much more widespread than ionotropic KAR signalling [12, 13] and recent discoveries have highlighted their previously unsuspected roles in neuromodulation. For example, they regulate inhibitory transmission by controlling surface expression of the chloride transporter KCC2 [14] and mediate certain forms of synaptic plasticity [15, 16]. For extensive reviews of metabotropic KARs see [4, 17].

Our aim here is to provide an overview of recent advances in understanding the cellular regulation of KARs and their interacting proteins, and how these processes influence KAR-mediated synaptic transmission and plasticity. We highlight what is known, what remains to be established, and outline the future perspectives for KAR research and how it will impact on our understanding of brain function and dysfunction in disease.

✉ Jeremy M. Henley
j.m.henley@bristol.ac.uk

✉ Kevin A. Wilkinson
Kevin.Wilkinson@bristol.ac.uk

[1] School of Biochemistry, Centre for Synaptic Plasticity, Biomedical Sciences Building, University of Bristol, Bristol BS8 1TD, UK

Published online: 21 December 2017

Nomenclature of KAR Subunits

Since their initial cloning [18, 19] the names of specific KAR subunits have changed to conform to a simpler, more systematic naming system. This can lead to considerable confusion in the field since many seminal early papers use the old nomenclature. Nonetheless, since 2009, the International Union of Basic and Clinical Pharmacology (IUPHAR) naming system has been almost universally adopted. Briefly, the subunits formerly most commonly referred to as GluR5, GluR6, GluR7, KA1 and KA2 are now named GluK1, GluK2, GluK3, GluK4 and GluK5, respectively, and the genes encoding these proteins are named *GRIK1-5* [20].

KARs from Birth to Maturity

KAR Structure and Assembly

KARs are heteromeric assemblies containing four subunits. Each subunit has a large extracellular N-terminal domain (NTD), helical transmembrane domains (TMD) including three membrane spanning domains (M1, M3 and M4) and a membrane re-entrant domain (M2), and an intracellular C-terminal domain (CTD). The latter part of the NTD (the last ~ 150 amino acids, S1) together with the extracellular loops between M3 and M4 (S2) form the ligand-binding domain (LBD) [21]. Recently, detailed structural information has been gained by solving the crystal structure of kainate receptor subunits and this is reviewed in detail elsewhere [22–25].

Heteromeric Assembly

Following protein synthesis, the NTDs initiate receptor assembly in the endoplasmic reticulum (ER) by facilitating dimer formation, and the dimerization of two dimers then leads to the formation of tetrameric receptors. Based on affinity for their ligand, KAR subunits have been grouped into low affinity (GluK1-3) and high affinity (GluK4-5) receptors. Studies on recombinant systems have shown that low affinity GluK1-3 subunits can form ion channels as both homomers and heteromers but high affinity GluK4 and GluK5 subunits can only form heteromeric functional ion channels when complexed with the low-affinity subunits [19, 26, 27]. The most abundant subunit combination in the brain comprises GluK2 and GluK5. This occurs, at least in part, because widely distributed contacts within the NTD of GluK2 and GluK5 favour the assembly of functional heteromeric receptors over homomeric receptors [28].

Alternative Splicing

Regions within the N- and C- terminal domains of KAR subunits can undergo alternative RNA splicing. For instance, the extracellular N-terminal domain of GluK1 can produce two variants, $GluK1_1$ and $GluK1_2$ [29], while the C-terminus has four splice variants, GluK1a, GluK1b, GluK1c and GluK1d [30, 31]. Splice variants have also been reported at the C-termini of both GluK2 and GluK3; GluK2a/GluK2b/GluK2c and GluK3a/GluK3b, respectively [32–34]. C-terminal alternative splicing of KAR subunits has been shown to greatly affect the ability of receptors to exit the ER and accumulate at the cell surface. Furthermore, different C-termini facilitate distinct protein–protein interactions and it is likely they provide mechanisms for nuanced tuning of specific KARs at particular locations [35–37].

RNA Editing

In addition to splicing, further diversity arises from varying degrees of RNA editing in GluK1 and GluK2 subunits [38, 39]. For example, Q/R editing in the pore-lining region of GluK2 results in a change from the genomically encoded glutamine residue to an arginine. This change alters the properties of the resultant KAR from calcium permeable to calcium impermeable and also alters the biophysical properties of the channel [40]. Furthermore, GluK2 Q/R editing reduces its ability to assemble with other subunits, leading to its accumulation as monomers and dimers that are retained in the ER [41].

It is well established that GluK1/GluK2 editing is developmentally controlled through regulation of the enzyme that also catalyses GluK1/2 RNA editing, ADAR2 [42–44]. For an excellent recent review see [45]. ADAR2 levels are low in embryonic brain and during development ADAR2 levels increase [46]. After birth ~ 80% of GluK2 and 40% GluK1 are edited, which leads to fewer surface KARs and lower conductance and Ca^{2+} permeability [47]. Furthermore, recent evidence has suggested that the ADAR2 dependent Q/R editing of GluK2 is also dynamically regulated during homeostatic scaling [48]. Suppression of synaptic activity with TTX results in upscaling of KAR surface expression, which is, at least in part, due to reduced Q/R editing of GluK2 [48]. Therefore, this developmental and homeostatic regulation of GluK2 Q/R editing likely control processes such as synaptogenesis [49, 50], plasticity [40] and pathology [47].

KAR Trafficking Through the Secretory Pathway

The accurate and timely delivery of KARs to specific pre-, post- and extrasynaptic locations is fundamental to many aspects of neuronal function. Most research efforts have

focused on the processes of transcription, endocytosis, recycling and degradation (for reviews see [4, 51]). However, after assembly, tetrameric KARs need to traffic through the secretory pathway to reach the cell surface and be appropriately targeted. Until recently, it was unknown whether these early KAR trafficking steps occur locally in dendrites and, importantly, how these processes are regulated.

Local Dendritic Translation and Secretory Pathway Trafficking

In neurons, mRNAs can be trafficked to distant sites in axons and dendrites for local translation and processing [52–57]. A range of neuronal transmembrane proteins, including AMPARs, NMDARs and $GABA_BRs$, can be translated using both somatic and dendritically localised ribosome patterned rough ER. They then traffic from the ER using dendritic ER exit sites and utilise the somatic Golgi or dendritic Golgi outposts for mature glycosylation [48, 58–62]. Importantly, all of the secretory pathway machinery appears to be present in neurites as iGluRs can mature in isolated dendrites [63]. For example, AMPAR mRNAs traffic into dendrites, under the control of synaptic activity, to create local utilizable pools of mRNA for local translation [64].

Recently, using the RUSH system, which allows the synchronous release and visualization of cargo proteins trafficking through the secretory pathway [65, 66], it has been demonstrated that GluK2-containing KARs utilise these local secretory pathway systems for their delivery to the cell surface [48] (Fig. 1). However, the functional consequences that result from KARs utilising these local secretory pathway systems remain to be established.

Activity Dependent Secretory Pathway Trafficking

Although there is a strong base of knowledge about the activity-dependent regulation of KAR endocytosis and recycling [13, 15, 67–71], compared to AMPARs [72] and tsVSVG cargo [73], little is known about the activity-dependence of secretory pathway trafficking of KARs. A very recent study reported that secretory pathway KAR trafficking is indeed highly regulated in multiple different cellular activity contexts [48]. Activation of surface KARs results in a decrease in secretory pathway trafficking of de novo GluK2-containing KARs from the ER to the cell surface, demonstrating that KAR secretory pathway trafficking is subject to a negative feedback mechanism controlling KAR surface levels. Mechanistically, this pathway is dependent on the PDZ ligand of GluK2, since a mutant lacking this

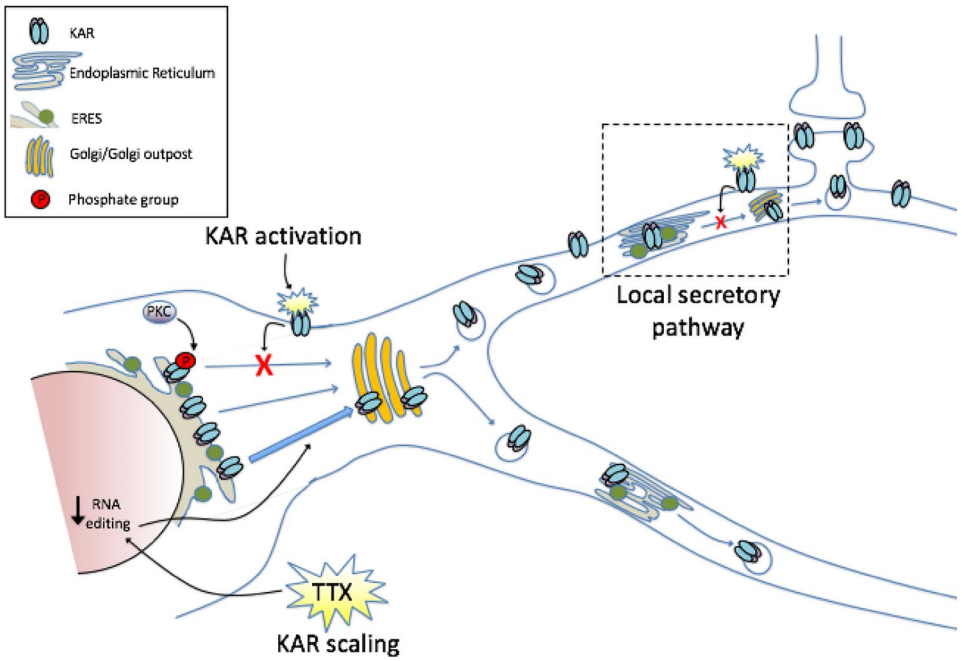

Fig. 1 Control of KAR trafficking through the secretory pathway. KAR trafficking is controlled at multiple levels under basal and activity-dependent conditions. PKC phosphorylation of the GluK2 subunit at S846 and S868 reduces ER exit of GluK2-containing receptors. Activation of surface KARs leads to a feedback mechanism that reduces forward trafficking of KARs from the ER, via a mechanism that requires the PDZ ligand of GluK2. Furthermore, induction of synaptic scaling via inhibiting neuronal activity with TTX leads to upscaling of KARs, at least in part via reduced RNA editing of the GluK2 subunit, favouring forward trafficking of GluK2-containing KARs. Finally, in addition to using somatic Golgi for post-ER processing, KARs can also use local secretory pathway systems in dendrites

protein interaction site is insensitive to the effects of kainate on secretory pathway trafficking, however the GluK2 interacting partner responsible remains to be determined [48].

Roles of GluK5 in Trafficking

As well as interactions with the GluK2 subunit, interactions with GluK5 also determine flux through the secretory pathway. ER retention sequences in the C-terminus of GluK5 facilitate its interaction with the COPI coat complex, driving retrograde Golgi to ER trafficking of KARs, and acting as an ER retrieval mechanism [74]. This interaction is disrupted by the heteromerization of GluK2 with GluK5 and binding to 14-3-3ζ, which promotes forward trafficking to the cell surface, both driving ER exit and favouring assembly of heteromeric KARs [74].

Post-translational Modifications

Further tight control of the ER exit and secretory pathway trafficking of KARs is also provided by post-translational modifications, most notably PKC phosphorylation of GluK2 at residues S846 and S868 [48, 75], which act to restrict forward trafficking of GluK2-containing KARs.

Thus, far from being a passive process, ER exit of KARs and flux through the secretory pathway is emerging as a major point of regulation in determining the surface expression of KARs under basal and activity-dependent conditions (summarised in Fig. 1).

Synaptic Positioning and Function of KARs

Given the highly-ordered targeting and localisation of KARs at distinct synaptic and sub-synaptic compartments, a key question in the field relates to how KARs are targeted to, and retained at, specific pre- or postsynaptic locations. While many of the factors that mediate this distribution are yet to be determined, as discussed below, recent data suggest that structural aspects of the receptor subunits, the presence of Neto auxiliary proteins in the KAR complex and the secreted C1q-like proteins play important roles in these processes (Fig. 2).

Postsynaptic KARs

Role of the GluK2 C-Terminus in Synaptic Localisation

In the cerebellum, KARs are located post-synaptically on cerebellar granule cells, which receive inputs from mossy fibres. These receptors comprise GluK2/5 and the auxiliary subunit Neto2 [76] (see below). Synaptic localisation of this complex is dependent on the GluK2 subunit, since ablation

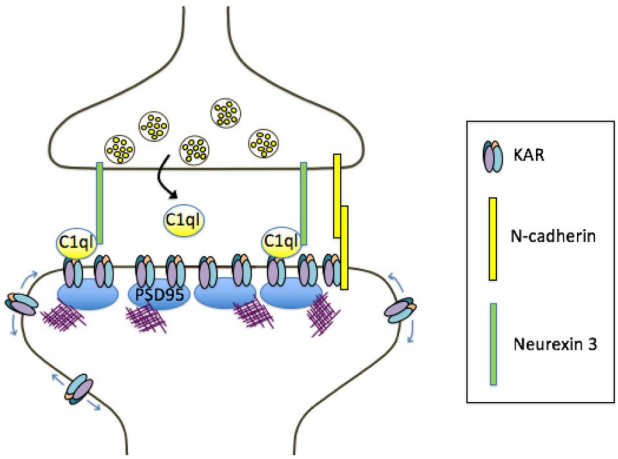

Fig. 2 Mechanisms of KAR synaptic localisation. At mossy fibre-CA3 (MF-CA3) synapses, presynaptically released C1ql proteins cluster KARs through binding to KAR subunit extracellular domains, and forming a tripartite trans-synaptic complex with presynaptic neurexin 3. KAR synaptic incorporation is also promoted through interactions between the GluK2 C-terminus and the trans-synaptic adhesion molecule N-cadherin, and through interactions between the C-termini of GluK1, GluK2 and GluK5 (and potentially Neto1) and PSD95

of GluK5 or Neto2 has no effect on levels of GluK2/Neto2 or GluK2/GluK5, respectively, in the postsynaptic density (PSD) fraction [76, 77]. Furthermore, knock-in mice in which the intracellular C-terminus of GluK2 is replaced with the C-terminus of the AMPAR subunit GluA1 do not exhibit synaptic KAR responses in cerebellar slices [77]. Notably, whole cell KAR currents were unaffected, demonstrating a specific role for the GluK2 C-terminus in synaptic incorporation of KARs at cerebellar synapses but not in receptor surface expression [77]. Furthermore, these mice show reduced postsynaptic KAR responses at MF-CA3 synapses in the hippocampus, the prototypical KAR-containing synapse in the brain, but no reduction in total KAR responses, again indicating a specific role for the GluK2 C-terminus in synaptic incorporation, but not surface expression, of KARs [77].

Roles of GluK4 and GluK5 in the Synaptic Specificity of KARs

While the C-terminus of GluK2 seems to be necessary for synaptic incorporation, synapse specificity in the hippocampus has been shown to be dependent on the GluK4 and GluK5 subunits. Postsynaptic KARs at MF-CA3 synapses are lost in mice lacking both of these subunits [78]. Moreover, in GluK4/5$^{-/-}$ mice there is a redistribution of GluK2 immunolabelling to more distal dendrites in CA3 pyramidal neurons [77], suggesting GluK4/5 are crucial determinants of the synapse specificity of KARs in the hippocampus. Interestingly, viral re-expression of GluK5 in the

hippocampus of GluK4/5$^{-/-}$ mice rescued GluK2 signal in stratum lucidum, but this did not occur for a GluK5 chimera in which the extracellular N-terminus was replaced with that of GluK2 [77], which the authors attribute to the ability of the N-terminus of GluK5 to bind to the mossy fibre-enriched C1q-like proteins (see below).

Proteins that Interact with KARs to Define Postsynaptic Localisation

N-Cadherin

The fact that MF-CA3 synapses in GluK2$^{-/-}$ mice lack postsynaptic KAR responses [79] has allowed examination of the factors required for their effective synaptic positioning by re-expressing wild-type or mutant GluK2 in CA3 neurons. The last 20 amino acids of GluK2 are required for KAR incorporation at MF-CA3 synapses [80] and this region mediates interactions between GluK2 and the neuronal cell adhesion molecule N-cadherin [81]. At MF-CA3 synapses in wild-type mice, expression of a dominant-negative N-cadherin reduced KAR EPSCs, as did knockdown of N-cadherin mediated by expression of Cre recombinase in CA3 cells from N-cadherin floxed mice [80]. Together, these findings demonstrate GluK2 binding to N-cadherin is a key determinant of GluK2 recruitment to MF-CA3 synapses.

PSD95

The synaptic scaffold protein PSD95 binds to the C-terminal PDZ ligands of the core KAR subunits GluK1, GluK2 and GluK5 [82, 83]. PSD95 also binds to the auxiliary subunit Neto1 [84], and accelerates the recovery of GluK2 from desensitisation [85]. The KAR component of the EPSC at MF-CA3 synapses is reduced in PSD95 knockout mice, suggesting a role for this interaction in KAR synaptic localisation [86]. However, whether this is due to direct binding of KARs to PSD95 and, if it is, which subunits are responsible, remains to be determined. Moreover, as discussed below, regulation of the interaction between GluK5 and PSD95 is required for long-term depression (LTD) of KARs at MF-CA3 synapses [87].

C1ql

The C1q-like proteins are a family of secreted synaptic organisers [88]. Two members of this family, C1ql2 and C1ql3, are highly expressed by hippocampal mossy fibres and contribute to the localisation of KARs to mossy fibre synapses in CA3 neurons [77, 89]. In heterologous cells, C1ql2 and 3 bind to the N-terminal domains of GluK2 and GluK4 [89], although another study instead observed binding to GluK5 [77]. C1ql2 and 3 are present at MF-CA3 synapses, and their levels are reduced in slices from GluK2$^{-/-}$ or GluK4$^{-/-}$ mice, suggesting GluK2 and GluK4 act as binding sites for C1ql2/3 [89]. Moreover, GluK2/3 immunoreactivity is markedly decreased in CA3 stratum lucidum in C1ql2/3 knockout mice, and KAR EPSCs at MF-CA3 synapses are reduced to levels similar to those observed in GluK2$^{-/-}$ mice. The presynaptic adhesion molecule neurexin 3 binds to secreted C1ql2/3 and a neurexin 3-C1ql-KAR complex was isolated in co-cultures of HEK293 cells expressing neurexin 3 and C1ql2/3 and neurons [89]. Thus, specific secretion of C1ql proteins at mossy fibres provides the basis for a trans-synaptic complex that clusters KARs postsynaptically at MF-CA3 synapses (Fig. 2).

Neto1 and Neto2

Neto1 and Neto2 are single pass transmembrane proteins that associate with KAR complexes through binding to the GluK1-3 subunits [90, 91]. Neto1 is expressed abundantly in the hippocampus and is a component of postsynaptic KARs at MF-CA3 synapses [91] whereas Neto2 is more highly expressed in the cerebellum [90]. The effects of Neto proteins on KAR channel properties have been studied extensively (reviewed in [92–95]), but, briefly, Neto proteins generally slow the deactivation kinetics of KARs, which accounts for their different properties in vivo compared to exogenously expressed KARs in cell lines that do not contain Netos. Furthermore, it has also recently been shown that Neto proteins control the function of both somatodendritic and presynaptic KARs in somatostatin, cholecystokinin/cannabinoid receptor 1, and parvalbumin-containing interneurons to regulate neuronal network inhibition [96]. However, as outlined below, how Neto proteins affect the trafficking and synaptic incorporation of KARs is less well established with the current literature containing apparently contradictory results.

Netos and GluK2

Initial studies observed no effect of Neto1 or Neto2 in mediating surface expression of GluK2 in heterologous systems [90, 91] nor any effects on the abundance of GluK2 or GluK5 in PSD fractions from Neto1 knockout mice [91]. Furthermore, co-expression of Neto1 or Neto2 did not enhance exogenous KAR responses in CA1 pyramidal neurons, which normally lack postsynaptic KAR EPSCs, arguing against a role for Netos in synaptic incorporation of GluK2-containing KARs [9]. Other studies, however, reported a reduction in synaptic GluK2 in the hippocampus of Neto1 knockout mice [97, 98], and from cerebellar PSD fractions from Neto2 knockout mice [99], supporting a role for Neto proteins in the synaptic targeting of GluK2.

Moreover, recent studies have reported that Neto1 and Neto2 enhance GluK2 surface expression in HEK293 cells [100] and that injection of Neto2 with GluK2 into oocytes potentiates GluK2 surface expression [77]. Given these apparently contradictory results, the precise roles of Neto proteins in the trafficking and targeting of GluK2-containing KARs remains to be defined.

Netos and GluK1

Neto proteins have also been reported to be involved in the trafficking of GluK1-containing KARs. Transfection of Neto2 with GluK1 promotes GluK1 surface expression in both COS-7 cells and cultured hippocampal neurons, and drives the synaptic incorporation of GluK1-containing KARs [101]. Consistent with this role, co-transfection of either Neto1 or Neto2 with GluK1 in CA1 pyramidal cells in hippocampal slice cultures enhances GluK1 surface expression and synaptic targeting [9, 102]. It should be noted, however, that since these studies rely on overexpression of KAR subunits in cells that do not usually express GluK1 [6, 103] or exhibit synaptic KAR responses [6–8], the relevance of Neto proteins to GluK1 trafficking *in vivo* requires further examination.

Overall, although there is not yet a clear consensus, accumulating evidence suggests Neto proteins do influence surface expression and synaptic targeting of KARs under some circumstances. The apparently conflicting data regarding the roles of Netos in KAR trafficking and synaptic positioning can, at least in part, be attributed to the use of different model systems, clonal cell lines and neuronal subtypes, and experimental conditions. Thus, the current inconsistencies may reflect a complex relationship between Netos and KARs, which can be affected differential subunit expression and the availability of cell type-specific interacting proteins. Moreover, GluK2 is subject to multiple, coordinated post-translational modifications (PTMs) including phosphorylation [75], SUMOylation [67, 69], ubiquitination [104, 105] and palmitoylation [71, 106], each of which could potentially directly or indirectly influence the actions of Netos. Clearly, further work is required to will determine the molecular mechanisms, under what circumstances, and for which subunit combinations Netos regulate KAR trafficking and targeting in vivo.

KAR Post-translational Modifications and Post-synaptic Localisation

CaMKII Phosphorylation of GluK5

LTD of KARs at MF-CA3 synapses is induced by a spike timing-, Ca^{2+} influx-, and CaMKII-dependent plasticity mechanism, which is absent in slices from GluK5$^{-/-}$ mice [87]. CaMKII phosphorylates the C-terminal domain of GluK5 in vitro and a phosphomimetic mutation enhances surface expression, but reduces synaptic localisation, in neurons. GluK5 phosphorylation enhances lateral mobility and reduces the interaction between GluK5 and PSD95. Moreover, while re-expression of GluK5 in GluK5$^{-/-}$ slices restored KAR-LTD, expression of a non-phosphorylatable GluK5 did not, demonstrating that direct phosphorylation of GluK5 by CaMKII is required for this form of KAR LTD [87]. Thus, these data indicate that CaMKII phosphorylation of GluK5-containing KARs regulates their synaptic localisation by antagonising the interaction between GluK5 and PSD95 (Fig. 3).

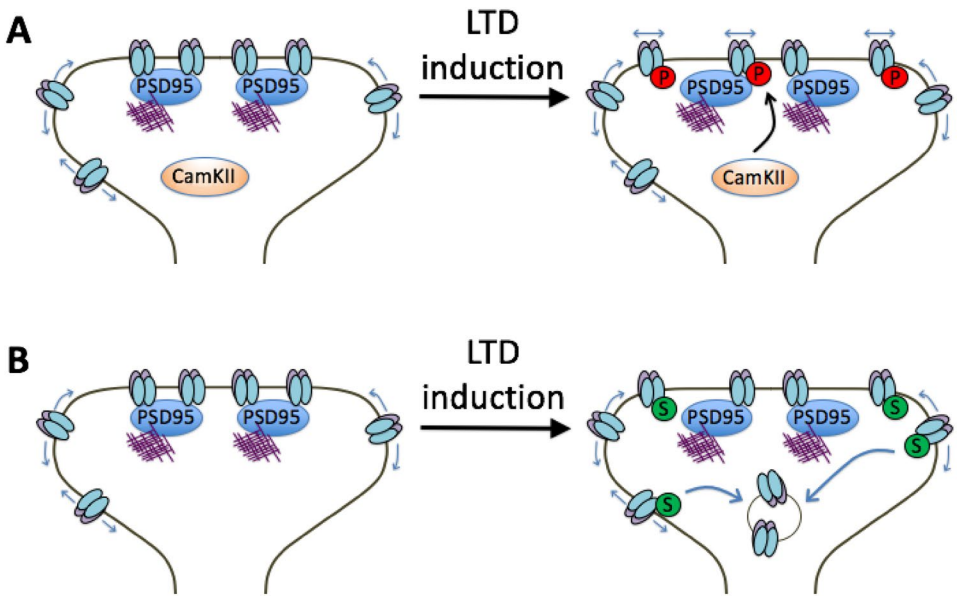

Fig. 3 Mechanisms of KAR-LTD. **a** At MF-CA3 synapses, LTD induction leads to CaMKII-mediated phosphorylation of the GluK5 subunit, reducing its ability to bind PSD95. This reduced anchoring of GluK5-containing KARs promotes their lateral mobility and diffusion away from the postsynapse, resulting in LTD of KAR EPSCs. **b** An alternative LTD mechanism results in PKC-dependent phosphorylation (not shown) and subsequent SUMOylation of the GluK2 subunit. This then leads to endocytosis of GluK2-containing KARs and LTD of KAR-mediated synaptic transmission

PKC Phosphorylation of GluK2

PKC phosphorylation of GluK2 at S846 and S868 regulates the surface expression of GluK2-containing KARs at several levels. It affects both GluK2 transit through the secretory pathway [48, 75] and KAR endocytosis and recycling back to the plasma membrane [15, 75]. Phosphorylation of S846 promotes basal internalisation of GluK2-containing KARs in both HeLa cells and neurons [75], potentially via regulating the interaction between GluK2 and 4.1 proteins [71]. Furthermore, phosphorylation of both sites occurs in response to kainate stimulation of cultured neurons, and phosphorylation at S868 is required for agonist-induced endocytosis of GluK2, by promoting SUMOylation at lysine 886 [15, 69, 107] (see below). It should be noted, however, that PKC phosphorylation of S868 also appears to be involved in recycling of endocytosed GluK2 back to the plasma membrane [15], suggesting that whether phosphorylation of S868 promotes insertion or removal of GluK2 from the plasma membrane is likely to be context-dependent.

SUMOylation

SUMOylation is a post-translational modification that results from the conjugation of a member of the ~ 11kD SUMO family to lysine residues in substrate proteins [108]. GluK2 is SUMOylated at a single lysine residue in its intracellular C-terminus, K886, resulting in agonist-induced internalisation of GluK2-containing KARs [67]. Infusion of the catalytic domain of the deSUMOylating enzyme SENP1 increases KAR currents at MF-CA3 synapses, highlighting SUMOylaton as an endogenous regulator of the number of synaptic KARs [67]. Subsequent studies have demonstrated that SUMOylation of GluK2 is enhanced by prior PKC-mediated phosphorylation of serine 868 and is required for LTD of kainate receptors at MF-CA3 synapses [15, 69].

Ubiquitination

One major functions of protein ubiquitination is to target proteins for lysosomal or proteasomal degradation [109]. A recent study identified that the Parkinson's disease-associated ubiquitin ligase Parkin directly interacts with and ubiquitinates the C-terminus of GluK2 [105]. Parkin ubiquitinates GluK2 in both heterologous cells and cultured neurons, and knockdown of Parkin increased GluK2 surface expression and increased vulnerability of hippocampal neurons to kainate-induced excitotoxicity. Furthermore, in a mouse model of autosomal recessive juvenile Parkinson's expressing a truncated form of Parkin, there are increased levels of GluK2 in substantia nigra and corresponding increases in cortex samples from human patients expressing mutations in Parkin [105]. Thus, GluK2 is a Parkin target that may contribute to the excitotoxic cell death of substantia nigra neurons in Parkinson's disease.

KARs in Plasticity

KARs are involved in both excitatory and inhibitory neurotransmission, controlling both short and longer-term plasticity. These properties have been extensively reviewed [2, 11] and we confine our discussion largely to the most recent findings relating to the role of postsynaptic KARs as inducers of long-term plasticity.

KAR Regulation of Excitatory Neurotransmission

Presynaptic KARs decrease glutamate release at CA3-CA1 pyramidal cell synapses [110–112]. Intriguingly, however, KARs have also been shown to facilitate glutamate release upon application of nanomolar concentrations of kainate. This facilitation of glutamate release requires KAR activation resulting in the accumulation of presynaptic calcium, the production of Ca^{2+}–calmodulin complexes and the activation adenylate cyclase and PKA [113–115]. Thus, at certain synapses, KARs can exert bidirectional modulatory actions on glutamate release related to the extent of their activation (for recent review see [3]).

Postsynaptic KARs at MF-CA3 synapses undergo plastic changes, and exhibit several forms of LTD that can be induced by different stimulation protocols [15, 87]. Chamberlain et al. showed that SUMOylation of GluK2 is required for activity-dependent long-term depression of kainate receptor-mediated synaptic transmission (KAR LTD). They We further demonstrated that a critical trigger for SUMOylation is GluK2 phosphorylation by protein kinase C (PKC) and that this sequence of events is required for KAR LTD and that SUMOylation can act as the switch between enhanced or decreased surface expression of KARs after PKC phosphorylation [15].

Furthermore, in cultured neurons, activity-dependent up- or down-regulation of surface KARs can be induced by differential agonist application protocols [13, 68]. KAR surface expression is also subject to homeostatic plasticity and can be 'scaled' by manipulating neuronal excitability [48]. Intriguingly, beyond being regulated by plasticity themselves, there is a growing appreciation that KARs also function as postsynaptic inducers of synaptic plasticity (Fig. 3).

Recently, a novel form of AMPAR-LTP was discovered at CA3-CA1 synapses that is mediated by activation of postsynaptic KARs ($KAR\text{-}LTP_{AMPAR}$ [16]). Despite the fact that CA1 pyramidal cells exhibit essentially no postsynaptic KAR EPSCs [6, 8, 9, 102, 116], activation of postsynaptic KARs by high-frequency stimulation of Schaffer collaterals inhibits a slow after-hyperpolarization current that regulates

excitability in hippocampus (IsAHP) through a metabotropic cascade [117, 118], suggesting receptors are postsynaptically localised. Remarkably, however, at these synapses, KARs, which have a classical ion channel structure, signal primarily through a G protein-dependent pathway (for review see [17]).

Consistent with this, stimulation protocols that activate postsynaptic KARs on CA1 neurons induce LTP of AMPARs via a metabotropic signalling pathway [16]. GluK2$^{-/-}$ mice lack this novel form of plasticity, indicating an absolute requirement for this subunit in induction of KAR-LTP$_{AMPAR}$ (Fig. 4). Similar to inhibition of IsAHP, KAR-LTP$_{AMPAR}$ is mediated by activation of pertussis toxin-sensitive G-proteins, and requires activation of PKC and PLC. Furthermore, similar to LTP induced by activation of NMDARs, KAR-LTP$_{AMPAR}$ is mediated by an increase in surface AMPARs supplied by recruitment of recycling endosomes to spines and also leads to structural plasticity, as determined by an increase in spine size and maturation [16].

Thus, although the exact mechanisms are still to be determined, it is clear that KAR metabotropic signalling plays a key role in directly mediating certain forms of AMPAR-mediated plasticity at CA1 synapses.

KAR Regulation of Inhibitory Neurotransmission

KAR Regulation of GABA Release

An important facet of KAR physiology is that they coordinate and regulate neuronal and network activity via regulation of both excitatory and inhibitory transmission. Presynaptic KARs downregulate GABA release from interneurons in the hippocampus through a metabotropic PKC and PLC dependent pathway that reduces inhibitory postsynaptic currents (IPSCs) [119].

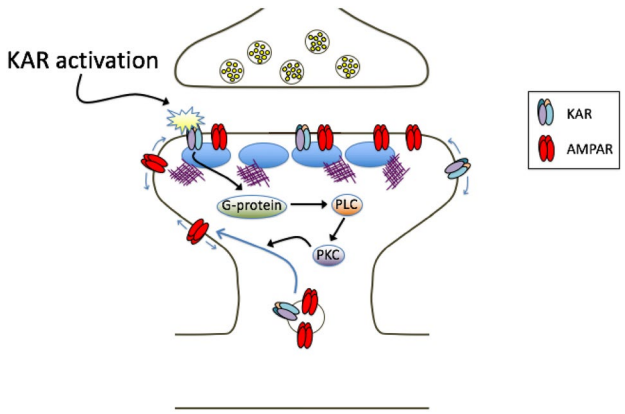

Fig. 4 Mechanism of KAR-LTP$_{AMPAR}$. At CA3-CA1 synapses, activation of postsynaptic KARs leads to LTP of AMPAR-mediated synaptic transmission. This occurs through KAR-mediated activation of a pertussis toxin-sensitive G protein, activation of phospholipase C (PLC), PKC, and increased exocytosis of AMPARs from recycling endosomes

KARs and GABA$_A$Rs

Moreover, postsynaptic KAR metabotropic signalling depresses synaptic GABA$_A$Rs while at the same time potentiating extrasynaptic GABA$_A$Rs, in a process that decreases synaptic inhibitory drive to facilitate synaptic plasticity, while simultaneously protecting against neuronal over-excitation by promoting extrasynaptic inhibition [120].

KARs and KCC2

In addition to this direct effect on GABA$_A$R-mediated transmission, KARs separately regulate the potassium-chloride cotransporter KCC2. KCC2 is crucial because it establishes the electrochemical chloride gradient for postsynaptic inhibition through GABA$_A$Rs [121, 122] and its dysregulation is implicated in autism spectrum disorder (ASD; [123]) and epilepsy [124]. KCC2 interacts with both Neto2 [125] and GluK2 [126], which increase the total abundance and enhance surface expression of KCC2 [14]. KCC2 and GluK2 form macromolecular assemblies that traffic together, and this complex regulates intraneuronal chloride homeostasis to support GABA$_A$R-mediated transmission [126]. In addition, this process is further controlled by phosphorylation of serines 846 and 868 in GluK2 to determine surface KCC2 levels [14]. These findings establish clear roles for KARs as modulators of postsynaptic inhibitory transmission.

KARs in Disease

Dysregulation of common molecular pathways underlies multiple neurological and neurodegenerative diseases and there is mounting evidence that KAR dysfunction could be one such feature (reviewed in [127, 128]).

Epilepsy

KAR dysfunction is particularly closely associated with temporal lobe epilepsy (TLE) [129], and GluK2$^{-/-}$ mice exhibit significantly fewer seizures than wild-type counterparts [79]. TLE is associated with abnormal sprouting of recurrent mossy fibres, which synapse onto dentate gyrus cells [130–132] and this abnormal sprouting is also reduced in GluK2$^{-/-}$ mice [133]. Consistent with the requirement for recruitment of KARs to postsynaptic sites for seizure activity, despite induction of MF sprouting in an animal model of TLE, C1ql2/3 double KO mice are resistant to seizures [89] and genetic silencing of KARs at CA3 synapses attenuates kainate-induced seizures [134]. Together, these

studies suggest that recurrent synaptic activity, mediated by postsynaptic KARs, drives seizure activity in TLE, and highlights KARs as an attractive therapeutic target in the treatment of this disorder.

KARs and Other Neurological Disorders

In addition to TLE, both gain [135] and loss [136, 137] of GluK2 have been reported to lead to ASD-like phenotypes. Furthermore, duplication of the GluK4 gene has been associated with autism [138] and, consistent with this, overexpression of GluK4 in the forebrain of mice causes severe anxiety and ASD-like behaviours [139]. Additionally, GluK4 has been linked with treatment-resistant depression [140], and disruption of the gene encoding GluK4 has been observed in a patient with schizophrenia and mental retardation [141].

Most recently it has been reported that complete ablation of all KAR subunits results in disrupted corticostriatal function and dramatic obsessive-compulsive-like behaviour with severe self-grooming [142]. Together with the previous studies, these new observations support the notion that KAR-mediated control of network activity is a key determinant of higher brain function, and that disruption of these pathways can lead to multiple neurological disorders.

Perspectives

Although historically much less studied than AMPARs or NMDARs, there is a currently a renaissance in KAR research fuelled by the realisation that they are multifunctional neuronal modulators that have roles in health and disease far beyond those previously appreciated.

To understand how KARs exert these regulatory effects, it is necessary to define how KARs themselves are controlled and how they interact with, and regulate, other proteins and systems. Furthermore, while there is a growing appreciation of the multifaceted roles played by KARs, a number of fundamental questions remain unanswered. For example, while it is widely-accepted that KARs can signal both ionotropically and metabotropically through G-proteins, how this dual signaling occurs, and what determines which 'mode' of signaling an individual KAR complex utilizes remains almost entirely unexplored. In addition, while we are beginning to understand the molecular events that control the specific distribution and synaptic localization of KARs, how these mechanisms cooperate to orchestrate the highly selective distribution of KARs in the brain remains an important unanswered question. Finally, although KARs can induce plasticity of AMPARs, exactly how this occurs, how widespread this form of plasticity is in the brain, and whether postsynaptic KARs can direct other forms of bidirectional synaptic plasticity remain unknown.

We expect that further studies examining how KAR localisation and signalling at pre- and postsynaptic sites impacts on neuronal function will answer many of these remaining questions, and will transform our understanding of the roles KARs play in development, plasticity and disease.

References

1. Sihra TS, Flores G, Rodriguez-Moreno A (2014) Kainate receptors: multiple roles in neuronal plasticity. Neuroscientist 20:29–43
2. Carta M, Fievre S, Gorlewicz A, Mulle C (2014) Kainate receptors in the hippocampus. Eur J Neurosci 39:1835–1844
3. Sihra TS, Rodriguez-Moreno A (2013) Presynaptic kainate receptor-mediated bidirectional modulatory actions: mechanisms. Neurochem Int 62:982–987
4. Lerma J, Marques JM (2013) Kainate receptors in health and disease. Neuron 80:292–311
5. Ruano D, Lambolez B, Rossier J, Paternain AV, Lerma J (1995) Kainate receptor subunits expressed in single cultured hippocampal neurons: molecular and functional variants by RNA editing. Neuron 14:1009–1017
6. Bureau I, Bischoff S, Heinemann SF, Mulle C (1999) Kainate receptor-mediated responses in the CA1 field of wild-type and GluR6-deficient mice. J Neurosci 19:653–663
7. Castillo PE, Malenka RC, Nicoll RA (1997) Kainate receptors mediate a slow postsynaptic current in hippocampal CA3 neurons. Nature 388:182–186
8. Granger AJ, Shi Y, Lu W, Cerpas M, Nicoll RA (2013) LTP requires a reserve pool of glutamate receptors independent of subunit type. Nature 493:495–500
9. Sheng N, Shi YS, Lomash RM, Roche KW, Nicoll RA (2015) Neto auxiliary proteins control both the trafficking and biophysical properties of the kainate receptor GluK1. eLife 4:e11682
10. Sheng N, Shi YS, Nicoll RA (2017) Amino-terminal domains of kainate receptors determine the differential dependence on Neto auxiliary subunits for trafficking. Proc Natl Acad Sci USA 114:1159–1164
11. Lerma J (2003) Roles and rules of kainate receptors in synaptic transmission. Nat Rev Neurosci 4:481–495
12. Lourenco J, Matias I, Marsicano G, Mulle C (2011) Pharmacological activation of kainate receptors drives endocannabinoid mobilization. J Neurosci 31:3243–3248
13. Gonzalez-Gonzalez IM, Henley JM (2013) Postsynaptic kainate receptor recycling and surface expression are regulated by metabotropic autoreceptor signalling. Traffic 14:810–822
14. Pressey JC, Mahadevan V, Khademullah CS, Dargaei Z, Chevrier J, Ye W, Huang M, Chauhan AK, Meas SJ, Uvarov P, Airaksinen MS, Woodin MA (2017) A kainate receptor subunit promotes the recycling of the neuron-specific K^+-Cl^- co-transporter KCC2 in hippocampal neurons. J Biol Chem 292:6190–6201
15. Chamberlain SE, Gonzalez-Gonzalez IM, Wilkinson KA, Konopacki FA, Kantamneni S, Henley JM, Mellor JR (2012) SUMOylation and phosphorylation of GluK2 regulate

kainate receptor trafficking and synaptic plasticity. Nat Neurosci 15:845–852
16. Petrovic MM, Viana da Silva S, Clement JP, Vyklicky L, Mulle C, Gonzalez-Gonzalez IM, Henley JM (2017) Metabotropic action of postsynaptic kainate receptors triggers hippocampal long-term potentiation. Nat Neurosci 20:529–539
17. Valbuena S, Lerma J (2016) Non-canonical signaling, the hidden life of ligand-gated ion channels. Neuron 92:316–329
18. Bettler B, Boulter J, Hermans-Borgmeyer I, O'Shea-Greenfield A, Deneris ES, Moll C, Borgmeyer U, Hollmann M, Heinemann S (1990) Cloning of a novel glutamate receptor subunit, GluR5: expression in the nervous system during development. Neuron 5:583–595
19. Egebjerg J, Bettler B, Hermans-Borgmeyer I, Heinemann S (1991) Cloning of a cDNA for a glutamate receptor subunit activated by kainate but not AMPA. Nature 351:745–748
20. Collingridge GL, Olsen RW, Peters J, Spedding M (2009) A nomenclature for ligand-gated ion channels. Neuropharmacology 56:2–5
21. Hughes TE (1994) Transmembrane topology of the glutamate receptors. A tale of novel twists and turns. J Mol Neurosci 5:211–217
22. Karakas E, Regan MC, Furukawa H (2015) Emerging structural insights into the function of ionotropic glutamate receptors. Trends Biochem Sci 40:328–337
23. Mollerud S, Frydenvang K, Pickering DS, Kastrup JS (2017) Lessons from crystal structures of kainate receptors. Neuropharmacology 112:16–28
24. Zhu S, Gouaux E (2017) Structure and symmetry inform gating principles of ionotropic glutamate receptors. Neuropharmacology 112:11–15
25. Meyerson JR, Chittori S, Merk A, Rao P, Han TH, Serpe M, Mayer ML, Subramaniam S (2016) Structural basis of kainate subtype glutamate receptor desensitization. Nature 537:567–571
26. Werner P, Voigt M, Keinanen K, Wisden W, Seeburg PH (1991) Cloning of a putative high-affinity kainate receptor expressed predominantly in hippocampal CA3 cells. Nature 351:742–744
27. Herb A, Burnashev N, Werner P, Sakmann B, Wisden W, Seeburg PH (1992) The KA-2 subunit of excitatory amino acid receptors shows widespread expression in brain and forms ion channels with distantly related subunits. Neuron 8:775–785
28. Kumar J, Schuck P, Mayer ML (2011) Structure and assembly mechanism for heteromeric kainate receptors. Neuron 71:319–331
29. Bettler B, Boulter J, Hermansborgmeyer I, Osheagreenfield A, Deneris ES, Moll C, Borgmeyer U, Hollmann M, Heinemann S (1990) Cloning of a novel glutamate receptor subunit, GluR5—expression in the nervous system during development. Neuron 5:583–595
30. Sommer B, Burnashev N, Verdoorn TA, Keinanen K, Sakmann B, Seeburg PH (1992) A glutamate receptor channel with high affinity for domoate and kainate. EMBO J 11:1651–1656
31. Pinheiro P, Mulle C (2006) Kainate receptors. Cell Tissue Res 326:457–482
32. Schiffer HH, Swanson GT, Heinemann SF (1997) Rat GluR7 and a corboxy terminal splice variant, GluR7b, are functional kainate receptor subunits with a low sensitivity to glutamate. Neuron 19:1141–1146
33. Jaskolski F, Coussen F, Nagarajan N, Normand E, Rosenmund C, Mulle C (2004) Subunit composition and alternative splicing regulate membrane delivery of kainate receptors. J Neurosci 24:2506–2515
34. Pahl S, Tapken D, Haering SC, Hollmann M (2014) Trafficking of kainate receptors. Membranes 4:565–595
35. Ren Z, Riley NJ, Needleman LA, Sanders JM, Swanson GT, Marshall J (2003) Cell surface expression of GluR5 kainate receptors is regulated by an endoplasmic reticulum retention signal. J Biol Chem 278:52700–52709
36. Coussen F, Perrais D, Jaskolski F, Sachidhanandam S, Normand E, Bockaert J, Marin P, Mulle C (2005) Co-assembly of two GluR6 kainate receptor splice variants within a functional protein complex. Neuron 47:555–566
37. Jaskolski F, Normand E, Mulle C, Coussen F (2005) Differential trafficking of GluR7 kainate receptor subunit splice variants. J Biol Chem 280:22968–22976
38. Egebjerg J, Kukekov V, Heinemann SF (1994) Intron sequence directs RNA editing of the glutamate receptor subunit GluR2 coding sequence. Proc Natl Acad Sci USA 91:10270–10274
39. Howe JR (1996) Homomeric and heteromeric ion channels formed from the kainate type subunits GluR6 and KA2 have very small, but different unitary conductances. J Neurophysiol 76:510–519
40. Vissel B, Royle GA, Christie BR, Schiffer HH, Ghetti A, Tritto T, Perez-Otano I, Radcliffe RA, Seamans J, Sejnowski T, Wehner JM, Collins AC, O'Gorman S, Heinemann SF (2001) The role of RNA editing of kainate receptors in synaptic plasticity and seizures. Neuron 29:217–227
41. Ball SM, Atlason PT, Shittu-Balogun OO, Molnar E (2010) Assembly and intracellular distribution of kainate receptors is determined by RNA editing and subunit composition. J Neurochem 114:1805–1818
42. Bernard A, Khrestchatisky M (1994) Assessing the extent of RNA editing in the TMII regions of Glur5 and Glur6 kainate receptors during rat brain development. J Neurochem 62:2057–2060
43. Schmitt J, Dux E, Gissel C, Paschen W (1996) Regional analysis of developmental changes in the extent of GluR6 mRNA editing in rat brain. Brain Res Dev Brain Res 91:153–157
44. Bernard A, Ferhat L, Dessi F, Charton G, Represa A, Ben-Ari Y, Khrestchatisky M (1999) Q/R editing of the rat GluR5 and GluR6 kainate receptors in vivo and in vitro: evidence for independent developmental, pathological and cellular regulation. Eur J Neurosci 11:604–616
45. Nishikura K (2016) A-to-I editing of coding and non-coding RNAs by ADARs. Nat Rev Mol Cell Biol 17:83–96
46. Behm M, Wahlstedt H, Widmark A, Eriksson M, Ohman M (2017) Accumulation of nuclear ADAR2 regulates adenosine-to-inosine RNA editing during neuronal development. J Cell Sci 130:745–753
47. Filippini A, Bonini D, La Via L, Barbon A (2016) The good and the bad of glutamate receptor RNA editing. Mol Neurobiol
48. Evans AJ, Gurung S, Wilkinson KA, Stephens DJ, Henley JM (2017) Assembly, secretory pathway trafficking, and surface delivery of kainate receptors is regulated by neuronal activity. Cell Rep 19:2613–2626
49. Tashiro A, Dunaevsky A, Blazeski R, Mason CA, Yuste R (2003) Bidirectional regulation of hippocampal mossy fiber filopodial motility by kainate receptors. A two-step model of synaptogenesis. Neuron 38:773–784
50. Sakha P, Vesikansa A, Orav E, Heikkinen J, Kukko-Lukjanov TK, Shintyapina A, Franssila S, Jokinen V, Huttunen HJ, Lauri SE (2016) Axonal kainate receptors modulate the strength of efferent connectivity by regulating presynaptic differentiation. Front Cell Neurosci. https://doi.org/10.3389/fncel.2016.00003
51. Contractor A, Mulle C, Swanson GT (2011) Kainate receptors coming of age: milestones of two decades of research. Trends Neurosci 34:154–163
52. Bramham CR, Wells DG (2007) Dendritic mRNA: transport, translation and function. Nat Rev Neurosci 8:776–789

53. Doyle M, Kiebler MA (2011) Mechanisms of dendritic mRNA transport and its role in synaptic tagging. EMBO J 30:3540–3552
54. Holt CE, Schuman EM (2013) The central dogma decentralized: new perspectives on RNA function and local translation in neurons. Neuron 80:648–657
55. Ho VM, Dallalzadeh LO, Karathanasis N, Keles MF, Vangala S, Grogan T, Poirazi P, Martin KC (2014) GluA2 mRNA distribution and regulation by miR-124 in hippocampal neurons. Mol Cell Neurosci 61:1–12
56. Buxbaum AR, Yoon YJ, Singer RH, Park HY (2015) Single-molecule insights into mRNA dynamics in neurons. Trends Cell Biol 25:468–475
57. Rangaraju V, Tom Dieck S, Schuman EM (2017) Local translation in neuronal compartments: how local is local? EMBO Rep 18:693–711
58. Horton AC, Ehlers MD (2004) Secretory trafficking in neuronal dendrites. Nat Cell Biol 6:585–591
59. Cui-Wang T, Hanus C, Cui T, Helton T, Bourne J, Watson D, Harris KM, Ehlers MD (2012) Local zones of endoplasmic reticulum complexity confine cargo in neuronal dendrites. Cell 148:309–321
60. Quassollo G, Wojnacki J, Salas DA, Gastaldi L, Marzolo MP, Conde C, Bisbal M, Couve A, Caceres A (2015) A RhoA signaling pathway regulates dendritic golgi outpost formation. Curr Biol 25:971–982
61. Valenzuela JI, Perez F (2015) Diversifying the secretory routes in neurons. Front Neurosci 9:358
62. Hanus C, Geptin H, Tushev G, Garg S, Alvarez-Castelao B, Sambandan S, Kochen L, Hafner AS, Langer JD, Schuman EM (2016) Unconventional secretory processing diversifies neuronal ion channel properties. eLife 5, e20609
63. Kacharmina JE, Job C, Crino P, Eberwine J (2000) Stimulation of glutamate receptor protein synthesis and membrane insertion within isolated neuronal dendrites. Proc Natl Acad Sci USA 97:11545–11550
64. Grooms SY, Noh KM, Regis R, Bassell GJ, Bryan MK, Carroll RC, Zukin RS (2006) Activity bidirectionally regulates AMPA receptor mRNA abundance in dendrites of hippocampal neurons. J Neurosci 26:8339–8351
65. Boncompain G, Perez F (2012) Synchronizing protein transport in the secretory pathway. Curr Protoc Cell Biol. https://doi.org/10.1002/0471143030.cb1519s57
66. Boncompain G, Perez F (2014) Synchronization of secretory cargos trafficking in populations of cells. Methods Mol Biol 1174:211–223
67. Martin S, Nishimune A, Mellor JR, Henley JM (2007) SUMOylation regulates kainate-receptor-mediated synaptic transmission. Nature 447:321–325
68. Martin S, Bouschet T, Jenkins EL, Nishimune A, Henley JM (2008) Bidirectional regulation of kainate receptor surface expression in hippocampal neurons. J Biol Chem 283:36435–36440
69. Konopacki FA, Jaafari N, Rocca DL, Wilkinson KA, Chamberlain S, Rubin P, Kantamneni S, Mellor JR, Henley JM (2011) Agonist-induced PKC phosphorylation regulates GluK2 SUMOylation and kainate receptor endocytosis. Proc Natl Acad Sci USA 108:19772–19777
70. González-González IM, Konopaki F, Rocca DL, Doherty AJ, Jaafari N, Wilkinson KA, Henley JM (2012) Kainate receptor trafficking. WIRES Membr Transp Signal 1:31–44
71. Copits BA, Swanson GT (2013) Kainate receptor post-translational modifications differentially regulate association with 4.1N to control activity-dependent receptor endocytosis. J Biol Chem 288:8952–8965
72. Pick JE, Khatri L, Sathler MF, Ziff EB (2016) mGluR long-term depression regulates GluA2 association with COPII vesicles and exit from the endoplasmic reticulum. EMBO J. https://doi.org/10.15252/embj.201694526
73. Hanus C, Kochen L, Tom Dieck S, Racine V, Sibarita JB, Schuman EM, Ehlers MD (2014) Synaptic control of secretory trafficking in dendrites. Cell Rep 7:1771–1778
74. Vivithanaporn P, Yan S, Swanson GT (2006) Intracellular trafficking of KA2 kainate receptors mediated by interactions with coatomer protein complex I (COPI) and 14–3-3 chaperone systems. J Biol Chem 281:15475–15484
75. Nasu-Nishimura Y, Jaffe H, Isaac JT, Roche KW (2010) Differential regulation of kainate receptor trafficking by phosphorylation of distinct sites on GluR6. J Biol Chem 285:2847–2856
76. Yan D, Yamasaki M, Straub C, Watanabe M, Tomita S (2013) Homeostatic control of synaptic transmission by distinct glutamate receptors. Neuron 78:687–699
77. Straub C, Noam Y, Nomura T, Yamasaki M, Yan D, Fernandes HB, Zhang P, Howe JR, Watanabe M, Contractor A, Tomita S (2016) Distinct subunit domains govern synaptic stability and specificity of the kainate receptor. Cell Rep 16:531–544
78. Fernandes HB, Catches JS, Petralia RS, Copits BA, Xu J, Russell TA, Swanson GT, Contractor A (2009) High-affinity kainate receptor subunits are necessary for ionotropic but not metabotropic signaling. Neuron 63:818–829
79. Mulle C, Sailer A, Perez-Otano I, Dickinson-Anson H, Castillo PE, Bureau I, Maron C, Gage FH, Mann JR, Bettler B, Heinemann SF (1998) Altered synaptic physiology and reduced susceptibility to kainate- induced seizures in GluR6-deficient mice. Nature 392:601–605
80. Fievre S, Carta M, Chamma I, Labrousse V, Thoumine O, Mulle C (2016) Molecular determinants for the strictly compartmentalized expression of kainate receptors in CA3 pyramidal cells. Nat Commun 7:12738
81. Coussen F, Normand E, Marchal C, Costet P, Choquet D, Lambert M, Mege RM, Mulle C (2002) Recruitment of the kainate receptor subunit glutamate receptor 6 by cadherin/catenin complexes. J Neurosci 22:6426–6436
82. Garcia EP, Mehta S, Blair LA, Wells DG, Shang J, Fukushima T, Fallon JR, Garner CC, Marshall J (1998) SAP90 binds and clusters kainate receptors causing incomplete desensitization. Neuron 21:727–739
83. Hirbec H, Francis JC, Lauri SE, Braithwaite SP, Coussen F, Mulle C, Dev KK, Coutinho V, Meyer G, Isaac JT, Collingridge GL, Henley JM (2003) Rapid and differential regulation of AMPA and kainate receptors at hippocampal mossy fibre synapses by PICK1 and GRIP. Neuron 37:625–638
84. Ng D, Pitcher GM, Szilard RK, Sertie A, Kanisek M, Clapcote SJ, Lipina T, Kalia LV, Joo D, McKerlie C, Cortez M, Roder JC, Salter MW, McInnes RR (2009) Neto1 is a novel CUB-domain NMDA receptor-interacting protein required for synaptic plasticity and learning. PLoS Biol 7:e41
85. Bowie D, Garcia EP, Marshall J, Traynelis SF, Lange GD (2003) Allosteric regulation and spatial distribution of kainate receptors bound to ancillary proteins. J Physiol 547:373–385
86. Suzuki E, Kamiya H (2016) PSD-95 regulates synaptic kainate receptors at mouse hippocampal mossy fiber-CA3 synapses. Neurosci Res 107:14–19
87. Carta M, Opazo P, Veran J, Athane A, Choquet D, Coussen F, Mulle C (2013) CaMKII-dependent phosphorylation of GluK5 mediates plasticity of kainate receptors. EMBO J 32:496–510
88. Matsuda K (2017) Synapse organization and modulation via C1q family proteins and their receptors in the central nervous system. Neurosci Res 116:46–53
89. Matsuda K, Budisantoso T, Mitakidis N, Sugaya Y, Miura E, Kakegawa W, Yamasaki M, Konno K, Uchigashima M, Abe M, Watanabe I, Kano M, Watanabe M, Sakimura K, Aricescu AR,

Yuzaki M (2016) Transsynaptic modulation of kainate receptor functions by C1q-like proteins. Neuron 90:752–767
90. Zhang W, St-Gelais F, Grabner CP, Trinidad JC, Sumioka A, Morimoto-Tomita M, Kim KS, Straub C, Burlingame AL, Howe JR, Tomita S (2009) A transmembrane accessory subunit that modulates kainate-type glutamate receptors. Neuron 61:385–396
91. Straub C, Hunt DL, Yamasaki M, Kim KS, Watanabe M, Castillo PE, Tomita S (2011) Distinct functions of kainate receptors in the brain are determined by the auxiliary subunit Neto1. Nat Neurosci 14:866–873
92. Copits BA, Swanson GT (2012) Dancing partners at the synapse: auxiliary subunits that shape kainate receptor function. Nat Rev Neurosci 13:675–686
93. Tomita S, Castillo PE (2012) Neto1 and Neto2: auxiliary subunits that determine key properties of native kainate receptors. J Physiol 590:2217–2223
94. Howe JR (2014) Modulation of non-NMDA receptor gating by auxiliary subunits. J Physiol. https://doi.org/10.1113/jphysiol.2014.273904
95. Han L, Howe JR, Pickering DS (2016) Neto2 influences on kainate receptor pharmacology and function. Basic Clin Pharmacol Toxicol 119:141–148
96. Wyeth MS, Pelkey KA, Yuan X, Vargish G, Johnston AD, Hunt S, Fang C, Abebe D, Mahadevan V, Fisahn A, Salter MW, McInnes RR, Chittajallu R, McBain CJ (2017) Neto auxiliary subunits regulate interneuron somatodendritic and presynaptic kainate receptors to control network inhibition. Cell Rep 20:2156–2168
97. Tang M, Pelkey KA, Ng D, Ivakine E, McBain CJ, Salter MW, McInnes RR (2011) Neto1 is an auxiliary subunit of native synaptic kainate receptors. J Neurosci 31:10009–10018
98. Wyeth MS, Pelkey KA, Petralia RS, Salter MW, McInnes RR, McBain CJ (2014) Neto auxiliary protein interactions regulate kainate and NMDA receptor subunit localization at mossy fiber-CA3 pyramidal cell synapses. J Neurosci 34:622–628
99. Tang M, Ivakine E, Mahadevan V, Salter MW, McInnes RR (2012) Neto2 interacts with the scaffolding protein GRIP and regulates synaptic abundance of kainate receptors. PLoS ONE 7:e51433
100. Palacios-Filardo J, Aller MI, Lerma J (2016) Synaptic targeting of kainate receptors. Cereb Cortex 26:1464–1472
101. Copits BA, Robbins JS, Frausto S, Swanson GT (2011) Synaptic targeting and functional modulation of GluK1 kainate receptors by the auxiliary neuropilin and tolloid-like (NETO) proteins. J Neurosci 31:7334–7340
102. Sheng N, Shi YS, Nicoll RA (2017) Amino-terminal domains of kainate receptors determine the differential dependence on Neto auxiliary subunits for trafficking. Proc Natl Acad Sci USA. https://doi.org/10.1073/pnas.1619253114
103. Paternain AV, Herrera MT, Nieto MA, Lerma J (2000) GluR5 and GluR6 kainate receptor subunits coexist in hippocampal neurons and coassemble to form functional receptors. J Neurosci 20:196–205
104. Salinas GD, Blair LA, Needleman LA, Gonzales JD, Chen Y, Li M, Singer JD, Marshall J (2006) Actinfilin is a Cul3 substrate adaptor, linking GluR6 kainate receptor subunits to the ubiquitin-proteasome pathway. J Biol Chem 281:40164–40173
105. Maraschi A, Ciammola A, Folci A, Sassone F, Ronzitti G, Cappelletti G, Silani V, Sato S, Hattori N, Mazzanti M, Chieregatti E, Mulle C, Passafaro M, Sassone J (2014) Parkin regulates kainate receptors by interacting with the GluK2 subunit. Nat Commun 5:5182
106. Pickering DS, Taverna FA, Salter MW, Hampson DR (1995) Palmitoylation of the GluR6 kainate receptor. Proc Natl Acad Sci USA 92:12090–12094
107. Wilkinson KA, Konopacki F, Henley JM (2012) Modification and movement: phosphorylation and SUMOylation regulate endocytosis of GluK2-containing kainate receptors. Commun Integr Biol 5:223–226
108. Wilkinson KA, Henley JM (2010) Mechanisms, regulation and consequences of protein SUMOylation. Biochem J 428:133–145
109. Finley D, Chau V (1991) Ubiquitination. Annu Rev Cell Biol 7:25–69
110. Chittajallu R, Vignes M, Dev KK, Barnes JM, Collingridge GL, Henley JM (1996) Regulation of glutamate release by presynaptic kainate receptors in the hippocampus. Nature 379:78–81
111. Kamiya H, Ozawa S (1998) Kainate receptor-mediated inhibition of presynaptic Ca^{2+} influx and EPSP in area CA1 of the rat hippocampus. J Physiol 509(Pt 3):833–845
112. Frerking M, Schmitz D, Zhou Q, Johansen J, Nicoll RA (2001) Kainate receptors depress excitatory synaptic transmission at CA3→CA1 synapses in the hippocampus via a direct presynaptic action. J Neurosci 21:2958–2966
113. Schmitz D, Mellor J, Frerking M, Nicoll RA (2001) Presynaptic kainate receptors at hippocampal mossy fiber synapses. Proc Natl Acad Sci USA 98:11003–11008
114. Rodriguez-Moreno A, Sihra TS (2011) Metabotropic actions of kainate receptors in the control of glutamate release in the hippocampus. Adv Exp Med Biol 717:39–48
115. Andrade-Talavera Y, Duque-Feria P, Sihra TS, Rodriguez-Moreno A (2013) Pre-synaptic kainate receptor-mediated facilitation of glutamate release involves PKA and Ca(2+) -calmodulin at thalamocortical synapses. J Neurochem 126:565–578
116. Castillo PE, Janz R, Sudhof TC, Tzounopoulos T, Malenka RC, Nicoll RA (1997) Rab3A is essential for mossy fibre long-term potentiation in the hippocampus. Nature 388:590–593
117. Melyan Z, Wheal HV, Lancaster B (2002) Metabotropic-mediated kainate receptor regulation of IsAHP and excitability in pyramidal cells. Neuron 34:107–114
118. Melyan Z, Lancaster B, Wheal HV (2004) Metabotropic regulation of intrinsic excitability by synaptic activation of kainate receptors. J Neurosci 24:4530–4534
119. Rodriguez-Moreno A, Lerma J (1998) Kainate receptor modulation of GABA release involves a metabotropic function. Neuron 20:1211–1218
120. Jiang L, Kang D, Kang J (2015) Potentiation of tonic GABAergic inhibition by activation of postsynaptic kainate receptors. Neuroscience 298:448–454
121. Chamma I, Chevy Q, Poncer JC, Levi S (2012) Role of the neuronal K-Cl co-transporter KCC2 in inhibitory and excitatory neurotransmission. Front Cell Neurosci 6:5
122. Woodin MA, Ganguly K, Poo MM (2003) Coincident pre- and postsynaptic activity modifies GABAergic synapses by postsynaptic changes in Cl- transporter activity. Neuron 39:807–820
123. Tyzio R, Nardou R, Ferrari DC, Tsintsadze T, Shahrokhi A, Eftekhari S, Khalilov I, Tsintsadze V, Brouchoud C, Chazal G, Lemonnier E, Lozovaya N, Burnashev N, Ben-Ari Y (2014) Oxytocin-mediated GABA inhibition during delivery attenuates autism pathogenesis in rodent offspring. Science 343:675–679
124. Woo NS, Lu J, England R, McClellan R, Dufour S, Mount DB, Deutch AY, Lovinger DM, Delpire E (2002) Hyperexcitability and epilepsy associated with disruption of the mouse neuronal-specific K-Cl cotransporter gene. Hippocampus 12:258–268
125. Ivakine EA, Acton BA, Mahadevan V, Ormond J, Tang M, Pressey JC, Huang MY, Ng D, Delpire E, Salter MW, Woodin MA, McInnes RR (2013) Neto2 is a KCC2 interacting protein required for neuronal Cl- regulation in hippocampal neurons. Proc Natl Acad Sci USA 110:3561–3566

126. Mahadevan V, Pressey JC, Acton BA, Uvarov P, Huang MY, Chevrier J, Puchalski A, Li CM, Ivakine EA, Airaksinen MS, Delpire E, McInnes RR, Woodin MA (2014) Kainate receptors coexist in a functional complex with KCC2 and regulate chloride homeostasis in hippocampal neurons. Cell Rep 7:1762–1770
127. Matute C (2011) Therapeutic potential of kainate receptors. CNS Neurosci Ther 17:661–669
128. Yuan H, Low CM, Moody OA, Jenkins A, Traynelis SF (2015) Ionotropic GABA and glutamate receptor mutations and human neurologic diseases. Mol Pharmacol 88:203–217
129. Crepel V, Mulle C (2015) Physiopathology of kainate receptors in epilepsy. Curr Opin Pharmacol 20:83–88
130. Tauck DL, Nadler JV (1985) Evidence of functional mossy fiber sprouting in hippocampal formation of kainic acid-treated rats. J Neurosci 5:1016–1022
131. Represa A, Trembley E, Ben-Ari Y (1987) Kainate binding sites in the hippocampal mossy fibres: localization and plasticity. Neuroscience 20:739–748
132. Epsztein J, Represa A, Jorquera I, Ben-Ari Y, Crepel V (2005) Recurrent mossy fibers establish aberrant kainate receptor-operated synapses on granule cells from epileptic rats. J Neurosci 25:8229–8239
133. Peret A, Christie LA, Ouedraogo DW, Gorlewicz A, Epsztein J, Mulle C, Crepel V (2014) Contribution of aberrant GluK2-containing kainate receptors to chronic seizures in temporal lobe epilepsy. Cell Rep 8:347–354
134. Yu LM, Polygalov D, Wintzer ME, Chiang MC, McHugh TJ (2016) CA3 synaptic silencing attenuates kainic acid-induced seizures and hippocampal network oscillations. eNeuro. https://doi.org/10.1523/ENEURO.0003-16.2016
135. Guzman YF, Ramsey K, Stolz JR, Craig DW, Huentelman MJ, Narayanan V, Swanson GT (2017) A gain-of-function mutation in the GRIK2 gene causes neurodevelopmental deficits. Neurol Genet 3:e129
136. Lanore F, Labrousse VF, Szabo Z, Normand E, Blanchet C, Mulle C (2012) Deficits in morphofunctional maturation of hippocampal mossy fiber synapses in a mouse model of intellectual disability. J Neurosci 32:17882–17893
137. Micheau J, Vimeney A, Normand E, Mulle C, Riedel G (2014) Impaired hippocampus-dependent spatial flexibility and sociability represent autism-like phenotypes in GluK2 mice. Hippocampus 24:1059–1069
138. Griswold AJ, Ma D, Cukier HN, Nations LD, Schmidt MA, Chung RH, Jaworski JM, Salyakina D, Konidari I, Whitehead PL, Wright HH, Abramson RK, Williams SM, Menon R, Martin ER, Haines JL, Gilbert JR, Cuccaro ML, Pericak-Vance MA (2012) Evaluation of copy number variations reveals novel candidate genes in autism spectrum disorder-associated pathways. Hum Mol Genet 21:3513–3523
139. Aller MI, Pecoraro V, Paternain AV, Canals S, Lerma J (2015) Increased dosage of high-affinity kainate receptor gene grik4 alters synaptic transmission and reproduces autism spectrum disorders features. J Neurosci 35:13619–13628
140. Milanesi E, Bonvicini C, Congiu C, Bortolomasi M, Gainelli G, Gennarelli M, Minelli A (2015) The role of GRIK4 gene in treatment-resistant depression. Genet Res 97:e14
141. Pickard BS, Malloy MP, Christoforou A, Thomson PA, Evans KL, Morris SW, Hampson M, Porteous DJ, Blackwood DH, Muir WJ (2006) Cytogenetic and genetic evidence supports a role for the kainate-type glutamate receptor gene, GRIK4, in schizophrenia and bipolar disorder. Mol Psychiatry 11:847–857
142. Xu J, Marshall JJ, Fernandes HB, Nomura T, Copits BA, Procissi D, Mori S, Wang L, Zhu Y, Swanson GT, Contractor A (2017) Complete disruption of the kainate receptor gene family results in corticostriatal dysfunction in mice. Cell Rep 18:1848–1857

https://www.jstage.jst.go.jp/article/jts/42/5/42_529/_article

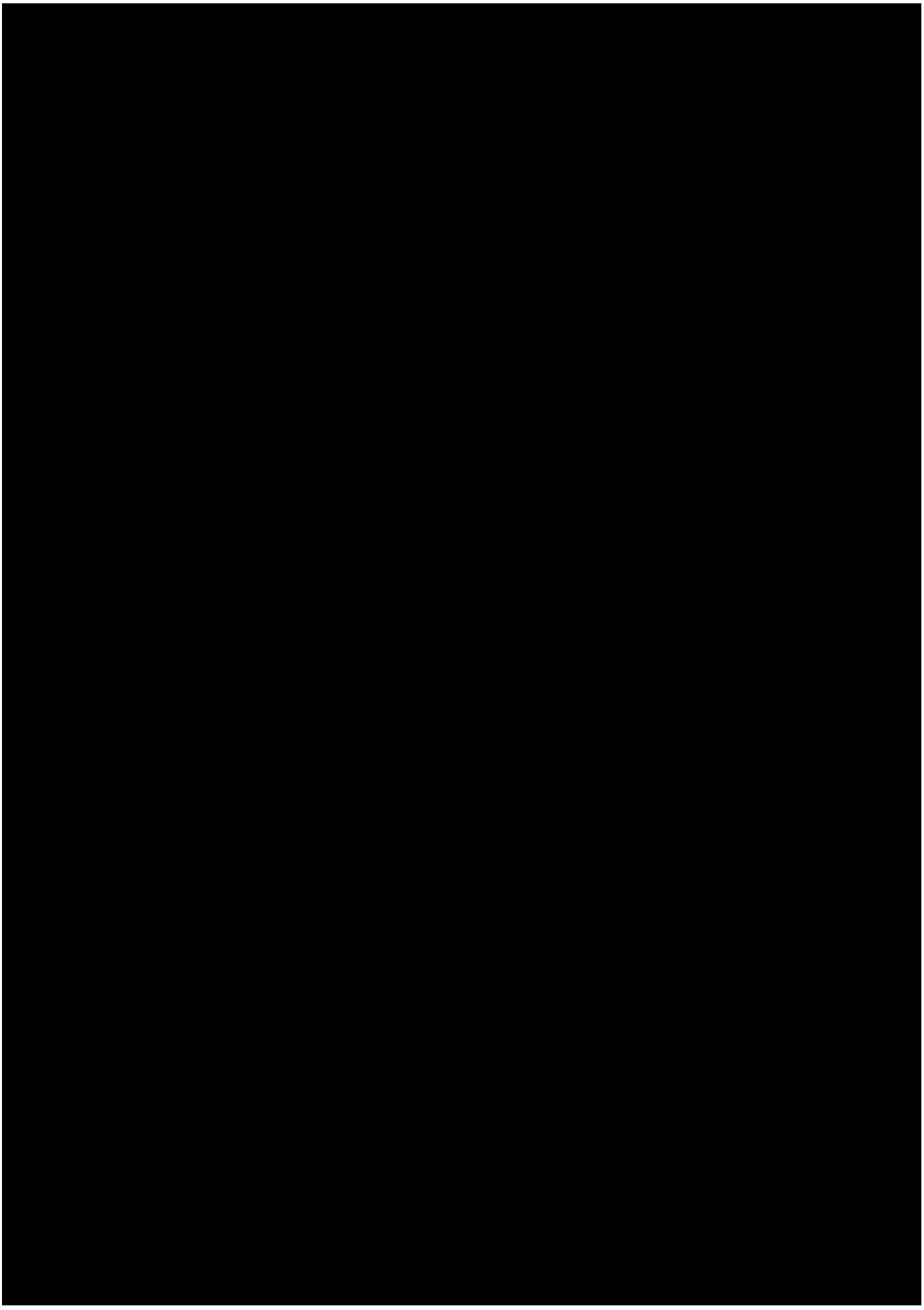

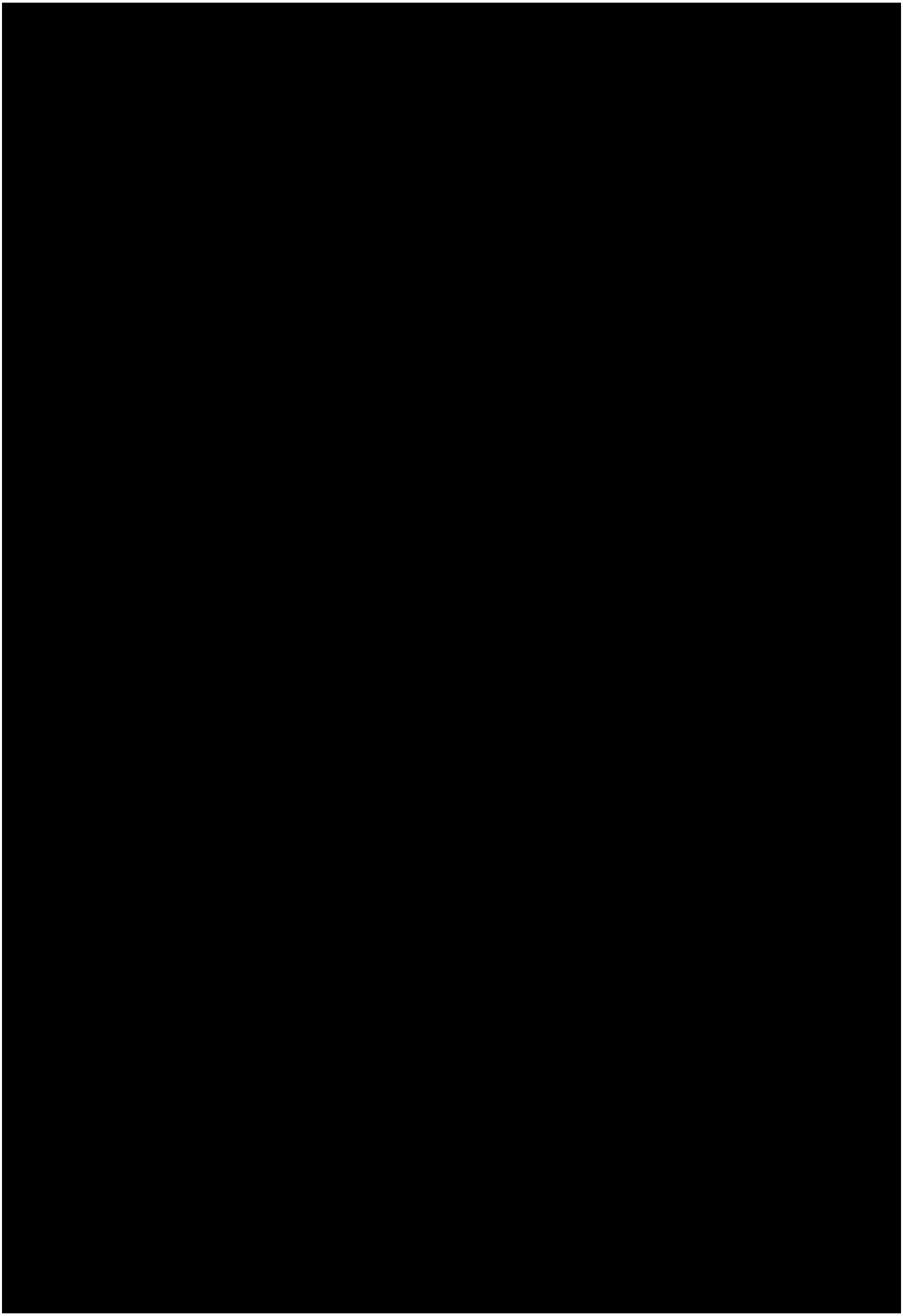

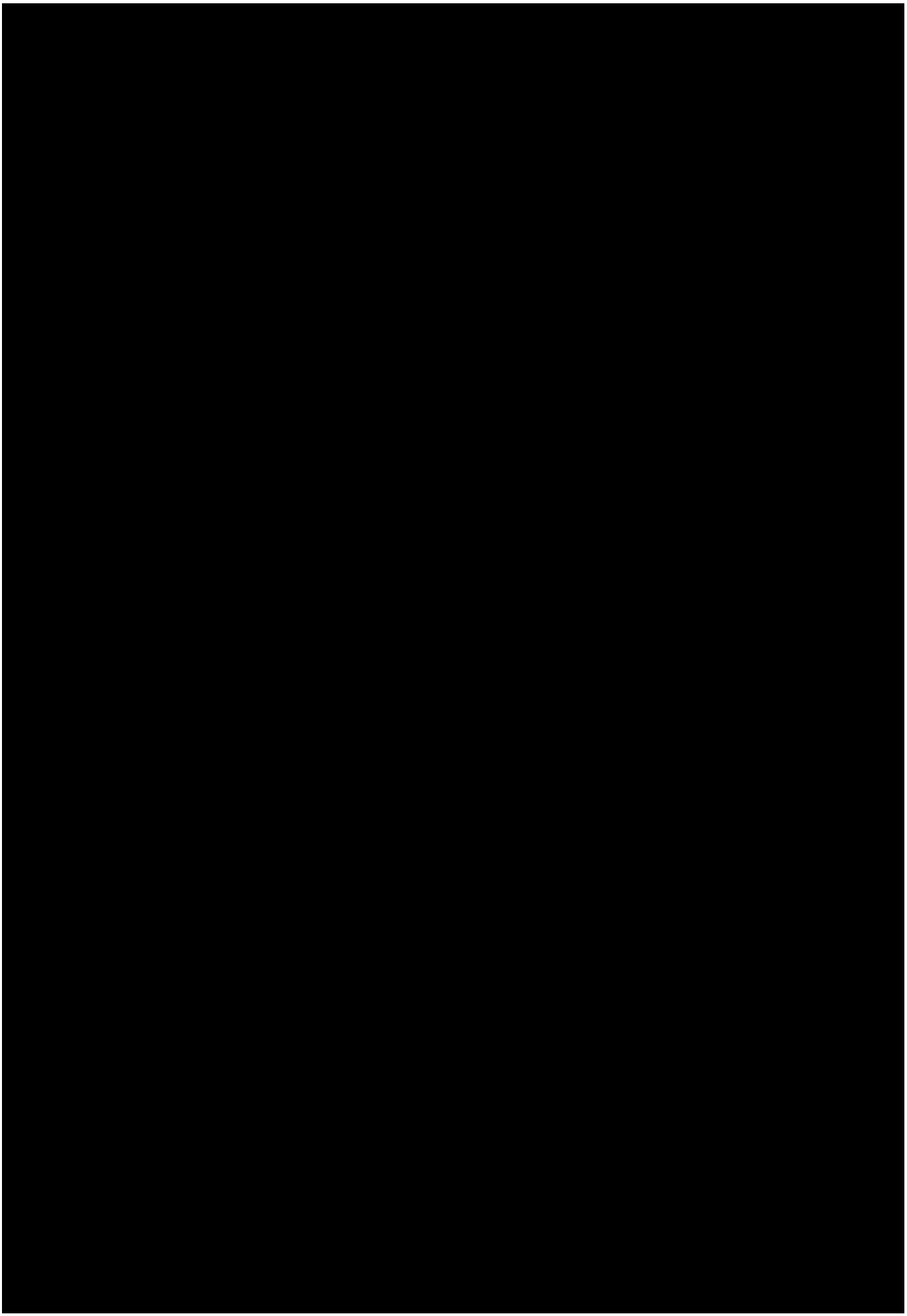

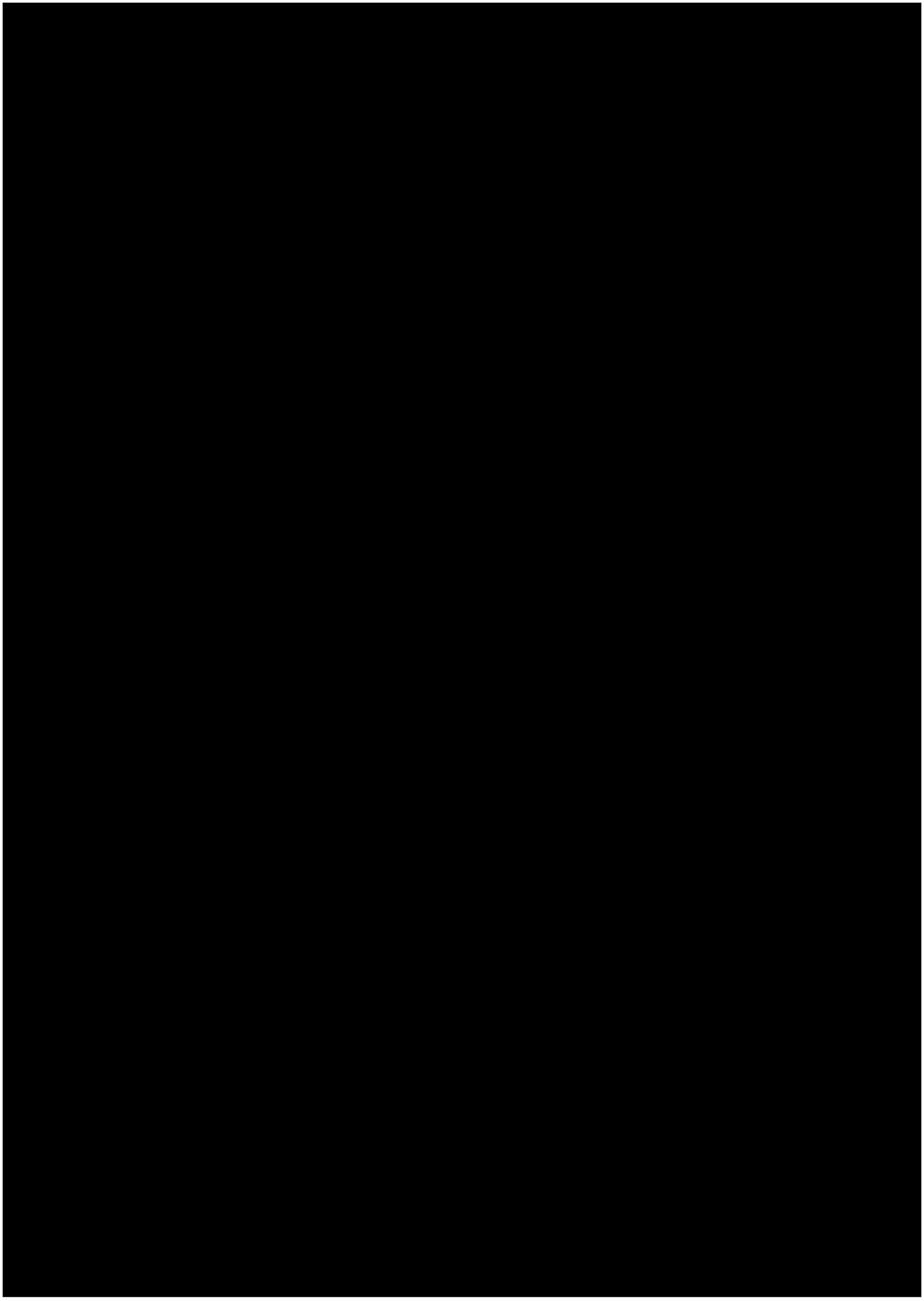

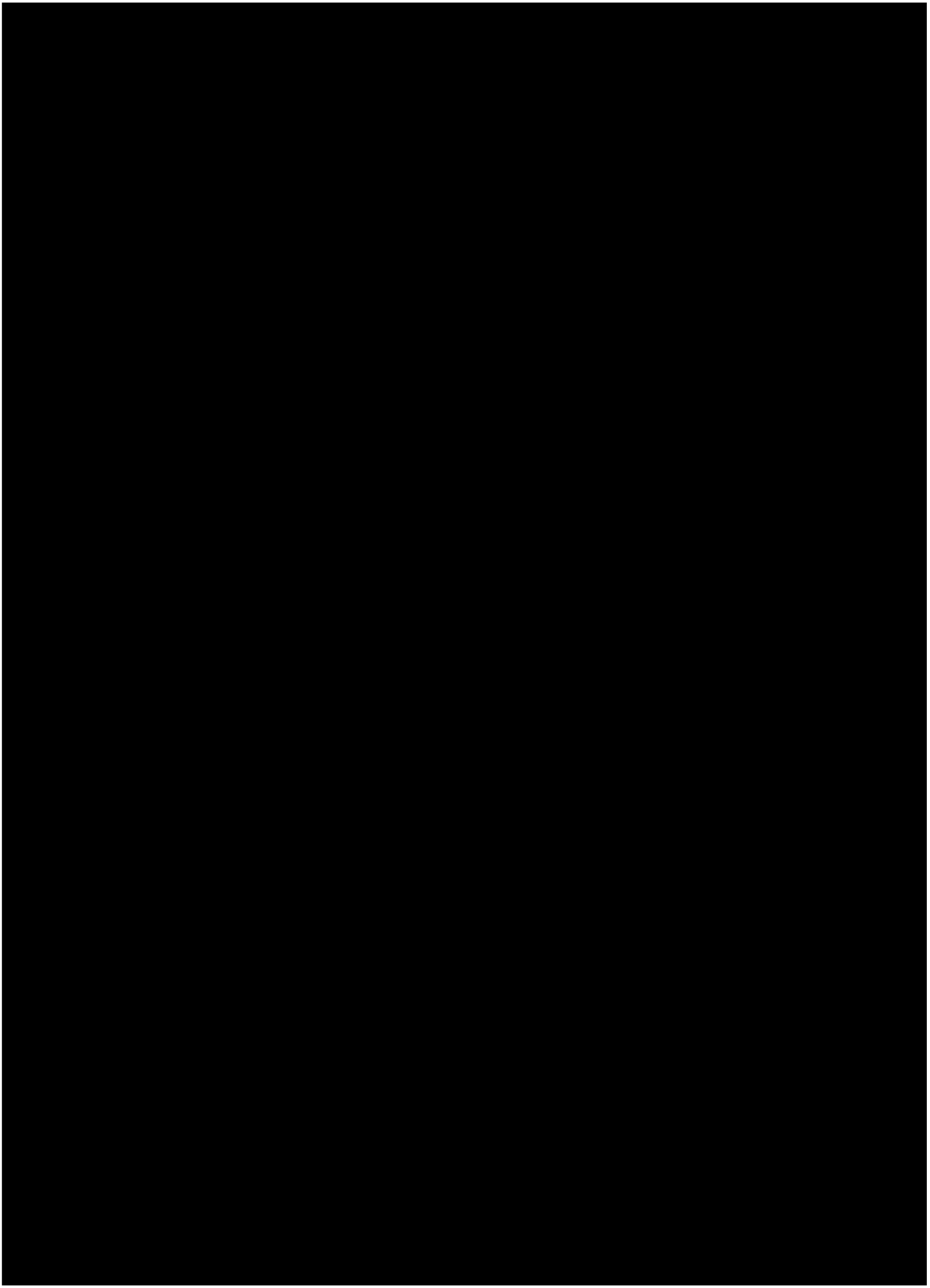

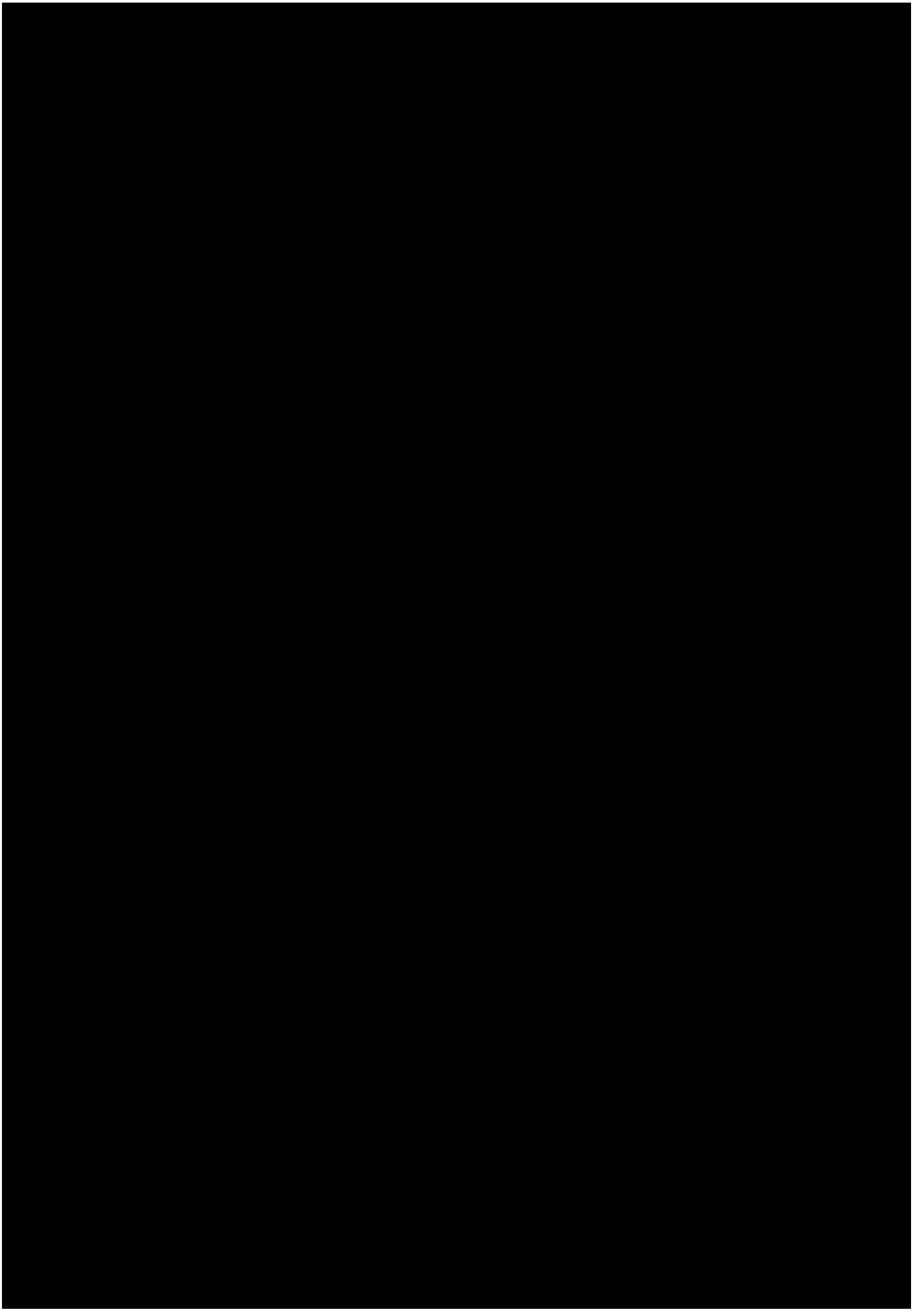

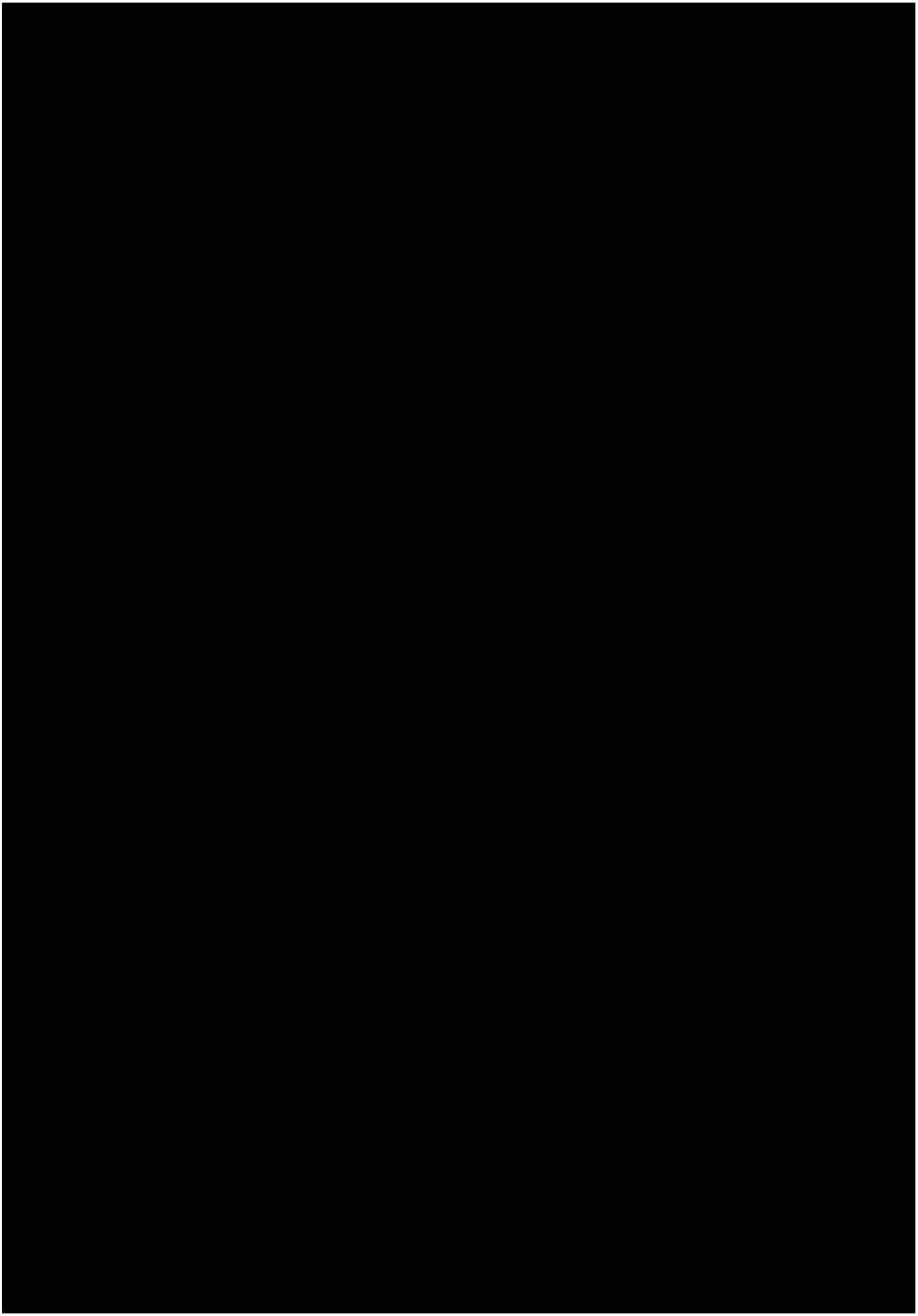

Article

Cell Reports

Assembly, Secretory Pathway Trafficking, and Surface Delivery of Kainate Receptors Is Regulated by Neuronal Activity

Graphical Abstract

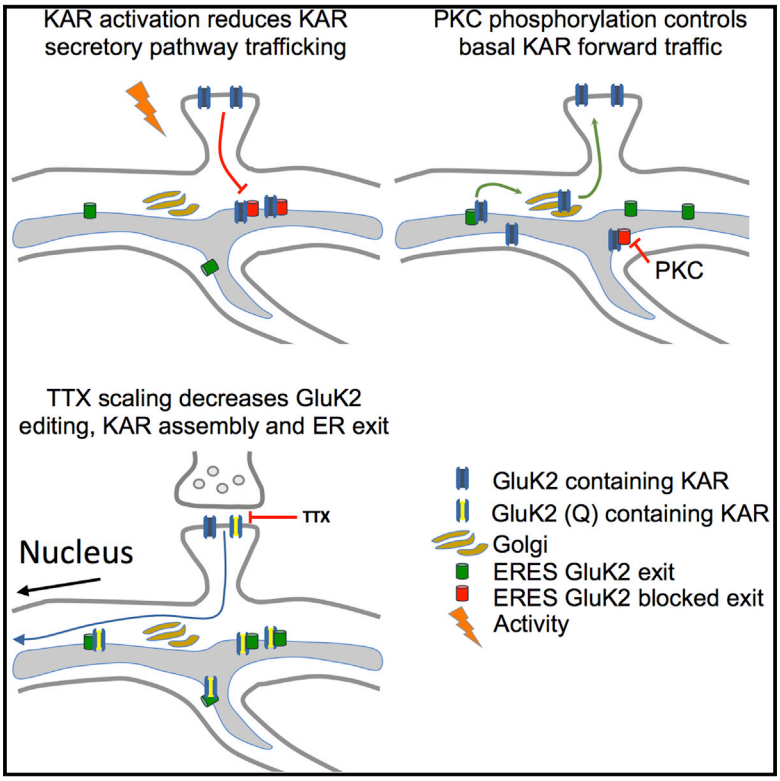

Highlights

- KARs can use a local dendritic secretory network for trafficking to the post-synapse
- Their secretory trafficking is highly activity-dependently regulated
- TTX decreases GluK2 editing, which promotes ER export of new KARs
- KAR activation slows KAR traffic via C-terminal PDZ ligand interactions on GluK2

Authors

Ashley J. Evans, Sonam Gurung, Kevin A. Wilkinson, David J. Stephens, Jeremy M. Henley

Correspondence

j.m.henley@bristol.ac.uk

In Brief

Evans et al. show that secretory pathway trafficking of KARs is highly activity-dependent. This medium-term regulatory mechanism demonstrates how neuronal excitability and network activity are regulated at multiple levels over a range of time courses.

Evans et al., 2017, Cell Reports *19*, 2613–2626
June 20, 2017
http://dx.doi.org/10.1016/j.celrep.2017.06.001

Cell Reports
Article

Assembly, Secretory Pathway Trafficking, and Surface Delivery of Kainate Receptors Is Regulated by Neuronal Activity

Ashley J. Evans,[1] Sonam Gurung,[1] Kevin A. Wilkinson,[1] David J. Stephens,[1] and Jeremy M. Henley[1,2,*]
[1]School of Biochemistry, Centre for Synaptic Plasticity, Biomedical Sciences Building, University of Bristol, University Walk, Bristol BS8 1TD, UK
[2]Lead Contact
*Correspondence: j.m.henley@bristol.ac.uk
http://dx.doi.org/10.1016/j.celrep.2017.06.001

SUMMARY

Ionotropic glutamate receptor (iGluR) trafficking and function underpin excitatory synaptic transmission and plasticity and shape neuronal networks. It is well established that the transcription, translation, and endocytosis/recycling of iGluRs are all regulated by neuronal activity, but much less is known about the activity dependence of iGluR transport through the secretory pathway. Here, we use the kainate receptor subunit GluK2 as a model iGluR cargo to show that the assembly, early secretory pathway trafficking, and surface delivery of iGluRs are all controlled by neuronal activity. We show that the delivery of de novo kainate receptors is differentially regulated by modulation of GluK2 Q/R editing, PKC phosphorylation, and PDZ ligand interactions. These findings reveal that, in addition to short-term regulation of iGluRs by recycling/endocytosis and long-term modulation by altered transcription/translation, the trafficking of iGluRs through the secretory pathway is under tight activity-dependent control to determine the numbers and properties of surface-expressed iGluRs.

INTRODUCTION

The morphological complexity of neurons presents unique challenges for the timely and appropriate supply of proteins to dynamic and metabolically active synapses. The ionotropic glutamate receptor (iGluR) family comprising N-methyl-D-aspartate (NMDA), α-amino-3-hydroxy-5-methyl-4-isoxazolepropionic acid (AMPA), and kainate receptors (NMDARs, AMPARs, and KARs, respectively) are critical for synaptic transmission and plasticity, and the mechanisms by which iGluRs are delivered to, retained at, and removed from synapses under basal, stimulated, and pathological conditions have been the focus of intense investigation for decades (Huganir and Nicoll, 2013; Granger and Nicoll, 2013; Lerma and Marques, 2013; Henley and Wilkinson, 2016).

The transcription (Liu et al., 2010; Jia et al., 2006; Grooms et al., 2006), RNA editing (Sanjana et al., 2012), translation (Schuman et al., 2006), post-translational modification (Martin et al., 2007; Copits and Swanson, 2013; Lussier et al., 2015; Wilkinson et al., 2012; Chamberlain et al., 2012; Konopacki et al., 2011), and surface endocytosis/recycling (Glebov et al., 2015; Boehm et al., 2006; Palmer et al., 2005; Beattie et al., 2000; Kennedy and Ehlers, 2011) of iGluRs are all activity-dependently regulated. Surprisingly, however, relatively little is known about whether and how the delivery of newly synthesized iGluRs through the secretory pathway is controlled by neuronal activity. Studies using temperature-sensitive vesicular stomatitis virus G transmembrane protein (tsVSV-G) as a cargo marker for the endomembrane system have reported that endoplasmic reticulum (ER) exit sites (ERESs) are both present and utilized in dendrites and that some VSV-G cargo subsequently colocalizes at dendritic Golgi outposts (Torre and Steward, 1996; Presley et al., 1997; Horton and Ehlers, 2003). Using mRNA trafficked from the soma, postsynaptic proteins can be locally translated and post-translationally modified (Cajigas et al., 2012; Holt and Schuman, 2013; Na et al., 2016). Furthermore, transmembrane proteins with an immature glycosylation profile can be surface-expressed, suggesting that not all secretory pathway cargo needs to be processed within the Golgi prior to plasma membrane insertion (Hanus et al., 2016).

Despite its widespread use, the fact that tsVSV-G is an exogenous viral protein and that temperature shifts are required to release it from the ER raise important questions about its fidelity as a reporter for endogenous neuronal proteins. Despite these caveats, neuronal activity can increase VSV-G-containing vesicle delivery through the secretory pathway to the cell surface (Hanus et al., 2014), suggesting, but not directly demonstrating, that the secretory pathway trafficking of endogenous cargos such as iGluRs is likely to be activity-dependently regulated. Furthermore, the secretory pathway trafficking of AMPARs can be regulated by interactions with coat protomer II (COPII) components following activation of metabotropic glutamate receptors (Pick et al., 2017).

To directly monitor iGluR processing and progression through the secretory pathway under basal and stimulated conditions, we adapted the retention using selective hooks (RUSH) system that allows the synchronous release and visualization of the

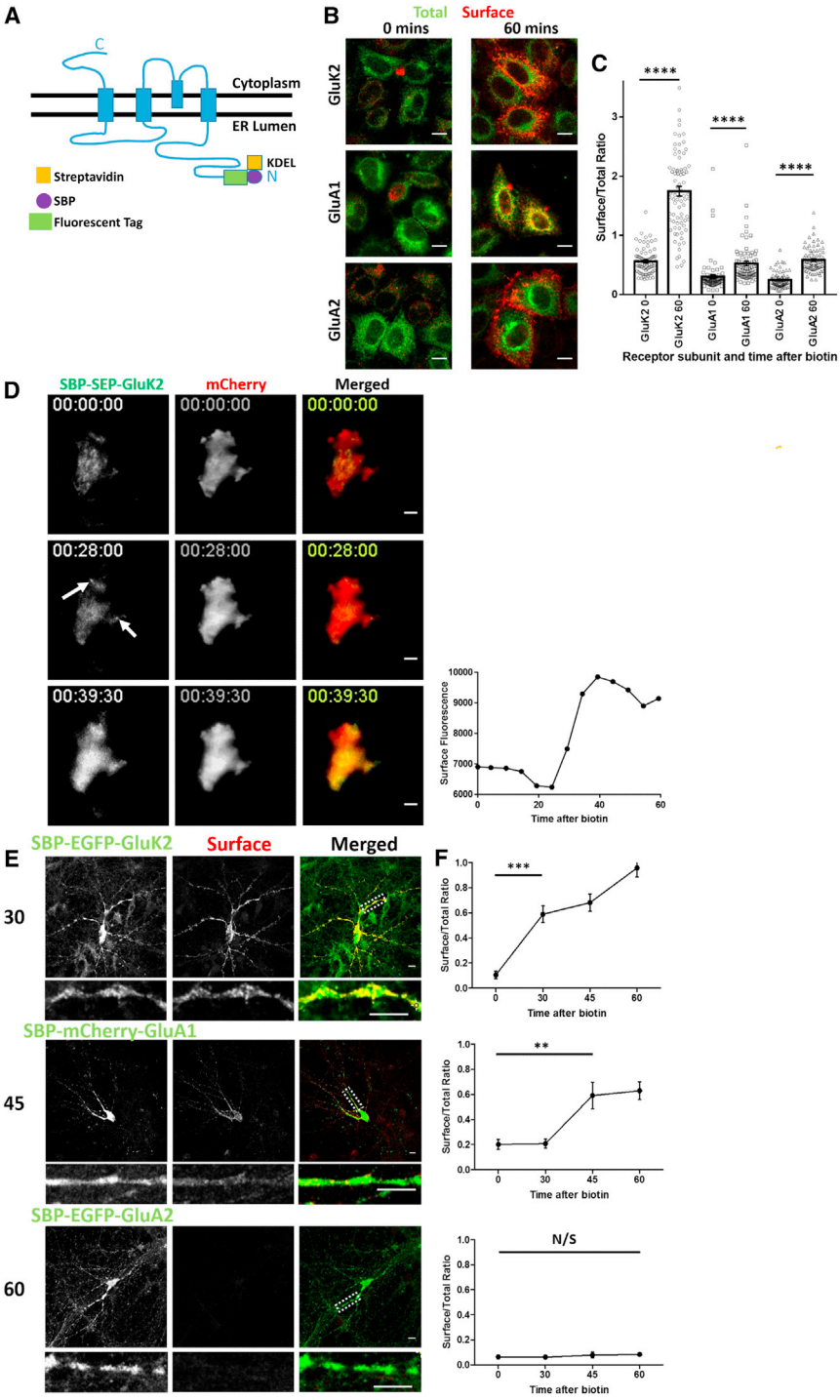

Figure 1. Construction and Validation of RUSH Glutamate Receptor Subunits in HeLa and Primary Hippocampal Neuronal Cells

(A) Schematic of a RUSH ionotropic glutamate receptor subunit. SBP, streptavidin-binding peptide.

(B) Representative confocal images of the AMPAR subunits SBP-mCherry-GluA1 and SBP-EGFP-GluA2 and the KAR subunit SBP-EGFP-GluK2 in HeLa cells. Receptors are retained in the ER (0 min) and synchronously released by biotin addition, allowing trafficking to the cell surface (60 min after biotin addition). Total, green; surface anti-SBP, red.

(C) Quantification of the data represented in (B); three independent experiments, n = 80 cells/condition. ****$p < 0.0001$, Welch's t test.

(D) Representative still frames of the TIRF microscopy video (Figure S1B; Movie S1), showing the time course of trafficking and analysis of cell surface delivery of SBP-SEP-GluK2 after biotin addition. Arrows indicate sites of exocytosis. Quantification of surface delivery over time is also shown. See also Figure S1B.

(E) Representative confocal images of primary hippocampal neurons showing the differential secretory pathway trafficking rates of SBP-EGFP-GluK2, SBP-mCherry-GluA1, and SBP-EGFP-GluA2 containing KARs and AMPARs, respectively. Surface-expressed receptors were visualized using anti-SBP (red) at the indicated times (minutes) after biotin release. White boxes positioned on the merged panels indicate the region of the zoom panel.

(F) Quantification of the data shown in (E); three independent experiments, n = 20–24 for each receptor per time point. ***$p < 0.001$, **$p < 0.01$, Welch's t test.

Scale bars, 10 μm.

trafficking of cargo through the secretory pathway (Boncompain et al., 2012). We used the KAR subunit GluK2 as a prototypic iGluR cargo. KARs are present at both pre- and postsynaptic membranes, where they perform distinct roles in modulating synaptic transmission, neuronal excitability, and network activity (Contractor et al., 2011; Lerma and Marques, 2013), and they are implicated in processes ranging from neuronal development and differentiation to neurodegeneration and neuronal cell death (Contractor et al., 2011; González-González et al., 2012).

We show that KARs can use a local dendritic secretory pathway. GluK2 editing is activity-dependently controlled, resulting in modulation of KAR assembly (Ball et al., 2010) and subsequent increases in unedited GluK2-containing, calcium-permeable KARs at the cell surface (Egebjerg and Heinemann, 1993). Under basal conditions, the secretory pathway trafficking of GluK2-containing KARs is regulated by protein kinase C (PKC) phosphorylation. In a distinct regulatory process, surface KAR activation slows the progression of newly synthesized KARs through the secretory pathway by modulating interactions at the C-terminal PDZ ligand of GluK2. Together, these data reveal that the delivery of de novo KARs to the cell surface is dynamically regulated in a sophisticated, multilayered manner. These mechanisms provide additional flexibility to neuronal responses to changing cellular environments and network activity.

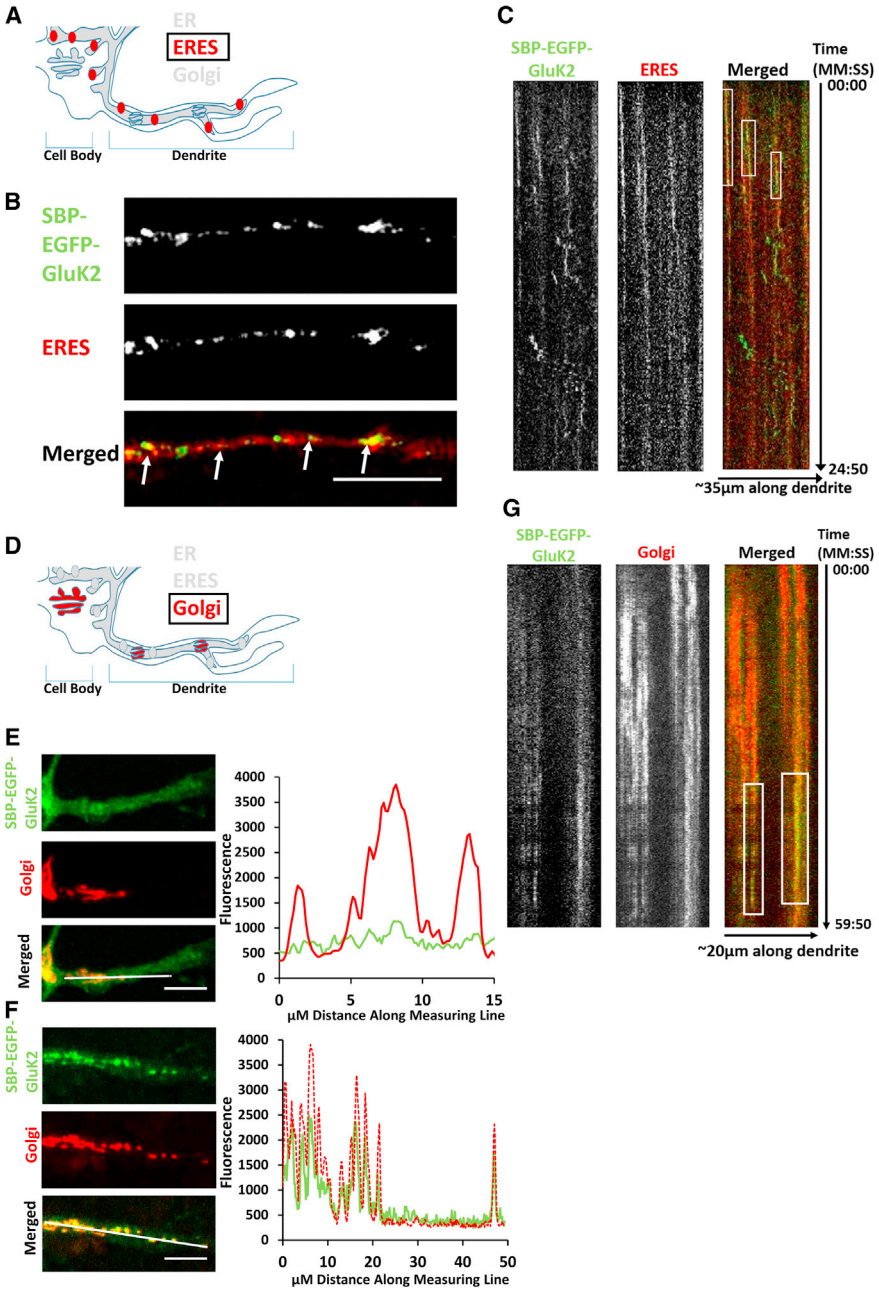

Figure 2. KARs Use Local Secretory Pathway Systems

(A) Schematic of dendritic local secretory pathways in neurons, focusing on ER exit sites.

(B) Representative fixed confocal images of dendritic ERESs (using the marker mRuby-Sec23a) and SBP-EGFP-GluK2 10 min after biotin addition. White arrows in the merged panel indicate colocalization.

(C) Kymograph (Movie S2) of SBP-EGFP-GluK2 and mRuby-Sec23a up to 24 min 50 s after biotin addition, with a frame being taken every 10 s. White boxes on the merged panel show the duration of colocalization.

(D) Schematic of dendritic local secretory pathways in neurons, focusing on the Golgi.

(E) Representative fixed confocal images of SBP-EGFP-GluK2 colocalization with the Golgi marker Sialyltransferase-mCherry (Golgi) before biotin release and a line trace illustrating lack of colocalization along the line indicated in white in the merged image.

(F) Representative fixed confocal images of SBP-EGFP-GluK2 30 min after biotin-induced release with Sialyltransferase-mCherry (Golgi) and line trace quantification.

(G) Kymograph (Movie S3) of SBP-EGFP-GluK2 and GalT-mCherry (Golgi) after biotin addition up to 59 min 50 s, with a frame being taken every 10 s. White boxes on the merged panel show colocalization duration.

Scale bars, 10 µm.

RESULTS

Using RUSH to Assay iGluR Secretory Pathway Trafficking

We utilized the RUSH system by tagging the GluK2 KAR subunit and both the GluA1 and GluA2 AMPAR subunits at the N terminus with a streptavidin-binding peptide (SBP) and a fluorescent tag. When these constructs are coexpressed with a streptavidin-KDEL "hook" that localizes to the lumen of the ER, the SBP-tagged subunits are anchored at the ER membrane (Figure 1A). The retained SBP-tagged receptors can then be synchronously released by biotin addition to monitor their trafficking through the secretory pathway (Figure S1A; Boncompain and Perez, 2012).

We first validated these RUSH constructs in HeLa cells. As expected, the SBP-tagged receptors are efficiently retained in the ER (0 min), and, upon addition of biotin, they are released and move through the secretory pathway, reaching the cell surface after 60 min (Figures 1B and 1C). Interestingly, each of the three different subunits had different kinetics, with much more GluK2 than GluA1 or GluA2 present at the cell surface after 60 min. Because GluK2 traffics most rapidly, we measured the dynamics of surface expression using super-ecliptic pHluorin (SEP)-tagged GluK2 (SBP-SEP-GluK2) (Ashby et al., 2004; Wilkinson et al., 2014) and total internal reflection fluorescence (TIRF) microscopy. GluK2 starts accumulating at the surface ~30 min after biotin-induced release from the ER (Figure 1D; Figure S1B; Movie S1).

Consistent with the results from HeLa cells, we observed different rates of secretory pathway trafficking for GluK2, GluA1, and GluA2 in hippocampal neurons (Figures 1E and 1F). In agreement with previous reports using endogenous subunits (Greger et al., 2002), SBP-mCherry-GluA1 traffics through the secretory pathway quicker than SBP-EGFP-GluA2. These data show that the RUSH system allows synchronized release of KARs and AMPARs from the ER in both clonal cell lines and neurons and that it provides a powerful tool to investigate the early trafficking steps of iGluRs.

KARs Use Dendritic ER Exit Sites and Golgi Outposts

VSV-G and NMDARs have been reported to use dendritic ERESs and Golgi outposts (Figures 2A and 2D) for post-translational modification, which is facilitated by the interacting proteins CASK and SAP97 (Horton and Ehlers, 2003; Jeyifous et al., 2009). Although KARs bind to both CASK and SAP97 through a PDZ ligand/domain interaction (Coussen et al., 2002; Hirbec et al., 2003), it is unknown whether KARs use local secretory pathways. We therefore investigated this using SBP-EGFP-GluK2 in neurons. SBP-EGFP-GluK2 colocalizes with mRuby-Sec23A-labeled ERESs (Budnik and Stephens, 2009; Hughes and Stephens, 2010) in dendrites after biotin-induced release (Figures 2B and 2C; Figure S2A; Movie S2).

VSV-G colocalizes with local Golgi outposts after release from dendritic ERESs (Horton and Ehlers, 2003; Figure 2D). Before release, SBP-EGFP-GluK2 is retained in the ER and does not colocalize with dendritic Golgi outposts (Figure 2E). However, 30 min after ER release by biotin, SBP-EGFP-GluK2 strongly colocalized at Golgi outposts (Figures 2F and 2G; Figure S2B; Movie S3), demonstrating that KARs utilize local secretory pathway systems.

Assembly and Surface Delivery of Newly Synthesized KARs Is Controlled by Chronic Changes in Synaptic Activity and Mediated by Changes in the RNA Editing of GluK2

NMDAR and AMPAR surface expression scales in response to chronic down- or upregulation of synaptic activity (Rao and Craig, 1997; Shepherd et al., 2006; Turrigiano, 2012). To address whether KARs also scale, we chronically suppressed synaptic activity in hippocampal neurons with tetrodotoxin (TTX) for 24 hr. As expected, TTX significantly increased GluA1-containing AMPAR surface expression and also increased GluK2-containing KARs at the cell surface with no change in surface epidermal growth factor receptors (EGFRs) (Figures 3A and 3B), indicating that chronic blockade of activity upscales GluK2-containing KARs.

The pre-mRNAs encoding GluA2 and GluK2 can undergo editing at a site within the channel pore that changes a glutamine (Q) residue to an arginine (R) in the translated subunit (Sommer et al., 1991). This Q/R editing alters the calcium permeability of surface-expressed AMPARs (Burnashev et al., 1992) and KARs (Köhler et al., 1993). Q/R editing also regulates AMPAR and KAR subunit assembly and ER exit (Greger et al., 2002; Ball et al., 2010). We generated RUSH variants of edited and unedited GluK2, and, consistent with previous observations (Ball et al., 2010), the edited (R) form of SBP-EGFP-GluK2 exhibited lower levels of surface expression compared with the unedited Q form in HeLa cells after 24 hr of biotin-induced release (Figures 3C and 3D; Figure S3A). Furthermore, TTX decreases Q/R editing of GluK2 (Figures 3E and 3F). We hypothesized that this change in GluK2 editing will promote KAR assembly and ER exit, resulting in increased surface expression. To test this, we knocked down ADAR2, the enzyme responsible for GluK2 editing (Nishikura, 2016; Figure S3B). ADAR2 knockdown reduced GluK2 editing similar to TTX treatment (Figure S3C) and upscaled surface GluK2 in the absence of TTX (Figures 3G and 3H), indicating that KAR scaling is mediated, at least in part, by activity-dependent regulation of GluK2 Q/R editing.

PKC Phosphorylation Regulates Basal KAR Trafficking through the Secretory Pathway

To measure the secretory pathway trafficking and surface expression of de novo KARs without confounding issues from endocytosis and recycling of KARs, we modified the RUSH protocol to measure all subunits that reach the cell surface by live labeling (Figure 4A). To ensure that this live labeling protocol faithfully reports only secretory pathway trafficking to the cell surface and is not affected by rates of endocytosis, we exposed SBP-EGFP-GluK2-expressing HeLa cells to kainate to promote KAR endocytosis (Figure S4A). Comparable surface delivery levels of SBP-EGFP-GluK2 were observed with and without kainate, confirming that this procedure only reports de novo KARs delivered by the secretory pathway (Figures 4B and 4C).

Serines 846 and 868 in the C terminus of GluK2 are phosphorylated by PKC, and phosphomimetic mutations of these residues

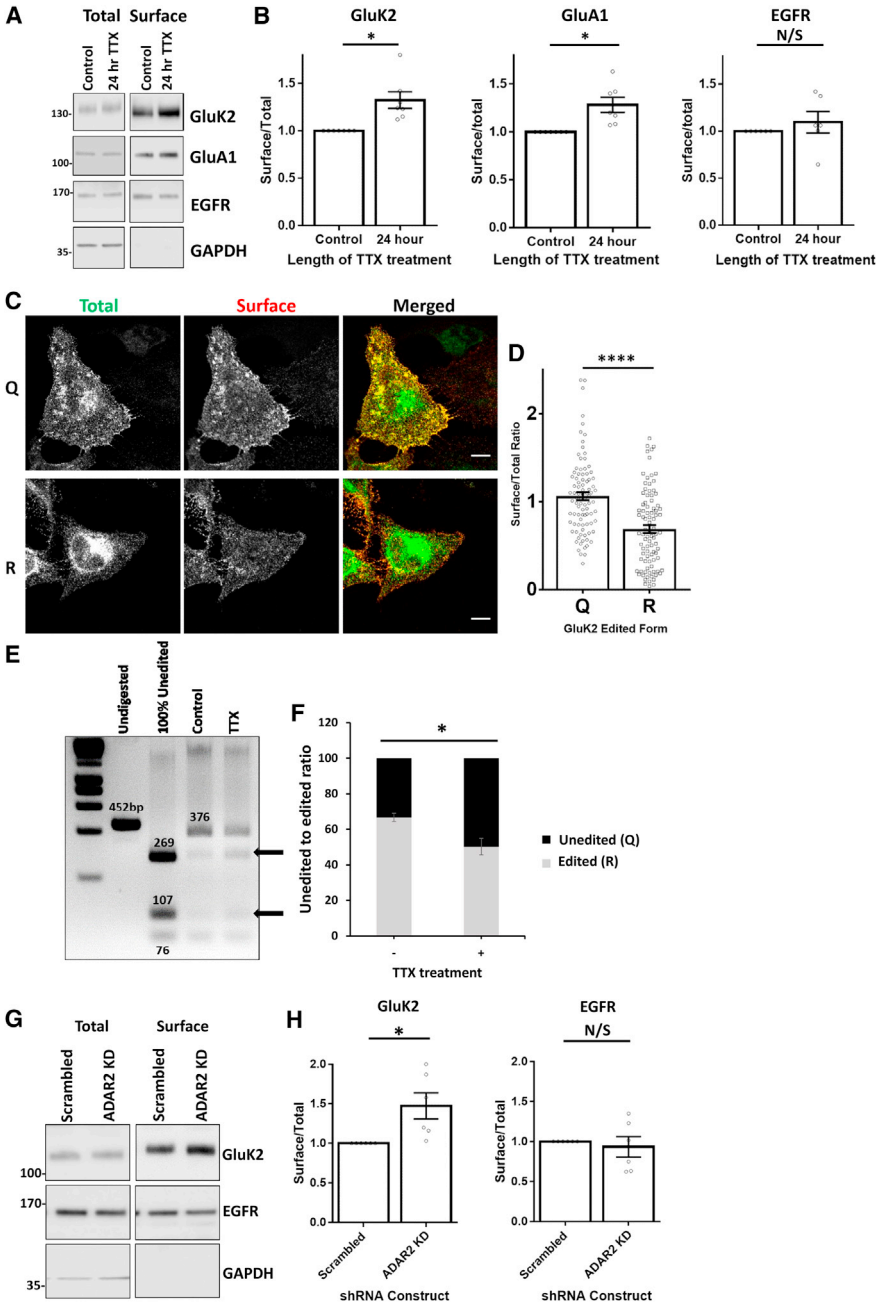

Figure 3. KAR ER Exit Is Regulated by Activity-Dependent Changes in RNA Editing of GluK2

(A) Representative western blots of surface-biotinylated KAR and AMPAR subunits and EGFR in hippocampal neurons. The blots show surface and total levels of subunits with or without 24-hr treatment with 1 μM TTX to suppress synaptic activity.

(B) Quantification of immunoblots and comparison of surface-to-total ratios from six (GluA1 and EGFR) and seven (GluK2) independent experiments. *$p < 0.05$, Wilcoxon matched pairs signed-rank test.

(C) SBP-EGFP-GluK2 unedited (Q) or edited (R) RUSH constructs transfected into HeLa cells with addition of biotin at the time of transfection to allow basal expression. Surface RUSH KARs were labeled with anti-SBP for a duration of 5 min. See also Figure S3A.

(D) Quantification from (C), representative of three independent experiments (n = 90). ****$p < 0.0001$, Welch's t test.

(E) RT-PCR and digestion analysis of levels of unedited and edited GluK2 with or without TTX treatment. Black arrows indicate unedited forms of GluK2.

(F) Quantification of unedited and edited GluK2 with or without TTX treatment (n = 5). *$p < 0.05$, Welch's t test.

(G) Representative western blots of surface-biotinylated GluK2 and EGFR after lentiviral infection of primary hippocampal neurons with either scrambled or ADAR2-targeting shRNA. The blots show both total and surface levels of GluK2 and EGFR after 5 days of knockdown. See also Figure S3B.

(H) Quantification of immunoblots and comparison of surface-to-total ratios from six independent experiments. *$p < 0.05$, Wilcoxon matched pairs signed-rank test.

cause ER retention (Konopacki et al., 2011). We therefore used the RUSH assay to assess the role of GluK2 phosphorylation in KAR trafficking through the secretory pathway. We mutated both S846 and S868 to non-phosphorylatable alanines (SBP-EGFP-GluK2-AA) or to phosphomimetic aspartic acid residues (SBP-EGFP-GluK2-DD). As predicted, the AA phospho-null mutant traffics more and the DD phosphomimetic mutant traffics less efficiently to the cell surface than the wild-type SBP-EGFP-GluK2 under non-stimulated conditions. In parallel, we tested the effect of the PKC activator phorbol 12-myristate 13-acetate (PMA) on surface accumulation. Consistent with the mutant data, PMA decreased the surface expression of SBP-EGFP-GluK2, whereas SBP-EGFP-GluK2-AA was unaffected (Figures 4D and 4E; Figure S4B). Our interpretation of these results is that a proportion of GluK2 is basally phosphorylated by PKC in the ER and that this provides a mechanism to regulate the ER exit and supply of de novo KARs for delivery to the cell surface.

Activation of Surface-Expressed KARs Regulates De Novo KAR Delivery to the Cell Surface

Our data demonstrate that, rather than being a constitutive process, the secretory pathway trafficking of KARs is subject to strict regulation. Under basal conditions, PKC phosphorylation limits the supply of GluK2-containing KARs, and chronic suppression of synaptic activity reduces Q/R editing, which promotes KAR assembly and ER exit. Therefore, we next tested the effects of direct activation of surface-expressed KARs on SBP-EGFP-GluK2 trafficking. We used our previously described transient kainate application protocol (5 min, 10 μM kainate + TTX followed by washout), which increases KAR surface expression (Martin et al., 2008; González-González and Henley, 2013). This transient kainate application prior to biotin-induced SBP-EGFP-GluK2 release from the ER caused a significant reduction in trafficking through the secretory pathway to the cell surface (Figures 5A and 5B). In contrast, the secretory pathway trafficking of SBP-EGFP-GluA1 was unaffected (Figures 5C and 5D). These results indicate that transient activation of surface KARs can selectively reduce the trafficking of de novo KARs through the secretory pathway to control the supply of receptors available for insertion at the cell surface (Figure S5). We initially hypothesized that phosphorylation of S846 and S868 may mediate the kainate-evoked reduction in the surface delivery of de novo KARs (Nasu-Nishimura et al., 2010; Konopacki et al., 2011). Contrary to our expectations, however, secretory pathway trafficking of the non-phosphorylatable SBP-EGFP-GluK2-AA was also significantly reduced by transient kainate stimulation (Figures 5E and 5F). Thus, kainate regulation of KAR secretory pathway trafficking appears to be mediated via a mechanism other than PKC phosphorylation.

The GluK2 PDZ Ligand Is Involved in Basal and Activity-Dependent Delivery of De Novo Receptors to the Cell Surface

The GluK2 PDZ ligand (^{905}ETMA^{908}) interacts with multiple PDZ domain-containing proteins, including SAP97, PICK1, PSD95, GRIP, syntenin, and CASK (Coussen et al., 2002; Hirbec et al., 2002), and inhibition of PDZ interactions using a competing peptide leads to a rundown in KAR excitatory postsynaptic currents (EPSCs) (Hirbec et al., 2003). We therefore mutated the extreme C-terminal PDZ ligand of SBP-EGFP-GluK2 from the wild-type sequence ETMA to EPAS, which cannot interact with PDZ domain-containing proteins (Hirbec et al., 2003).

In HeLa cells, secretory pathway trafficking for both wild-type SBP-EGFP-GluK2-ETMA and the PDZ ligand mutant SBP-EGFP-GluK2-EPAS was comparable (Figures 6A and 6B; Figure S6A). Similarly, there was no difference between the wild-type and EPAS mutant when expressed in neurons with addition of biotin at the same time as transfection to allow continuous release of the receptor from the ER to determine their steady-state localization (Figures 6C and 6D; Figure S6B).

We next performed experiments corresponding to those shown in Figure 5, where biotin was added to elicit synchronized release of SBP-EGFP-GluK2 or SBP-EGFP-GluK2-EPAS with or without a transient kainate stimulation prior to biotin application. This transient kainate stimulation significantly decreased the secretory pathway trafficking of wild-type SBP-EGFP-GluK2-ETMA (Figures 6E and 6F). Interestingly, the secretory pathway trafficking of SBP-EGFP-GluK2-EPAS was significantly reduced compared with SBP-EGFP-GluK2-ETMA under basal conditions. Furthermore, the secretory pathway trafficking of SBP-EGFP-GluK2-EPAS was not further decreased by kainate application, indicating that preventing PDZ interactions occludes the kainate-induced reduction in secretory pathway trafficking (Figures 6E and 6F; Figure S6B). Together, these results demonstrate that, although the GluK2 PDZ interactions do not affect the steady-state localization of GluK2-containing KARs, they regulate their activity-dependent secretory pathway trafficking.

DISCUSSION

Here we show that GluK2-containing KARs use a local secretory pathway system close to their sites of membrane delivery. Rather than being a constitutive process, KAR traffic through the secretory pathway is tightly and differentially regulated under chronically suppressed, basal, and transiently stimulated conditions.

Validation of the RUSH System in Neurons

RUSH provides a powerful system for investigating the dynamics of AMPAR and KAR trafficking to the cell surface. We show that the RUSH GluA1 and GluA2 AMPAR subunits and GluK2 KAR subunit are effectively retained at the ER membrane and can be synchronously released on demand by addition of biotin in both clonal cells and primary neurons. Importantly, the rates of traffic through the secretory pathway we measured for GluA1 and GluA2 agree well with rates reported for endogenous AMPAR subunits monitored by pulse-chase radiolabeling, with GluA1 trafficking more rapidly than GluA2 (Greger et al., 2002; Greger and Esteban, 2007).

KAR Scaling Is Mediated by GluK2 Editing

AMPARs and NMDARs scale in response to a prolonged decrease or increase in synaptic activity (Turrigiano, 2012). Given their importance in neuronal circuit development and both pre- and postsynaptic function (Contractor et al., 2011; Lerma and Marques, 2013) we reasoned that it is likely that KARs also need to be tuned in response to overall activity changes. Consistent with this, KARs are scaled by chronic

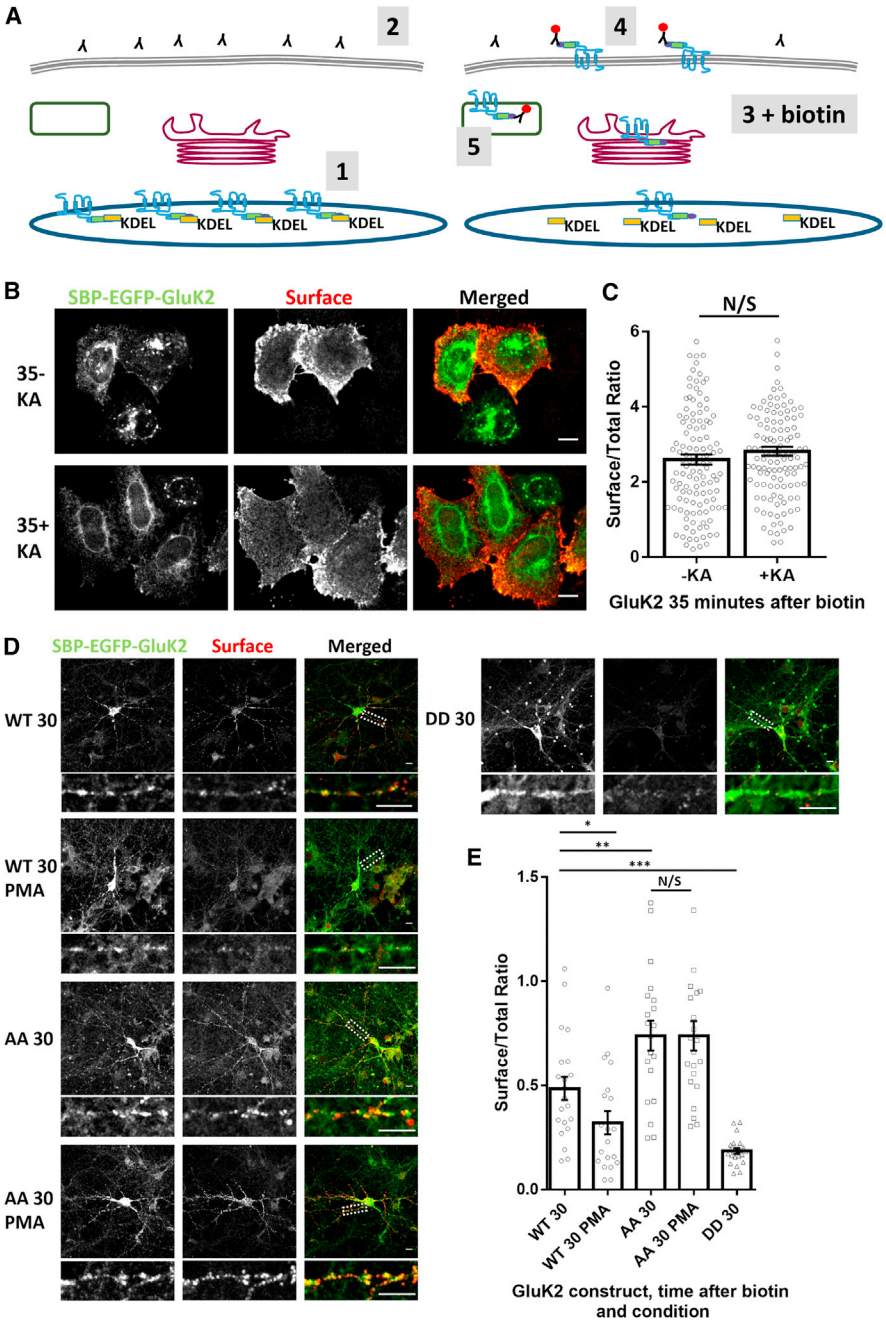

Figure 4. Basal PKC Phosphorylation Suppresses Surface Delivery of KARs

(A) Schematic illustrating the live labeling protocol used to exclude any contribution of changes in endocytosis. 1: hooked RUSH receptor before the addition of biotin. 2: live label with anti-SBP antibody. 3: addition of biotin allows release of receptors and accumulation at the cell surface. 4: anti-SBP antibodies bind to newly exposed SBP-tagged receptors. 5: a proportion of receptors internalize, but cells are permeabilized and labeled with a secondary antibody labeling all receptors that have been surface-exposed.

(B) Representative images of the live labeling protocol showing that 100 μM KA does not change the secretory pathway delivery and extent of surface expression of SBP-EGFP-GluK2 in HeLa cells 35 min after biotin addition. See also Figure S4A.

(C) Quantification of the data shown in (B); two independent experiments, n = 80. $p > 0.05$, Welch's t test.

(D) Representative images of hippocampal neurons expressing SBP-EGFP-GluK2 WT, SBP-EGFP-GluK2 S846A/S868A, or SBP-EGFP-GluK2 S846D/S868D 30 min after biotin in the presence or absence of PMA. Total receptor distribution was measured using the EGFP tag, and surface-expressed receptors were determined using live labeling with anti-SBP. See also Figure S4B.

(E) Quantification of three independent experiments (n = 17–22). ***$p < 0.0005$, **$p < 0.01$, *$p < 0.05$; Welch's t test.

Scale bars, 10 μm.

suppression of synaptic activity (Yan et al., 2013). We propose a mechanism analogous to NMDAR scaling whereby changes in RNA editing regulate the ER exit and, consequently, the availability of new NMDARs for delivery to the surface (Mu et al., 2003). We show that chronic suppression of synaptic activity decreases Q/R editing of GluK2, which promotes KAR assembly, ER exit, and delivery to the cell surface (Figure 7). This mechanism to restrict the amount of KARs reaching the cell surface likely plays a key role in controlling neuronal excitability, and it is notable that transgenic mice deficient in Q/R editing display increased seizure vulnerability (Vissel et al., 2001).

PKC Phosphorylation of GluK2 Controls Basal Trafficking through the Secretory Pathway

Agonist activation of surface-expressed KARs causes PKC phosphorylation of GluK2 at S846 and S868, which promotes SUMOylation and KAR endocytosis (Martin et al., 2007; Konopacki et al., 2011; Chamberlain et al., 2012). Furthermore, phosphomimetic serine-to-aspartate mutations of residues 846 and 868 in GluK2 impede KAR traffic to the cell surface (Nasu-Nishimura et al., 2010; Konopacki et al., 2011). Here we show that these PKC phosphorylation sites are involved in ER exit of KARs and that preventing PKC phosphorylation of GluK2 by mutating S846 and S868 to alanine increases basal rates of secretory pathway trafficking. Thus, PKC phosphorylation of S846 and S868 in GluK2 exerts multiple levels of control over KAR trafficking, including regulating the number of GluK2-containing KARs that can exit the ER and enter the secretory pathway (Figure 7).

Transient Kainate Receptor Activation Downregulates the Delivery of Newly Synthesized KARs

Transient KAR activation can elicit a lasting upregulation of KARs at the cell surface because of increased recycling back to the surface (Martin et al., 2008; González-González and Henley, 2013), and this form of KAR activation can also induce long-term potentiation (LTP) of AMPARs (Petrovic et al., 2017; Sanjana et al., 2012). Here we show that transient kainate stimulation decreases the supply of de novo KARs through the secretory pathway. We interpret these results to indicate a negative feedback mechanism that can limit the extent of the increase in KAR surface expression. Thus, following a kainate-induced increase in surface expression of locally available KARs, the supply of new receptors is restricted to prevent positive feedback, leading to further increases in KAR surface expression and uncontrolled neuronal excitability and excitotoxicity. This agonist-mediated regulation of KAR secretory pathway trafficking is not due to changes in the phosphorylation status of S846 and S868 because secretory pathway traffic of the PKC non-phosphorylatable GluK2 mutant was also reduced by transient kainate application. Furthermore, this regulatory system is KAR-specific because kainate stimulation does not regulate the secretory pathway traffic of AMPARs.

GluK2 PDZ Interactions and the Activity-Controlled Secretory Pathway

The PDZ ligand of GluK2 binds to an array of interacting proteins, including PSD95, SAP97, PICK1, GRIP, CASK, and syntenin (Coussen et al., 2002; Hirbec et al., 2003) that control many aspects of KAR localization and function. C-terminal truncations of GluK2 that removed the PDZ ligand did not result in major defects in trafficking in heterologous cells, indicating that the PDZ ligand is not required for folding or ER exit (Yan et al., 2004). Consistent with this, secretory pathway trafficking is similar for GluK2 containing either the wild-type (ETMA) or mutated non-binding (EPAS) PDZ ligand. Furthermore, the steady-state localization of PDZ ligand mutants was also unchanged, suggesting that, although PDZ interactions are important for the dynamics of secretory pathway trafficking, they are not required for correct localization of GluK2.

Disruption of the GluK2 PDZ ligand did, however, significantly decrease basal secretory pathway trafficking in neurons, which occluded the kainate-induced reduction of secretory pathway trafficking. This is consistent with our previous observation that a peptide corresponding to the PDZ ligand of GluK2 can out compete endogenous interactions and, consequently, causes rundown of KAR-mediated EPSCs (Hirbec et al., 2003) and long-term depression of kainate receptor-mediated synaptic transmission (Park et al., 2006). Both of these reductions in KAR-mediated transmission are sustained over long periods, and we propose that they are attributable, at least in part, to the activity-dependent reductions in KAR secretory pathway trafficking we describe here.

In summary, the secretory pathway trafficking of KARs occurs through local secretory pathways using ERES in distal dendrites and Golgi outposts. We note, however, that it has recently been reported that KARs with an immature glycosylation state accumulate at the cell surface, suggesting that not all KARs are processed within the Golgi (Hanus et al., 2016). Like long-term regulation of iGluR synthesis by transcription and translation and short-term regulation by endocytosis and recycling of surface-expressed iGluRs, the intermediate-term processes of trafficking through the secretory pathway are also under tight activity-dependent control. These additional medium-term regulatory mechanisms add further flexibility and subtlety to neuronal excitability and network activity. Consistent with this general idea, the secretory pathway trafficking of the GluA2 AMPAR subunit can be regulated by an activity-dependent interaction with COPII vesicle proteins during mGluR-mediated, long-term depression (Pick et al., 2017). These findings open exciting avenues of research into how defects in this local secretory trafficking of KARs contribute to diseases such as epilepsy and autism, in which misregulation of KARs have been strongly implicated.

EXPERIMENTAL PROCEDURES

Primary Neuronal Culture

Embryonic hippocampal neurons were isolated from E18 Wistar rats as described previously (Martin and Henley, 2004). The cells were then plated out at various densities and cultured for up to 2 weeks. Plating medium was left on the cells for the first 24 hr: Neurobasal (Gibco) medium supplemented with horse serum (10%), GS21 (GlobalStem), and 2 mM Glutamax. Then this was changed to feeding medium (lacking horse serum) for the duration of the culture. Animal care and all experimental procedures were conducted in accordance with UK Home Office and University of Bristol guidelines.

DNA Construct Generation and Transfection

All RUSH iGluR constructs were assembled in the RUSH vector system as described previously (Boncompain and Perez, 2013). Briefly, glutamate

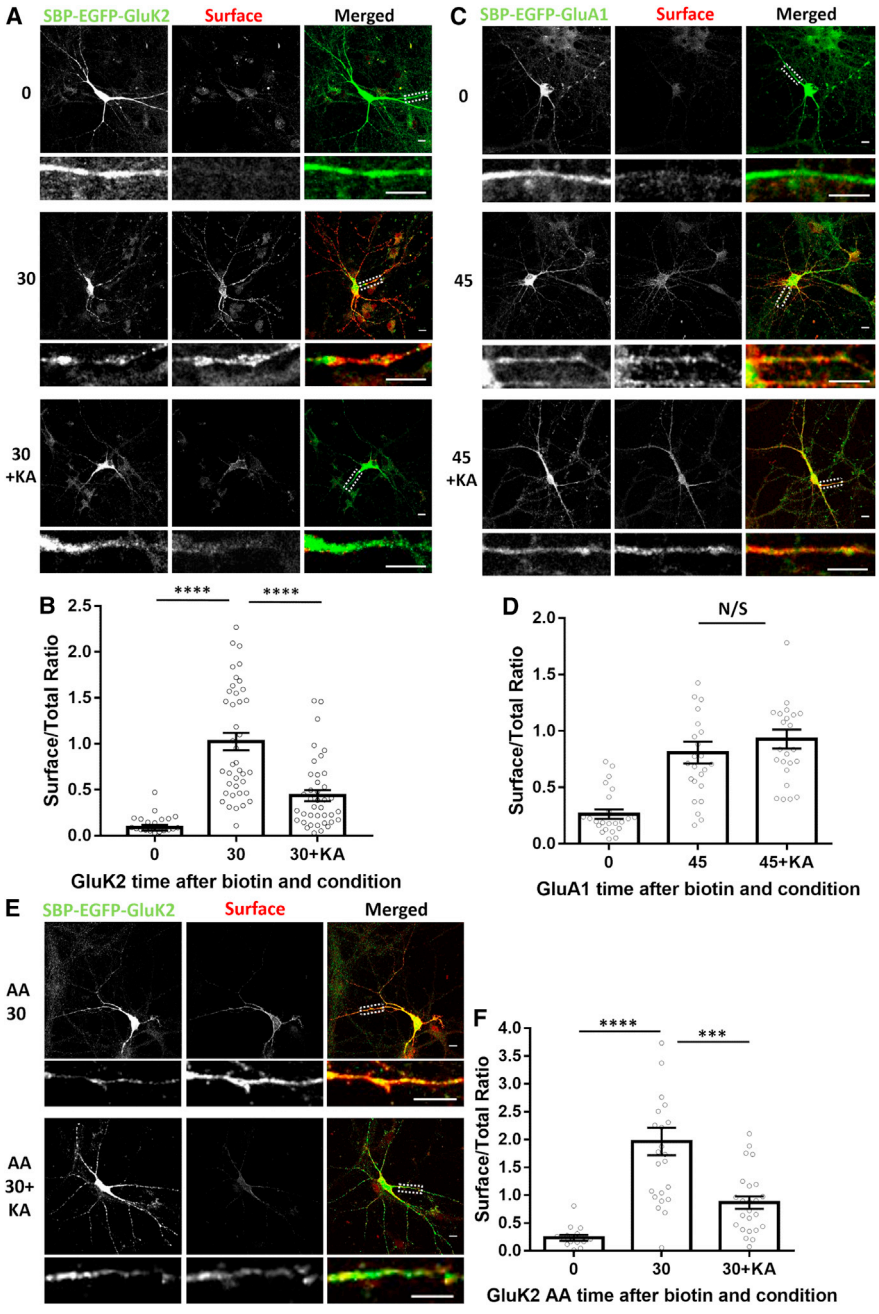

Figure 5. KAR Progress through the Secretory Pathway Is Regulated by Transient KAR Stimulation

(A) Representative images of SBP-EGFP-GluK2 without biotin (0), with biotin for 30 min (30), or with a transient 5-min pre-treatment with 10 μM kainate before biotin addition (30+KA). Total SBP-EGFP-GluK2 was visualized with EGFP, and the surface-expressed SBP-EGFP-GluK2 was live-labeled with anti-SBP.

(B) Quantification of five independent experiments (n = 24–40). ****$p < 0.0001$, Welch's t test.

(C) Representative images of SBP-EGFP-GluA1 without biotin (0), with biotin for 45 min (45), or with a transient 5-min pre-treatment with 10 μM kainate before biotin addition (45+KA). Total SBP-EGFP-GluA1 was visualized with EGFP, and the surface-expressed SBP-EGFP-GluA1 was live-labeled with anti-SBP antibody.

(D) Quantification of three independent experiments; n = 24 for all conditions. $p > 0.05$, Welch's t test.

(E) Representative images of SBP-EGFP-GluK2 S846A/S868A, 30 min after biotin (AA 30), or with a transient 5-min pre-treatment with kainate before biotin addition (AA 30+KA). Total SBP-EGFP-GluK2 S846A/S868A was visualized with EGFP, and surface-expressed SBP-EGFP-GluK2 S846A/S868A was live-labeled with anti-SBP antibody.

(F) Quantification of three independent experiments; n = 15–30. ****$p < 0.0001$, ***$p < 0.001$, Welch's t test.

Scale bars, 10 μm.

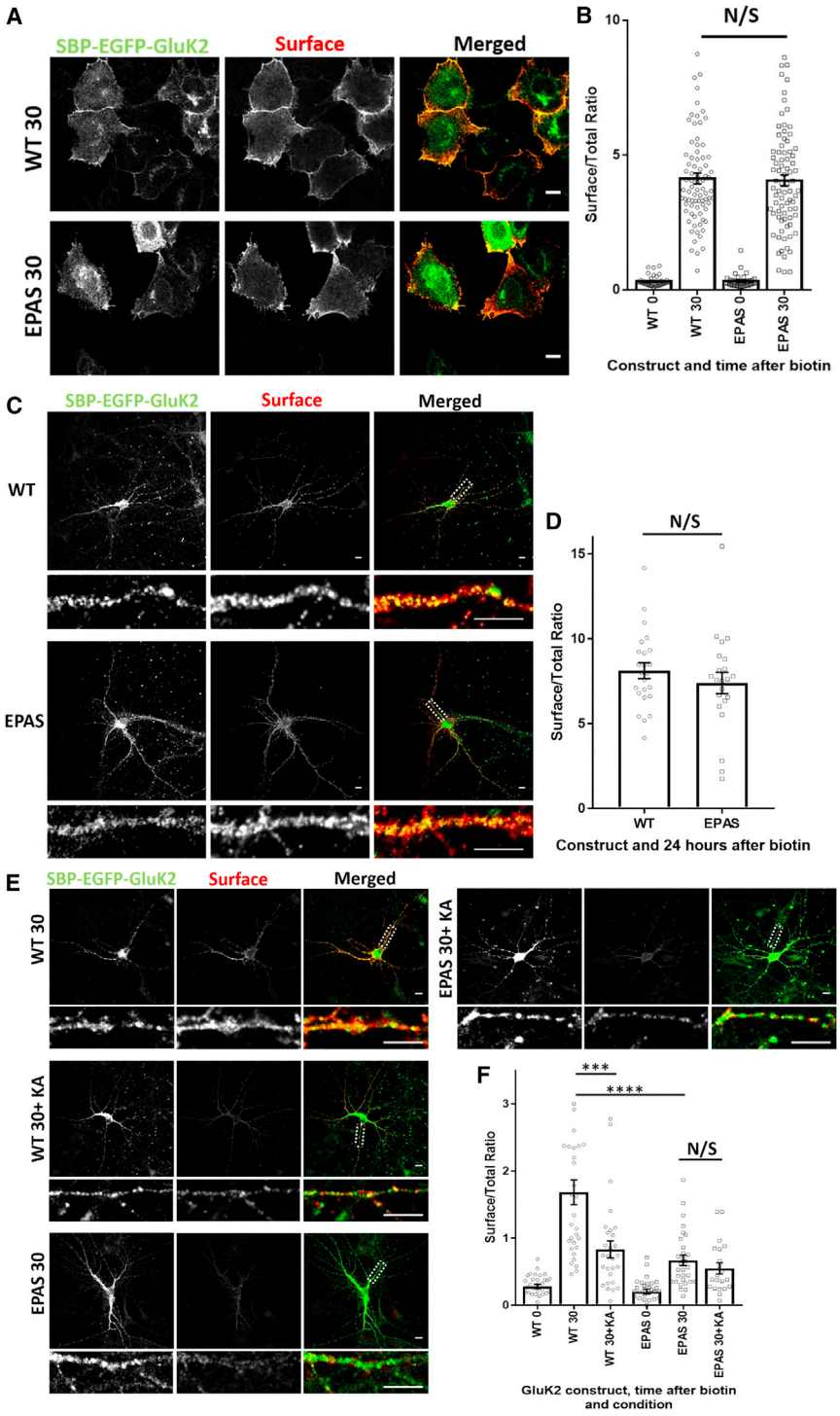

Figure 6. The PDZ Ligand of GluK2 Is Involved in Both Basal and Activity-Dependent Progression of KARs through the Secretory Pathway

(A) Representative images of HeLa cells showing the distributions of exogenously expressed SBP-EGFP-GluK2-ETMA or SBP-EGFP-GluK2-EPAS before and 30 min after addition of biotin. In all cases, EGFP was used to visualize total receptors, and surface-expressed KARs were visualized by live labeling with anti-SBP antibody.

(B) Quantification of two independent experiments; n = 40 for 0 and n = 80 for 30. $p > 0.05$, Welch's t test. See also Figure S6A.

(C) Representative images of hippocampal neurons expressing SBP-EGFP-GluK2-ETMA or SBP-EGFP-GluK2-EPAS 24 hr after addition of biotin. EGFP was used to visualize total receptors, and surface-expressed KARs were visualized by live labeling with anti-SBP antibody.

(D) Quantification of three independent experiments; n = 22–24. $p > 0.05$, Welch's t test.

(E) Representative images of hippocampal neurons expressing SBP-EGFP-GluK2-ETMA or SBP-EGFP-GluK2-EPAS before or 30 min after addition of biotin, with or without a transient 5-min pretreatment of 10 μM kainate. EGFP was used to visualize total receptors, and surface-expressed KARs were visualized by live labeling with anti-SBP antibody. See also Figure S6B.

(F) Quantification of four independent experiments; n = 21–32. ****$p < 0.0001$, ***$p < 0.001$, Welch's t test.

Scale bars, 10 μm.

receptors were cloned so that the fluorescent protein (FP) and the SBP were positioned immediately after an N-terminal signal peptide (in all cases, the interleukin-2 signal peptide was used). The structure is therefore SP-SBP-FP-glutamate receptor. All GluK2 constructs had an additional myc tag on the N terminus, and all SBP-EGFP-GluK2 constructs used, unless specified otherwise, were Q-edited versions (Martin et al., 2007). The R-edited version of SBP-EGFP-GluA2 was used throughout. For each iGluR construct, a forward primer was designed with an FseI restriction site and the reverse primer with a PacI site, followed by cloning of the PCR product using standard molecular biology techniques. QuikChange mutagenesis was used to introduce point mutations. Fluorescent tags were switched using forward and reverse primers with SbfI and FseI sites, respectively. DH5α was used to clone and amplify DNA. A Lipofectamine 2000 method from Invitrogen was used to introduce DNA into hippocampal neurons (days in vitro [DIV] 13–14) and HeLa cells. Cells were incubated at 37°C and 5% CO_2 for 18–24 hr before fixation or live imaging (Boncompain et al., 2012).

Virus Generation and shRNA

For ADAR2 knockdown experiments, a short hairpin RNA (shRNA)-targeting ADAR2 (target sequence AACAAGAAGCTTGCCAAGGCC) under the control of an H1 promoter was cloned into a modified form of the lentiviral vector pXLG3. Lentiviruses were then produced using HEK293T cells, harvested, and added to DIV 9/10 hippocampal cells for 5 days, followed by surface biotinylation (Rocca et al., 2017).

Live Cell Surface Labeling and Fixation

All experiments with surface staining were performed using a live imaging protocol. RUSH-transfected hippocampal neurons or HeLa cells were live-labeled using an anti-SBP (Millipore, monoclonal, clone 20, MAB10764) primary antibody.

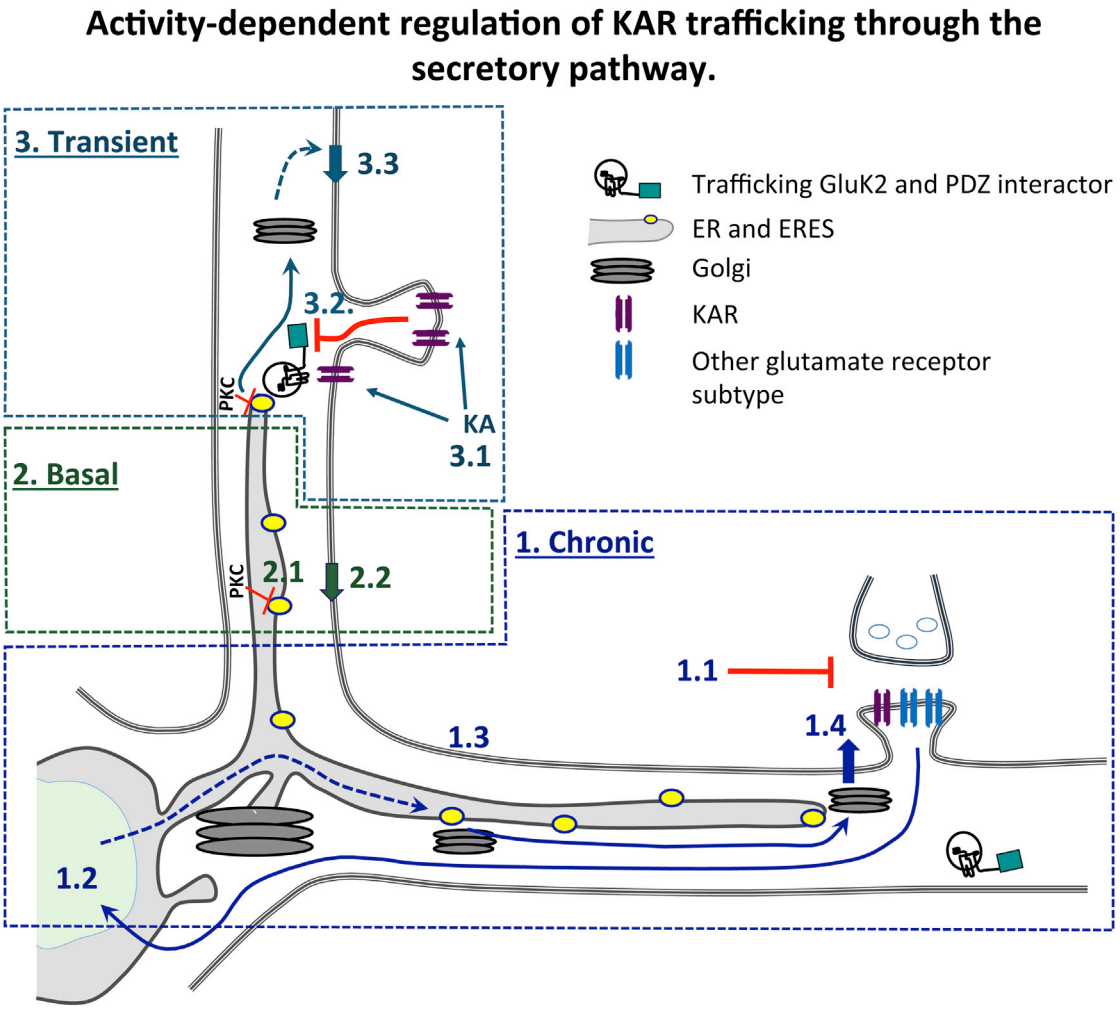

1. Chronic

1.1 TTX addition.

1.2 Less RNA editing.

1.3 Decreased editing leads to increased KAR assembly and ER exit.

1.4 Increased surface GluK2.

2. Basal

2.1 PKC phosphorylation of S846 and S868 reduces ER exit.

2.2 Decreased surface GluK2.

3. Transient

3.1. Transient activation of KARs.

3.2. Reduced secretory pathway trafficking of GluK2 via PDZ ligand interaction.

3.3. Decreased delivery of *de novo* GluK2 to the surface.

Figure 7. Model

Shown is a schematic summarizing our results.

For activity experiments, cells were incubated for 5 min in 1 μM TTX with or without 10 μM kainate (Tocris Bioscience) and then washed with PBS. GYKI53655 (40 μM, Abcam) was included to block AMPARs. The PKC activator PMA (12-O-tetradecanoylphorbol-13-acetate [TPA], Cell Signaling Technology) was used at 1 μM, and DMSO was used as a vehicle. HEPES-buffered saline (HBS) (NaCl, 140 mM; KCl, 5mM; glucose, 15 mM; HEPES, 25 mM; $CaCl_2$, 1.5 mM; and $MgCl_2$, 1.5 mM) containing D-biotin (40 μM, Sigma) was added to the cells in the presence of the anti-SBP antibody (1/500 dilution) for different times. The 0 time point was incubated with just anti-SBP and no biotin but always for the longest time being tested. After completion, cells were washed with PBS multiple times before fixing in 4% paraformaldehyde (PFA) for 8–10 min and quenched in 100 mM glycine (Severn Biotech). Cells were then incubated with PBS + 3% BSA (Sigma) with 0.1% Triton X-100 (Fisher Scientific) for 10 min and then with PBS + 3% BSA for a further 10 min.

For all non-live labeling experiments, the medium was removed from cells on the day of fixation. The cells were then washed with PBS, and methanol (−20°C) was added to the cells and incubated at −20°C for 4 min. The cells were then washed in PBS.

Fixed Immunostaining and Secondary Antibody Labeling

After fixation, the cells were washed in PBS before addition of primary antibodies diluted in PBS + 3% BSA for an incubation time of 60 min. Cells were washed in PBS before adding secondary antibodies (Jackson ImmunoResearch Laboratories), which were used at 1:400 dilution in PBS + 3% BSA. The cells were then washed again in PBS and mounted onto glass slides using Fluoromount-G with DAPI (eBioscience).

Imaging and Analysis

A Leica SP5 confocal microscope was used to image both the total (EGFP/mCherry) and surface (anti-SBP) fluorescence, and a surface-to-total ratio was calculated after analysis. ImageJ was used to analyze surface-to-total ratios. Multiple boxes were drawn onto proximal and secondary dendrites that had an EGFP/mCherry signal present. The total fluorescence was measured, and then the channel was switched to surface fluorescence to measure the surface. A surface-to-total ratio was measured, and then an average of the multiple box measurements gave a cell surface-to-total ratio. At least eight cells were analyzed per experiment, and experiments were repeated at least three times using cells from independent dissections. TIRF analysis was done using the mCherry signal to mark the cell surface. ImageJ was used to then measure the accumulation of SEP fluorescence. Prism and either Welch's t tests (direct comparison of two time points/conditions/receptors) or Wilcoxon matched-pairs signed-rank (normalized control sample) tests were used to determine statistical significance. Data are represented as mean, and SEM values are used for error bars. Kymograph live imaging representations and colocalization line traces were made using ImageJ. The scale bars used throughout all figures represent 10 μm.

RUSH Wide-Field Imaging

A Nikon Ti microscope with a Plan Apo VC 60× oil differential interference contrast (DIC) lens and an Andor DU-885 camera were used to acquire live wide-field RUSH images. The heated stage was pre-heated to 37°C. The cell medium was replaced with 1 mL pre-warmed HBS. When RUSH-transfected cells were found, biotin was added to the cells by diluting biotin to a 2× working solution in HBS. 1 mL of this 2× biotin working solution was added to the original 1 mL of imaging medium already on the cells. The cells were imaged over time periods of up to 60 min, with a frame being taken every 5 or 10 s.

RUSH TIRF Imaging

A Leica AM TIRF MC system attached to a Leica DMI 6000 inverted epifluorescence microscope was used to image the surface of cells. A 63× oil lens was used. HBS was added to the cells, and the cells were found and focused, and the cell surface plane (mCherry) was found using automated TIRF angles. Frames were taken every 30 s.

Scaling, Surface Biotinylation, and Western Blot

Hippocampal neurons (DIV 14–15) plated at a density of 500,000 per well of a 6-well dish were treated with 1 μM TTX for 24 hr. All steps were performed on ice with ice-cold buffers unless stated otherwise. After the stated treatments, hippocampal neurons were washed twice in PBS. Surface proteins were labeled with membrane-impermeable Sulfo-NHS-SS biotin (0.3 mg/mL, Thermo Scientific) for 10 min on ice and washed three times with PBS. 50 mM NH_4Cl was added to quench free biotin-reactive groups, and cells were extracted with lysis buffer (50 mM Tris [pH 7.4], 150 mM NaCl, 1% Triton, 0.1% SDS, and protease inhibitor [Complete, Roche]), incubated on ice for 30 min, and centrifuged (15,000 × *g*, 4°C, 20 min) to remove insoluble cell debris. For isolation of surface proteins, samples were incubated with streptavidin beads (Sigma) for 90 min at 4°C. Following three washes, the samples were boiled with 2× sample buffer at 95°C for 10 min, resolved by SDS-PAGE, and immunoblotted. Antibodies used were as follows: GluA1 and GluK2 (Millipore), glyceraldehyde 3-phosphate dehydrogenase (GAPDH) and EGFR (Abcam), and ADAR2 (Sigma). Western blots were imaged and quantified using LI-COR Biosciences Image Studio software. The surface levels of GluA1, GluK2, and EGFR were normalized to their respective total levels to determine surface expression. Treated samples were normalized to their control samples.

RNA Extraction and RT-PCR

RNA samples were extracted from DIV 14 hippocampal neurons after the stated treatments using the RNeasy Mini RNA extraction kit (QIAGEN) following the manufacturer's protocol. 1 μg of RNA was used per condition and reverse-transcribed to cDNA using the RevertAid First Strand cDNA Synthesis Kit following the manufacturer's protocol (Thermo Scientific). The following primers (spanning the M2 region of GluK2) were used, giving a PCR product of 452 bp: GluK2 F, 5′-GGTATAACCCACACCCTTGCAACC-3′; GluK2 R, 5′-TGACTCCATTAAGAAAGCATAATCCGA-3′. To determine the level of GluK2 RNA editing, BbvI (New England Biolabs) digestion was used (Bernard et al., 1999). Digestion of the PCR product was performed at 37°C for 2 hr. All of the digested product was run on 4% agarose gel, and the ethidium bromide-stained bands were imaged using a UV transilluminator and quantified using NIH ImageJ. To determine the level of editing, the following formula was used: (intensity of 376 [edited] / intensity of [376 (edited) + 269 (unedited)]) × 100. The band at 76 bp was used to determine equal loading.

SUPPLEMENTAL INFORMATION

Supplemental Information includes six figures and three movies and can be found with this article online at http://dx.doi.org/10.1016/j.celrep.2017.06.001.

AUTHOR CONTRIBUTIONS

A.J.E. performed the imaging experiments. S.G. performed the scaling and RNA editing experiments. K.A.W. helped design and make the constructs and provided practical advice and training. D.J.S. initiated the use of RUSH with A.J.E. in non-neuronal cells, and J.M.H. managed the project. A.J.E. and J.M.H. wrote the first draft of the paper. All authors made intellectual contributions and participated in editing the paper.

ACKNOWLEDGMENTS

K.A.W. and J.M.H. are funded by the MRC (MR/L003791). A.J.E. and S.G. are funded by the Wellcome Trust Dynamic Cell Biology Ph.D. program (102388/Z/13/Z to A.J.E. and 105384/Z/14/Z to S.G.). J.M.H. is also grateful for financial support from the BHF (PG/14/60/31014) and BBSRC (BB/K014366 and BB/K014358). We thank Franck Perez and Gaelle Boncompain for providing us with RUSH mCherry E-Cadherin, which we used as the template for our iGluR constructs. We thank Prof. Viki Allan for the UBC6-mCherry DNA construct. We also thank the Wolfson Bioimaging facility at the University of Bristol.

Received: December 28, 2016
Revised: April 17, 2017
Accepted: May 25, 2017
Published: June 20, 2017

REFERENCES

Ashby, M.C., Ibaraki, K., and Henley, J.M. (2004). It's green outside: tracking cell surface proteins with pH-sensitive GFP. Trends Neurosci. *27*, 257–261.

Ball, S.M., Atlason, P.T., Shittu-Balogun, O.O., and Molnár, E. (2010). Assembly and intracellular distribution of kainate receptors is determined by RNA editing and subunit composition. J. Neurochem. *114*, 1805–1818.

Beattie, E.C., Carroll, R.C., Yu, X., Morishita, W., Yasuda, H., von Zastrow, M., and Malenka, R.C. (2000). Regulation of AMPA receptor endocytosis by a signaling mechanism shared with LTD. Nat. Neurosci. *3*, 1291–1300.

Bernard, A., Ferhat, L., Dessi, F., Charton, G., Represa, A., Ben-Ari, Y., and Khrestchatisky, M. (1999). Q/R editing of the rat GluR5 and GluR6 kainate receptors in vivo and in vitro: evidence for independent developmental, pathological and cellular regulation. Eur. J. Neurosci. *11*, 604–616.

Boehm, J., Kang, M.G., Johnson, R.C., Esteban, J., Huganir, R.L., and Malinow, R. (2006). Synaptic incorporation of AMPA receptors during LTP is controlled by a PKC phosphorylation site on GluR1. Neuron *51*, 213–225.

Boncompain, G., and Perez, F. (2012). Synchronizing protein transport in the secretory pathway. Curr. Protoc. Cell Biol. *Chapter 15*, Unit 15.19.

Boncompain, G., and Perez, F. (2013). Fluorescence-based analysis of trafficking in mammalian cells. Methods Cell Biol. *118*, 179–194.

Boncompain, G., Divoux, S., Gareil, N., de Forges, H., Lescure, A., Latreche, L., Mercanti, V., Jollivet, F., Raposo, G., and Perez, F. (2012). Synchronization of secretory protein traffic in populations of cells. Nat. Methods *9*, 493–498.

Budnik, A., and Stephens, D.J. (2009). ER exit sites–localization and control of COPII vesicle formation. FEBS Lett. *583*, 3796–3803.

Burnashev, N., Monyer, H., Seeburg, P.H., and Sakmann, B. (1992). Divalent ion permeability of AMPA receptor channels is dominated by the edited form of a single subunit. Neuron *8*, 189–198.

Cajigas, I.J., Tushev, G., Will, T.J., tom Dieck, S., Fuerst, N., and Schuman, E.M. (2012). The local transcriptome in the synaptic neuropil revealed by deep sequencing and high-resolution imaging. Neuron *74*, 453–466.

Chamberlain, S.E., González-González, I.M., Wilkinson, K.A., Konopacki, F.A., Kantamneni, S., Henley, J.M., and Mellor, J.R. (2012). SUMOylation and phosphorylation of GluK2 regulate kainate receptor trafficking and synaptic plasticity. Nat. Neurosci. *15*, 845–852.

Contractor, A., Mulle, C., and Swanson, G.T. (2011). Kainate receptors coming of age: milestones of two decades of research. Trends Neurosci. *34*, 154–163.

Copits, B.A., and Swanson, G.T. (2013). Kainate receptor post-translational modifications differentially regulate association with 4.1N to control activity-dependent receptor endocytosis. J. Biol. Chem. *288*, 8952–8965.

Coussen, F., Normand, E., Marchal, C., Costet, P., Choquet, D., Lambert, M., Mège, R.M., and Mulle, C. (2002). Recruitment of the kainate receptor subunit glutamate receptor 6 by cadherin/catenin complexes. J. Neurosci. *22*, 6426–6436.

Egebjerg, J., and Heinemann, S.F. (1993). Ca^{2+} Permeability of Unedited and Edited Versions of the Kainate Selective Glutamate Receptor GluR6. Proc. Natl. Acad. Sci. USA *90*, 755–759.

Glebov, O.O., Tigaret, C.M., Mellor, J.R., and Henley, J.M. (2015). Clathrin-independent trafficking of AMPA receptors. J. Neurosci. *35*, 4830–4836.

González-González, I.M., and Henley, J.M. (2013). Postsynaptic kainate receptor recycling and surface expression are regulated by metabotropic autoreceptor signalling. Traffic *14*, 810–822.

González-González, I.M., Konopaki, F., Rocca, D.L., Doherty, A.J., Jaafari, N., Wilkinson, K.A., and Henley, J.M. (2012). Kainate Receptor Trafficking. WIRES Membrane Transport and Signaling *1*, 31–44.

Granger, A.J., and Nicoll, R.A. (2013). Expression mechanisms underlying long-term potentiation: a postsynaptic view, 10 years on. Philos. Trans. R. Soc. Lond. B Biol. Sci. *369*, 20130136.

Greger, I.H., and Esteban, J.A. (2007). AMPA receptor biogenesis and trafficking. Curr. Opin. Neurobiol. *17*, 289–297.

Greger, I.H., Khatri, L., and Ziff, E.B. (2002). RNA editing at arg607 controls AMPA receptor exit from the endoplasmic reticulum. Neuron *34*, 759–772.

Grooms, S.Y., Noh, K.M., Regis, R., Bassell, G.J., Bryan, M.K., Carroll, R.C., and Zukin, R.S. (2006). Activity bidirectionally regulates AMPA receptor mRNA abundance in dendrites of hippocampal neurons. J. Neurosci. *26*, 8339–8351.

Hanus, C., Kochen, L., Tom Dieck, S., Racine, V., Sibarita, J.B., Schuman, E.M., and Ehlers, M.D. (2014). Synaptic control of secretory trafficking in dendrites. Cell Rep. *7*, 1771–1778.

Hanus, C., Geptin, H., Tushev, G., Garg, S., Alvarez-Castelao, B., Sambandan, S., Kochen, L., Hafner, A.S., Langer, J.D., and Schuman, E.M. (2016). Unconventional secretory processing diversifies neuronal ion channel properties. eLife *5*.

Henley, J.M., and Wilkinson, K.A. (2016). Synaptic AMPA receptor composition in development, plasticity and disease. Nat. Rev. Neurosci. *17*, 337–350.

Hirbec, H., Perestenko, O., Nishimune, A., Meyer, G., Nakanishi, S., Henley, J.M., and Dev, K.K. (2002). The PDZ proteins PICK1, GRIP, and syntenin bind multiple glutamate receptor subtypes. Analysis of PDZ binding motifs. J. Biol. Chem. *277*, 15221–15224.

Hirbec, H., Francis, J.C., Lauri, S.E., Braithwaite, S.P., Coussen, F., Mulle, C., Dev, K.K., Coutinho, V., Meyer, G., Isaac, J.T., et al. (2003). Rapid and differential regulation of AMPA and kainate receptors at hippocampal mossy fibre synapses by PICK1 and GRIP. Neuron *37*, 625–638.

Holt, C.E., and Schuman, E.M. (2013). The central dogma decentralized: new perspectives on RNA function and local translation in neurons. Neuron *80*, 648–657.

Horton, A.C., and Ehlers, M.D. (2003). Dual modes of endoplasmic reticulum-to-Golgi transport in dendrites revealed by live-cell imaging. J. Neurosci. *23*, 6188–6199.

Huganir, R.L., and Nicoll, R.A. (2013). AMPARs and synaptic plasticity: the last 25 years. Neuron *80*, 704–717.

Hughes, H., and Stephens, D.J. (2010). Sec16A defines the site for vesicle budding from the endoplasmic reticulum on exit from mitosis. J. Cell Sci. *123*, 4032–4038.

Jeyifous, O., Waites, C.L., Specht, C.G., Fujisawa, S., Schubert, M., Lin, E.I., Marshall, J., Aoki, C., de Silva, T., Montgomery, J.M., et al. (2009). SAP97 and CASK mediate sorting of NMDA receptors through a previously unknown secretory pathway. Nat. Neurosci. *12*, 1011–1019.

Jia, Y.H., Zhu, X., Li, S.Y., Ni, J.H., and Jia, H.T. (2006). Kainate exposure suppresses activation of GluR2 subunit promoter in primary cultured cerebral cortical neurons through induction of RE1-silencing transcription factor. Neurosci. Lett. *403*, 103–108.

Kennedy, M.J., and Ehlers, M.D. (2011). Mechanisms and function of dendritic exocytosis. Neuron *69*, 856–875.

Köhler, M., Burnashev, N., Sakmann, B., and Seeburg, P.H. (1993). Determinants of Ca2+ permeability in both TM1 and TM2 of high affinity kainate receptor channels: diversity by RNA editing. Neuron *10*, 491–500.

Konopacki, F.A., Jaafari, N., Rocca, D.L., Wilkinson, K.A., Chamberlain, S., Rubin, P., Kantamneni, S., Mellor, J.R., and Henley, J.M. (2011). Agonist-induced PKC phosphorylation regulates GluK2 SUMOylation and kainate receptor endocytosis. Proc. Natl. Acad. Sci. USA *108*, 19772–19777.

Lerma, J., and Marques, J.M. (2013). Kainate receptors in health and disease. Neuron *80*, 292–311.

Liu, Y., Formisano, L., Savtchouk, I., Takayasu, Y., Szabó, G., Zukin, R.S., and Liu, S.J. (2010). A single fear-inducing stimulus induces a transcription-dependent switch in synaptic AMPAR phenotype. Nat. Neurosci. *13*, 223–231.

Lussier, M.P., Sanz-Clemente, A., and Roche, K.W. (2015). Dynamic Regulation of N-Methyl-d-aspartate (NMDA) and α-Amino-3-hydroxy-5-methyl-4-isoxazolepropionic Acid (AMPA) Receptors by Posttranslational Modifications. J. Biol. Chem. *290*, 28596–28603.

Martin, S., and Henley, J.M. (2004). Activity-dependent endocytic sorting of kainate receptors to recycling or degradation pathways. EMBO J. *23*, 4749–4759.

Martin, S., Nishimune, A., Mellor, J.R., and Henley, J.M. (2007). SUMOylation regulates kainate-receptor-mediated synaptic transmission. Nature *447*, 321–325.

Martin, S., Bouschet, T., Jenkins, E.L., Nishimune, A., and Henley, J.M. (2008). Bidirectional regulation of kainate receptor surface expression in hippocampal neurons. J. Biol. Chem. *283*, 36435–36440.

Mu, Y., Otsuka, T., Horton, A.C., Scott, D.B., and Ehlers, M.D. (2003). Activity-dependent mRNA splicing controls ER export and synaptic delivery of NMDA receptors. Neuron *40*, 581–594.

Na, Y., Park, S., Lee, C., Kim, D.K., Park, J.M., Sockanathan, S., Huganir, R.L., and Worley, P.F. (2016). Real-Time Imaging Reveals Properties of Glutamate-Induced Arc/Arg 3.1 Translation in Neuronal Dendrites. Neuron *91*, 561–573.

Nasu-Nishimura, Y., Jaffe, H., Isaac, J.T., and Roche, K.W. (2010). Differential regulation of kainate receptor trafficking by phosphorylation of distinct sites on GluR6. J. Biol. Chem. *285*, 2847–2856.

Nishikura, K. (2016). A-to-I editing of coding and non-coding RNAs by ADARs. Nat. Rev. Mol. Cell Biol. *17*, 83–96.

Palmer, C.L., Lim, W., Hastie, P.G., Toward, M., Korolchuk, V.I., Burbidge, S.A., Banting, G., Collingridge, G.L., Isaac, J.T., and Henley, J.M. (2005). Hippocalcin functions as a calcium sensor in hippocampal LTD. Neuron *47*, 487–494.

Park, Y., Jo, J., Isaac, J.T., and Cho, K. (2006). Long-term depression of kainate receptor-mediated synaptic transmission. Neuron *49*, 95–106.

Petrovic, M., Viana Da Silva, S., Clement, J.P., Vyklicky, L., Mulle, C., González-González, I.M., and Henley, J.M. (2017). Metabotropic action of postsynaptic kainate receptors triggers hippocampal LTP. Nat. Neurosci. *20*, 529–539.

Pick, J.E., Khatri, L., Sathler, M.F., and Ziff, E.B. (2017). mGluR long-term depression regulates GluA2 association with COPII vesicles and exit from the endoplasmic reticulum. EMBO J. *36*, 232–244.

Presley, J.F., Cole, N.B., Schroer, T.A., Hirschberg, K., Zaal, K.J., and Lippincott-Schwartz, J. (1997). ER-to-Golgi transport visualized in living cells. Nature *389*, 81–85.

Rao, A., and Craig, A.M. (1997). Activity regulates the synaptic localization of the NMDA receptor in hippocampal neurons. Neuron *19*, 801–812.

Rocca, D.L., Wilkinson, K.A., and Henley, J.M. (2017). SUMOylation of FOXP1 regulates transcriptional repression via CtBP1 to drive dendritic morphogenesis. Sci. Rep. *7*, 877.

Sanjana, N.E., Levanon, E.Y., Hueske, E.A., Ambrose, J.M., and Li, J.B. (2012). Activity-dependent A-to-I RNA editing in rat cortical neurons. Genetics *192*, 281–287.

Schuman, E.M., Dynes, J.L., and Steward, O. (2006). Synaptic regulation of translation of dendritic mRNAs. J. Neurosci. *26*, 7143–7146.

Shepherd, J.D., Rumbaugh, G., Wu, J., Chowdhury, S., Plath, N., Kuhl, D., Huganir, R.L., and Worley, P.F. (2006). Arc/Arg3.1 mediates homeostatic synaptic scaling of AMPA receptors. Neuron *52*, 475–484.

Sommer, B., Köhler, M., Sprengel, R., and Seeburg, P.H. (1991). RNA editing in brain controls a determinant of ion flow in glutamate-gated channels. Cell *67*, 11–19.

Torre, E.R., and Steward, O. (1996). Protein synthesis within dendrites: glycosylation of newly synthesized proteins in dendrites of hippocampal neurons in culture. J. Neurosci. *16*, 5967–5978.

Turrigiano, G. (2012). Homeostatic synaptic plasticity: local and global mechanisms for stabilizing neuronal function. Cold Spring Harb. Perspect. Biol. *4*, a005736.

Vissel, B., Royle, G.A., Christie, B.R., Schiffer, H.H., Ghetti, A., Tritto, T., Perez-Otano, I., Radcliffe, R.A., Seamans, J., Sejnowski, T., et al. (2001). The role of RNA editing of kainate receptors in synaptic plasticity and seizures. Neuron *29*, 217–227.

Wilkinson, K.A., Konopacki, F., and Henley, J.M. (2012). Modification and movement: Phosphorylation and SUMOylation regulate endocytosis of GluK2-containing kainate receptors. Commun. Integr. Biol. *5*, 223–226.

Wilkinson, K.A., Ashby, M.C., and Henley, J.M. (2014). Validity of pHluorin-tagged GluA2 as a reporter for AMPA receptor surface expression and endocytosis. Proc. Natl. Acad. Sci. USA *111*, E304.

Yan, S., Sanders, J.M., Xu, J., Zhu, Y., Contractor, A., and Swanson, G.T. (2004). A C-terminal determinant of GluR6 kainate receptor trafficking. J. Neurosci. *24*, 679–691.

Yan, D., Yamasaki, M., Straub, C., Watanabe, M., and Tomita, S. (2013). Homeostatic control of synaptic transmission by distinct glutamate receptors. Neuron *78*, 687–699.

Cell Reports, Volume *19*

Supplemental Information

Assembly, Secretory Pathway Trafficking, and Surface Delivery of Kainate Receptors Is Regulated by Neuronal Activity

Ashley J. Evans, Sonam Gurung, Kevin A. Wilkinson, David J. Stephens, and Jeremy M. Henley

Supplemental Information

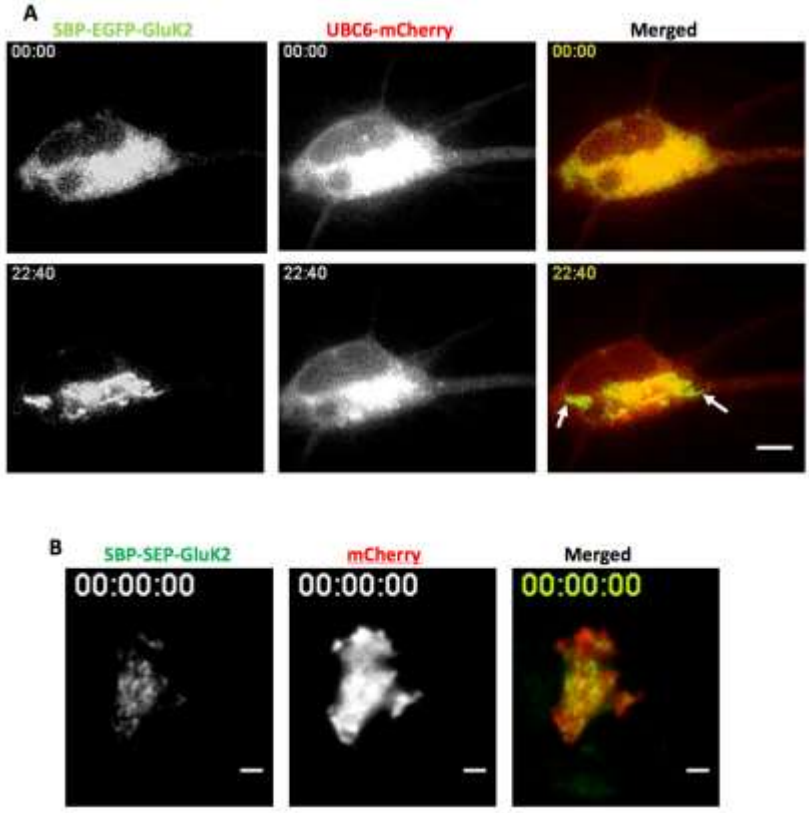

Figure S1. RUSH GluK2 receptor leaving the ER and exocytosing into the cell surface. Related to Figure 1. (see Supplemental Movie S1)

A) Primary hippocampal neurons were transfected with SBP-EGFP-GluK2 and an ER marker UBC6-mCherry (Wozniak et al., 2009). Frames were takien every 5 seconds after biotin addition. Still frames are shown demonstrating that before biotin there is colocalisation between SBP-EGFP-GluK2 and UBC6-mCherry and then a seperation after biotin addition (white arrows indicate seperation).

B) Movie from Figure 1D. HeLa cells were transfected for 20-24 hours with SBP-SEP-GluK2 and mCherry (to outline the cell). The bottom of the cell was found using TIRF imaging and biotin was added to release the 'hooked' receptor. Time is indicated in HR:MN:SC and split panels are shown for both SBP-SEP-GluK2, mCherry and a merged panel is also shown. Scale bars in all panels = 10µm.

Reference

Wozniak, M.J., Bola, B., Brownhill, K., Yang, Y.C., Levakova, V. & Allan, V.J. 2009. Role of kinesin-1 and cytoplasmic dynein in endoplasmic reticulum movement in VERO cells. *J Cell Sci,* 122**,** 1979-89.

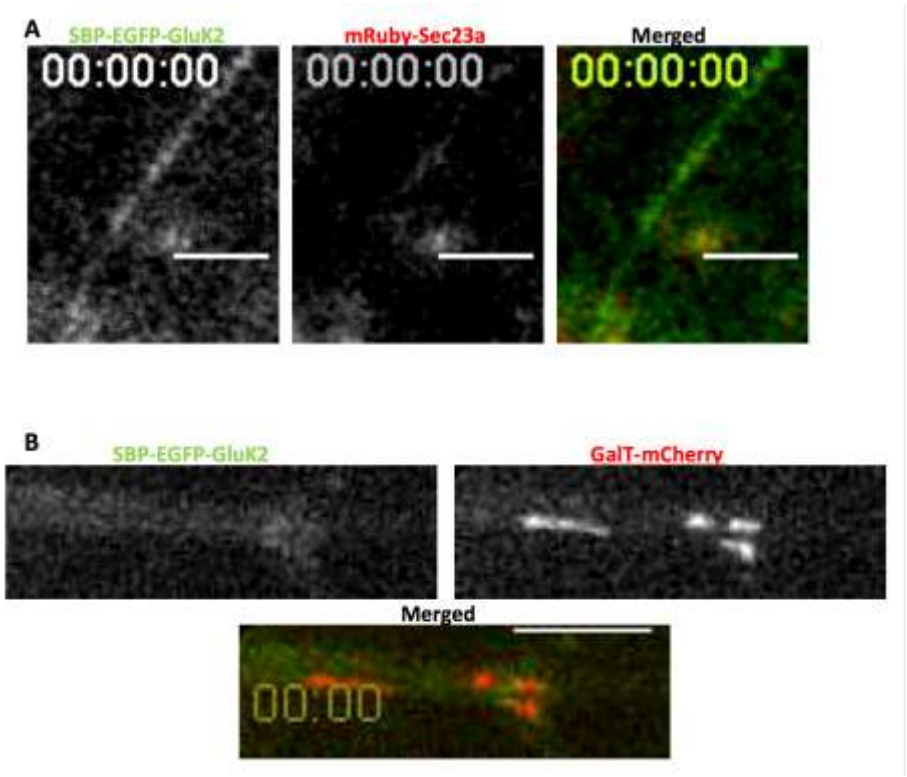

Figure S2: SBP-EGFP-GluK2 uses a local dendritic secretory pathway. Related to Figure 2.

A) Still image from the Kymograph shown in Figure 2C, please see Supplemental Movie S2. Primary hippocampal neurons were cotransfected for 20-24 hours with SBP-EGFP-GluK2 and mRuby-Sec23a to mark ER exit sites. Time is indicated in HR:MN:SC after the addition of biotin at the beginning of the movie.

B) Still image Kymograph shown in Figure 2G, please see Supplemental Movie S3. Primary hippocampal neurons were cotransfected for 20-24 hours with SBP-EGFP-GluK2 and GalT-mCherry to mark dendritc Golgi ouposts. Time is indicated MN:SC after the addition of biotin at the beginning of the movie.

Scale bars in all panels = 10µm.

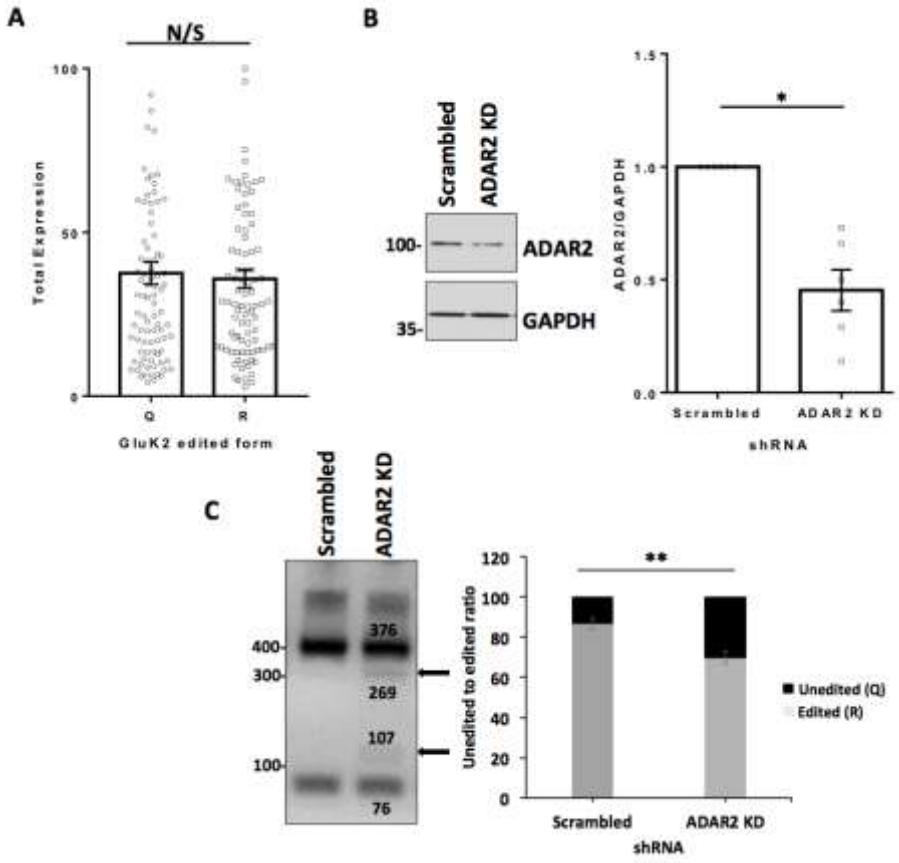

Figure S3: The GluK2 unedited (Q) and edited (R) are expressed at comparable levels and ADAR2 shRNA knocks down ADAR2 resulting in a decrease in GluK2 editing in primary neuronal culture. Related to Figure 3.

A) Total EGFP measurements (from Figure 3C, D) are compared from HeLa cells transfected for 20-24 hours with either SBP-EGFP-GluK2 (Q) or SBP-EGFP-GluK2 (R). This is to ensure there is no difference in the expression levels of the two different DNA constructs. 3 independent experiments and n=90. $p>0.05$, Welch's T Test.

B) Primary hippocampal neurons were infected with lentivirus expressing either scrambled or ADAR2 targeting shRNA, lysed and immunoblotted for ADAR2 and GAPDH. Graph shows quantification from 6 independent experiments. *=$p<0.05$, Wilcoxon matched-pairs signed rank test.

C) Primary hippocampal neurons were infected with lentivirus expressing either scrambled or ADAR2 targeting shRNA. Black arrows indicate unedited forms of GluK2. RT-PCR was performed on samples and digestion analysis of levels of unedited and edited GluK2 are displayed with quantification. **=$p<0.01$, Welch's T Test.

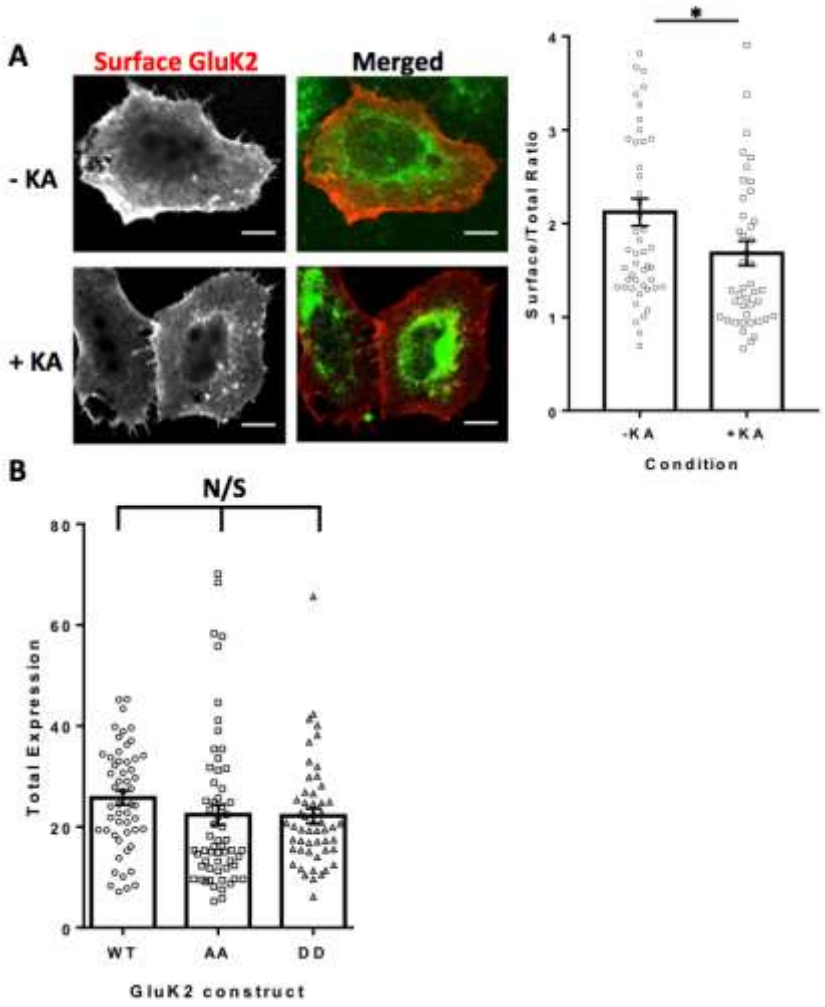

Figure S4: Kainate causes kainate receptor internalisation in HeLa cells and GluK2, GluK2 AA and GluK2 DD are all expressed at comparable levels. Related to Figure 4.

A) HeLa cells were transfected with SBP-mCherry-GluK2 (no hook, non RUSH variant) for 20-24 hours. Cells were untreated or exposed to kainate (100µM) and surface GluK2 labelled with Anti-SBP for 5 minutes. Cells were fixed in 4% PFA and not permeablised allowing labelling of just the receptors that remain at the cell surface and not the internilised population. Scale bars = 10µm. n=44-50, 2 independent experiments. *=p<0.05, Welch's T Test.

B) Total EGFP measurements (from Figure 4D, C) are compared from neurons transfected for 20-24 hours with SBP-EGFP-GluK2, SBP-EGFP-GluK2-AA or SBP-EGFP-GluK2-DD. This is to ensure there is no difference in the expression levels of the three different DNA constructs. 3 independent experiments, n=53-60. p>0.05, Welch's T Test.

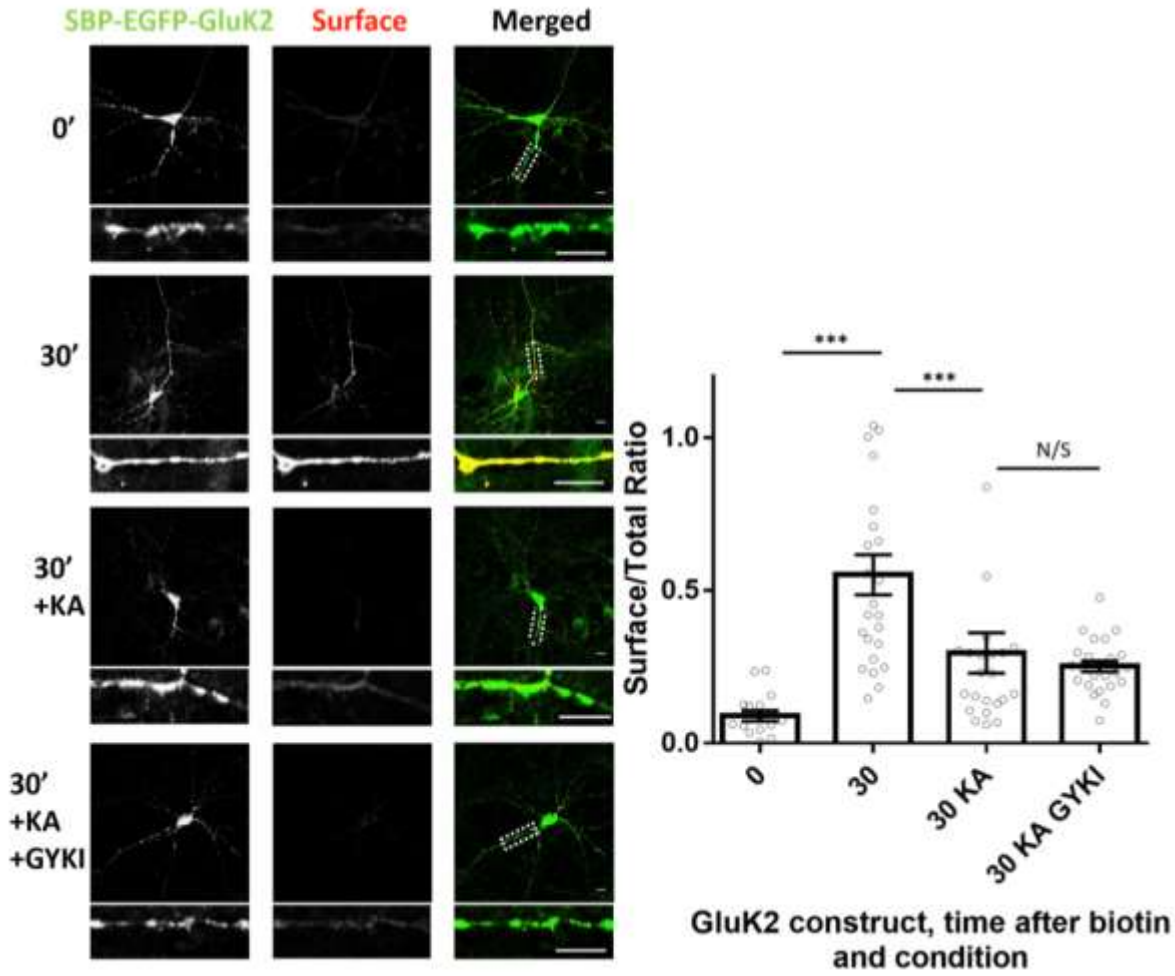

Figure S5: The transient kainate-mediated decrease in secretory pathway trafficking of de novo KARs is not mediated by activation of AMPARs. Related to Figure 5.

Primary hippocampal neurons were transfected with SBP-EGFP-GluK2 and released with biotin with or without a pre-biotin stimulation with 10µM KA or 10µM KA with 40µM GYKI-52466. KA still causes a decrease in *de novo* receptor surface delivery of KARs even in the presence of GYKI which inhibits AMPARs. ***=p<0.001, Welch's T Test. Scale bars = 10µm.

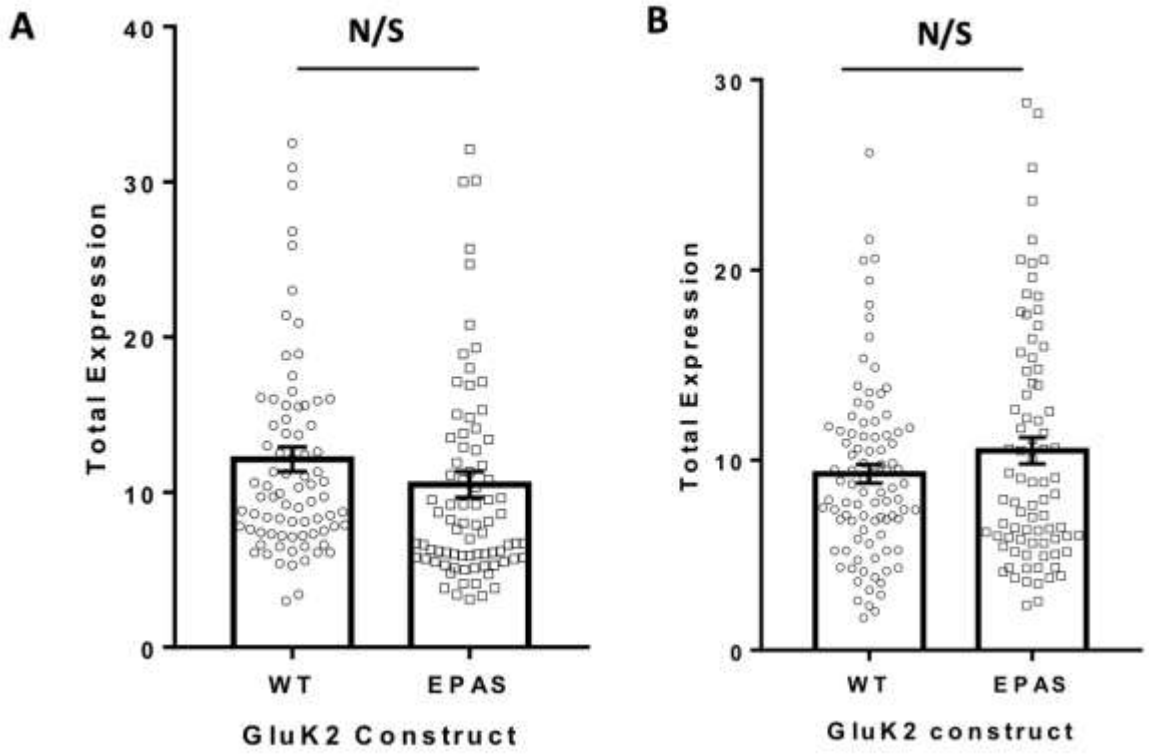

Figure S6: The GluK2 WT and EPAS mutant are expressed at comparable levels in both HeLa cells and neurons. Related to Figure 6.

A) Total EGFP measurements (from Figure 6A, B) are compared from HeLa cells transfected for 20-24 hours with either SBP-EGFP-GluK2 or SBP-EGFP-GluK2 EPAS. This is to ensure there is no difference in the expression levels of the two different DNA constructs. 3 independent experiments, n=80. $p>0.05$, Welch's T Test.

B) Total EGFP measurements (from Figure 6E, F) are compared from neurons transfected for 20-24 hours with either SBP-EGFP-GluK2 or SBP-EGFP-GluK2 EPAS. This is to ensure there is no difference in the expression levels of the two different DNA constructs. 4 independent experiments and n=82-92. $p>0.05$, Welch's T Test.